Ecosystem Status Report 2020
Eastern Bering Sea

Edited by:
Elizabeth Siddon
Auke Bay Laboratories, Alaska Fisheries Science Center, NOAA Fisheries

With contributions from:

Don Anderson, Kerim Aydin, Shaun W. Bell, Nick Bond, Lyle Britt, Caroline Brown, Greg Buck, Dan Cooper, Jessica Cross, Deana Crouser, Curry J. Cunningham, Seth Danielson, Lauren Divine, Elizabeth Dobbins, Sherri Dressel, Darcy Dugan, Ginny Eckert, Serafima Edelen, Anne Marie Eich, Lisa Eisner, Benjamin Fissel, Sarah Gaichas, Jeanette C. Gann, Colleen Harpold, Jordan Head, Kris Holderied, Kirstin Holsman, Jim Ianelli, Tim Jones, Robb Kaler, Stephen Kasperski, Kelly Kearney, Esther Kennedy, David Kimmel, Alexander Kitaysky, Joseph Krieger, Kathy Kuletz, Elizabeth Labunski, Carol Ladd, Ned Laman, Geoffrey M. Lang, Kari Lanphier, Jean Lee, Kathi Lefebvre, Dennis Lekanof, Aaron Lestenkof, Jackie Lindsey, Christopher Long, Rosie Masui, Paul Melovidov, Sara Miller, Calvin W. Mordy, Franz Mueter, Peter Murphy, Jens M. Nielsen, Elena Oaks, Jim Overland, Darren Pilcher, Chandra Poe, Melissa Rhodes-Reese, Sean Rohan, Marc Romano, Kate Savage, Gay Sheffield, Punguk Shoogukwruk, Kalei Shotwell, Elizabeth Siddon, Kim Sparks, Ingrid Spies, Phyllis Stabeno, Richard L. Thoman, Grant Thompson, Stacy Vega, Andie Wall, Muyin Wang, Jordan T. Watson, George A. Whitehouse, Tom Wilderbuer, Alexis Will, Sarah Wise, and Ellen Yasumiishi

Reviewed by:
The Bering Sea and Aleutian Islands Groundfish Plan Team
November 17, 2020
North Pacific Fishery Management Council
1007 West Third, Suite 400
Anchorage, AK 99501

Eastern Bering Sea 2020 Report Card

For more information on individual Report Card indicators, please see 'Description of the Report Card indicators' (p. 25). For more information on the methods for plotting the Report Card indicators, please see 'Methods Description for the Report Card Indicators' (p. 205).
* indicates Report Card information updated with 2020 data.

- * The **North Pacific Index (NPI)** was lower (i.e., lower sea level pressure) during summer 2019 then peaked during the winter of 2019–2020. The NPI effectively represents the state of the Aleutian Low with higher values signifying high sea level pressure. The NPI relaxed back to a near normal state in the summer of 2020. The Nov–Mar average **NPI value remains above the long-term mean.**
- * The mean **sea ice extent** across the Bering Sea (1 Aug–31 Jul; western and eastern) exhibited no long term trend, although a **steep decline in ice extent** was observed from 2012 (highest extent on record) to 2018 (lowest extent on record). The 2019–2020 daily mean extent of 231,518 km^2 is **within 1 standard deviation of the long-term mean**. Seasonal sea ice extent has implications, for example, to the cold pool, spring bloom strength and timing, and bottom-up productivity.
- * Summer bottom temperatures and spatial extent of the **cold pool were average** based on the ROMS hindcast model (see Physical Environment Synthesis 69).
- The acoustic survey that provides estimates of **euphausiid density** occurs biennially in even years. **Look for an update in 2021** based on saildrone acoustic information collected in summer 2020 that was not yet available for this Report.
- The biomass of **motile epifauna** sampled during the 2019 bottom trawl survey remained above the long-term mean. Trends in motile epifauna biomass **indicate benthic productivity**, although individual species and/or taxa may reflect varying time scales of productivity.
- The biomass of **benthic foragers** remained low in 2019 and was largely due to yellowfin sole and northern rock sole being below their long-term means. Trends in benthic forager biomass are variable over the time series and **indicate availability of infauna** (i.e., prey of these species).
- The biomass of **pelagic foragers** in 2019 was up from 2018 but remained below the long-term mean. Trends in pelagic forager biomass **indicate availability of forage fish** (i.e., prey to upper trophic levels) as well as **predator abundance** within the ecosystem.
- The biomass of **fish apex predators** remained at the long-term mean in 2019. Trends in apex predator biomass reflect relative **predation pressure on zooplankton and juvenile fishes**.

- The **multivariate seabird breeding index** indicated that seabirds bred earlier and had better reproductive success in 2019 compared to recent very poor years. Reproductive success and/or early breeding are assumed to be mediated through food supply, therefore above-average values indicate better than average recruitment of year classes that seabirds feed on (e.g., age-0 pollock), or better than average supply of forage fish that commercially-fished species feed on (e.g., capelin eaten by both seabirds and Pacific cod).
- **Northern fur seal pup production** at St. Paul Island in 2018 **continued a declining trend since 1998** that may be partially attributed to low pup growth rates.
- Seafloor **habitat disturbance due to fishing gear** (pelagic and non-pelagic trawl, longline, and pot) as of December 2018 showed interactions have remained **below the long-term average** since 2011. Fishing gear can affect habitat used by a fish species for the processes of spawning, breeding, feeding, or growth to maturity.

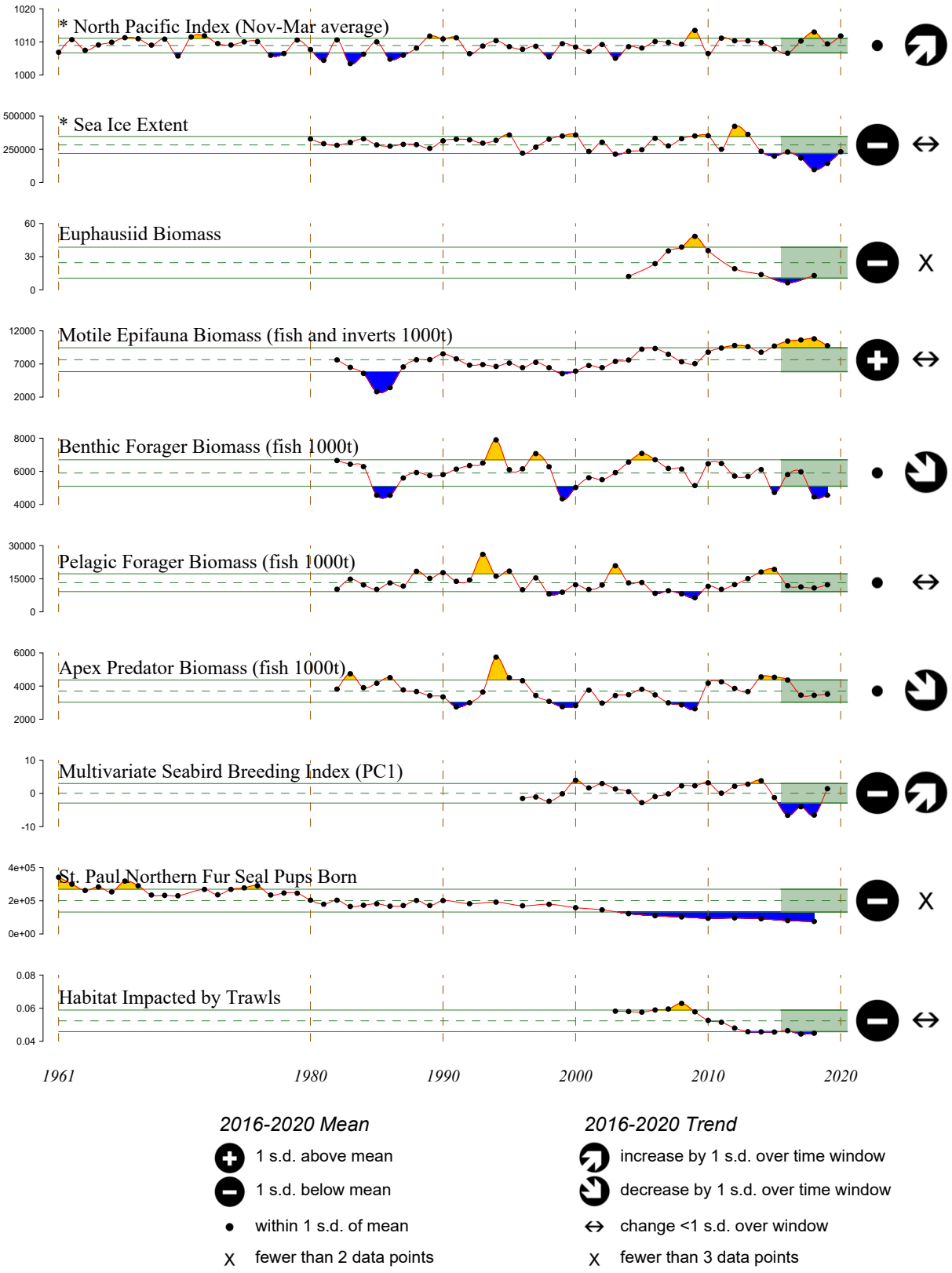

Figure 1: Eastern Bering Sea ecosystem assessment indicators; see text for descriptions.
* indicates time series updated in 2020.

Ecosystem Assessment

Elizabeth Siddon
Auke Bay Laboratories, Alaska Fisheries Science Center, NOAA Fisheries
Contact: elizabeth.siddon@noaa.gov

Last updated: November 2020

Introduction

The primary intent of this assessment is to summarize and synthesize climate and fishing effects (historical and future) on the eastern Bering Sea shelf and slope regions from an ecosystem perspective. The Ecosystem Status Reports of the Groundfish Stock Assessment and Fishery Evaluations (SAFE) provide the historical perspective of status and trends of ecosystem components and ecosystem-level attributes using an indicator approach. For the purposes of management, this information must be synthesized to provide a coherent view of the ecosystem effects to clearly recommend precautionary thresholds, if any, required to protect ecosystem integrity. The eventual goal of the synthesis is to provide succinct indicators of current ecosystem conditions and a prognosis of how fish stocks are expected to fare, given concurrent information on ecosystem status. To perform this synthesis, a blend of data analysis and modeling is required annually to assess current ecosystem status in the context of historical and future climate conditions.

Complete Recap of the 2019 Ecosystem State

Some ecosystem indicators are updated to the current year (2020), while others can only be updated to the previous year (or earlier) due to the nature of the data collected, sample processing, or modeling efforts. Therefore, some of the "new" updates in each Ecosystem Status Report reflect information from the previous year(s). Below is a complete summary of 2019 that includes information from both previous and current indicators. The next section (Current Conditions: 2020) provides a summary of the 2020 ecosystem state based on indicators updated this year.

The eastern Bering Sea experienced the second year with little winter sea ice (winter 2018/2019) and reduced cold pool extent (summer 2019), prompting the expression of a 'double whammy' for ecosystem impacts. A Noteworthy contribution to the 2020 ESR identifies thresholds of marine heatwave conditions for the southeastern and northern Bering Sea (p. 42). The threshold has

been been persistently exceeded in both the southeastern and northern Bering Sea for much of the last five years, but is particularly evident during winters 2017/2018 and 2018/2019 in the northern Bering Sea. The observed ecosystem conditions in 2019 are discussed below in terms of (i) reflecting 2018 conditions, (ii) reflecting 2019 conditions, and (iii) reflecting cumulative impacts of continued warm conditions from winter 2017/2018 through summer 2019.

Reflective of 2018 conditions:
Ecosystem responses that may reflect 2018 conditions include the gray whale Unusual Mortality Event (UME) and the short-tailed shearwater die-off event. Lagged (delayed) impacts of poor feeding conditions experienced during 2018 are hypothesized to at least partially explain the mortality events. Both species feed in the Bering Sea during summer; gray whales are benthic feeders (e.g., amphipods) while shearwaters are planktivorous (e.g., euphausiids). Both species embark on long migrations to the southern hemisphere for breeding during the austral summer. Therefore, the 2019 mortality events may reflect 2018 feeding conditions in the Bering Sea, conditions experienced during the breeding season in the southern hemisphere, or lack of available prey to complete the migration back to the Bering Sea in 2019. Seabird bycatch rates are influenced, in part, by prey supply and a link exists between poor ocean conditions and peak bycatch years. The numbers of seabirds estimated to be caught incidentally in the eastern Bering Sea fisheries in 2019 increased 49% from 2018 largely attributed to the shearwater mortality event that occurred throughout Alaska in 2019.

The gray whale UME has continued in 2020; gray whale strandings remained elevated, but at slightly lower numbers than in 2019 (p. 48). The continuation of the UME indicates insufficient benthic productivity over the feeding grounds of the northern Bering Sea and Chukchi Sea. Conversely, the magnitude of short-tailed shearwater mortalities was far lower in 2020. Shearwaters consume euphausiids, along with larvae and small fish, therefore they are indicators of feeding conditions for planktivorous groundfish species. It seems possible that prey availability (i.e., zooplankton and ichthyoplankton) in the upper water column improved from winter 2019/2020 through summer 2020.

Reflective of 2019 conditions:
It is important to remember that the 2018/2019 winter sea ice accumulation differed from winter 2017/2018. While residual heat delayed freeze up until mid-December (similar to 2017/2018), accumulation approached the long-term mean sea ice extent through January 2019 (whereas 2018 sea ice never approached normal levels) before southerly winds persisted during February and reduced sea ice (similar timing between years). The impact and subsequent ecosystem effects of early 2019 sea ice formation are not fully understood, although it is hypothesized the small, retracted cold pool (i.e., thermal barrier) may have contributed to the increased biomass of pollock over the southern shelf in 2019.

The spring bloom fuels secondary production of the zooplankton prey community that forms the base of energy transfer for upper trophic levels (e.g., fish, seabirds, mammals). Chlorophyll-a concentrations in 2019 reached the long-term mean (baseline 2003–2020) over the northern shelf and Bering Strait while concentrations over the southern shelf remained below the long-term mean (p. 74), indicating higher potential for energy transfer through the food web in the northern Bering Sea in 2019 but lower energy transfer in the southeastern Bering Sea. The timing of the peak spring bloom in 2019, estimated from satellite data, was about a week earlier than the long term average and earlier than 2018. In 2019, the zooplankton community was dominated by small copepods, which is typical of warm-year conditions over the shelf, while large copepod and euphausiid abundance was low. Warm temperatures increase copepod secondary production rates;

combined with an earlier bloom, this may have resulted in sustained production and energy transfer into summer 2019. However, larger, lipid-rich copepods and euphausiids remained low across the shelf and could have affected energy storage and survival of juvenile fish within the region. Jellyfish, which are pelagic consumers of zooplankton and small fishes, showed a sharp increase in abundance in the 2019 bottom trawl survey from 2018 yet the catch of jellyfish in groundfish fisheries in 2019 was the 3rd lowest since 2011 and was about half the catch in 2018.

At the Pribilof Islands, reproductive success of several seabird species improved in 2019, indicating that birds (especially fish-eating species) were able to find sufficient food resources to support reproductive efforts during 2019. Successful breeding events occurred for murres at St. George, red-faced cormorants at St. Paul, and both species of kittiwakes at both islands. Successful foraging by these fish-eating seabirds is further corroborated by the below-average coccolithophore bloom index for 2019 and the high abundance of age-0 pollock collected in the northern Bering Sea surface trawl survey. For planktivorous species, including least and crested auklets, which feed primarily on copepods and euphausiids, oceanographic surveys showed the zooplankton community dominated by small copepods.

Unprecedented warmth in the inner domain during summer 2019 likely resulted in increased metabolic demands and may have impacted fish distributions. For example, the increased warmth may have pushed Pacific cod away from warm inshore waters and made them more available to the bottom trawl survey (L. Britt, pers comm), contributing to the large increase in abundance of young fish in 2019. Based on thermal conditions experienced between late summer 2019 and the following spring 2020, the 2019 pollock year class is predicted to have below-average recruitment to age-4 in 2023. In Bristol Bay, sockeye salmon returns remained high. The large inshore run in 2019 suggests these stocks experienced positive conditions at entry into the eastern Bering Sea in the summers of 2016 and 2017, and winters of 2016/2017 and 2017/2018.

Reflective of cumulative impacts:
The method used to calculate groundfish condition was revised for the 2020 ESR (p. 96) and updated time series through 2019 resulted in changes compared to last year's condition indicator. An upward trend was still evident for most species over the southern shelf relative to 2017–2018. Residuals were positive relative to historical averages for pollock (>250 mm), northern rock sole, yellowfin sole, arrowtooth flounder, and Alaska plaice, suggesting a possible shift to a benthic-dominated system. Residuals were near historical averages for age 1–2 pollock (100–250 mm), Pacific cod, and flathead sole. In the northern Bering Sea, a separate length-weight regression was calculated using this year's method. Positive residuals were observed in 2019 for pollock (>250mm), Pacific cod, yellowfin sole, and Alaska plaice while residuals for pollock (100–250 mm) were neutral.

The 2018 pollock year class showed strong overwinter survival to age-1. However, several mechanistic relationships based on bottom-up pathways predicted below-average recruitment success for the 2018 year class. The occurrence of strong recruitment in light of low sea ice, above-average water temperatures, and poor prey quality/quantity challenges our current understanding of recruitment processes for pollock. One hypothesis stems from the anomalous February winds from the southwest. Winds brought warm, moist air from the south over the shelf, but may have also increased on-shelf flow and upwelling conditions. Upwelling of productivity during winter may have subsidized energy transfer and contributed to increased survival of age-0 pollock. In combination with greater overwinter survival, the 2018 year class may have experienced reduced predation pressure from cannibalism because recruitment of recent year classes has been low. Pollock age-1 natural mortality peaked in 2016, but has declined in recent years and the 2019 estimate was at

the long-term mean, also demonstrating reduced predation pressure for the 2018 year class.

The declaration of an Unusual Mortality Event for ice seals reflects cumulative impacts of conditions in 2018 and 2019. The increased mortality of seals and the apparent decline in pup condition demonstrate immediate and delayed impacts of the loss of sea ice habitat for pupping and nursing in both years. They could also demonstrate broader ecosystem effects, such as competition for prey from northward shifts of fish populations. At the Pribilof Islands, community members reported unusually high numbers of male fur seals overwintering at St. Paul (i.e., they never left from the 2018 season). Overwintering may have occurred due to good feeding conditions or lack of sufficient energy stores for migrations, potentially reflective of the continuous warmth throughout the year.

Groundfish Community Indicators:
The total CPUE of fish and invertebrates sampled in the eastern Bering Sea bottom trawl survey declined between 2014–2018, but increased again in 2019 (p. 122) likely reflecting the 75% increase in pollock biomass. Both the latitudinal and depth distribution of the demersal community on the eastern Bering Sea shelf show strong directional trends over the last four decades, with significant shifts to the north and into shallower waters (p. 125). The mean lifespan of the demersal fish community (including pollock) in 2019 was 30.2 years, and is the second highest in the time series (p. 130). The stability of groundfish biomass increased dramatically in 2019 to the highest of the time series (p. 133).

Fishing and Human Dimensions Indicators:
Landings in the eastern Bering Sea remained stable through 2019, predominantly driven by trends in pollock which saw increased prices in 2018 and 2019. Landings of Pacific cod, driven by TAC levels, dropped in 2019, but were off-set by landings increases in flatfish and rockfish. First-wholesale value, a more comprehensive measure of value to the fishing industry, fell in 2018–2019 as Pacific cod landings decreased and the average price of sablefish declined.

The unemployment rate in southeastern Bering Sea communities decreased to 2.7% in 2019 and have been consistently lower than State and national rates. The population increased 0.58%, yet 47% of communities within the region experienced population decline. School enrollment rates for schools under 20 students appears to have stabilized after 2017.

The unemployment rate in northern Bering Sea communities decreased to 11.5% in 2019, but have been consistently higher than State and national rates. The population increased 6.1% with 74.8% of communities experiencing population increase. Northern Bering Sea school district enrollment rates are generally stable, yet most districts have graduation rates that are well below state graduation averages.

Current Conditions: 2020

Overview
Following two years of physical oceanographic perturbations, the eastern Bering Sea experienced a return to near-normal climatic conditions in 2020. The winters of 2017/2018 and 2018/2019 had unprecedentedly low sea ice and reduced spatial extent of the cold pool, removing the thermal barrier between the southern and northern Bering Sea shelves. Distributional shifts in groundfish stocks were observed (e.g., more than 50% of the overall biomass of Pacific cod biomass occurred

in the northern Bering Sea in 2018). Ecosystem impacts in response to these conditions include changes in overall productivity and the potential for new trophic pathways. Considerable cooling during winter 2019/2020 allowed for rapid build-up of sea ice, exceeding median ice extent in parts of February and March 2020. However, ice thickness was low, and retreated quickly in spring. This ephemeral ice was sufficient to form a cold pool of average spatial extent, but above-average sea surface temperatures returned in spring and remained above average through summer 2020. The southeastern and northern Bering Sea are experiencing a persistent warm stanza, greater in both magnitude and duration than that of the early 2000s.

Data and Information Mitigation Strategies

During 2020, the vast majority of NOAA Fisheries surveys were canceled in the eastern and northern Bering Sea due to COVID-19 travel restrictions. This was an on-year for the biennial NOAA ecosystem and acoustics surveys, in addition to annual trawl surveys, therefore numerous contributions of ecosystem information for this Report were unable to be updated this year. While gaps exist throughout the Report (e.g., forage fish), NOAA scientists, state/university partners, tribal governments, and coastal community members provided new and innovative contributions to inform our understanding of the current ecosystem state.

The Bering 10K Regional Ocean Modeling System (ROMS) hindcast simulation provided critical information of bottom water conditions over the Bering Sea shelf in 2020. First, the evolution of modeled bottom temperatures between November of the previous year through the beginning of August placed 2020 in historical context as an 'average' year in terms of $<2^{o}$C and $<0^{o}$C waters in the standard bottom trawl survey area and spatial extent of the cold pool. Second, a new indicator of ocean acidification, based on Ωarag undersaturation, estimates the percent of the Bering Sea shelf where bottom waters are corrosive. This operationalizing of the ROMS model has great potential for the Ecosystem Status Report (ESR) as well as groundfish and crab Ecosystem and Socioeconomic Profiles (ESPs).

Satellite-derived indicators were developed this year to better describe and understand oceanographic conditions. Sea surface temperature is a foundational metric; new analyses presented in 2020 may help to identify mechanisms or critical periods through which SST has the greatest impacts on Bering Sea ecosystem and fisheries. As an example, the accumulation of SST throughout the year provides a better understanding of the annual thermal exposure experienced by the system. Marine heatwave thresholds were defined and demonstrate that recent heatwaves have been persistent and intense. Heatwaves occurred during early years of the time series, but the frequency and durations have increased dramatically, especially in the northern Bering Sea, where residual heat and low sea ice extent resulted in dramatically increased cumulative annual thermal exposure.

The 2020 Eastern Bering Sea ESR includes the Integrated Seabird Information section and the Physical Environment Synthesis, both intended to incorporate information from a variety of knowledge sources and provide comprehensive overviews and implications for fisheries management. In fact, the U.S. Fish and Wildlife Service was unable to conduct seabird research in the eastern and northern Bering Sea in 2020 due to COVID-19 travel restrictions. Coastal community members, tribal governments, and state/university partners provided all information on seabird dynamics for this Report and the U.S. Fish and Wildlife biologists helped to synthesize this information and provide implications.

Bridging Across Gaps

Due to survey limitations in 2020, the contributions received ranged from basin-scale, satellite-

derived indicators to local-scale community observations. The mesoscale patterns gleaned from comprehensive shelf-wide surveys were absent. Trophic gaps in information occurred, as well. For example, for 2020, no indicators from zooplankton to adult fish were available. The interpretation of the current ecosystem state bridges across these gaps and hinges on existing understanding of mechanistic relationships and dynamics in the eastern Bering Sea.

The Defining Role of Sea Ice

Tracking the seasonal progression and retreat of sea ice over the shelf highlights the interactive roles of water temperature (i.e., residual warmth in the system) and winds. Late arrival of sea ice is more and more common with a strong negative linear trend of early ice (Oct–Dec) over the past 40 years. Delayed freeze-up leads to shortened ice seasons that has impacts on ice thickness, ice algae, and thermal modulation as well as impacts to transportation and subsistence activities. After two years of little to no sea ice over the Bering Sea shelf, the near-normal ice extent observed in 2020 appeared to have only minimal mitigating effects on the warmth in the upper water column (i.e., sea surface temperatures), but did result in an 'average' cold pool extent. This vertical stratification of the water column is more typical of shelf conditions and affects predator/prey dynamics.

Chlorophyll-a concentrations were lower in 2020 than 2019 in all regions except the southern outer domain. Chl-a concentrations over the southern inner and middle shelves have been below average since 2016. In the northern Bering Sea, the concentrations over the inner and middle shelves were below average and the outer shelf was low and continued a decreasing trend since 2014. Primary producers provide fundamental energy and nutrients for zooplankton grazers and higher trophic level species; these trends indicate lower energy transfer to support the food web over the southern and northern Bering Sea shelves in 2020. The timing of the peak spring bloom in 2020 was earlier than the long-term average; for the southern inner and middle shelves it occurred about a week earlier. This contrasts with 2018 which was among the latest while 2017 was among the earliest spring blooms. The coccolithophore bloom index was below average in 2018 and 2019 but increased, particularly on the middle shelf, in 2020. Coccolithophores may be a less desirable food source for microzooplankton in this region and smaller coccolithophores result in longer trophic chains. The striking milky aquamarine color of the water during a coccolithophore bloom can also reduce foraging success for visual predators. Combined, these indicators of primary production suggest limited and/or poor quality of the prey base to support trophic energy transfer (e.g., juvenile fish, seabirds) in 2020.

The 2020 Togiak herring population is predominantly comprised of age-6 and age-7 fish (the 2013 and 2014 year classes). The 2014 year class remains the largest estimated recruitment since 1982. Oceanographic conditions over the southeastern Bering Sea shelf transitioned from below-average (i.e., cold) in 2013 to above-average (i.e., warm) in 2014 and neither year experienced temperatures that exceeded the marine heatwave threshold. While the recruitment of age-4 fish to the spawning population in 2018 was still the largest estimated recruitment since 1982, the magnitude of that recruit class was estimated in the 2020-forecast model to be lower than was previously estimated. 2018 was above-average (i.e., warm) with little cooling effect from sea ice and just over 200 days that exceeded the marine heatwave threshold.

Preliminary data from ADF&G for 2020 commercial salmon harvests indicate that statewide total harvests are below the preseason forecast but nearing the 2018 total harvest (as of 22 Sept 2020). The 2020 Bristol Bay salmon inshore run was the 5th largest on record and 74.5% higher than the 1963–2019 average. The current period of high Bristol Bay sockeye salmon production now exceeds the previous high production stanza that occurred 1989–1995. A projected decrease in the

number of pink salmon in 2020 could have a positive impact on fish-eating seabirds (i.e., less prey competition).

In 2020, at the Pribilof Islands, seabird attendance appeared similar to recent years while breeding observations suggest that it was an average, to slightly below average, year for most fish-eating species (e.g., kittiwakes, murres). Planktivorous species (i.e., auklets) have been declining in recent years and continued to be low in 2020, at least for St. Paul Island. Warmer water temperatures from 2014–2019 seem to have negatively affected least auklets, and likely parakeet auklets, as evidenced by declines in reproductive success and colony attendance. In the northern Bering Sea, on St. Lawrence Island, reproductive success and colony attendance differed among fish-eating and planktivorous seabirds suggesting foraging impacts across trophic levels. In the Bering Strait region, emaciation and starvation were observed in some individuals throughout the summer and beach-cast carcasses of several species of seabirds were observed on the eastern and western sides of the Bering Strait.

Direct and indirect indicators of groundfish recruitment success provide information on the status of recent year classes. The 2020 springtime drift pattern was mixed, indicating larvae (e.g., pollock) may have be retained over the southern middle shelf. Lower primary production in this region may limit the prey base to support trophic energy transfer to large, lipid-rich copepod taxa (i.e., *Calanus* spp.). The 2019 pollock year class experienced unfavorable temperature conditions from age-0 to age-1 and is predicted to have below-average recruitment to age-4 in 2023. Concurrently, low abundance of large copepods during late-summer in 2017–2019 indicate poor overwinter survival and recruitment to age-3 in 2020–2022. Recent years of low recruitment for pollock have resulted in lower rates of cannibalism. The climate-enhanced multispecies model (CEATTLE) estimates of age-1 predation mortality for pollock is at the long-term mean as declines in total predator biomass are contributing to reduced predation rates and mortality.

Executive Summary of Recent Trends in the Eastern Bering Sea

This section provides highlights and links to full contributions contained in this Report. The links are organized within four sections: Noteworthy, Physical Environment Trends, Ecosystem Trends, and Fishing and Human Dimensions Trends.

Noteworthy

- The vast majority of surveys and field research in the eastern Bering Sea were not conducted during 2020 due to COVID-19 travel restrictions. This year's Report is therefore absent contributions that rely on samples and data collected during those field efforts. While some gaps have been filled through new contributions, other gaps remain throughout the Report.
- In response to COVID-19, Alaska Governor Mike Dunleavy declared a state of emergency on 11 March 2020. Subsequent travel mandates impacted fishing and processing businesses, although considered "essential businesses", in order to maintain safe working environments for employees and minimize spread to local communities (p. 29).
- The incidental catch of herring in the 2020 directed pollock fishery was unusual because it occurred during a period of relatively high nominal CPUE values for pollock fishing and was highest in the winter pollock A season. Several hypotheses pertaining to changes in the herring or pollock populations or ecosystem-driven changes could explain the high PSC catch in 2020 (p. 30).
- An increase in marine debris has been reported in Bering Strait communities from July through October 2020. The debris was predominantly foreign in manufacture, with identifiable Russian and Korean writing, and adds to existing concerns in the Bering Strait region regarding food security and economic impacts with an increase in large scale commercial fishing/processing activities and other industrial vessel traffic (p. 36).
- A new indicator of ocean acidification conditions based on aragonite saturation states suggests that seasonal bottom water corrosive conditions peaked in 2013 and have slowly improved since. Modeled conditions from ROMS hindcast for summer 2020 indicate a more strongly corrosive outer shelf domain compared to the 2003–2019 average (p. 39).
- New metrics of sea surface temperature provide added detail and enable exploration of mechanisms or critical periods of thermal exposure over the eastern Bering Sea shelf. The threshold for a marine heatwave has been been persistently exceeded in both the southeastern and northern Bering Sea for much of the last five years (p. 42).
- Since January of 2019, elevated numbers of eastern North Pacific gray whale mortalities have occurred along the west coast of North America, stretching from Mexico to Alaska. In May of 2019, an Unusual Mortality Event (UME) was declared. In 2020, gray whale strandings remained elevated, but at slightly lower numbers than in 2019 (p. 48).

Physical Environment Trends

- Following two years of physical oceanographic perturbations, the eastern Bering Sea experienced a return to near-normal climatic conditions in 2020 (p. 51).
- Residual warmth delayed sea ice formation until late 2019. Considerable cooling then allowed for rapid build-up of sea ice, even exceeding median ice extent in parts of February and March 2020. However, ice thickness was low, and retreated quickly in spring (p. 54).
- Early season sea ice extent shows a strong negative linear trend during the past 40 years (p. 54).
- Annual sea ice extent showed a steep decline from 2012 (highest ice extent on record) to 2018 (lowest ice extent on record). The 2019–2020 mean extent was within 1 standard deviation of the long-term mean (p. 54).
- Winters 2017/2018 and 2018/2019 were among 5 years with the strongest south winds, which contributed to low sea ice extent. South winds also drive on-shelf and cross-shelf advection. Winter 2019/2020 had wind speed direction near the long-term average (p. 57).
- A relatively high sea level pressure anomaly in the central and eastern North Pacific in spring (Mar-May) of 2020 brought anomalous winds from the south over the eastern and northern Bering Sea and contributed to rapid sea ice retreat (p. 57).
- The 2020 springtime (1 Apr–30 Jun) drift pattern was mixed, with an early period of eastward drift followed by a period of westward drift (p. 57).
- Late winter 2019 sea surface temperatures were closer to the long-term mean, reaching -1.8°C in the NBS denoting ice cover. Above-average temperatures returned in spring over the southeastern and northern Bering Sea and remained above average through 25 October 2020, similar to those observed in 2019 (p. 61).
- The southeastern and northern Bering Sea are experiencing a persistent warm stanza, greater in both magnitude and duration than that of the early 2000s (p. 61).
- Water temperatures collected from St. Paul Island indicate 2020 was relatively cool compared to 2014–2020 and cooling of the water column continued into March 2020. Chlorophyll-a measurements did not detect the spring bloom until May 2020 (p. 61).
- Seasonal projections of SST from the National Multi-Model Ensemble (NMME) indicate positive anomalies for the entire Bering Sea and north of Bering Strait through the end of 2020. However, a reduction in magnitude of the positive anomalies is forecast through April 2021 (p. 61).
- Summer bottom temperatures and spatial extent of the cold pool were average based on the ROMS hindcast model and observations from the 2020 *Oscar Dyson* cruise (p. 69).
- The vertical structure of the water column over the shelf was typical in 2020, with a warm surface layer, colder bottom layer, and a sharp interface (p. 69).

Ecosystem Trends

- Chlorophyll-a concentrations over the southern inner and middle shelves have been below average since 2016. The southern outer region had above-average values in 2020. In the northern Bering Sea, the concentrations over the inner and middle shelves were below average and the outer shelf was low and continued a decreasing trend since 2014 (p. 74).
- The timing of the peak spring bloom in 2020 was earlier than the long-term average; for the southern inner and middle shelves it occurred about a week earlier. This contrasts with 2018 which was among the latest while 2017 was among the earliest spring blooms (p. 74).
- The coccolithophore bloom index was below average in 2018 and 2019 but increased, particularly on the middle shelf, in 2020 (p. 79).
- Time series of zooplankton abundance from spring (1996–2019) and late-summer (1998–2019) surveys over the southern Bering Sea shelf indicate large copepod abundances are more variable, especially during late-summer, small copepods show less interannual variability in spring or late-summer, and euphausiid abundances were higher and more variable in spring compared to late-summer. Time series from late-summer (2002–2019) surveys over the northern Bering Sea show large copepod abundances are lower than over the southern shelf, small copepods showed little interannual variability, and euphausiid abundances were very low overall and trends did not appear to correspond to 'warm' or 'cold' periods (p. 82).
- The Togiak herring forecast for 2020 is 215,826 short tons. The 2020 population is predominantly age-6 and age-7 fish (the 2013 and 2014 year classes). The 2014 year class remains the largest estimated recruitment since 1982 (p. 87).
- Commercial harvest of salmon in the Bering Sea varied across regions in 2019. Chinook salmon abundance was low in the Yukon area with no commercial fishing season and harvests in Bristol Bay were 23% below average. Coho abundance in the Yukon area resulted in the 4th highest catch on record while harvests in Bristol Bay were below average. Chum salmon harvest in Norton Sound was low, but was above average in Bristol Bay (p. 90).
- The 2020 Bristol Bay salmon inshore run of 58.2 million sockeye is the 5th largest on record since 1963 and 74.5% higher than the 1963–2019 average. Inshore run sizes in 2015–2020 all exceeding 50 million salmon; the current period of high Bristol Bay sockeye salmon production now exceeds the previous high production stanza of 1989–1995 (p. 92).
- The diet of large (60cm+) Pacific cod consists of fish, crustaceans, and other large invertebrates. Over the southeast shelf, pollock were the dominant prey in most years, but were extremely low from 2008–2012 and were replaced with a mix of *Chionoecetes* spp. and flatfish. Over the northwest shelf, pollock were dominant except for short periods (e.g., 2016–2019 *Chionoecetes* spp. and octopus increased). In the northern Bering Sea, *Chionoecetes* spp. (primarily snow crab) were the largest portion of cod diet, except in 2010 when flatfish and forage fish were the main prey items (p. 94).
- The positive trend in groundfish condition observed over the last 2–3 years in the eastern and northern bottom trawl surveys (i.e., increasingly positive length-weight residuals) could be related to concurrent trends in other ecosystem covariates. *Note: The method used to calculate groundfish condition was updated in 2020 (through 2019 survey data) and further revisions to the indicator are planned for 2021* (p. 96).
- The climate-enhanced multispecies model (CEATTLE) estimates of age-1 predation mortality for all three species (walleye pollock, Pacific cod, arrowtooth flounder) continue to decline from the recent 2016 peak mortality. Age-1 predation mortality for pollock is at the long-term mean, while age-1 Pacific cod and arrowtooth flounder mortality rates have declined relative to past years and remain below the long-term mean (p. 103).
- The temperature change index predicts survival and recruitment of juvenile pollock. Based on thermal conditions experienced between late summer and the following spring, the 2016 and 2019 year classes are predicted to have below-average recruitment to age-4 in 2020 and 2023 (p. 108).

- The abundance of large copepods during late-summer is correlated with recruitment to age-3 pollock; low abundance of large copepods during late-summer 2017 and 2018 indicate poor overwinter survival and recruitment to age-3 in 2020 and 2021 (p. 109).
- At the Pribilof Islands, seabird attendance in 2020 appeared similar to recent years. Least auklet attendance at the colonies and abundance in the waters around the island has declined in recent years. St. George Island reported that birds returned at the usual time and in typical abundance with good colony attendance throughout the summer 2020. In the Bering Strait region, emaciation and starvation were observed and beach-cast carcasses were reported on the eastern and western sides of the Bering Strait in 2020.
- Total CPUE of fish and invertebrates in the eastern Bering Sea bottom trawl survey shows an increasing trend. The highest observed value occurred in 2014 and total CPUE declined thereafter with a sharp drop between 2017 and 2018. Total CPUE increased again in 2019 (p. 122).
- Species richness and diversity in the eastern Bering Sea bottom trawl survey have varied from 1982 to 2019. The average number of species increased from 1995 to 2004, remained relatively high through 2011, and then both richness and diversity decreased through 2014, followed by a return to relatively high levels with an unusually high Shannon diversity observed in 2018 (p. 123).
- Both the latitudinal and depth distribution of the demersal community on the eastern Bering Sea shelf show strong directional trends over the last four decades, with significant shifts to the north and into shallower waters (p. 125).
- The mean lifespan of the southeastern Bering Sea demersal fish community (including pollock, the dominant species by biomass) in 2019 was 30.2 years, and is the second highest in the time series. This is up from 27.6 years in 2018 and above the long-term mean of 28.2 years (p. 130). Excluding pollock, the mean lifespan is slightly less, although patterns and trends are similar. The exception was 1985 when the mean lifespan was 32.0 with pollock included and 32.9 without pollock (p. 130).
- The mean length of the southeastern Bering Sea demersal fish community (including pollock) in 2019 was 37.2 cm, which is only slightly less than the 2018 peak value of 37.6cm. Excluding pollock, the 2018 peaked reached 38.0 cm and dropped to 34.4 cm in 2019 (p. 131).
- The stability of groundfish biomass within the southeastern Bering Sea demersal fish community (including pollock) increased dramatically in 2019 to the highest of the time series. Excluding pollock, the time series shows a steady upward trend to the peak value in 2019 (p. 133).
- Results from shellfish and phytoplankton monitoring showed a consistent presence of harmful algal blooms (HABs) throughout the Gulf of Alaska and Aleutian Islands in 2020; results from samples collected in the northern Bering Sea are still pending (p. 136).

Fishing and Human Dimensions Trends

- Through week 36 of 2020, discard biomass across the entire EBS is consistent with the 2015–2019 period for the trawl non-pollock sector. Trawl pollock sector discards to date in 2020 are trending slightly higher than the 2015–2019 period, while fixed gear discards are trending lower. This contribution includes FMP targeted groundfish species only and does not include PSC species (e.g., halibut, herring, crab, salmon) or other non-target ecosystem component species (e.g., forage fish) (p. 139).
- The catch of jellyfish in groundfish fisheries in 2019 was the 3rd lowest since 2011 and was about half the catch in 2018. The catch of structural epifauna has been relatively steady from 2011 to 2019. The catch of assorted invertebrates (e.g., seastars) increased 23% from 2018 to 2019 (p. 142).
- The numbers of seabirds estimated to be caught incidentally in the eastern Bering Sea fisheries in 2019 increased 49% from 2018 and was above the 2010– 2018 average. Northern fulmars, shearwaters, and gulls were the most common species or species groups caught incidentally in 2019 that could be identified (p. 145).
- As of June 30, 2020, no BSAI groundfish stock or stock complex is subject to overfishing, is known to be overfished, or known to be approaching an overfished condition. The decrease in overall Fish Stock Sustainability Index (FSSI) score from 2019 to 2020 is the net result of changes in the stocks included in the FSSI plus a loss of one point for the biomass of Norton Sound red king crab decreasing to below 80% of B_{MSY} (p. 152).
- Landings in the eastern Bering Sea remained stable through 2019. Landings are predominantly from the pelagic forager group dominated by pollock. Trends in the apex predator group are driven by TAC levels in Pacific cod which dropped in 2019 but were off-set by increases in flatfish and rockfish (p. 157).
- In 2018 and 2019 prices for pollock increased. First-wholesale value fell in 2018–2019 in the apex predator group as Pacific cod landings decreased and the average price of sablefish declined (p. 159).
- The unemployment rate in southeastern Bering Sea communities decreased to 2.7% in 2019; the peak unemployment of 3.6% occurred in 2014. Unemployment rates in this region have been consistently lower than State and national rates. The unemployment rate in northern Bering Sea communities decreased to 11.5% in 2019, but have been consistently higher than State and national rates (p. 164).
- Between 2010–2019, the population in the southeastern Bering Sea increased 0.58%, which was lower than State trends (2.9%), yet 47% of communities within the region experienced population decline. The population in the northern Bering Sea increased 6.06% with 74.8% of communities experiencing population increase (p. 169).
- In the southeastern Bering Sea, school enrollment rates for schools under 20 students appears to have stabilized after 2017. Northern Bering Sea school district enrollment rates are generally stable. Alaska's average graduation rates have been 75.6% (2015), 76.1% (2016), and 78.2% (2017); most NBS districts have graduation rates that are well below state graduation averages (p. 175).

Contents

† indicates new contribution
* indicates contribution updated with 2020 data

List of Tables

List of Figures

Ecosystem Indicators

Description of the Report Card Indicators

1. The North Pacific Index (NPI) (Nov–Mar average): The NPI was selected as the single most appropriate index for characterizing the climate forcing of the Bering Sea. The NPI is a measure of the strength of the Aleutian Low, specifically the area-weighted sea level pressure (SLP) for the region of 30° to 65°N, 160°E to 140°W (Trenberth and Hurrell, 1994). A lower NPI indicates a stronger Aleutian low.

The advantageous aspects of the NPI include its systematic relationship to the primary causes of climate variability in the Northern Hemisphere, especially the El Niño-Southern Oscillation (ENSO) phenomenon, and to a lesser extent the Arctic Oscillation (AO). It may also respond to North Pacific SST and high-latitude snow and ice cover anomalies, but it is difficult to separate cause and effect.

The NPI also has some drawbacks: (1) it is relevant mostly to the atmospheric forcing in winter, (2) it relates mainly to the strength of the Aleutian Low rather than its position, which has also been shown to be important to the seasonal weather of the Bering Sea (Rodionov et al., 2007), and (3) it is more appropriate for the North Pacific basin as a whole than for a specific region (i.e., Bering Sea shelf).

Implications: to the Bering Sea are that the strength of the Aleutian Low relates to wintertime temperatures, with a deeper low (lower SLP values) associated with a greater preponderance of maritime air masses and hence warmer conditions.

Contact: Muyin.Wang@noaa.gov

2. Bering Sea Ice Extent: The Bering Sea ice year is defined as 1 August–31 July. Bering Sea ice extent data is from the National Snow and Ice Center's Sea Ice Index, version 3 (Fetterer et al., 2017), and uses the Sea Ice Index definition of the Bering Sea, effectively south of the line from Cape Prince of Wales to East Cape, Russia. The daily mean annual ice extent integrates the full ice season into a single value. *Implications:* Seasonal sea ice coverage impacts, for example, the extent of the cold pool, bloom strength and timing, and bottom-up productivity.

Contact: rthoman@alaska.edu

3. Euphausiid Biomass: Macrozooplankton are intermediaries in the transfer of carbon from primary production to living marine resources (commercial fisheries and protected species). Understanding the mechanisms that control secondary production is an obvious goal toward building better ecosystem syntheses. In the absence of direct measurements of secondary production in the eastern Bering Sea, we rely on estimates of biomass. We use an estimate of euphausiid biomass as determined from acoustic data collected during the biennial eastern Bering Sea summer acoustic-trawl survey. *Implications:* Euphausiids are food for many species of both ecological and commercial importance in the eastern Bering Sea, including walleye pollock.

Contact: Patrick.Ressler@noaa.gov

4., 5., 6., 7. Description of the Fish and Invertebrate Biomass Indices: We present four guilds to indicate the status and trends for fish and invertebrates in the eastern Bering Sea: motile epifauna, benthic foragers, pelagic foragers, and apex predators. Each is described in detail below. The full guild analysis involved aggregating all eastern Bering Sea species included in a food web model (Aydin and Mueter, 2007) into 18 guilds by trophic role, habitat, and physiological status (Table 1). For each guild, time trends of biomass are presented for 1977–2019. Eastern Bering Sea biomass trends are summed stock assessment model estimates or scaled survey data (from the eastern Bering Sea summer bottom trawl survey), where available, for each species within the guild. If neither time series is available, the species is assumed to have a constant biomass equal to the mid-1990s mass balance level estimated in Aydin and Mueter (2007). Catch data were taken directly from the Catch Accounting System and/or stock assessments for historical reconstructions.

Contact: Kerim.Aydin@noaa.gov or Andy.Whitehouse@noaa.gov

4. Motile Epifauna (fish and benthic invertebrates): This guild includes both commercial and non-commercial crabs, sea stars, snails, octopuses, and other mobile benthic invertebrates. Information is based on summer bottom trawl survey data. There are ten commercial crab stocks in the current Fishery Management Plan for Bering Sea/Aleutian Islands King and Tanner Crabs; we include seven on the eastern Bering Sea shelf: two red king crab *Paralithodes camtschaticus* (Bristol Bay, Pribilof Islands), two blue king crab *P. platypus* (Pribilof District and St. Matthew Island), one golden king crab *Lithodes aequispinus* (Pribilof Islands), and two Tanner crab stocks (southern Tanner crab *Chionoecetes bairdi* and snow crab *C. opilio*). The three dominant species comprising the eelpout group are marbled eelpout (*Lycodes raridens*), wattled eelpout (*L. palearis*), and shortfin eelpout (*L. brevipes*). The composition of seastars in shelf trawl catches are dominated by the purple-orange seastar (*Asterias amurensis*), which is found primarily in the inner/middle shelf regions, and the common mud star (*Ctenodiscus crispatus*), which is primarily an inhabitant of the outer shelf. Stock assessments for crabs have not been included to date, but could be in the future. *Implications:* Trends in the biomass of motile epifauna indicate benthic productivity and/or predation pressure, although individual species and/or taxa may reflect shorter or longer time scales of integrated impacts of bottom-up or top-down control.

5. Benthic Foragers (fish only): The species which comprise the benthic foragers group are the Bering Sea shelf flatfish species, juvenile arrowtooth flounder (*Atheresthes stomias*), and the sculpins. The major species of this group are surveyed annually and have abundances estimated by statistical models, therefore our confidence in their time-trend of abundance is high. *Implications:* Trends in the biomass of benthic foragers indicate availability of infauna (i.e., prey of these species).

6. Pelagic Foragers (fish and squid only): This guild includes adult and juvenile Walleye pollock (*Gadus chalcogrammus*), other forage fish such as Pacific herring (*Clupea pallasi*), Capelin (*Mallotus villosus*), Eulachon (*Thaleichthys pacificus*), and Sandlance, pelagic rockfish, salmon, and squid. Information quality ranges from a sophisticated highly quantitative stock assessment for pollock (the biomass dominant in the guild) through relatively high variance eastern Bering Sea shelf survey data for forage fish, to no time series data for salmon and squid. *Implications:* Trends in the biomass of pelagic foragers largely track Walleye pollock which is an important component of the Bering Sea ecosystem, both as forage and as a predator.

Table 1: Composition of foraging guilds in the eastern Bering Sea.

Motile Epifauna	Benthic Foragers	Pelagic Foragers	Fish Apex Predators
Eelpouts	P. cod (juv)	W. pollock (juv)	P. cod
Octopuses	Arrowtooth (juv)	W. pollock	Arrowtooth
Tanner crab	P. halibut (juv)	P. herring (juv)	Kamchatka fl. (juv)
King crab	Yellowfin sole (juv)	P. herring	Kamchatka fl.
Snow crab	Yellowfin sole	Gr. turbot (juv)	P. halibut
Sea stars	Flathead sole (juv)	Sablefish (juv)	Alaska skate
Brittle stars	Flathead sole	P. ocean perch	Large sculpins
Other echinoderms	N. rock sole (juv)	Sharpchin rockfish	
Snails	N. rock sole	Northern rockfish	
Hermit crabs	Alaska plaice	Dusky rockfish	
Misc. crabs	Dover sole	Other Sebastes	
	Rex sole	Atka mackerel (juv)	
	Misc. flatfish	Atka mackerel	
	Shortraker rockfish	Misc. fish shallow	
	Thornyhead rockfish	Squids	
	Greenlings	Salmon returning	
	Other sculpins	Salmon outgoing	
		Bathylagidae	
		Myctophidae	
		Capelin	
		Eulachon	
		Sandlance	
		Other pelagic smelts	
		Other managed forage	
		Scyphozoid jellies	

7. Apex Predators (shelf fish only): This guild includes Pacific cod (*Gadus macrocephalus*), arrowtooth flounder, Kamchatka flounder (*Atheresthes evermanni*), Pacific halibut (*Hippoglossus stenolepis*), Alaska skate, and large sculpins. Pacific cod and arrowtooth flounder time series are from stock assessments, and the remaining time series are from the annual eastern Bering Sea shelf summer bottom trawl survey. *Implications:* Trends in the biomass of apex predators indicate relative predation pressure on zooplankton and juvenile fishes within the ecosystem.

8. Multivariate Seabird Breeding Index: This index represents the dominant trend among 17 reproductive seabird data sets from the Pribilof Islands that include diving and surface-foraging seabirds. The trend of the leading principal component (PC1) represents all seabird hatch timing and the reproductive success of murres and cormorants. *Implications:* Above-average index values reflect high reproductive success and/or early breeding (assumed to be mediated through food supply) and indicate better than average recruitment of year classes that seabirds feed on (e.g., age-0 pollock), or better than average supply of forage fish that commercially-fished species feed on (e.g., capelin eaten by both seabirds and Pacific cod).

Contact: Stephani.Zador@noaa.gov

9. St. Paul Northern Fur Seal Pup Production: Pup production on St. Paul Island was chosen as an index for pinnipeds on the eastern Bering Sea shelf because the foraging ranges of females that breed on this island are largely on the shelf, as opposed to St. George Island which, to a greater extent, overlap with deep waters of the Basin and slope. Bogoslof Island females forage almost exclusively in pelagic habitats of the Basin and Bering Canyon and, as such, would not reflect foraging conditions on the shelf. *Implications:* Pup production reflects foraging conditions over the eastern Bering Sea shelf with above-average values indicating good foraging conditions.

Contact: Rod.Towell@noaa.gov

10. Habitat Impacted by Trawls: Fishing gear can affect habitat used by a fish species for the processes of spawning, breeding, feeding, or growth to maturity. This new indicator uses output from the Fishing Effects (FE) model to estimate the habitat reduction of geological and biological features over the Bering Sea domain, utilizing spatially-explicit VMS data. The indicator more accurately reflects an estimate of time that gear is in contact with the substrate; disturbance is assumed cumulative over the year, therefore the December value is plotted here. *Implications:* An estimate of the area of seafloor disturbed by trawl gear provides an indication of habitat disturbance.

Contact: John.V.Olson@noaa.gov

Noteworthy (formerly Hot Topics)

Here we present items that are new or noteworthy and of potential interest to fisheries managers.

COVID-19 Pandemic Impacts to the Fisheries Sector in Alaska

Alaska Governor Mike Dunleavy declared a state of emergency on 11 March 2020 and the first confirmed case occurred on 12 March 2020. Restaurants, bars, breweries, and food trucks all closed beginning on 18 March 2020, which may have limited some amount of seafood sales in some communities. However, the large scale and global nature of Alaska fisheries means that restaurant closures throughout the lower 48 and globally are more likely to impact Alaska seafood sales. The Governor announced on 23 March 2020 that "All people arriving in Alaska, whether resident, worker or visitor, are required to self-quarantine for 14 days and monitor for illness. Arriving residents and workers in self-quarantine, should work from home, unless you support critical infrastructure (see Attachment A)." Fishing and processing businesses are included in Attachment A as "essential businesses", which allowed many fishing operations to continue in 2020, albeit at a substantial cost to the harvesting and processing industries in Alaska to maintain a safe working environment for their employees and minimize spread to local community residents. More information on the actions of the State of Alaska in response to this crisis can be found on the State of Alaska webpage for COVID-19 Health Mandates[1].

Industry has reported that they have spent over $50 million[2] to reduce the risk of COVID-19 transmission among harvesters, processors, and the local communities while still providing important seafood for the U.S. and international markets, as well as providing food security for many Alaskans. The seafood industry has been fairly successful in Alaska limiting virus spread, but they had to deal with a substantial reduction in transportation options in many Western Alaska and Aleutian Islands communities and limited ability to switch crews throughout the fishing seasons to date. The NMFS Alaska Regional Office has been instrumental in devising solutions with industry to allow the continuation of fishing operations and limit the need for fisheries closures which would otherwise lead to vessel downtime and higher crew turnover increasing the risk of COVID-19 transmission.

Given this unprecedented disruption in the fishing industry in 2020, AFSC has developed a series of in-season ex-vessel revenue estimates for 2020 to provide the North Pacific Fishery Management Council, industry, and the public with more near real-time economic information for the annual groundfish harvest specifications process for 2021. This information is titled "Groundfish and Halibut In-season Ex-Vessel Revenue Estimates for 2020" and is included as Section 6 of the Groundfish Economic SAFE.

Contributed by Stephen Kasperski (NOAA/AFSC)

[1] https://covid19.alaska.gov/health-mandates/

[2] https://www.alaskaseafood.org/covid-19-impact-reports/

Incidental Catch of Herring in Groundfish Fisheries Increased in 2020

Background

Pacific herring are identified as Prohibited Species Catch (PSC) in the BSAI Groundfish Fisheries Management Plan. Herring PSC is incidentally caught primarily in the directed pollock fishery; the pollock fleet also actively avoids bycatch of all PSC species, with Chinook and chum salmon avoidance of highest priority. By regulation, herring PSC may not be retained and must be discarded at sea.

The PSC limit for BSAI groundfish fisheries is set at 1% of the forecasted eastern Bering Sea (EBS) herring biomass established by the State of Alaska. The PSC limit is further apportioned to fisheries categories recommended by the Council and published by NMFS in the harvest specifications. The forecast of EBS herring mature biomass is submitted to the NPFMC annually by the Alaska Department of Fish and Game (ADF&G; Figure 2, black line; also see p. 87). If the herring PSC limit is exceeded, seasonal herring savings areas may be closed to directed fishing for that fishery category (Figure 3). These time and area closures were established in 1991 during a decline in the herring population. The Winter Herring Savings Area has been closed twice, first for directed fishing for pollock with trawl gear in October 2012 and a second time in 2020. Summer Herring Savings Area I was closed to directed fishing for pollock in 2020, however a temporary rule opened directed pollock fishing for the shoreside, mothership, and CDQ sectors within Summer Herring Savings Area II in 2020.

The incidental catch of herring in the 2020 directed pollock fishery was unusual because it occurred during a period of relatively high nominal CPUE values for pollock fishing and also was highest in the winter fishing A season (in nearly all years, herring PSC is higher in summer B season; Figure 4). Pollock fishing masters noted that the herring were lower in the water column during the day (exhibiting a diurnal feeding pattern) and difficult to tell apart from pollock on the fish finder. Based on observer data, there appeared to be two modes in the size distribution of the herring PSC (150g and 400g). Due to the size disparity among herring stocks in the EBS (i.e., Togiak herring are generally larger at age than EBS herring stocks north of Togiak) it is unknown what age-classes make up these size groups.

Hypotheses Explaining Increased Herring Catch

Several hypotheses pertaining to changes in the herring or pollock populations could explain the high PSC catch in 2020, including: (i) increase in herring abundance through strong recruitment of recent year classes and an underestimate of the 2020 forecasted herring abundance from the stock assessment model, (ii) change in herring migration timing and/or route leading to overlap with pollock earlier in the year (during pollock A season), (iii) change in herring distribution apart from the spawning migration, either spatially over the shelf or vertically in the water column (captains observed herring occupying the near bottom waters during daylight hours in 2020 but typically herring are visible higher in the water column on echosounders); this could be due to availability of prey resources.

In addition to population dynamics, ecosystem-driven changes may have led to greater overlap between herring and pollock in 2020. Shifts in species distributions in response to temperature or sea ice extent have been documented, and species distributions may have been especially influenced given the unprecedented low levels of sea ice in the Bering Sea over winters 2017/2018 and 2018/2019. However, during winter 2019/2020, sea ice was fairly extensive over the shelf, including in the Gulf of Anadyr. It is possible that following two years of unprecedented low levels of sea ice, the near-normal extent of sea ice 'pushed' adult pollock and herring over a smaller portion of the southern EBS shelf and increased overlap between the species. In addition, such physical oceanographic perturbations may have altered prey distributions for either herring or pollock, resulting in greater overlap in 2020.

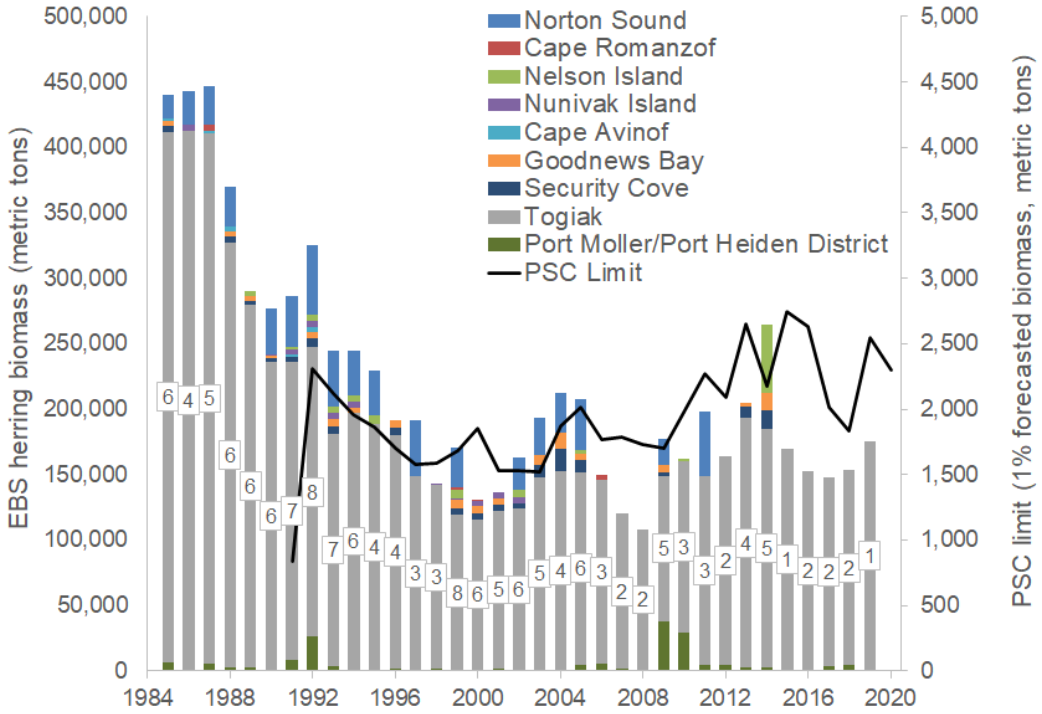

Figure 2: Biomass (t) of forecast (single year forecast for PSC management) and hindcast (from survey or catch-at-age assessment model estimates) eastern Bering Sea herring stocks (left axis). Stacked bars (left axis) indicate hindcast biomass of individual stocks from south to north with data labels showing the number of stocks with estimates out of nine stocks in each respective year. Line indicates forecasted biomass (t; left axis) and prohibited species catch (PSC) limit (t; right axis). PSC limit is set at 1% of forecast biomass of nine combined EBS stocks.

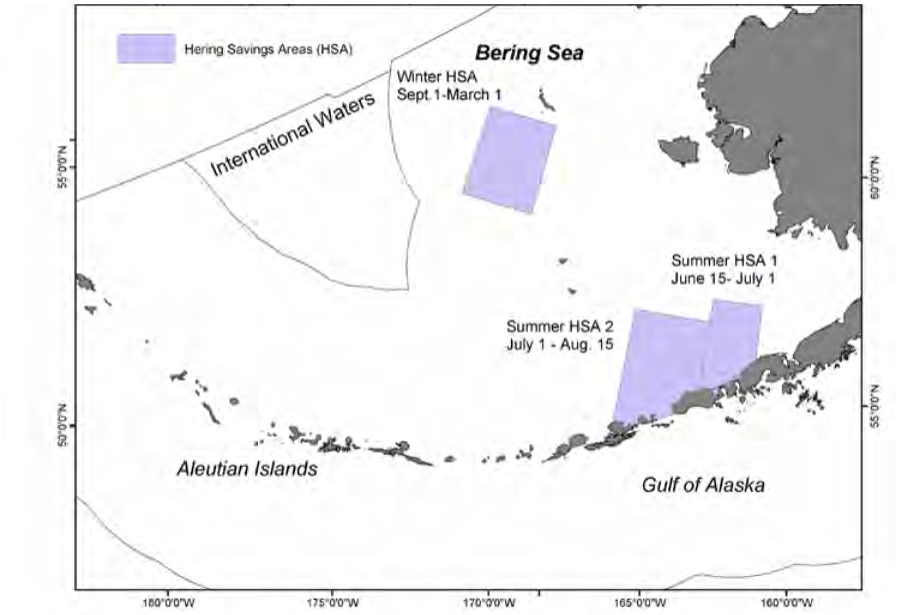

Figure 3: Herring Savings Areas in the eastern Bering Sea. Time of closures are denoted next to each area closure.

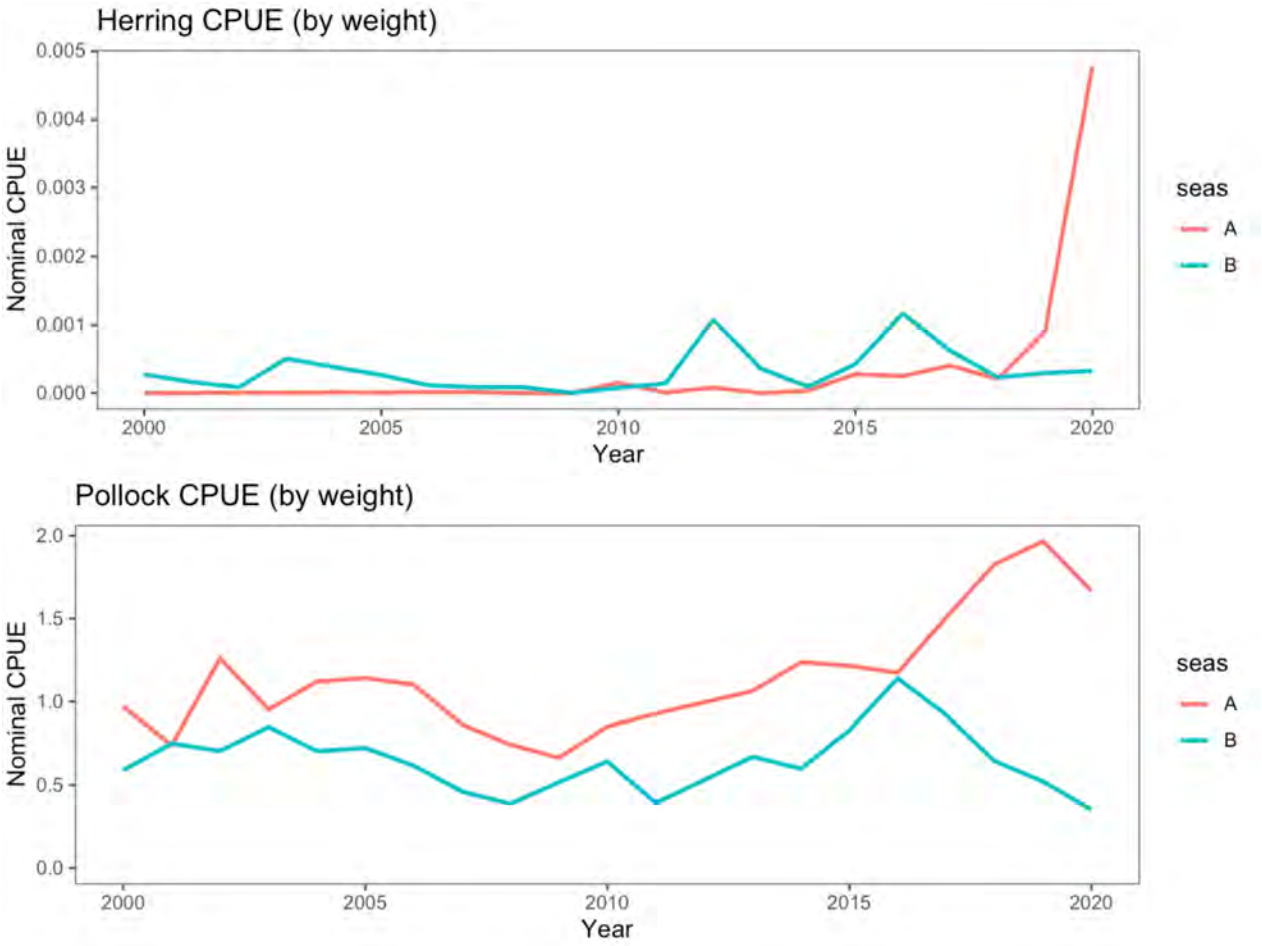

Figure 4: Herring PSC by season (upper panel) compared to pollock catch per time spent fishing (lower panel).

The distribution of fishing effort in time and space by the pollock fleet changes in response to the distribution of pollock (i.e., following the fish), in response to high PSC catch (e.g., to avoid Chinook bycatch), and in response to a myriad of other regulations including spatio-temporal catch limits of pollock within the Steller Sea Lion (SSL) Conservation Area (SCA). By regulation, only 62% of the A season pollock allocations may be harvested inside the SCA prior to 1 April. The A season pollock fishing traditionally begins in the Unimak Pass area up to Amak Island along the Alaska peninsula and then follows the 50 fathom curve up towards the Pribilofs following the spawn timing of pollock and also as SCA catch limits are reached and vessels are forced to move northwest due to SSL regulations.

It appears unlikely that a change in the pollock fishing distribution is the cause of increased herring catch in 2020. The A season pollock fishery spatial distribution (fishery footprint) has been remarkably consistent over the long time series and 2020 exhibited no departure from the historical fishing effort of the pollock fleet (Figure 5). There is significant overlap between the spatial distribution of bycatch of herring in the 2020 A season and the pollock fishery footprint in all historical years. If herring had been present at the levels seen in 2020 in recent years, it is expected that the pollock fleet would have encountered them. In addition, the distribution of herring, as sampled by the pollock fleet over the last nine years, indicates that herring have been caught in similar locations as those seen in 2020. However, it is difficult to tell whether the distribution of herring has changed over time due to the low herring PSC in the pollock A season prior

to 2020 (Figure 6). Fishery-independent observations of herring and pollock from 2020 are not available at this time; however, pollock fishermen conclude the increased bycatch was not due to a change in spatial or temporal overlap between pollock and herring, but due to an increased abundance of herring on the grounds.

Conclusions and Future Research

We conclude by highlighting several areas of research that could help inform the above hypotheses and further our understanding of herring population dynamics in the EBS, including:

1. Stock identification of individual spawning stocks (e.g., genomic sequencing, otolith shape analysis);
2. Investigate mixing of herring stocks outside of the spawning season, once stock identification methods have been established, to determine if PSC is likely to have a disproportionate impact on any individual stocks;
3. Herring age composition (surveys and bycatch);
4. Spawning herring age composition by stock throughout the entire spawning event (current sampling for herring in the Togiak District of Bristol Bay is restricted to the early portion of the spawning period when the directed commercial sac roe fishery occurs and other EBS herring stocks are not currently sampled for age composition);
5. Estimates of maturity for EBS herring;
6. Re-evaluation of herring spawning migration by stock;
7. Re-evaluation of Herring Savings Areas (HSAs) with respect to their effectiveness for protecting herring or exploration of other ways of reducing herring PSC; and
8. Juvenile life history dynamics.

Contributed by Elizabeth Siddon and Jim Ianelli (NOAA/AFSC)
and Sherri Dressel (ADF&G)

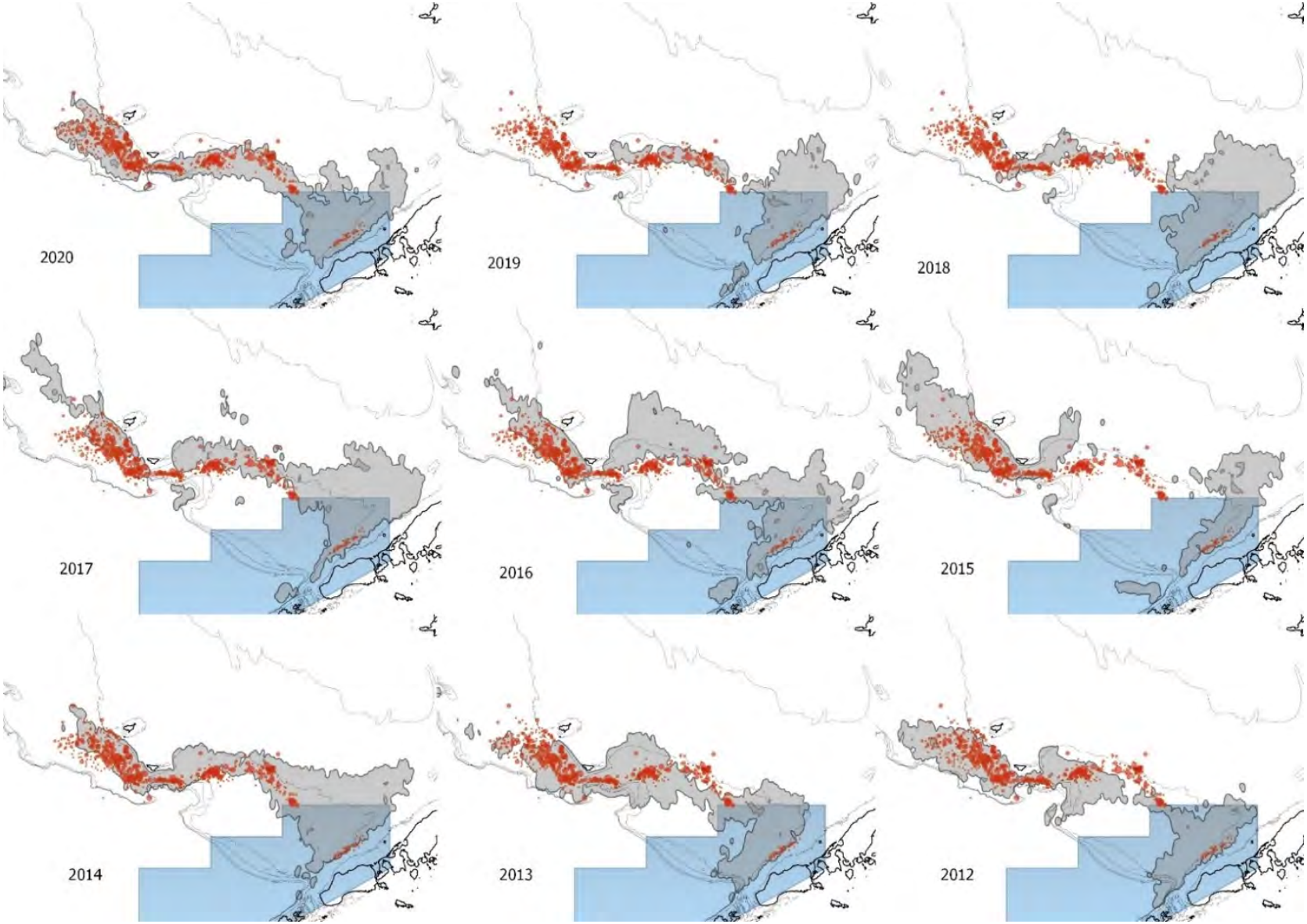

Figure 5: Pollock A season fishing footprint in 2012–2020 overlaid with 2020 herring bycatch. Size of the circles is related to the amount of herring bycatch in the hauls. Figure provided by SeaState, Inc.

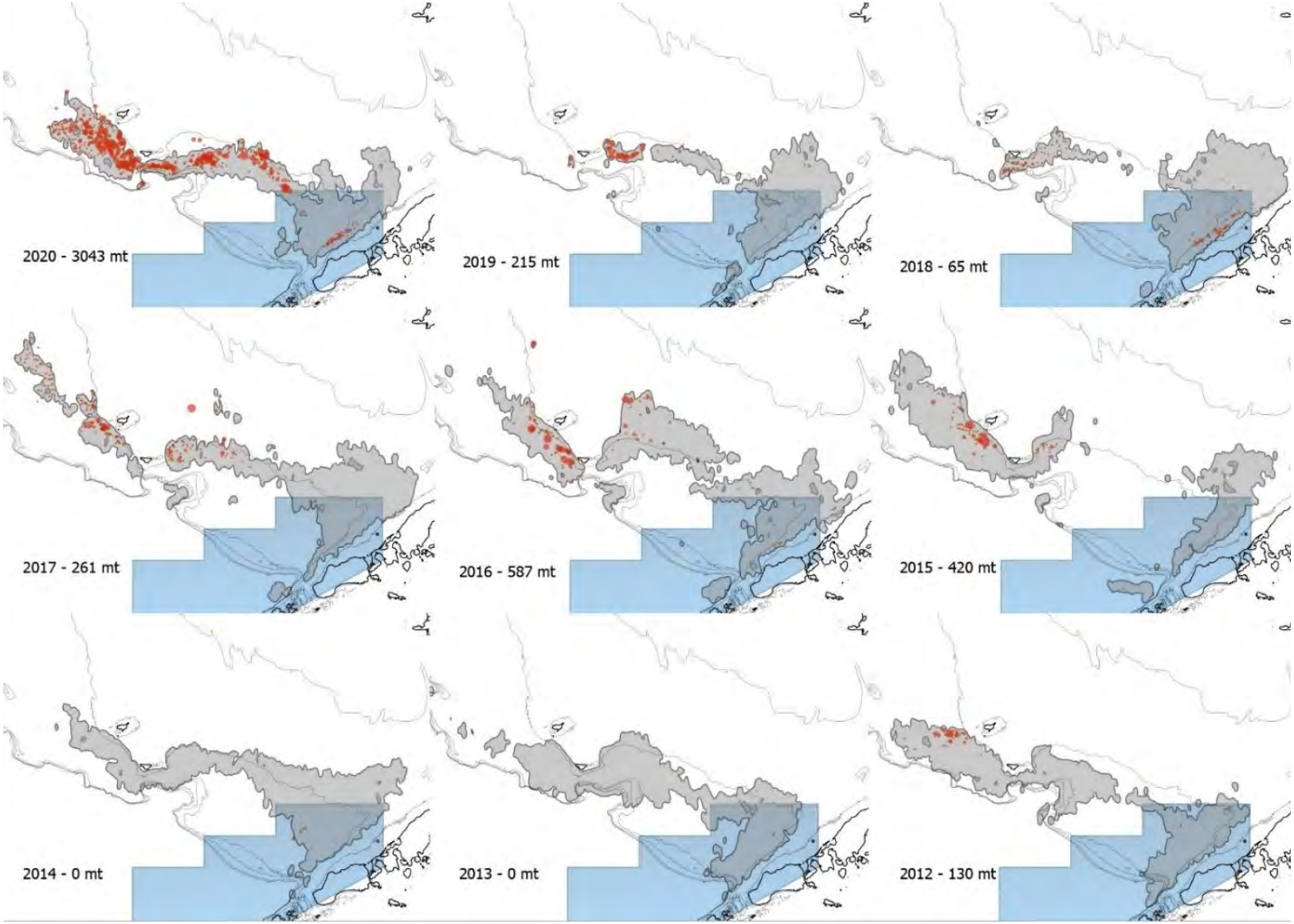

Figure 6: Pollock A season fishing footprint in 2012–2020 overlaid with associated herring bycatch. Size of the circles is related to the amount of herring bycatch in the hauls, and the scale (size of circle vs herring size) in all years is the same as that established for 2020. Hauls with <100kg of herring were omitted as hauls with trace amounts of herring can be very numerous (>1000) but have not summed to more than 32t of herring in this dataset. Figure provided by SeaState, Inc.

Bering Strait Debris Event

Debris Event

Starting in the last few days of July 2020, communities in the Bering Strait region began reporting a notably increased amount of marine debris, with volumes and types of debris well outside the baseline "normal" debris typically observed. The debris was predominantly foreign in manufacture, with Russian and Korean being readily identifiable by reporting parties and reviewers (Figure 7).

Initial sightings of the debris began on the north shore of St. Lawrence Island on July 27th, with reports of bags, debris, and floating food items outside of Savoonga, followed by reports on July 30th near Gambell. Also on July 30th, a large number of varied plastic containers (beverage bottles, cleaners, chemicals, etc.) were reported outside of Nome, followed by additional reports of similar debris ranging from eastern Norton Sound into the Bering Strait. In the following days and weeks, reports of sightings expanded northward to communities on the southern Chukchi Sea. Reports continued into October, though in diminishing concentrations, with generally fewer items being reported per area. Later reports also included relatively fresh debris, which could indicate recirculation of the initial debris or a further debris loss/introduction event.

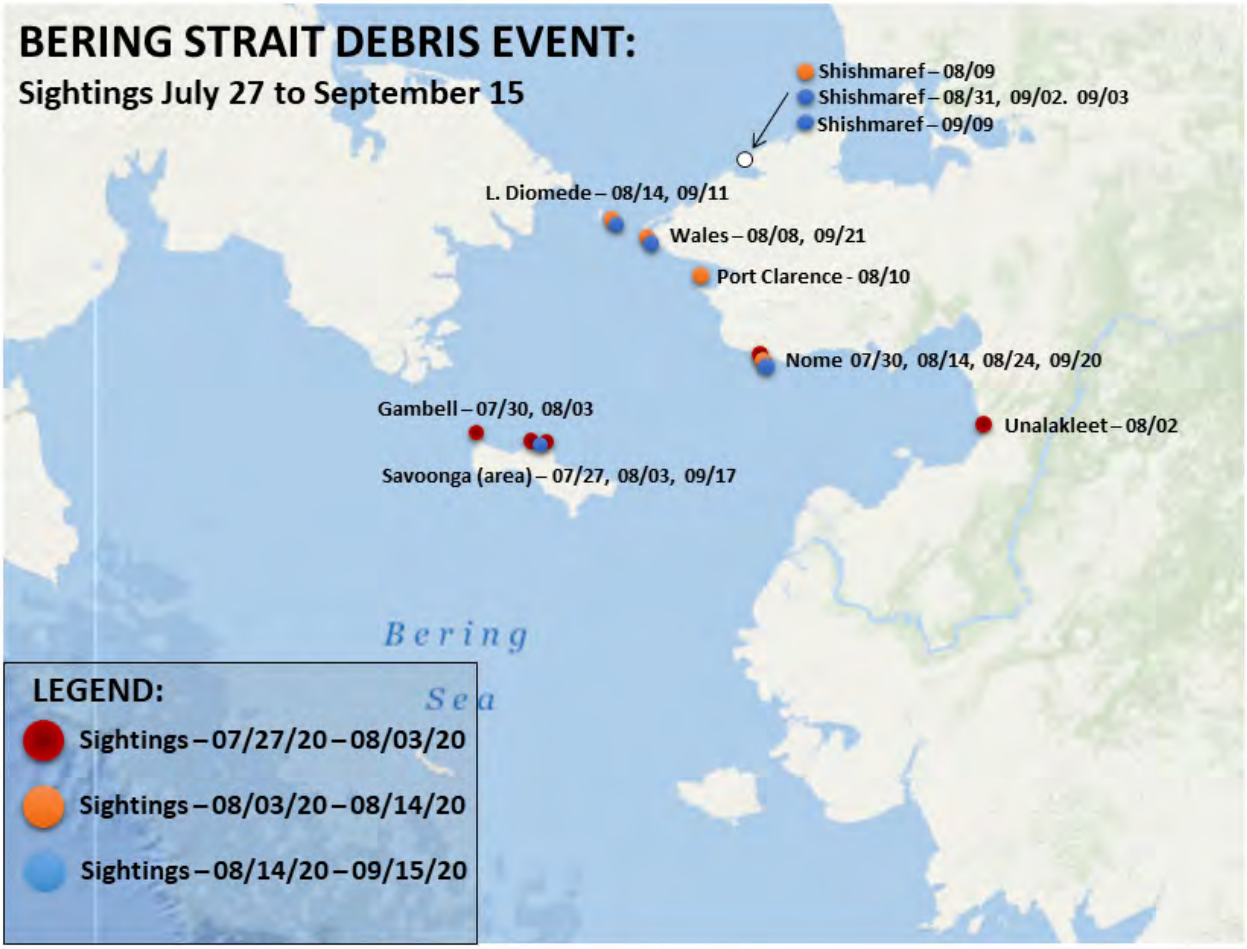

Figure 7: Map showing the location and date of marine debris in the northern Bering Sea and Bering Strait regions.

Debris Types
Debris types varied by location, but the general composition was primarily consumer debris: beverage bottles, food containers, personal product containers, household aerosol cans, chemical cleaners, and cooking oils. Several reports included identified or suspected hazardous material such as lubricating oils and chemical cleaning products. Intermixed with these consumer items were items associated with fishing industry activities. These fishing items included deck boots, primarily orange in color; blue bags that resembled bucket liners used in fishing fleets; and longline equipment with labeling from a Russian fishing firm. The majority of the initially reported debris appeared to have only recently entered the ocean, as many labels were still affixed and clear, the plastic was not degraded, and some items showed dates of manufacture or expiry in 2020. The diverse nature of the debris creates the potential for diverse impacts ranging from entanglements (in line or fishing gear) to ingestion of plastics (both initially or in the future as items degrade).

Possible Sources of Debris
Given this information, the initial assessment of the NOAA Office of Response and Restoration's Marine Debris Program (MDP) and Emergency Response Division (ERD) team was that the debris patterns appeared consistent with a point source debris release, such as accidental loss or intentional dumping from a vessel. This was supported by multiple factors: 1) the debris being of a roughly consistent composition and age, 2) debris appearing in a large amount in a compressed time period, 3) the presence of clearly "new" items, including fresh foods such as fruit and vegetables in some instances, and 4) debris diminishing in concentration with time and space from the initial sightings locations. The debris reported was also different from what is typically observed in the northern Bering Sea and Bering Strait region, which historical categorized removal data indicates generally includes comparatively more fishery-related debris (net, line, floats, banding, etc.). Foreign language consumer items have been a component of debris in the Bering Strait region dating back to the earliest data available, but at lower levels than has been observed during this incident.

Debris Event Context This debris event added to existing concerns in the Bering Strait region regarding food security and economic impacts from increased maritime activity. Potential threats to essential marine resources may be caused by immediate and long term impacts of debris. This event highlights concerns for local community domain awareness and human safety based on the presence and proximity of commercial fishing/processing activities and industrial vessel traffic, which can directly impact local economic and maritime subsistence activities. Potential impacts to marine resources that reside or migrate through the Bering Strait region are diverse and wide-ranging, including debris entanglements, vessel strikes, debris ingestion, and behavioral impacts to feeding or migration patterns and/or timing based on maritime human activity.

Response
Organizations collaborated to establish an ad-hoc task force including federal and state agencies, local debris community organizations, and coastal communities. The goal of this task force is to share information, build common situational awareness, and identify needs and opportunities for direct actions to address this incident. Specific actions have included:

- Hindcast Modeling: In partnership with USCG, NOAA MDP worked to apply NOAA ERD oceanographic modeling tools to evaluate the ability to "hindcast", or retrospectively model, the pathways of debris to identify potential location and timing when it was introduced into the ocean. Initial results indicated that, based on wind and current patterns in late July, the most likely debris pathway would have been from the West and South of St. Lawrence Island, though the likely source area increased significantly with time based on the variability of both debris behavior and conditions.
- Reporting System: The team created a reporting system for community members and included reporting protocols, regional phone contacts, and activated a dedicated email-based reporting account[3]. This information was widely distributed to tribal leadership and the general public throughout the Bering Strait region. Regional coastal responders, whose reporting was critical to raising initial awareness, continued to provide debris sightings through regional organizations such as Alaska Sea Grant and Kawerak, Inc.

[3]Email: incident.debris@noaa.gov

- Support Assessment: NOAA worked with regional partners to identify and scope best structures to deploy support to areas where targeted direct funding could be most helpful and effective to execute immediate removal and disposal, as well as ongoing monitoring to aid in identifying and sourcing future incidents.
- International Engagement: In anticipation of potential international engagement, the Marine Debris Program coordinated with the NOAA Office of International Affairs, USCG, and other international organizations to assess appropriate international government-to-government and industry channels for debris tracing and prevention actions under appropriate authorities and conventions.

Contributed by Peter Murphy
NOAA Marine Debris Program
Office of Response and Restoration
with Gay Sheffield
University of Alaska Fairbanks
Alaska Sea Grant

Ocean Acidification

The oceanic uptake of anthropogenic CO_2 is decreasing ocean pH and carbonate saturation states in a process known as ocean acidification (OA). The cold, carbon rich waters of the Bering Sea are already naturally more corrosive than most other regions of the global ocean, making this region more vulnerable to rapid changes in ocean chemistry. Ship-based sampling has already identified subsurface waters corrosive to aragonite (a soluble form of calcium carbonate used by many marine shell-building organisms), denoted by aragonite saturation states (Ωarag) < 1 (Mathis et al., 2011). The projected areal expansion and shallowing of these waters with continued absorption of anthropogenic CO_2 from the atmosphere poses a direct threat to marine calcifiers and an indirect threat to other species through trophic interactions.

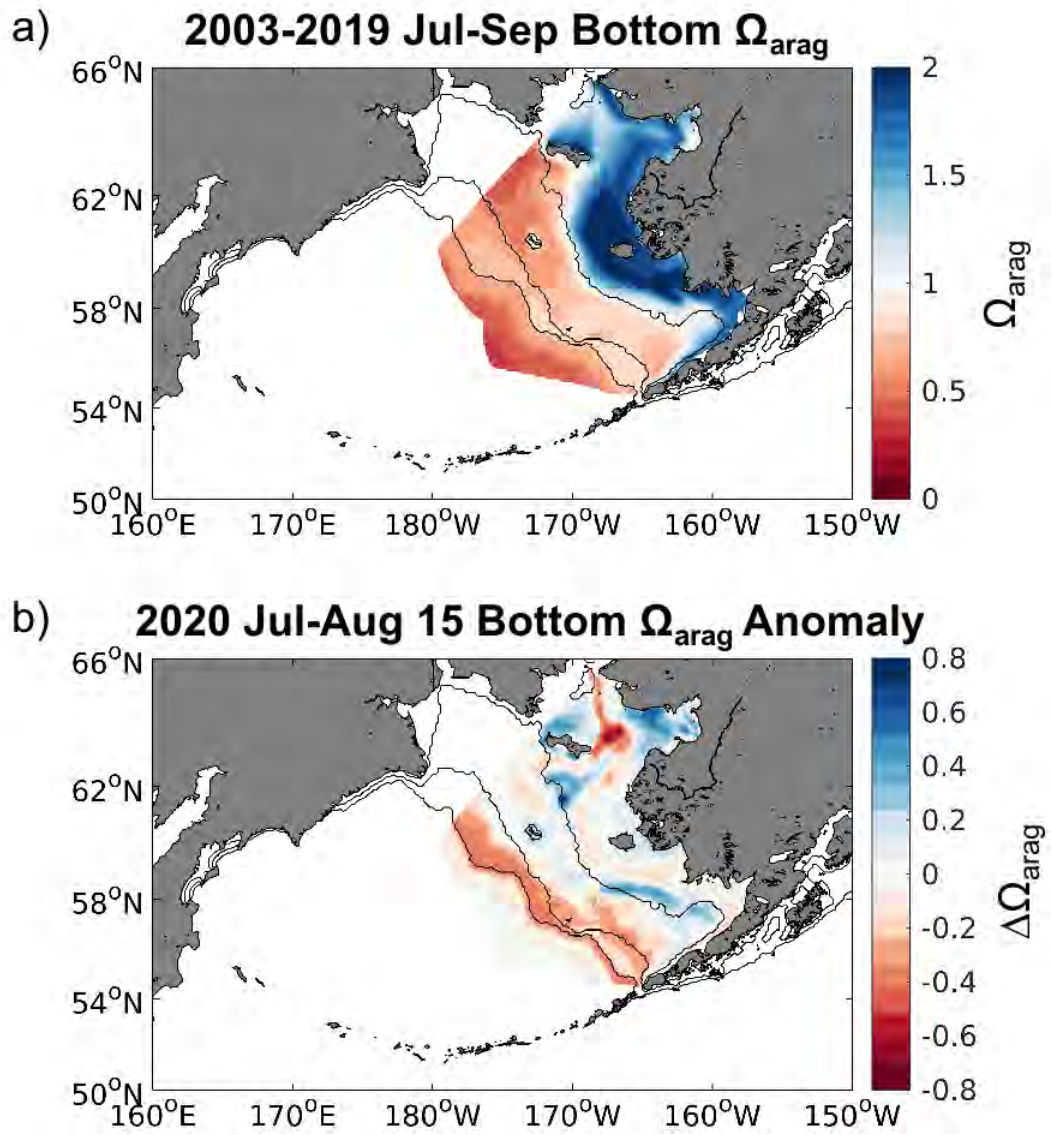

Figure 8: Preliminary spatial map of July–September averaged bottom water Ωarag for the (a) 2003–2019 model hindcast and (b) the 2020 model nowcast (updated through Aug 15th) anomaly compared to the 2003–2019 average. Contour lines denote the 50m, 100m, and 200m isobaths. Regions that are outside of the eastern Bering Sea region are omitted.

These OA risks demonstrate a clear need to track and forecast the spatial extent of acidified waters in the Bering Sea. To this end, we have developed carbonate chemistry for the Bering Sea ROMS NPZ model (Bering 10K; Kearney et al. (2020)), also utilized for reporting bottom water temperature forecasts (see p. 69). Previous work demonstrates model skill in simulating carbonate chemistry variables in hindcast mode (Pilcher et al., 2019). From 2003–2019, the model results illustrate corrosive bottom water Ωarag throughout the middle and outer Bering Sea shelf, but more resilient, buffered conditions within the inner shelf domain in late summer (Figure 8a). Previous work has shown that these corrosive conditions likely result from the bacterial respiration of organic carbon produced by phytoplankton that has sunk below the mixed layer (Mathis et al., 2011, 2014; Cross et al., 2013). Conversely, waters in the inner shelf domain have higher values of Ωarag during July–September because it is more challenging for corrosive conditions to form in shallower, well-ventilated water. Notably, modeled conditions in the summer of 2020 indicate a more strongly corrosive outer shelf domain compared to the 2003–2019 average (Figure 8b).

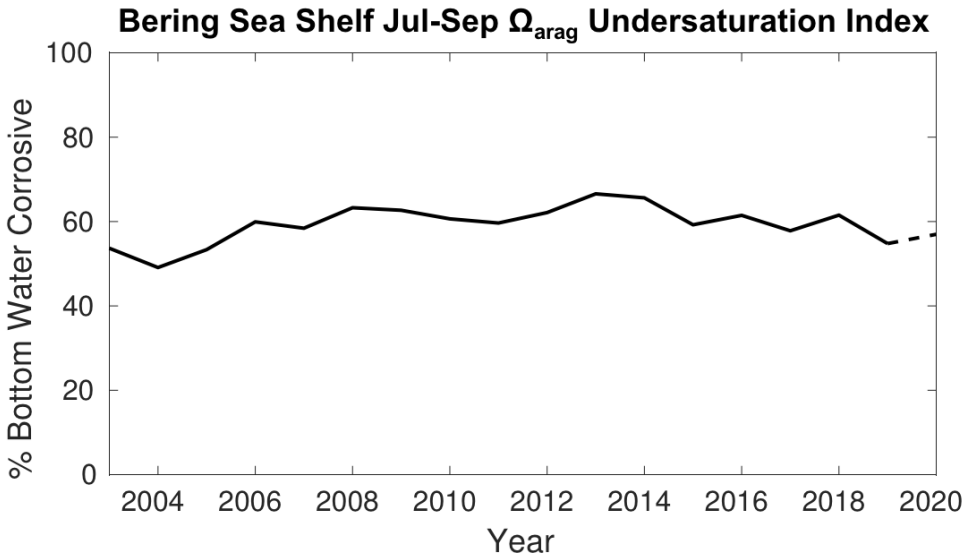

Figure 9: Model time series of the July–September Ωarag undersaturation index. Here, the Ωarag undersaturation index is calculated as the percent of spatial area of the eastern Bering Sea region (Figure 8) where bottom waters have a July–September average Ωarag < 1. The dashed portion at the end represents the incomplete 2020 value, which is run up through August 15^{th}.

In addition to providing updated model hindcasts of carbonate variables each year, our ultimate goal is to develop seasonal forecasts. These forecasts, initialized in spring, will provide a 4–5 month lead-time for corrosive conditions forecasted during the summer field season. The forecasts will be provided annually and compared to observed ship-based data collected every other year to track and improve the accuracy of the forecast. The first iteration of this forecast was planned for 2020, but has been delayed to 2022 by the COVID-19 pandemic. We envision a final product to consist of an annual Ωarag undersaturation index, shown as a time series that illustrates the historical context and forecasted conditions.

There are many possible ways to articulate the severity of ocean acidification across the Bering Sea shelf. The goal is that this index time series, along with the spatial anomaly plot (e.g., Figure 8b) will provide an assessment of the summer water conditions compared to previous years. Our first iteration of this index is calculated as the areal percentage of bottom waters in the eastern Bering Sea region with a July–September average Ωarag value less than 1 (Figure 9). This time series suggests that seasonal bottom water corrosive conditions peaked in 2013 and have slowly improved since. We further note that this format of a Ωarag undersaturation index is a first order attempt utilizing experimental model results, and we anticipate that the index will be modified and/or expanded following further model development. We especially invite and welcome stakeholder feedback on the strengths and limitations of this index and suggestions for improvement.

Case Study: Bristol Bay Red King Crab

In addition to a general Ωarag undersaturation index for the Bering Sea shelf, there is a pressing need to develop specific indices for commercial fisheries in the region. As an initial test, we examined correlations between the modeled carbonate system variables from 2003–2012 and adult Bristol Bay red king crab (RKC) spatial distributions. First, we decomposed the oceanographic variables (carbonate variables, including Ωarag, and temperature) and crab distributions into paired spatial maps and time series outlining a positive or negative phase (see Hermann et al. (2016) and Thorson et al. (2020) for methods).

Over this time period, the temperature shift from a warm to a cool stanza in 2007–2008 was readily apparent and dominated the response of all other oceanographic variables. The temperature phase was highly correlated with the RKC time series, and even more so when crab distributions were lagged by 1 year. During warmer years, RKC expand onto the central Bristol Bay shelf. During cooler years, they are much more concentrated along the Alaska Peninsula and in the northeast coastal Bering Sea, avoiding the cold waters in the central shelf. Colder waters were also highly correlated with reduced Ωarag, so the crabs' avoidance of colder waters also avoids more corrosive water. However, there are no indications that current Ωarag levels were independently correlated with red king crab movements.

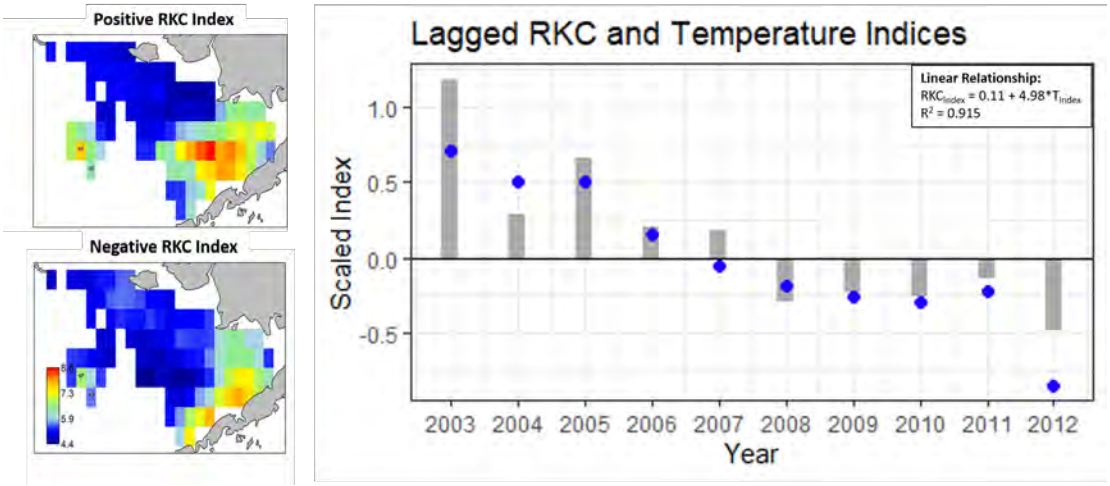

Figure 10: Heat maps of typical Bristol Bay RKC distributions during years with a positive RKC index (top left) and a negative RKC index (bottom left). Right: time series of temperature (blue) and RKC indices. RKC values have been lagged by one year relative to the temperature, while the temperature index has been rescaled by a factor of 5.

On longer time scales, we expect to see this temperature-OA relationship decouple as the Bering Sea warms and becomes more corrosive. Adult RKC can migrate within a year or less to avoid unfavorable temperatures. That mobility could allow them to seek less corrosive, warmer patches of water, avoiding some of the direct impacts of OA. However, this mobility does not apply to juvenile crabs, who are confined to crevices until they grow large enough to escape predation. Juvenile crab are missing from our dataset and have been shown to be more vulnerable to OA than adults (Long et al., 2013; Swiney et al., 2017). Future work will update this correlation study with the additional 2013–2019 Bering 10K model output and continued work toward a red king crab-specific Ωarag undersaturation index.

Contributed by Darren Pilcher (CICOES, NOAA/PMEL),
Jessica Cross (NOAA/PMEL),
Esther Kennedy (UC Davis),
Elizabeth Siddon (NOAA/AFSC), and
Christopher Long (NOAA/AFSC)
(PMEL contribution number 5176)

Marine Heatwaves in the Eastern Bering Sea

Sea surface temperature (SST) is one of the foundational metrics often used to describe the Bering Sea environment. Combined with sea ice extent, SST and several other simple metrics (e.g., cold pool extent) are often distilled into single annual or seasonal values used to describe the environment as relatively warm, average, or cold. We did a deeper dive on the intra- and inter-annual dynamics of SST in the southeastern and northern Bering Sea, with the hopes that more detail may help to identify mechanisms or critical periods through which SST has the greatest impacts on Bering Sea ecosystems and fisheries. Specifically, we explored SST throughout the annual sea ice cycle and examined the cumulative SST within each year to better understand the annual thermal exposure experienced by the system. We also explored finer scale daily data in the context of marine heatwaves.

Methods

Satellite SST data (source: NOAA Coral Reef Watch Program) were accessed via the NOAA CoastWatch West Coast Node ERDDAP server[4]. Daily data were averaged within the southeastern (south of 60°N and northern (60°N–65.75°N) Bering Sea shelf (10–200 m depth). Detailed methods are online[5]. We defined the annual cycle in the Bering Sea to begin on 1 September of each year and end on 31 August of the following year in order to most closely align with the seasonal sea ice cycle. Seasons were defined as fall (Sept–Nov), winter (Dec–Feb), spring (Mar–May), and summer (Jun–Aug), starting on 1 September 1985 and ending on 31 August 2020.

Marine heatwave calculations were performed using the heatwaveR package (Schlegel and Smit, 2018) with the earliest complete 30-yr period as the baseline (1 Sept 1985–31 Aug 2014).

Description of the indicators

Sea ice dynamics in the Bering Sea drive a unique and intense pattern of thermal exposure for the system throughout the year. As seen in Figure 11, the cumulative annual SST (i.e., the sum of daily SST throughout the year) does not reveal a linear pattern of increasing temperature, rather a non-linear, ice-derived pattern in both the southeastern and northern Bering Seas. In both systems, the cumulative SST increases throughout the fall as sea ice begins to form and in the north especially, persistent negative temperatures reduce the cumulative thermal exposure throughout the winter and spring. An inflection point appears around June in both regions, and a linear increase in cumulative SST persists for the remainder of the year (i.e., the end of August).

The end points, or the total cumulative SST, for each year demonstrate the stark difference in thermal exposure that each region experiences across years. These inter-annual differences in cumulative totals within each region are clearly illustrated in the form of anomalies (Figure 12). The warm stanza of the early 2000s and the recent warm years have far exceeded one standard deviation (horizontal dashed line) above average, with several years exceeding this common threshold several fold.

[4] https://coastwatch.pfeg.noaa.gov/erddap/griddap/NOAA_DHW.html
[5] github.com/jordanwatson/EcosystemStatusReports/tree/master/SST

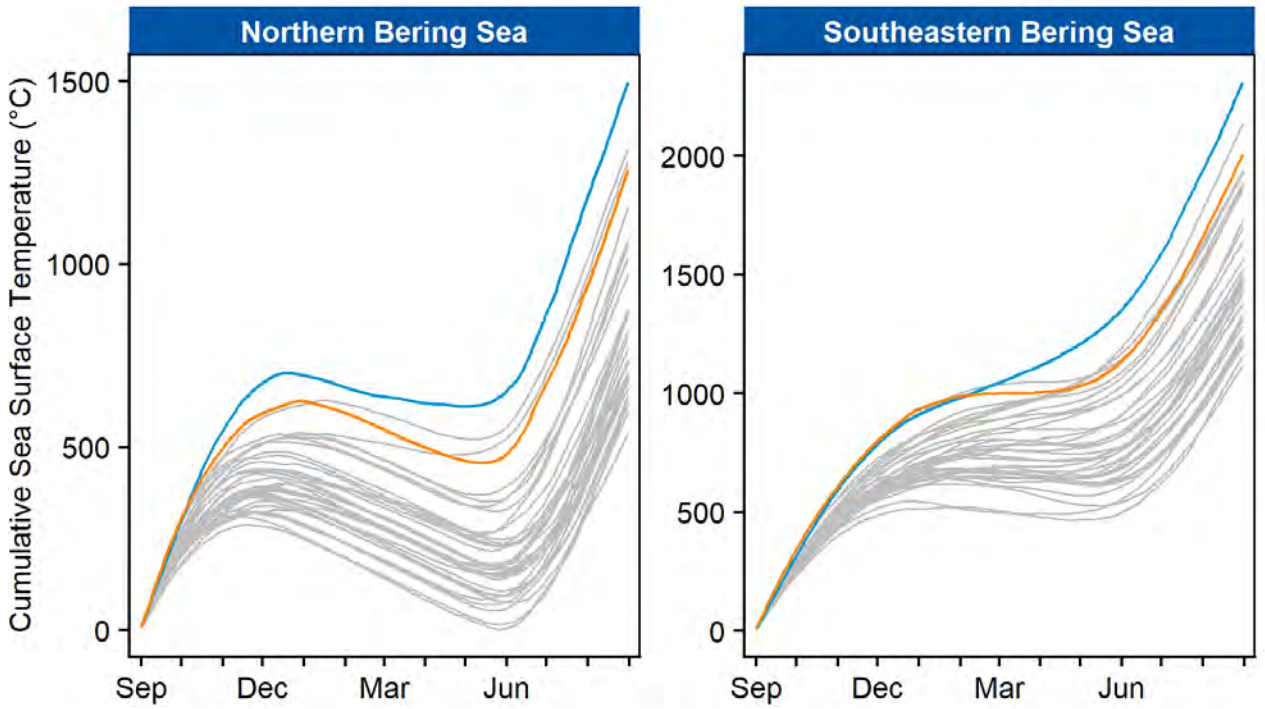

Figure 11: Cumulative sea surface temperatures (sum of daily temperatures) for years ending in 1986–2020 (annual cycles from 1 Sept–31 Aug of the following year). Orange lines are 2020 (i.e., 1 Sept 2019–31 Aug 2020), blue lines are 2019, and gray lines are all previous years.

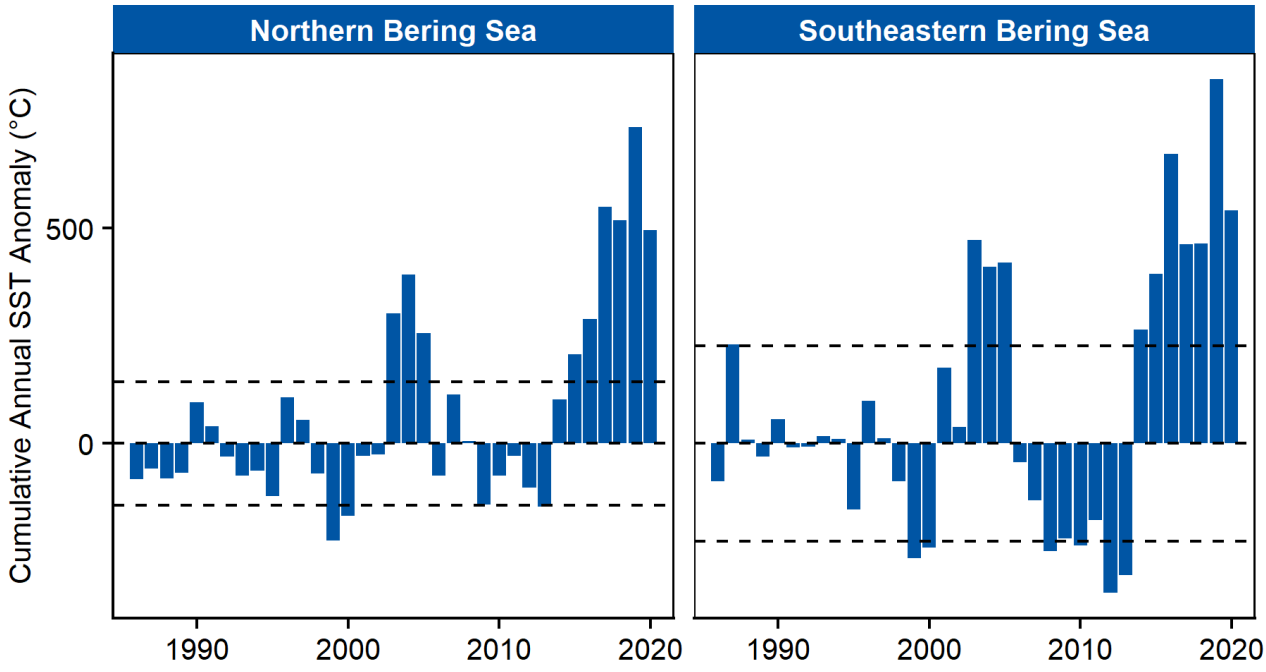

Figure 12: Anomaly of the total cumulative sea surface temperature (sum of daily temperatures) at the end of each year. Horizontal lines are ±1 SD from the mean during the 30-yr baseline period (1 Sept 1985–31 Aug 2014).

Ecologically, it is important to identify anomalous conditions relative to thermal exposure and compare oceanographic trends to stock dynamics. For example, Figure 13 summarizes the total cumulative SST for each year by the seasonal contribution to the thermal exposure. In the northern Bering Sea, predominantly negative SST in the winter and spring served to reduce the total cumulative SST in the earlier years, whereas more recently, there was negligible negative forcing from these seasons. Meanwhile, along the southeastern Bering Sea shelf, spring appears to have undergone much more variable inter-annual contributions to the cumulative SST, with a greater positive contribution in the recent warm years.

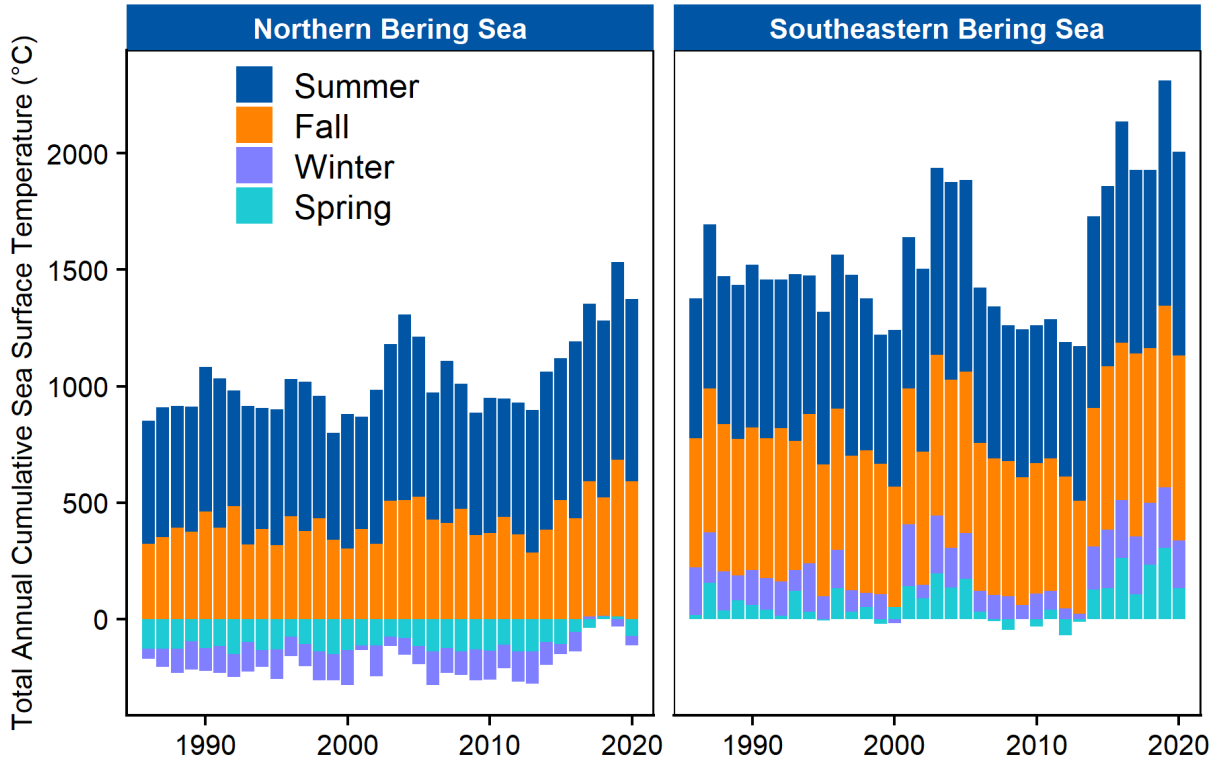

Figure 13: Total cumulative sea surface temperature (sum of daily temperatures) for each year, apportioned by season: summer (Jun–Aug), fall (Sept–Nov), winter (Dec–Feb), spring (Mar–May). Negative values are the result of sea surface temperatures below zero.

While the patterns from Figure 13 can be helpful for summarizing seasonal effects in aggregate, they may obscure annual or intra-annual patterns. Flamingo plots (Figure 14) illustrate the intra-annual variability more clearly. These figures show the same line plots as Figure 11, but displayed in chronological order instead of overlaid. Qualitative differences across years are readily discerned via the height at which inflection points begin, and the depth of the downward trend (a greater downward extent points to a more protracted period of cooling within the system). The most prominent feature in the northern Bering Sea is the shallowing of the inflection during recent years, as the cooling effect of sea ice dissipates. Meanwhile, in the south, there is a striking absence of a turning point (i.e., no downward turn) during the warm years (those ending in 2003–2005 and 2014–2020). **Note:** the red portions of each line represent periods defined as marine heatwaves (see more on marine heatwaves below).

We consider marine heatwaves to occur when SST exceeds a particular threshold for five or more days. That threshold is the 90th percentile of temperatures for a particular day of the year based on a 30-year baseline (Hobday et al., 2016). The intensity of a heatwave can be further characterized by examining the difference between the 90th percentile threshold for a given day and the baseline ("normal") temperature for that day.

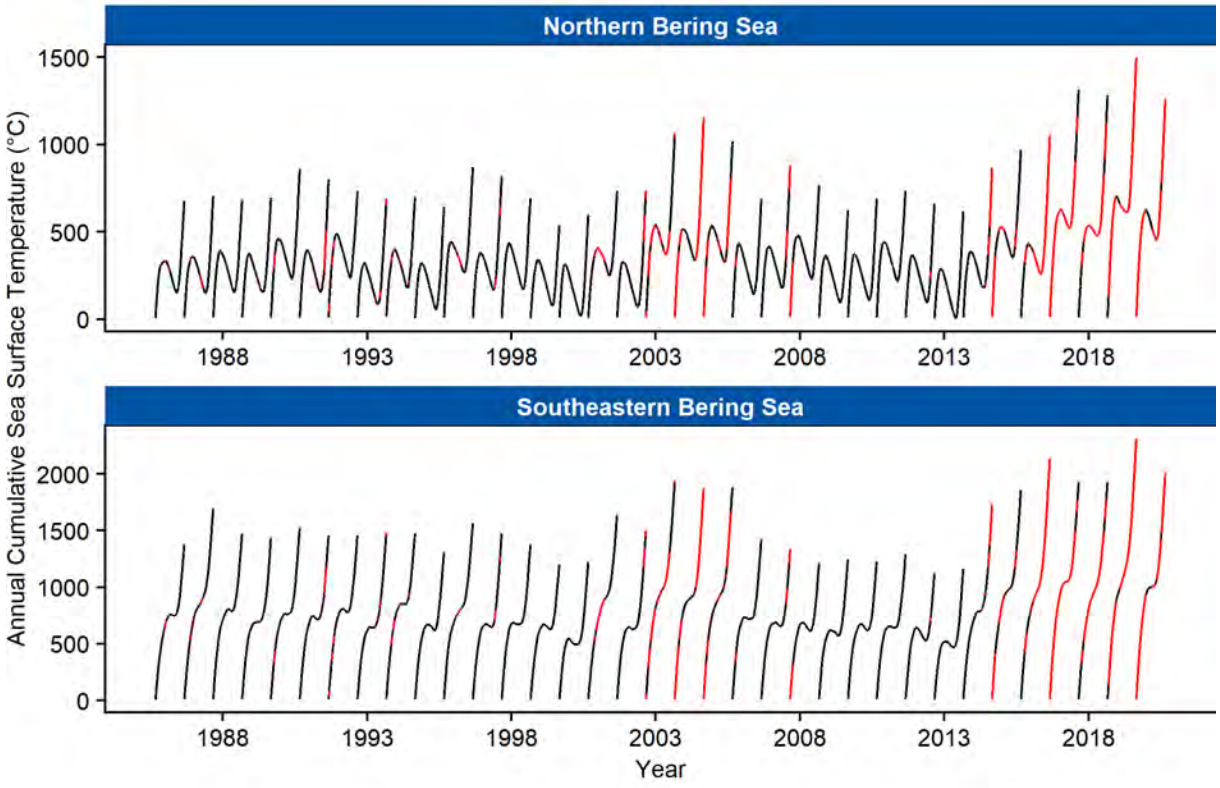

Figure 14: Cumulative sea surface temperatures (sum of daily temperatures) for years ending in 1986–2020 (annual cycles from 1 Sept–31 Aug of the following year). For each year, lines illustrate the accumulation of thermal exposure throughout the year, with downturns representing sea surface temperatures below zero. Red portions of each line represent periods defined as marine heatwaves.

If the threshold is exceeded, the event is characterized as moderate, strong (2 times the difference between then threshold and normal), severe (3 times the difference between the threshold and normal), or extreme (>=4 times the difference) (Hobday et al., 2018).

The recent marine heatwaves observed in Figure 14 have been particularly persistent and intense, reaching into the extreme category in the winters of 2017/2018 and 2018/2019 in the northern Bering Sea (Figure 15). While the extreme periods were relatively brief, heatwaves have been persistent in both the southeastern and northern Bering Sea for much of the last five years. These total annual heatwave durations are summarized in Figure 16, with the cumulative heatwave days by season. While heatwaves occurred during early years of the time series, the frequency and durations have increased dramatically, especially in the northern Bering Sea, where residual heat and low sea ice extent result in dramatically increased cumulative annual thermal exposure.

Many factors can influence sea surface temperatures, and subsequently the formation of marine heatwaves, including a suite of weather, climatic, and oceanographic factors (Holbrook et al., 2019). Meanwhile, defining or contextualizing heatwaves depends upon the selection of baseline years (in this case, 1 Sept 1985–31 Aug 2014). As long-term climate change leads to warmer temperatures, the baseline used to define 'normal' will change as well, requiring consideration of how baseline selection affects our interpretation of deviations from normal and thus, events like marine heatwaves (Jacox, 2019; Schlegel and Smit, 2018).

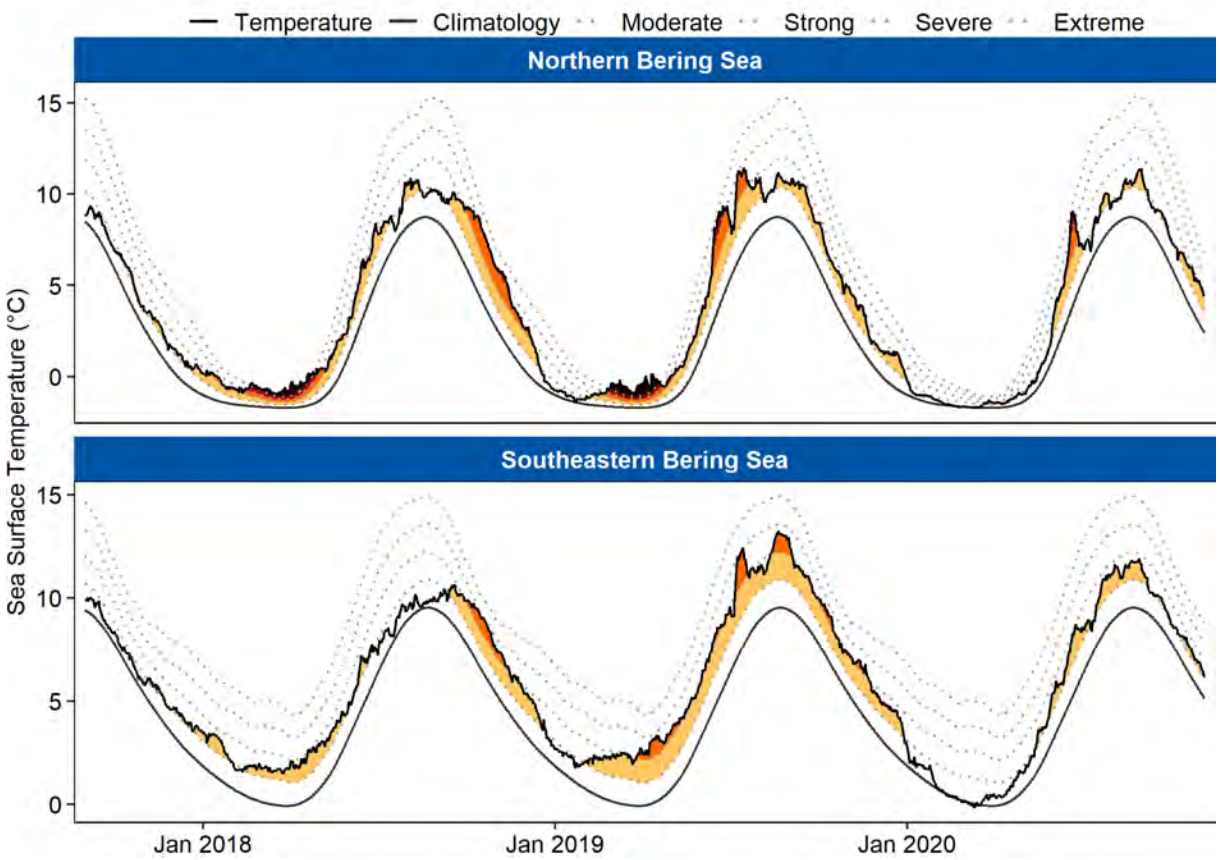

Figure 15: Marine heatwaves in the southeastern and northern Bering Sea since September 2017. Smoothed solid black line represents the baseline average temperature (i.e., climatology) for each day during the 30-yr baseline period (1 Sept 1985–31 Aug 2014). Jagged solid black line is the observed (satellite-derived) sea surface temperature for each day. Dotted lines illustrate thresholds for increasing heatwave intensity categories (moderate, strong, severe, extreme). Colored portions indicate periods during which marine heatwaves occurred, with lightest colors indicating moderate intensity heatwave events and intensity increasing as colors darken.

Contributed by Jordan Watson (NOAA/AFSC)

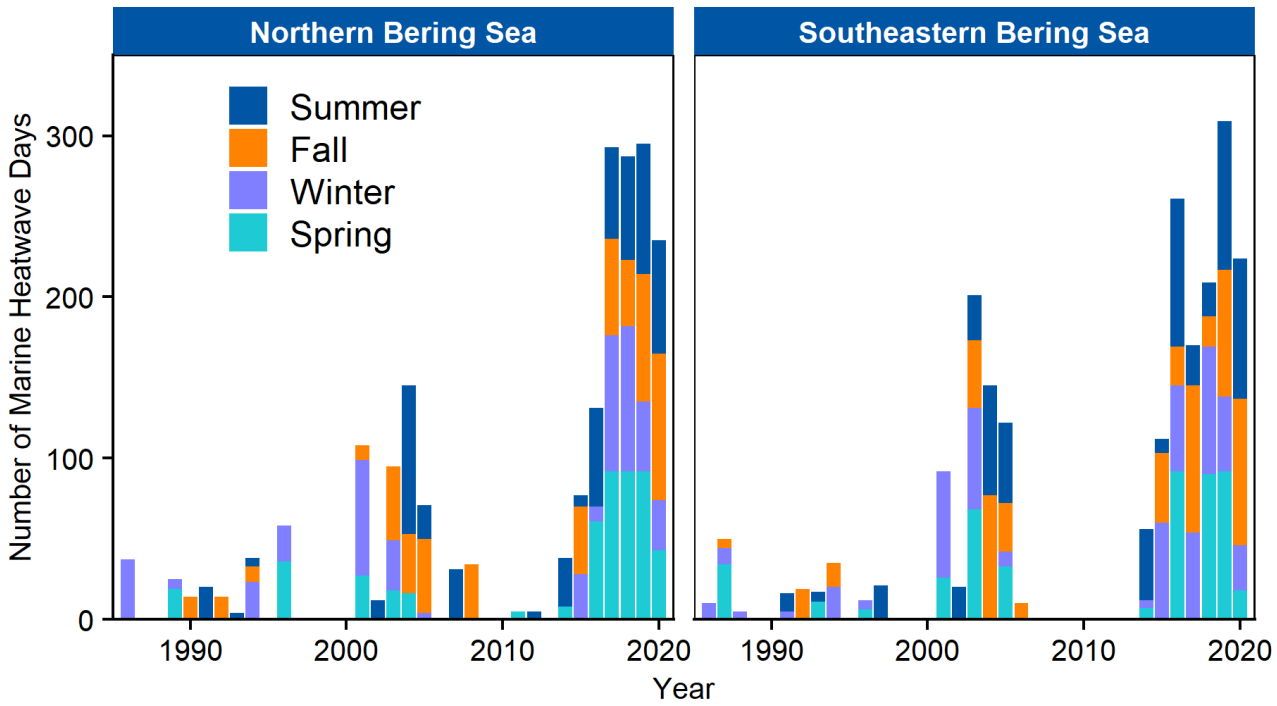

Figure 16: Number of days per year during which marine heatwaves occurred, by season: summer (Jun–Aug), fall (Sept–Nov), winter (Dec–Feb), spring (Mar–May).

2019-2020 Gray Whale Unusual Mortality Event

Since January of 2019, elevated numbers of eastern North Pacific gray whale (*Eschrichtius robustus*) mortalities have occurred along the west coast of North America, stretching from Mexico to Alaska. In May of 2019, the increased strandings were declared an Unusual Mortality Event (UME). In 2020, gray whale strandings remained elevated, but at slightly lower numbers than in 2019 (Table 2, Figure 17).

Table 2: Total number of gray whale strandings by location from 1 January 2019–15 October 2020.

Location	2019	2020
Canada	10	5
US Total	122	77
–Alaska	48	44
–Washington	34	12
–Oregon	6	3
–California	34	18
Mexico	81	87
Total	213	169

Gray whale life history includes an annual round-trip migration of up to 20,000 km. In 2019, the mortalities started off the western coast of southern Baja California Peninsula where gray whales overwinter to mate and calve, and followed the late winter/spring migration up to Alaskan waters where foraging occurs before the fasting return journey south. This pattern was repeated in 2020. The first Alaskan gray whale stranding in 2020 occurred on April 21 in Port Heiden in the Bering Sea. Mortalities continued throughout the summer with hotspots around Kodiak Island, Bristol Bay, and coastal waters of the Bering Sea and southern Chukchi (Figure 18).

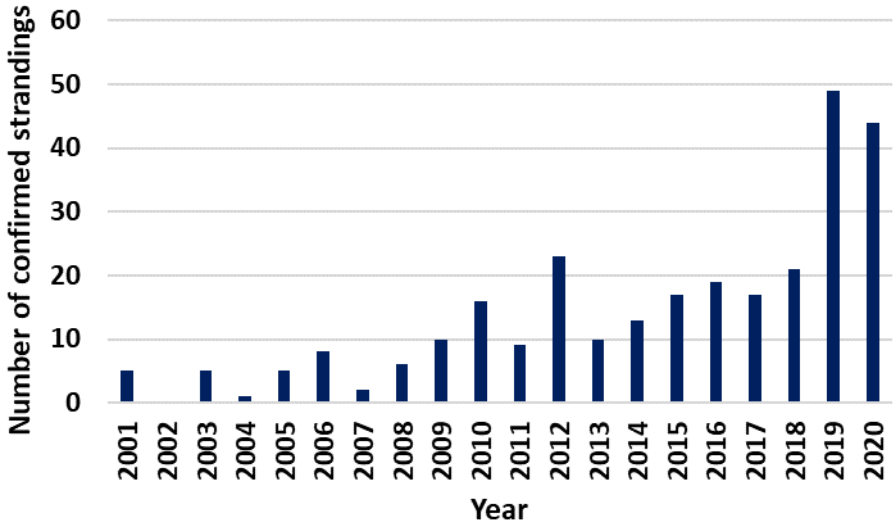

Figure 17: Number of gray whale strandings in Alaska by year, 2001–2020 (2020 numbers through 15 October).

Abnormal behaviors of live whales were also reported on occasion in both years. On May 25, 2020, a yearling gray whale in poor body condition was observed approximately 1.5 miles up from the mouth of the Twenty Mile River in Turnagain Arm. The whale remained upriver until June 3, then moved downstream where it

was live-stranded by a low tide near the river mouth. Once freed with the high tide, the whale moved out into Turnagain Arm. On June 12, a dead whale reported near the Theodore River mouth in upper Cook Inlet was thought to be the same whale.

The cause of the UME has not yet been determined and the investigation is continuing. Preliminary findings in several of the whales have shown evidence of emaciation; however, these findings are not consistent across all of the whales examined. Furthermore, while benthic prey, primarily ampelecid amphipods, in the Bering, Chukchi, and Beaufort Seas are considered the mainstay of gray whale foraging, there is also significant variability in foraging behavior depending on the location, season and year, and subset of whales (Moore et al., 2007; Calambokidis, 2013).

The eastern North Pacific gray whale is considered something of an "ecosystem sentinel" for the North Pacific and western arctic ecosystems. Correlations between changes in the distribution and behavior of gray whales and environmental change in these regions indicates the species may be effective sentinels (Moore, 2008).

A gray whale UME also occurred along the West Coast from Mexico to Alaska in 1999/2000. Although no definite conclusion was reached, the most likely precipitating factor was considered malnutrition, possibly associated with a decrease in the quantity and quality of prey items or the numbers of gray whales overwhelming the prey base as the population reached carrying capacity.

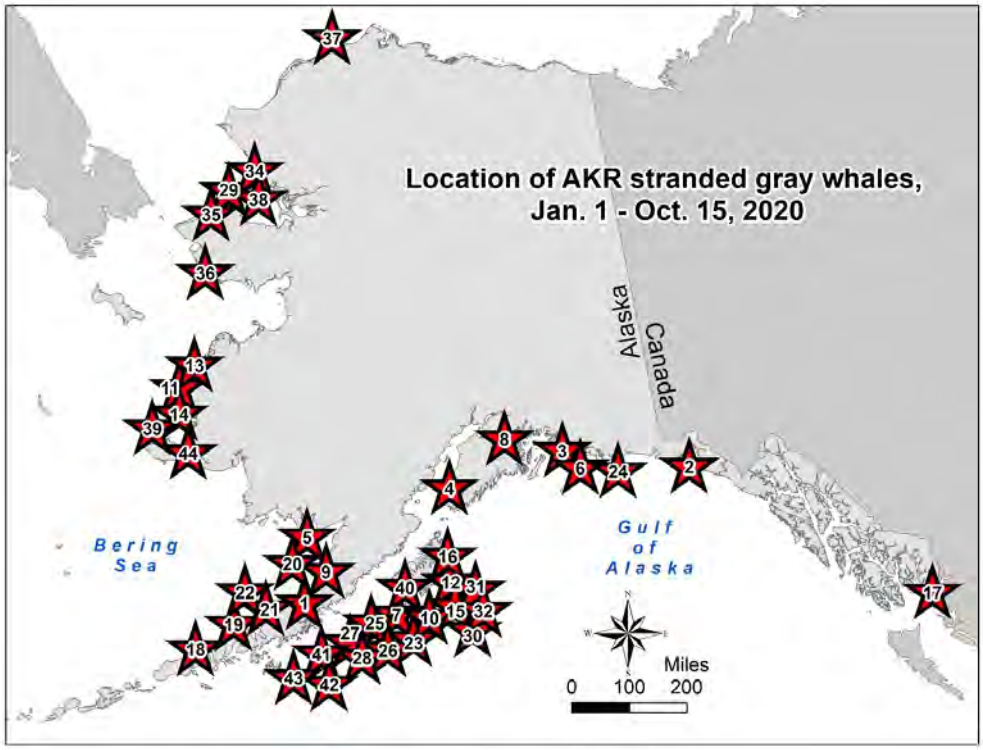

Figure 18: Locations of gray whale strandings in Alaska (NOAA/NMFS Alaska Region Marine Mammal Stranding Network unpublished data).

Contributed by Kate Savage, DVM
NOAA Fisheries
Protected Resources Division

Ecosystem Status Indicators

Indicators presented in this section are intended to provide detailed information and updates on the status and trends of ecosystem components. Older contributions that have not been updated are excluded from this edition of the report. Please see archived versions available at: `http://access.afsc.noaa.gov/reem/ecoweb/index.php`

Physical Environment Synthesis

This synthesis section provides an overview of physical oceanographic variables and contains contributions from (in alphabetical order):

Nick Bond (University of Washington, Cooperative Institute for Climate, Ocean, and Ecosystem Studies [CICOES])
Dan Cooper (NOAA Fisheries, Alaska Fisheries Science Center, Resource Assessment and Conservation Engineering Division)
Seth Danielson (University of Alaska Fairbanks, College of Fisheries and Ocean Sciences)
Lauren Divine (Ecosystem Conservation Office at Aleut Community of St. Paul Island)
Elizabeth Dobbins (University of Alaska Fairbanks, College of Fisheries and Ocean Sciences)
Kelly Kearney (University of Washington, Cooperative Institute for Climate, Ocean, and Ecosystem Studies [CICOES] and NOAA Fisheries, Alaska Fisheries Science Center)
Aaron Lestenkof (Ecosystem Conservation Office at Aleut Community of St. Paul Island)
Jim Overland (NOAA - Pacific Marine Environmental Lab [PMEL])
Phyllis Stabeno (NOAA - Pacific Marine Environmental Lab [PMEL])
Rick Thoman (University of Alaska Fairbanks, International Arctic Research Center)
Jordan Watson (NOAA Fisheries, Alaska Fisheries Science Center, Auke Bay Laboratories)
Tom Wilderbuer (NOAA Fisheries, Alaska Fisheries Science Center, Resource Ecology and Fisheries Management Division [retired])

Last updated: October 2020

Summary Statement
Following two years of physical oceanographic perturbations, the eastern Bering Sea experienced a return to near-normal climatic conditions in 2020. Residual warmth delayed sea ice formation until late 2019. Considerable cooling then allowed for rapid build-up of sea ice, even exceeding median ice extent in parts of February and March 2020. However, ice thickness was low, and retreated quickly in spring. Summer sea surface temperatures through August were above average in the southern and northern Bering Sea, similar to those observed in 2019. Summer bottom temperatures and spatial extent of the cold pool were average based on the ROMS hindcast model and observations from the 2020 *Oscar Dyson* cruise.

Introduction
In this section, we provide an overview of the physical oceanographic conditions impacting the eastern Bering Sea, describe conditions observed during 2020, and place 2020 in context to recent years. The physical environment has implications for ecosystem dynamics and productivity important to fisheries within the system and their management. We merge across information sources, from broad-scale to local-scale, as follows:

Outline

1. Climate Overview
2. Regional Highlights
3. Sea Ice
4. Winds
5. Sea Surface Temperature
6. Bottom Temperature

1. Climate Overview

Contributed by Nick Bond, *nicholas.bond@noaa.gov*
Climate indices provide an alternative means of characterizing the state of the North Pacific atmosphere-ocean system. Five commonly used indices are presented here: the NINO3.4 index for the state of the El Niño/Southern Oscillation (ENSO) phenomenon, PDO index (the leading mode of North Pacific SST variability), North Pacific Index (NPI), North Pacific Gyre Oscillation (NPGO), and Arctic Oscillation (AO). The time series of these indices from 2009 into spring/summer 2020 are plotted in Figure 19. Two indices, the NPI and the AO, best represent conditions impacting the eastern Bering Sea shelf and are described in more detail below.

The NPI effectively represents the state of the Aleutian low, with negative (positive) values signifying relatively low (high) sea level pressure (SLP). The NPI tended to be weakly negative during the summer of 2019 before entering a strongly positive phase during the winter of 2019–2020. This was especially the case in February 2020, during which the average SLP in the region used to specify the NPI (30-65°N, 160°E-140°W) was the greatest on record for that month. The Aleutian low tends to be stronger, i.e., the NPI is negative, during El Niño. This is opposite to what occurred in the winter of 2019–2020, and to a lesser extent in the previous winter of 2018–2019. The NPI relaxed back to a near normal state in the summer of 2020.

The AO represents a measure of the strength of the polar vortex, with positive values signifying anomalously low pressure over the Arctic and high pressure over the North Pacific and North Atlantic at a latitude of roughly 45°N. As for the NPI, early 2020 was highly unusual with a peak value of the AO approaching +4 standard deviations in terms of a seasonal (3-month) mean. This set-up helped bring about the coldest winter (Dec–Feb) for Alaska as a whole since 1998–1999, with mean temperatures on the order of 6°C colder than those during 5 of the 6 winters immediately preceding. A marked decline in the AO occurred during the spring of 2020 to near neutral values in summer 2020.

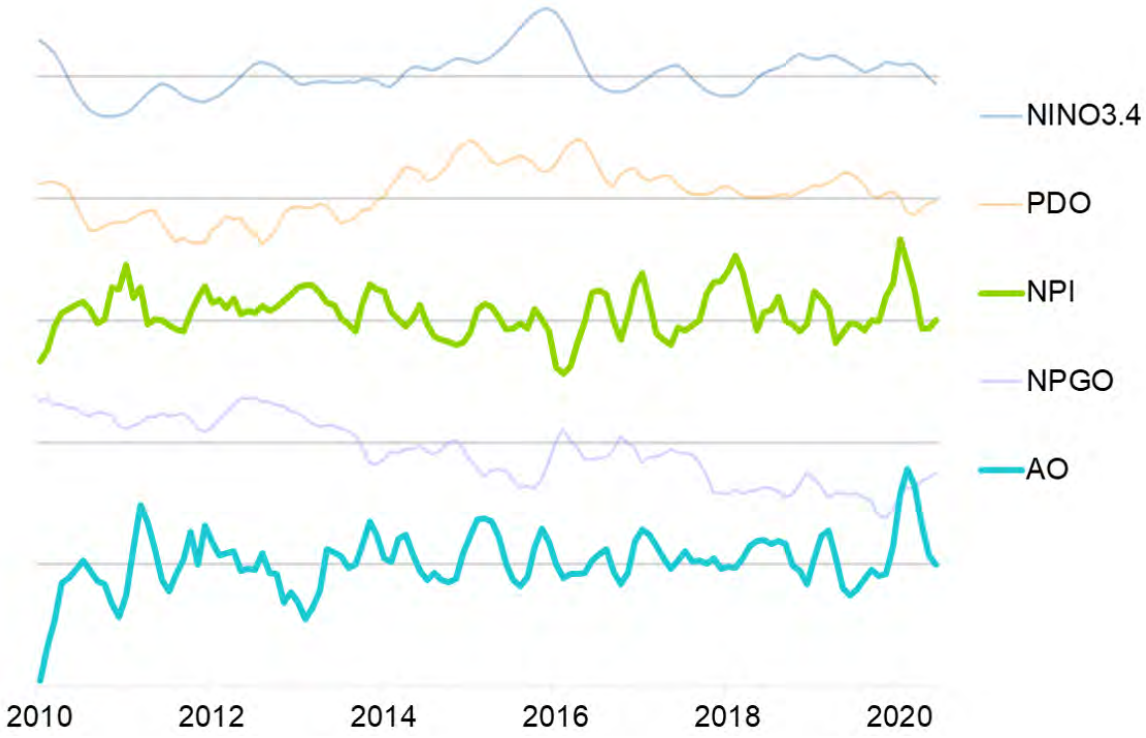

Figure 19: Time series of the NINO3.4, PDO, NPI, NPGO, and AO indices (ordered from top to bottom) for 2010–2020. Each time series represents monthly values that are normalized using a climatology based on the years of 1981–2010, and then smoothed with the application of three-month running means. The distance between the horizontal grid lines represents 2 standard deviations. More information on these indices is available from NOAA's Physical Sciences Laboratory at `https://psl.noaa.gov/data/climateindices/`.

2. Regional Highlights

Contributed by Nick Bond, *nicholas.bond@noaa.gov*

Summary
The North Pacific atmosphere-ocean climate system during autumn 2019 through summer 2020 featured generally higher than normal SLP and above-normal upper ocean temperatures south of Alaska. The anomalously high pressure was especially prominent during the winter of 2019–2020 and coincided with an intense polar vortex, as indicated by a strongly positive state for the Arctic Oscillation. This regional atmospheric circulation pattern occurred despite the co-existence of weak-moderate El Niño conditions in the tropical Pacific, with the latter usually accompanied by a strong Aleutian low (i.e., negative SLP anomalies). The sea surface temperature (SST) pattern during the period considered here represented a strongly negative state of the North Pacific Gyre Oscillation, particularly during the latter portion of 2019; the Pacific Decadal Oscillation transitioned from moderately positive in summer 2019 to moderately negative during much of 2020. The climate models used for seasonal weather predictions are indicating elevated odds (85%) of La Niña for the winter of 2020–2021. Model projections for early 2021 indicate that SSTs in the North Pacific are likely to remain warmer than normal in the central North Pacific south of 50°N, with near-normal temperatures for the central and eastern Aleutians and southeast Bering Sea shelf, and typical to slightly cool temperatures for the northern Gulf of Alaska.

Alaska Peninsula
Air temperatures in the vicinity of the Alaska Peninsula were mostly warmer than normal, especially during autumn 2019 and summer 2020, with more typical temperatures from late winter through much of spring 2020. Wind speeds were on the whole lower than normal. The SSTs were also on the warm side, but not to an extreme, with positive anomalies on the order of 0.5 to 1°C in coastal areas. The warmth at depth noted in the Gulf of Alaska extended southwestward along the shelfbreak on the south side of the Alaska Peninsula during summer and fall of 2019, with rapid cooling beginning near the end of 2019 continuing into 2020 bringing more normal temperatures.

Aleutian Islands
The Aleutian Islands experienced relatively warm weather in the early fall of 2019 with a transition to more normal air temperatures in winter 2020. The weather was quite variable in spring followed by a warm summer in 2020. The western portion of the Aleutian Islands tended to be relatively stormy in winter and spring 2020, with the central and eastern portions of this region on the quiet side, in large part due to an Aleutian low that was much weaker than usual. The sub-surface marine heat wave noted for the GOA and Alaska Peninsula regions appears to have not extended farther westward along the southside of the Aleutians. According to GODAS, NOAA's operational ocean analysis, and considering temperatures in the 100 to 250 meters layer relative to historical averages, the western Aleutians have been cool and the central and eastern Aleutians have been warm since about 2016. There are relatively few direct sub-surface observations to constrain the GODAS analysis in this region so these results are tentative.

Eastern Bering Sea
The eastern Bering Sea shelf was quite warm in the autumn 2019, and experienced a late arrival of sea ice, as now seems to be the rule. The following winter of 2019–2020, however, had colder weather than that during the last 4 years. This can be partly attributed to the high-latitude atmospheric circulation that included a very strong polar vortex (i.e., a positive state for the AO), which served to suppress the delivery of mild air masses of maritime origin. Especially cold weather, and rapid advance of seasonal sea ice, occurred for an extended period near the beginning of 2020, and then for shorter periods intermittently from late January through mid-March 2020. The wind anomalies were from the southwest in an overall sense; with the north portion of the shelf experiencing stormier conditions than the south portion from fall 2019 through spring 2020, compared to normal. SSTs over the eastern Bering Sea shelf warmed over the course of spring and summer 2020 to temperatures that were about 1 to 1.5°C above their climatological norms.

Bering Sea Deep Basin
The western, deep portion of the Bering Sea experienced anomalous winds from the west off the eastern

tip of Siberia during much of the winter of 2019–2020, resulting in cooling to normal SSTs after a warm fall in 2019. The weather in spring was variable, with some warming of the upper portion of the water column relative to seasonal norms. There is the suggestion that some of this warming can be attributed to warm water south of the Alaska Peninsula being transported through passes (particularly Amukta Pass) in the eastern Aleutian Island chain and subsequently being entrained in the northward flowing Bering Slope Current along the eastern Bering Sea shelf break. But again, direct measurements are scant and it is highly uncertain whether the GODAS product can properly account for the processes that result in the transport of Pacific water into the Bering Sea, and the subsequent fate of this water. At any rate, by summer 2020 the upper part of the water column in the deep basin of the Bering Sea was relatively warm in the north and cool in the south.

Arctic
The Arctic region of northern Alaska featured warm conditions in terms of atmospheric and upper ocean temperatures during the fall of 2019. For the Arctic as a whole, the ice cover in September 2019 was essentially tied with that in 2007 and 2016 for the 2nd lowest areal extent in the 41-year historical record. But the following winter brought some quite cold temperatures beginning in the latter part of December, with particularly frigid weather from late January into March 2020. The summer of 2020 included an ice edge far north of its usual position north of Russia in the East Siberian Sea extending across the dateline to the Chukchi Sea; the width of the open water farther east in the Beaufort Sea north of Alaska was not nearly as anomalous. Given the relatively warm weather occurring in northern Alaska in the latter part of summer 2020, and an ice edge well north of its usual latitude in the Chukchi Sea, it seems to be a safe bet that the onset of sea ice during the upcoming autumn and winter will be late yet again for the Chukchi Sea and northern Bering Sea (see 'Early Season Ice Extent' below for historical trends).

3. Sea Ice

Contributed by Rick Thoman, *rthoman@alaska.edu*
Early Season Ice Extent
While mean annual ice extent in the Bering Sea (both eastern and western) has shown no significant trend until recently, this is not the case for early season ice. The presence or absence of early sea ice in the Bering Sea is important because, at least during the passive microwave era, nearly all ice in the Bering Sea is first year ice, therefore Bering Sea ice thickness is related to both the air temperature and the age of the ice.

Trends
The mean daily extent for the two months from October 15 through December 15 show considerable inter-annual variability, but with a strong negative linear trend during the past 40 years (Figure 20). This trend was robust even prior to the two recent low ice seasons and is a realization of delayed ice formation due to residual warmth in the system. The mean early season ice extent for 2019 of 49,944 km^2 was below 1 standard deviation of the long-term mean.

Annual Bering Sea Ice Extent
The Bering Sea has historically been ice-free in the middle and late summer, with ice developing during the second half of October. To account for this seasonal cycle, the Bering Sea ice year is defined as 1 August to 31 July. Bering Sea ice extent data are from the National Snow and Ice Center's Sea Ice Index, version 3 (Fetterer et al., 2017), and use the Sea Ice Index definition of the Bering Sea (effectively south of the line from Cape Prince of Wales to East Cape, Russia).

Trends
The mean sea-ice extent exhibited no long term trend, although a steep decline in ice extent was observed from 2012 (highest ice extent on record) to 2018 (lowest ice extent on record) (Figure 21). The 2019–2020 daily mean extent of 231,518 km^2 is within 1 standard deviation of the long-term mean.

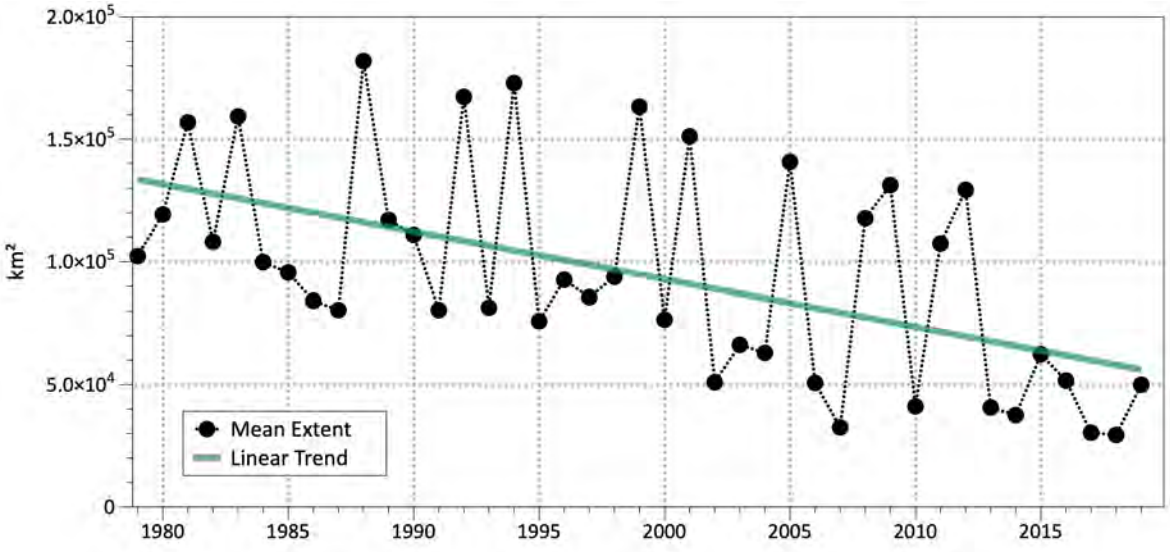

Figure 20: Early (15 Oct–15 Dec) mean sea-ice extent in the Bering Sea, 1979–2019.

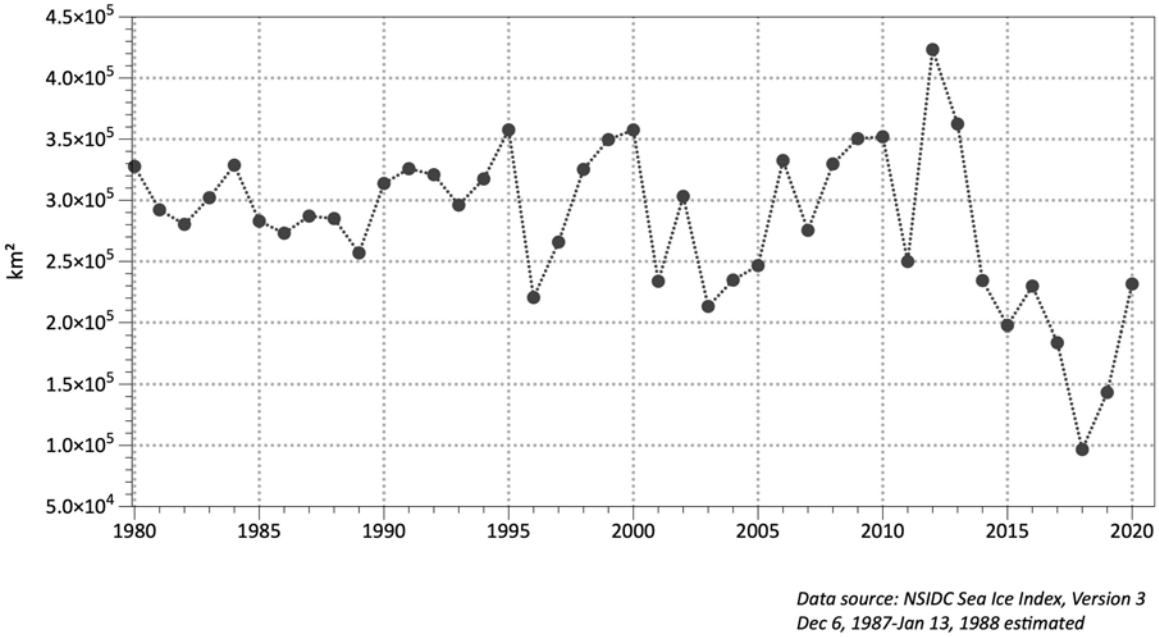

Figure 21: Mean sea-ice extent in the Bering Sea from 1 August to 31 July, 1979/1980–2019/2020.

Bering Sea Daily Ice Extent

Tracking the seasonal progression and retreat of sea ice highlights the interactive roles of water temperature (i.e., warmth in the system) and winds (Figure 22). For winter 2019–2020, residual warmth delayed sea-ice formation until late December 2019. Considerable cooling then allowed for rapid build-up of sea ice, even exceeding median ice extent in parts of February and March 2020. However, ice thickness was low, and retreated quickly in spring.

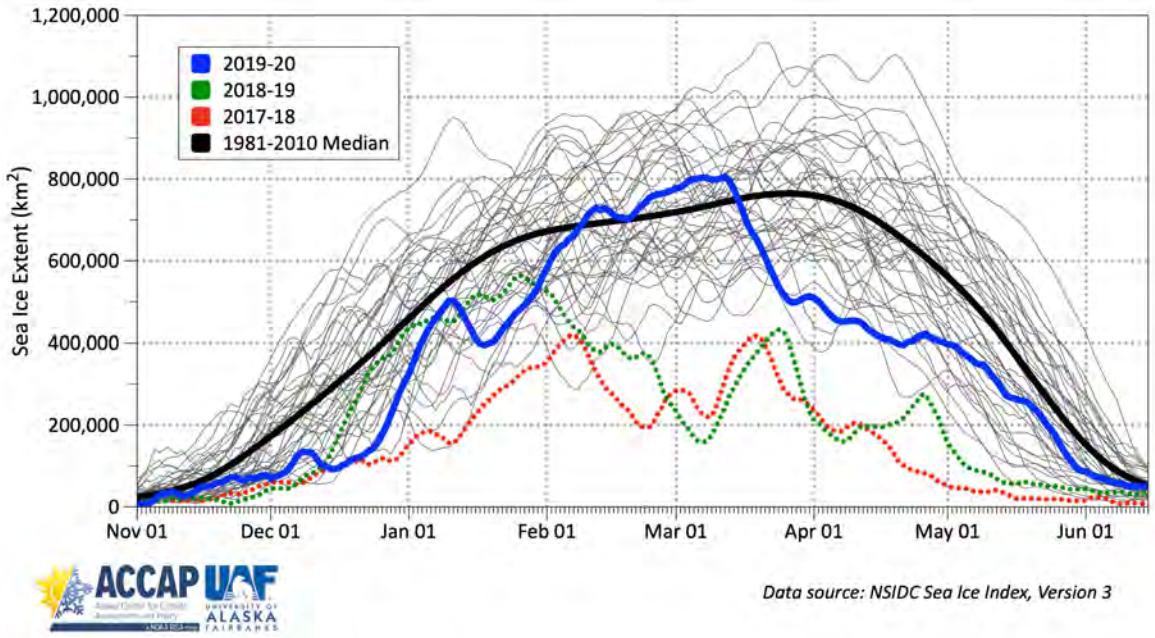

Figure 22: Daily ice extent in the Bering Sea. The most recent year (2019–2020) is shown in blue, recent years in dotted green (2018–2019) and red (2017–2018) lines, and the historical median shown in black. Individual years in the time series are shown in gray.

4. Wind

Sea Level Pressure Anomalies
Contributed by Nick Bond, *nicholas.bond@noaa.gov*
Broad-scale wind patterns over the North Pacific depicted as seasonal mean sea level pressure (SLP) anomalies are summarized here. The anomalies are relative to mean conditions over the period of 1981–2010. The data are from the NCEP/NCAR Reanalysis project and are made available by NOAA's Physical Sciences Laboratory (PSL)[6].

The SLP pattern during autumn (Sep–Nov) 2019 (Figure 23a) featured a positive anomaly centered over the Gulf of Alaska (GOA) and negative anomalies from the Sea of Okhotsk to the eastern tip of Siberia. The southeasterly wind anomalies accompanying the GOA positive SLP anomaly contributed to warm SSTs and upwelling-favorable winds in the northern and eastern GOA.

The winter (Dec–Feb) of 2019-2020 (Figure 23b) featured a large positive SLP anomaly of extreme magnitude (peak value approaching 10 millibar [mb]) centered between the Hawaiian Islands and mainland Alaska. This pattern implies substantial suppression of the storminess between 30 and 50°N across the North Pacific, especially east of the dateline. It also indicates wind anomalies from the west on the north side of the SLP anomaly center, particularly for the GOA, and hence anomalous equatorward Ekman transports for the upper ocean mixed layer in that region.

Relatively high SLP anomaly (exceeding 8mb) continued to dominate the central and eastern North Pacific through spring (Mar-May) of 2020 (Figure 23c), centered just south of the Alaska Peninsula. The circulation around this high SLP center brought anomalous winds with a component from the south over the eastern and northern Bering Sea. It also implies a continuation of westerly wind anomalies for the central GOA, and upwelling-favorable northwesterly wind anomalies for the coastal regions of the eastern GOA and British Columbia.

The distribution of SLP anomalies across the North Pacific during summer (Jun–Aug) of 2020 is shown in Figure 23d. Low pressure occurred over the GOA with higher pressure to the south between Alaska and the Hawaiian Islands in a similar sense to that of the previous winter, but with much weaker magnitudes. The SLP over the western North Pacific was lower than normal north of about 35°N and higher than normal from northeast of the Philippines to east of Japan with peak anomaly magnitudes of 1-2mb.

[6] `https://www.psl.noaa.gov/cgi-bin/data/composites/printpage.pl`.

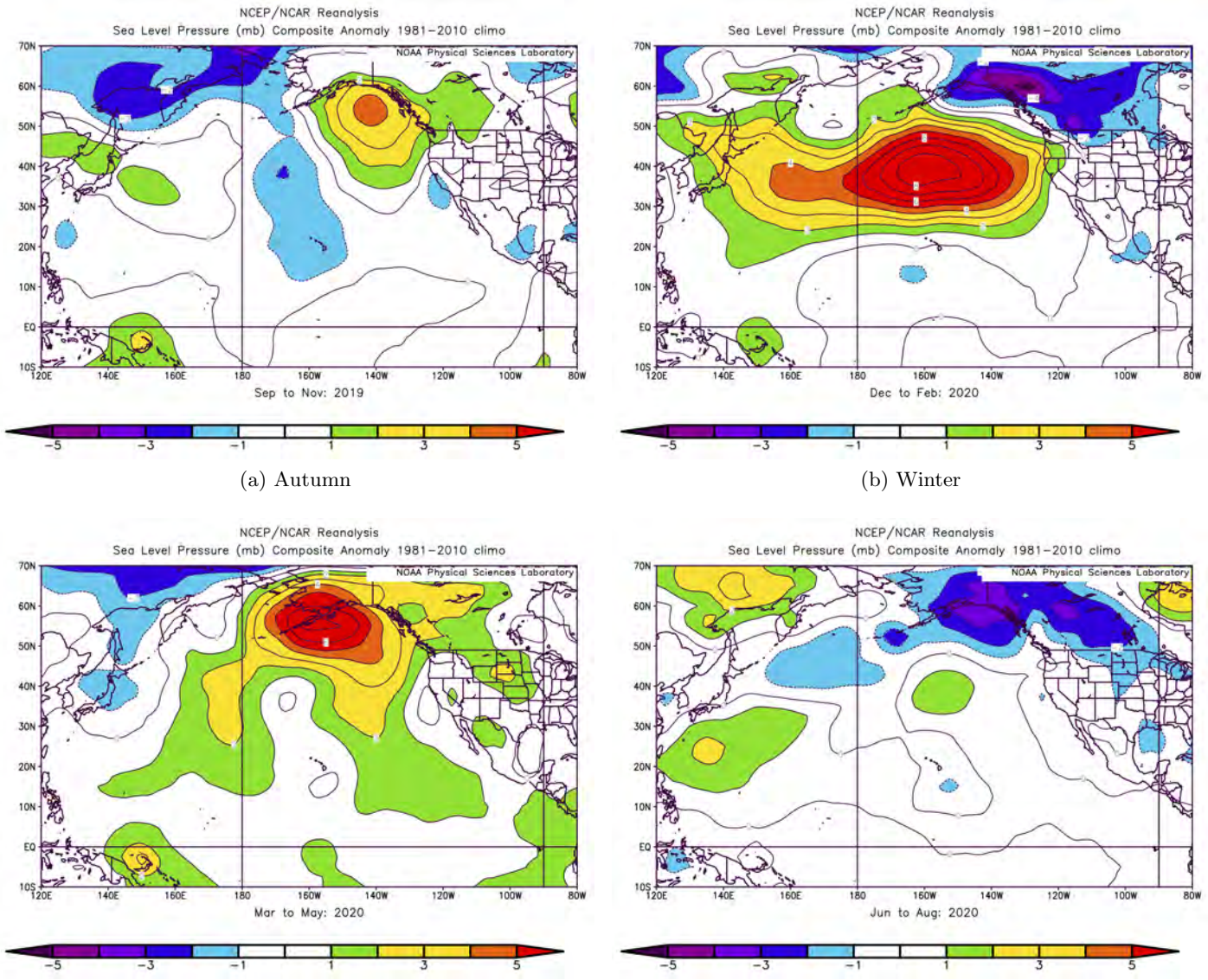

(a) Autumn

(b) Winter

(c) Spring

(d) Summer

Figure 23: SLP anomolies for autumn (Sept–Nov 2019), winter (Dec 2019–Feb 2020), spring (Mar–May 2020), and summer (Jun–Aug 2020).

Winter Wind Speed and Direction

Contributed by Rick Thoman, *rthoman@alaska.edu*)

The average winter (Nov–Mar) wind speed categorizes years as having prevailing north winds or south winds. No long-term trend is exhibited, although winters ending in 2018 and 2019 were among 5 years with the strongest south winds, which contributed to low sea ice extent in those years. The most recent winter (ending in 2020) had wind speed direction near the long-term average (Figure 24).

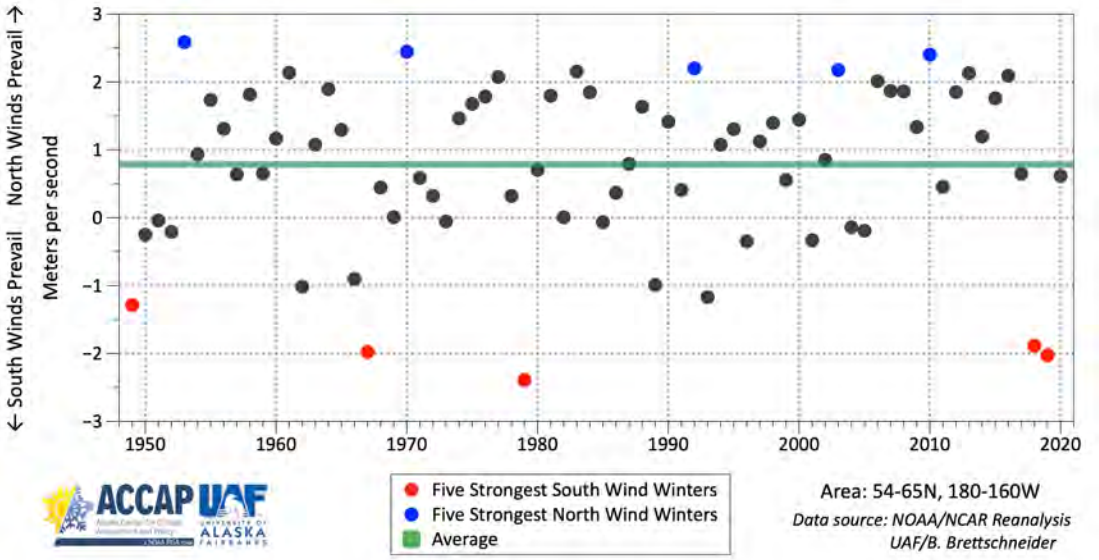

Figure 24: Winter (Nov–Mar) average north-south wind speed in the Bering Sea, 1949–2020. **Note:** the north-south (meridional) component of the wind is plotted inverse to meteorological convention with south to north as negative values and north to south as positive values.

Spring Jet Stream and Sea Level Pressure

Contributed by James Overland, *james.e.overland@noaa.gov*)

The jet stream describes atmospheric dynamics at higher altitude. In spring (Mar-May) 2020, the jet stream was located very far south (i.e., over Japan) and set up a 'warm ridge' over the eastern Bering Sea (Figure 25). Additionally, a low pressure system at sea level brought warm south winds over the eastern Bering Sea shelf and warm temperatures to the northern Bering Sea (Figure 26).

OSCURS Wind Forcing

Contributed by Dan Cooper and Tom Wilderbuer, *dan.cooper@noaa.gov*

Wilderbuer et al. (2002, 2013) summarized a study examining the recruitment of winter-spawning flatfish in relation to decadal atmospheric forcing, linking favorable recruitment to the direction of wind forcing during spring. Only two years (2015 and 2018) out of the past ten have OSCURS runs that are consistent with those which produced above-average recruitment in the original analysis. Estimates of northern rock sole (*Lepidopsetta polyxystra*) recruitment in recent years are consistent with this larval drift hypothesis (Cooper et al., 2020). For arrowtooth flounder (*Atheresthes stomias*) and flathead sole (*Hippoglossoides elassodon*), the correspondence between the springtime drift pattern from OSCURS and estimates of year class strength have weakened since the 1990s. Tidal transport may also play a role in larval dispersal (Wilderbuer et al., 2016).

Trends

The 2020 springtime drift pattern was mixed, with an early period of eastward drift followed by a period of westward drift during the 90-day index (Figure 27). In 2019, winds were consistently westward during the drift period consistent with below-average recruitment for winter spawning flatfish. In contrast, 2018 was favorable with predominant northward and eastward drift.

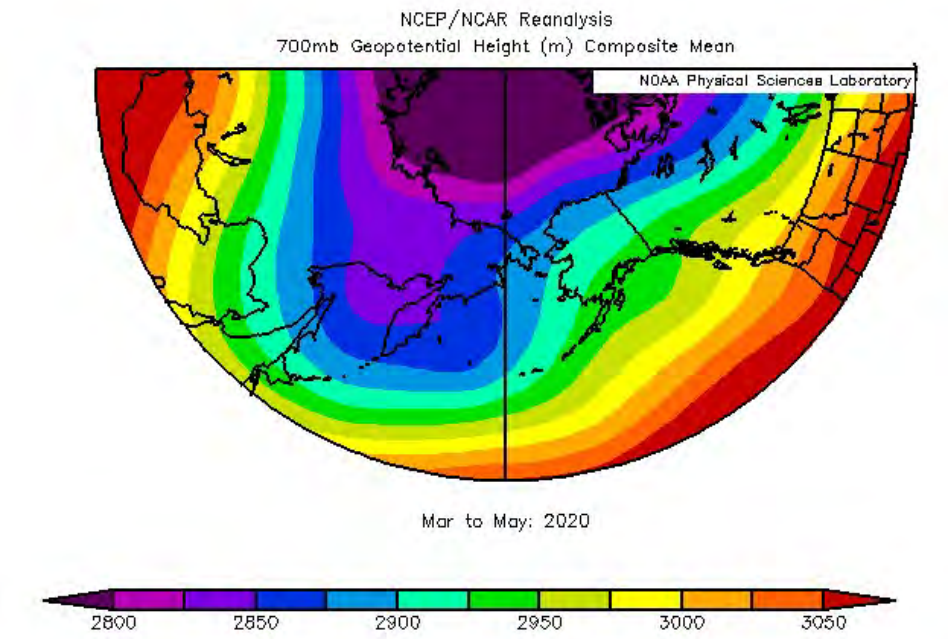

Figure 25: Spring (Mar-May) 2020 realization of the jet stream location over the North Pacific.

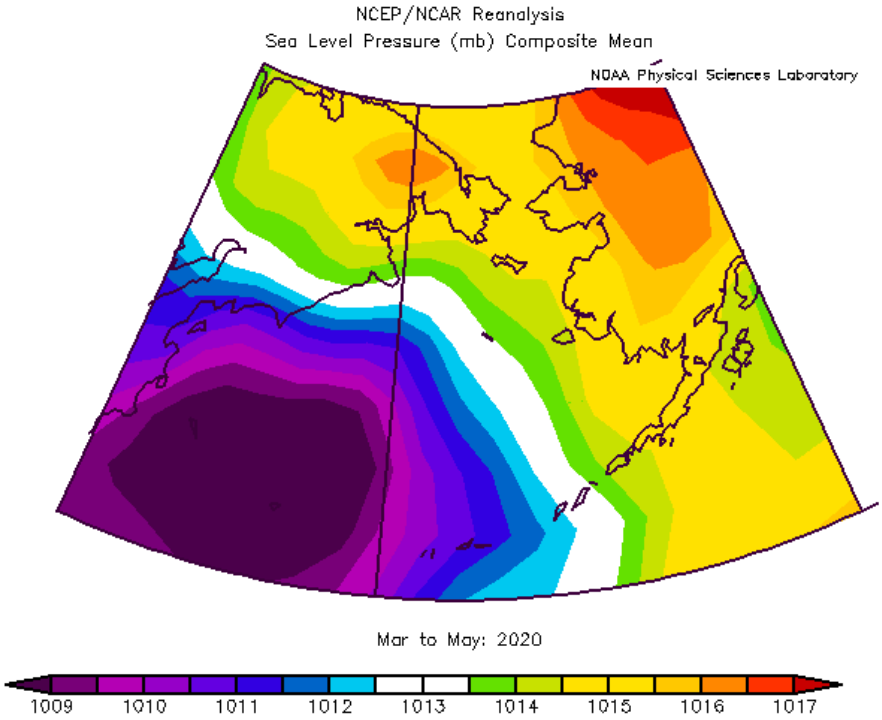

Figure 26: Spring (Mar-May) 2020 sea level pressure (actual values) over the North Pacific.

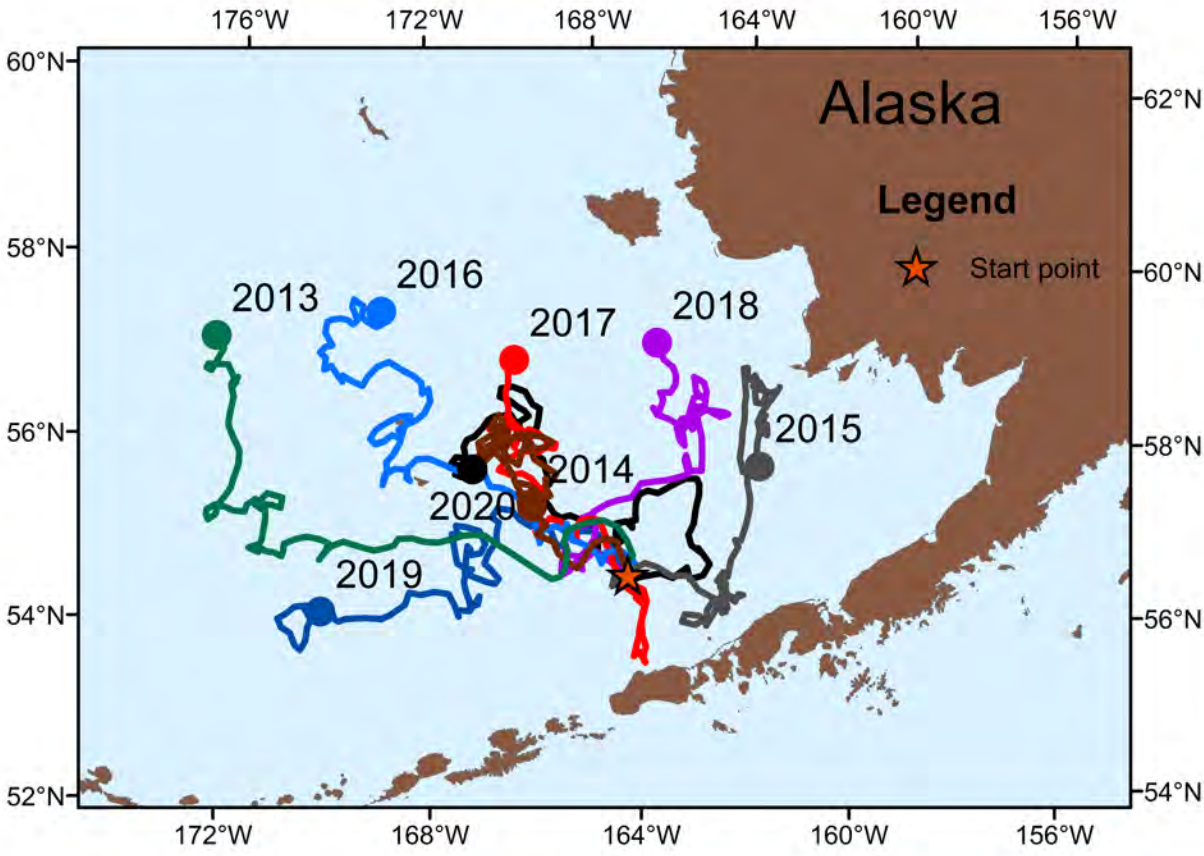

Figure 27: OSCURS (Ocean Surface Current Simulation Model) trajectories from starting point 56°N, 164°W from 1 April–30 June for 2013–2020.

5. Sea Surface Temperature

North Pacific Sea Surface Temperature (SST) Anomalies
Contributed by Nick Bond, *nicholas.bond@noaa.gov*
Broad-scale SST patterns over the North Pacific depicted as seasonal mean SST anomalies are summarized here. Similar to SLP, the anomalies are relative to mean conditions over the period of 1981–2010. The data are from NOAA's Optimum Interpolation Sea Surface Temperature (OISST) analysis and are made available by NOAA's Physical Sciences Laboratory (PSL).

The SST during the autumn of 2019 (Figure 28a) was warmer than normal for almost the entirety of the eastern North Pacific Ocean. Warm conditions also occurred in the western North Pacific between 30 and 45°N from the Korean Peninsula to 160°E. Especially prominent positive anomalies extended from the Chukchi Sea to a broad region between the Hawaiian Islands and the Pacific coast. The magnitude of the SST anomalies exceeded 2°C over much of the southeastern Bering Sea shelf and south of the GOA. Warmer than normal but more moderate SSTs were present along the west coast of North America from California to the northern GOA. The lesser anomalies in this coastal strip are consistent with the upwelling-favorable wind anomalies discussed in the previous section. It is noted that temperatures at depth (roughly 100 to 250 meters) in the western GOA were considerably warmer than normal during autumn 2019 from a historical perspective (not shown). The equatorial Pacific had a patch of SST anomalies greater than 1°C just west of the dateline but otherwise near normal temperatures.

The distribution of SST anomalies during winter (Dec–Feb) of 2019–2020 (Figure 28b), relative to the previous fall season, featured moderation in the magnitudes of the positive anomalies south of mainland Alaska, and considerable cooling on the southeastern Bering Sea shelf. The latter conditions represent a marked contrast with the warm to extremely warm winters of that region during the preceding 5 years. The equatorial Pacific included a patch of SST anomalies slightly greater than +1°C near the dateline in association with a weak El Niño of the central Pacific.

The spring (Mar-May) of 2020 (Figure 28c) included relatively warm SSTs throughout much of the North Pacific. The water that was more than 1°C warmer than usual south of Alaska increased in area from the previous season. There was also a substantial increase in temperatures in the southeastern Bering Sea, relative to seasonal norms, accompanying a rapid retreat of sea ice driven by southerly wind anomalies. The coastal waters of western North America from the GOA to northern California had near normal temperatures. The weak El Niño of the previous winter continued to fade, with some warmth remaining along the equator west of the dateline and near normal conditions in the east.

The large-scale SST anomaly pattern in the North Pacific during the summer (Jun–Aug) of 2020 (Figure 28d) featured mostly continued warmth east of the dateline between Alaska and the Hawaiian Islands. Cooling in an overall sense occurred west of the dateline, relative to the previous spring, with the development of negative anomalies from the western Aleutians to the entrance to the Sea of Okhotsk, and a diminishing of positive anomalies between about 30 and 45°N. Prominent warm anomalies on a smaller spatial scale developed on the southeastern Bering Sea shelf and in the southeastern Chukchi Sea along the northwest coast of Alaska. Cold SSTs were present in the eastern equatorial Pacific, with the vestiges of the warm temperatures of the past winter and spring confined to the far western portion. The latter portion of this period featured the development of positive SST anomalies of substantial magnitude (1.5–2°C) in the central and western GOA. This warming was associated with wind anomalies from the north; this kind of flow in summer tends to bring relatively warm and dry air off of mainland Alaska over the water, resulting in enhanced warming during this time of year.

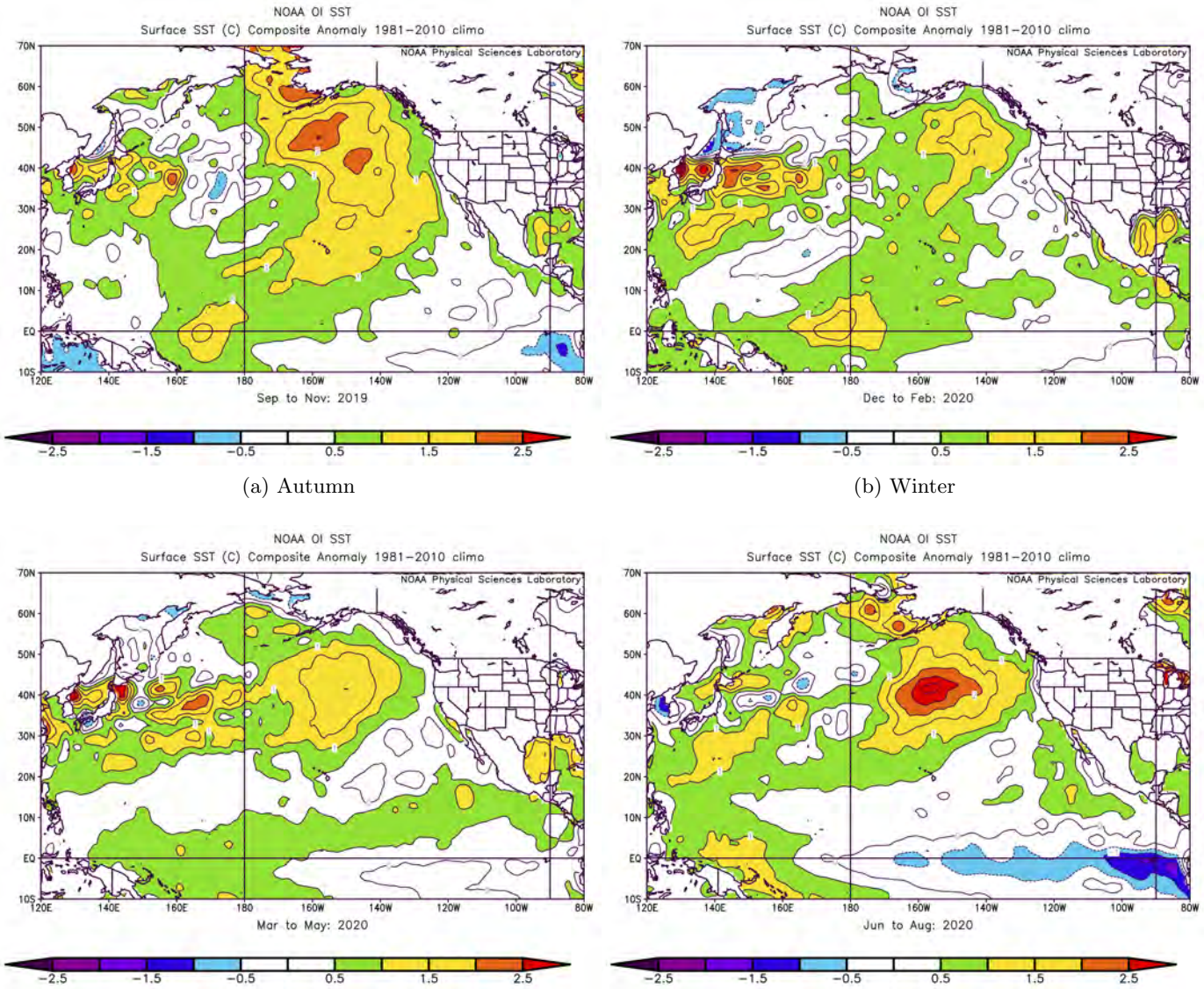

(a) Autumn (b) Winter

(c) Spring (d) Summer

Figure 28: SST anomolies for autumn (Sept–Nov 2019), winter (Dec 2019–Feb 2020), spring (Mar–May 2020), and summer (Jun–Aug 2020).

Bering Sea SST Trends and Anomalies
Contributed by Jordan Watson, *jordan.watson@noaa.gov*
Satellite SST data (source: NOAA Coral Reef Watch Program) were accessed via the NOAA CoastWatch West Coast Node ERDDAP server[7]. Daily data were averaged within the southeastern (south of 60°N) and northern (60°–65.75°N) Bering Sea shelf (10–200m depth). Detailed methods are available online[8].

SST Trends
Late winter 2019 SSTs were closer to the long-term mean, reaching -1.8°C in the NBS denoting ice cover. Above-average temperatures returned in spring and summer, especially over the southeastern shelf. Summer temperatures remained above average through October 25, 2020, similar to those observed in 2019 (Figure 29).

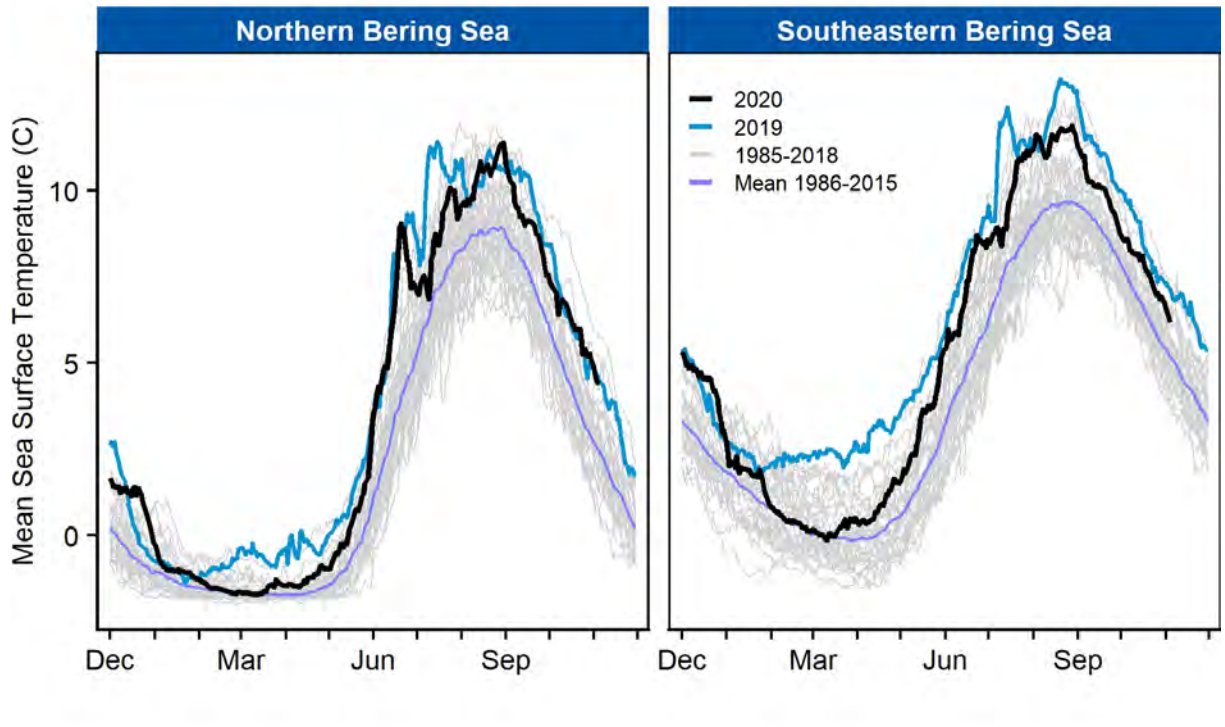

Figure 29: Mean SST for the northern (left) and southeastern (right) Bering Sea shelves. The most recent year (2019–2020; through Nov 4) is shown in orange, winter 2018/2019 is shown in blue, and the historical mean is shown in black. Individual years in the time series are shown in gray.

SST Time Series Trends
Trend analysis removed seasonality and noise from the SST time series (Edullantes, 2019) to better illustrate the long term trends in the SST data (Figure 30). Trends are compared to the mean (±1 SD) from a 30-yr baseline (1986–2015) and demonstrate that both the northern and southeastern Bering Sea are experiencing a persistent warm stanza, greater in both magnitude and duration than that of the early 2000s.

Marine Heatwave Index
Contributed by Jordan Watson, *jordan.watson@noaa.gov*
Please see Noteworthy contribution: 'Marine Heatwaves in the Eastern Bering Sea' (p. 42).

[7] `https://coastwatch.pfeg.noaa.gov/erddap/griddap/NOAA_DHW.html`
[8] `github.com/jordanwatson/EcosystemStatusReports/tree/master/SST`

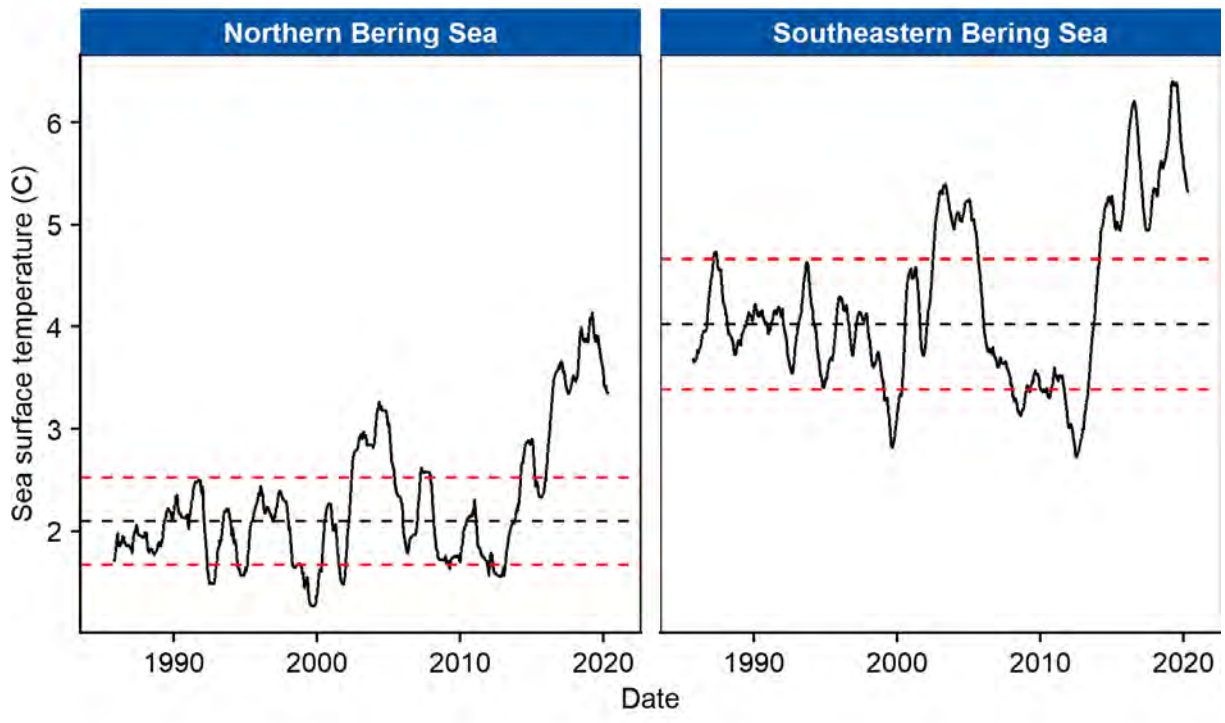

Figure 30: Time series trend of SST (seasonality and noise removed) for the northern (left) and southeastern (right) Bering Sea shelves. Black horizontal line is the 30-year mean (1986–2015) of the trend and red lines are ±1 SD.

St. Paul Island Temperature and Salinity

Contributed by Seth Danielson, Lauren Divine, Elizabeth Dobbins, and Aaron Lestenkof, *lmdivine@alaska.edu*

Temperature and salinity observations from North Dock on the St. Paul Island breakwater have been made since 2014 using CTD dataloggers (Figure 31). Instrumentation used since 2015 also had a sensor for chlorophyll-a fluorescence, which provides a measure of phytoplankton concentration. Water depth at the sample site is approximately 8m. Water column profiles are collected nominally weekly and have been averaged into monthly means here.

Trends

Water temperatures collected since 2014 from St. Paul Island indicate that 2016, 2018 (first half), and 2019 showed warmer water temperatures than the 6-year mean for most months while 2017, the latter half of 2018, and 2020 were relatively cool intervals. However, across the North Pacific as a whole, 2014 through 2020 has been appreciably warmer than the long-term average and the anomalies shown here all likely significantly underestimate the actual temperature offset relative to the climatology (e.g., Danielson et al. (2020)). Unlike 2018 and 2019 when the annual temperature minimum occurred in January, cooling of the water column in 2020 continued into March.

Salinity, however, shows an increasing trend over the time period. Contributing factors to salinity variability on the Bering Sea shelf include river discharge, precipitation, evaporation, ice advection, inflows from the Gulf of Alaska, and cross-slope exchanges with the basin (Aagaard et al., 2006). Instrument sensor drift over time is also possible; the root cause of the observed salinity trend is not presently understood but is under investigation.

Chlorophyll-a fluorescence measurements show year-to-year variations in the timing of the spring phytoplankton bloom. In particular, the bloom was not detected until May in 2019 and 2020, but the fluorescence did significantly increase above low winter values in April 2016, 2017, and 2018. The timing of phytoplankton bloom conditions has implications for zooplankton and microzooplankton blooms and grazing and growth rates.

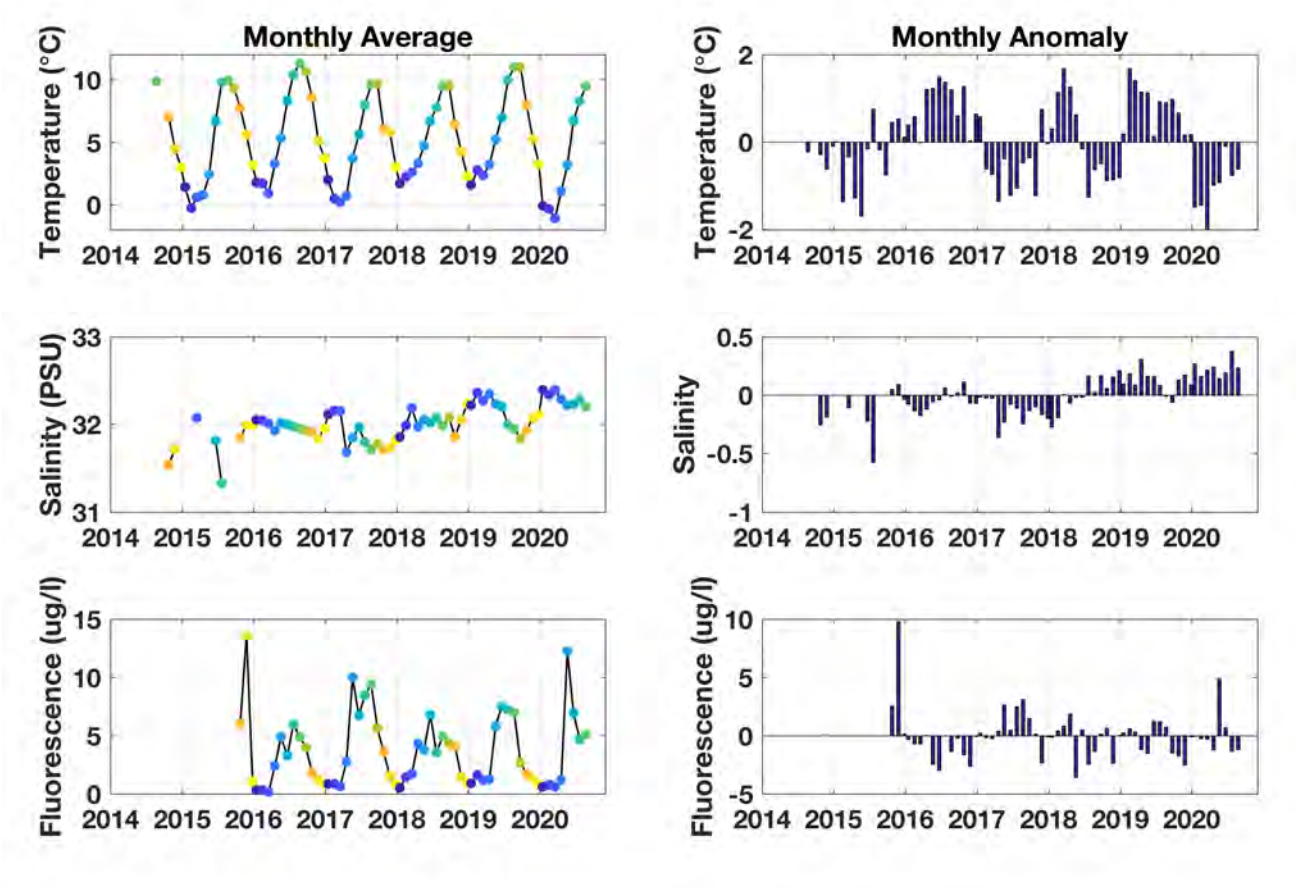

Figure 31: Temperature (top), salinity (middle), and chlorophyll-a fluorescence (bottom) measured at St. Paul Island. Left column shows monthly mean values over 2014–2020 and the right column shows monthly anomalies relative to 2014–2020. Colors in the left column delineate the month of year starting in January (blue) through December (yellow).

SST Projections from the National Multi-Model Ensemble
Contributed by Nick Bond, *nicholas.bond@noaa.gov*
Seasonal projections of SST from the National Multi-Model Ensemble (NMME) are shown in Figure 32a-c. An ensemble approach incorporating different models is appropriate for seasonal and longer-term simulations; the NMME represents the average of eight climate models. The uncertainties and errors in the predictions from any single climate model can be substantial. More detail on the NMME, and projections of other variables, are available at the National Weather Service Climate Prediction Center[9].

First, the projections from a year ago are reviewed. The model forecasts from August 2019 for the following fall and winter indicated a continuation of positive SST anomalies south of Alaska and moderation of the initially warmer conditions along the Alaska coast from the Alaska Peninsula to the SE Alaska panhandle. The sense of the evolution in the anomalies for the coastal waters of Alaska was correct, but for the models as a whole, the predictions indicated less cooling, relative to seasonal norms, than was observed. In addition, the models predicted winter conditions that were warmer than observed for the Bering Sea shelf; the longer-term forecasts for late winter into spring were superior. Anomalies of weak to moderate magnitude were forecast and observed for the Aleutian Island region, with the model forecasts being too warm in the western portion. With regards to the tropical Pacific, the models failed to fully account for the weak central Pacific El Niño that was present in fall 2019 into early 2020, but did properly predict near neutral conditions in spring 2020. Qualitatively, these model projections do not have quite as much overall skill as in the previous 4 years, but the signs of the SST anomalies were forecast correctly for most locations.

The NMME forecasts of three-month average SST anomalies indicate a continuation of a large region of warm water between Alaska and the Hawaiian Islands through the end of 2020 (Oct–Dec 2020; Figure 32a). Positive anomalies are predicted for the entire Bering Sea and north of Bering Strait, with a peak value in the Chukchi Sea off the coast of northwest Alaska. The latter can probably be attributed to a predicted delay in sea ice formation, which is highly plausible given the very low sea ice extent in the central Arctic during summer 2020. The predictions also indicate warm SSTs for the Alaska Peninsula and Aleutian Islands. Conversely, the coastal waters of the GOA are predicted to have near normal temperatures. A band of cold SST is projected in the tropical Pacific commensurate with that of a weak-moderate La Niña.

The overall pattern of SST anomalies across the North Pacific is maintained through the periods of December 2020–February 2021 (Figure 32b) and February–April 2021 (Figure 32c) with mostly decreases in the magnitude of anomalies, especially on the eastern Bering Sea shelf. The near coastal waters of the GOA are forecast to become slightly cooler than normal, consistent with atmospheric circulation anomalies being forecast for the North Pacific that feature a weaker Aleutian low than usual (i.e., positive SLP anomalies south of the Alaska Peninsula). The SLP pattern being forecast is similar to what was observed in the winter of 2019–2020 but of considerably weaker amplitude (not shown). La Niña does tend to be accompanied by atmospheric anomalies resembling those associated with the sets of predictions shown here, but it is uncertain whether the perturbation in the tropical Pacific will yield a substantial response in the North Pacific. The model forecasts indicate a moderation of cold conditions in the tropical Pacific by spring 2021. Coming out of the winter of 2020–2021, they suggest mostly near normal temperatures along the coast from British Columbia to the Alaska Peninsula, modestly warm conditions on the eastern Bering Sea shelf (i.e., light ice year), and slightly warm SSTs for the central and western Aleutian Islands.

[9] `http://www.cpc.ncep.noaa.gov/products/NMME/`

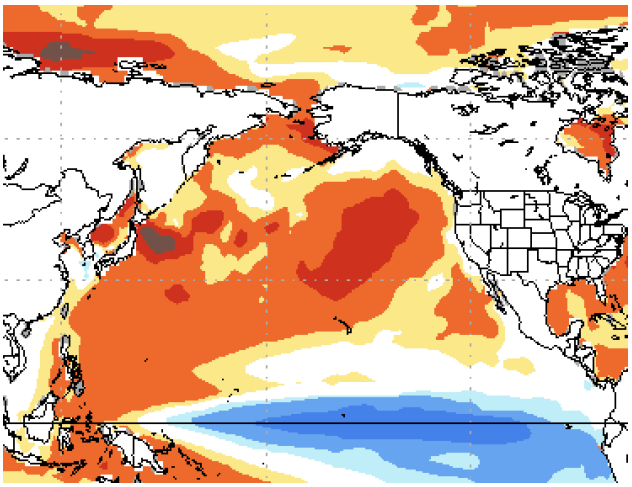

(a) Months Oct–Nov–Dec

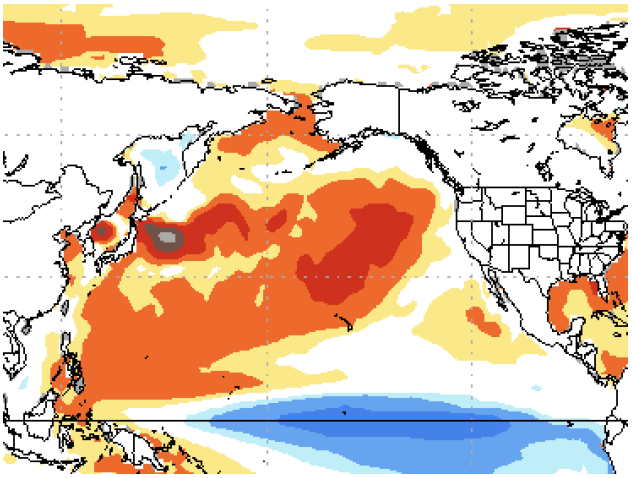

(b) Months Dec–Jan–Feb

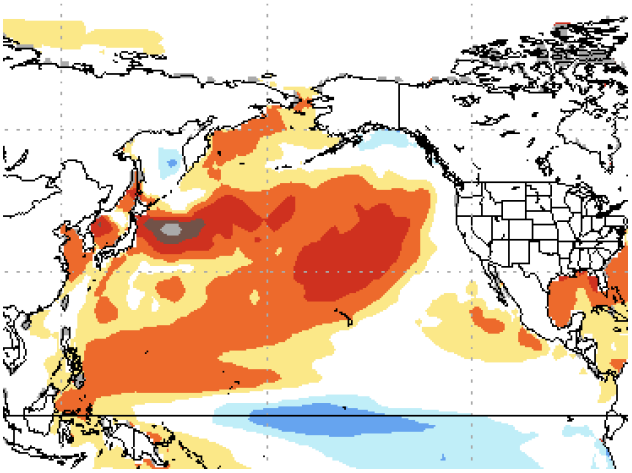

(c) Months Feb–Mar–Apr

Figure 32: Predicted SST anomalies from the NMME model for Oct–Nov–Dec (1-month lead), Dec–Jan–Feb (3-month lead), and Feb–Mar–Apr (5-month lead) for the 2020–2021 season.

6. Bottom Temperature

ROMS Modeled Bottom Temperature
Contributed by Kelly Kearney, *kelly.kearney@noaa.gov*
The Bering 10K Regional Ocean Modeling System (ROMS) hindcast simulation was extended to the near-present, using reanalysis-based input forcing. This hindcast simulation now extends from 15 Jan 1970–15 Aug 2020.

Trends
The Bering 10K hindcast simulation places 2020 as an average year, with slightly more <2°C water and slightly less than average <0°C water within the standard bottom trawl survey area at the beginning of July. This is in contrast to 2018 and 2019, which were two of the warmest years in this simulation period (Figure 33).

Examining the evolution of bottom temperatures between November of the previous year through the beginning of August, 2020 most closely resembles 1997. Both years were preceded by a warm year, with almost no water less than 2°C on the shelf at the start of the preceding winter. Throughout the winter, <2°C water fractions increased to above average levels, peaking in mid-May and remaining at just above average quantities into late summer. The <0°C water followed a similar pattern through May, but then dropped rapidly and nearly disappeared by the end of summer. A similar pattern was observed in the 2°C water a handful of other years (1971, 1974, 1992, and 1999), but the <0°C water did not see the same sharp summer decline in these years as in 1997 and 2020. In addition, 1997 and 2020 follow very similar trends when we examine bottom temperatures at the locations of the M2 and M8 moorings.

In terms of summer spatial patterns across the entire southeastern Bering Sea shelf, 2020 falls into a cluster of years with average to above-average 2°C water and average to below-average 0°C water, including 1995, 1997, 2000, and 2011.

Eastern Bering Sea Cold Pool Observations
Contributed by Phyllis Stabeno, *phyllis.stabeno@noaa.gov*
With the cancellation of most of the cruises to the eastern Bering Sea in 2020 there are few measurements of bottom temperature. The cold pool extent is largely determined by ice extent. Maximum sea-ice extent was fairly typical in 2020, so the expectation was that the cold pool in 2020 would be average. The comparison of bottom temperatures measured on NOAA Ship *Oscar Dyson* in September to the ROMS Bering 10K model hindcast for 15 August (latest available) showed good correlation over the northern shelf, but observed temperatures over the southern shelf were warmer than predicted. Based on observed temperatures, the cold pool (defined as <2°C) extended to ∼59°N (Figure 34).

The vertical structure of the water column on the eastern Bering Sea shelf was fairly typical in 2020, with a warm surface layer, colder bottom layer, and a sharp interface (Figure 35).

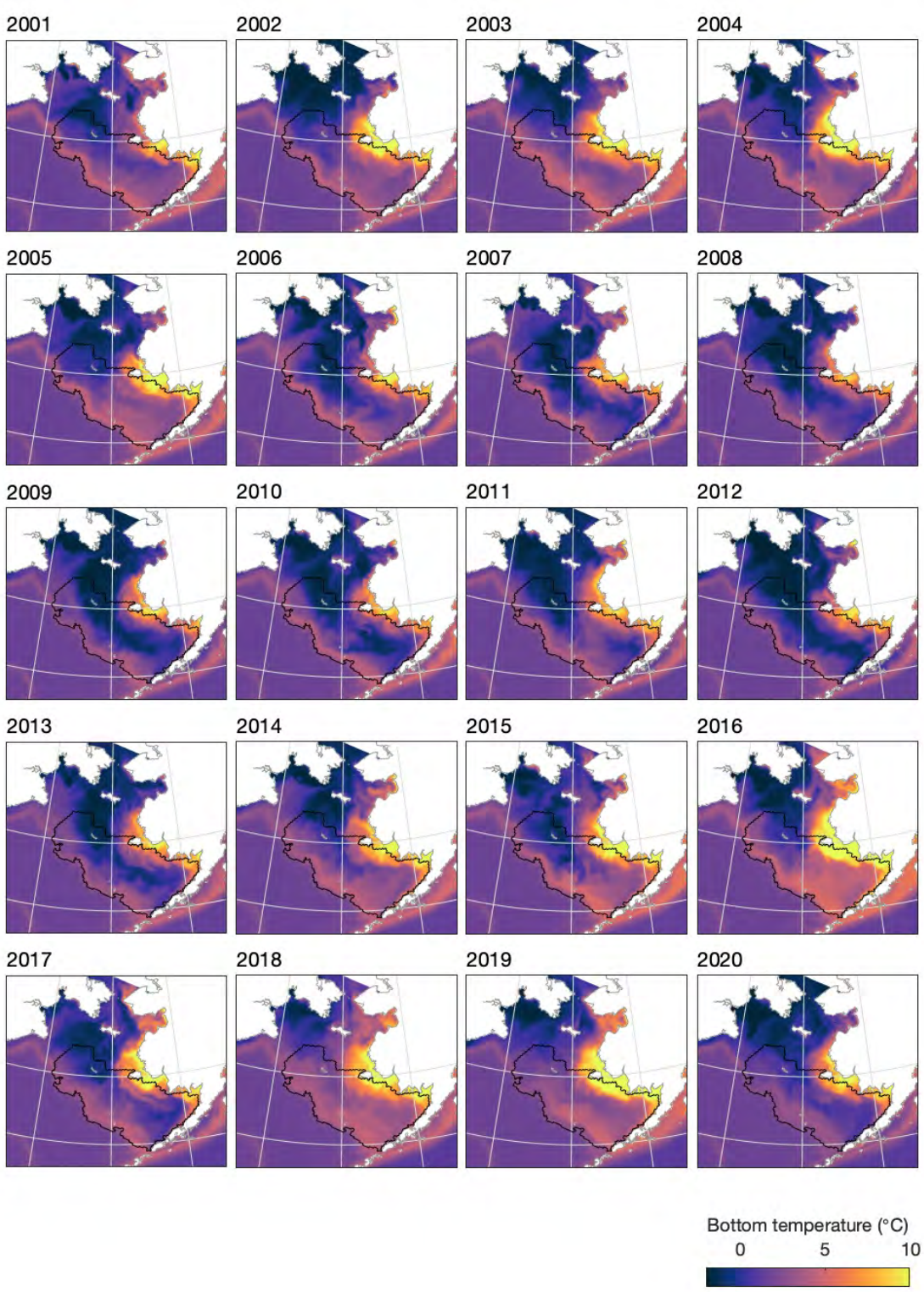

Figure 33: Bering 10K ROMS hindcast of bottom water temperature, extracted on July 1 of each year, for the Bering Sea, 2001–2020. The black outline denotes the standard bottom trawl survey grid.

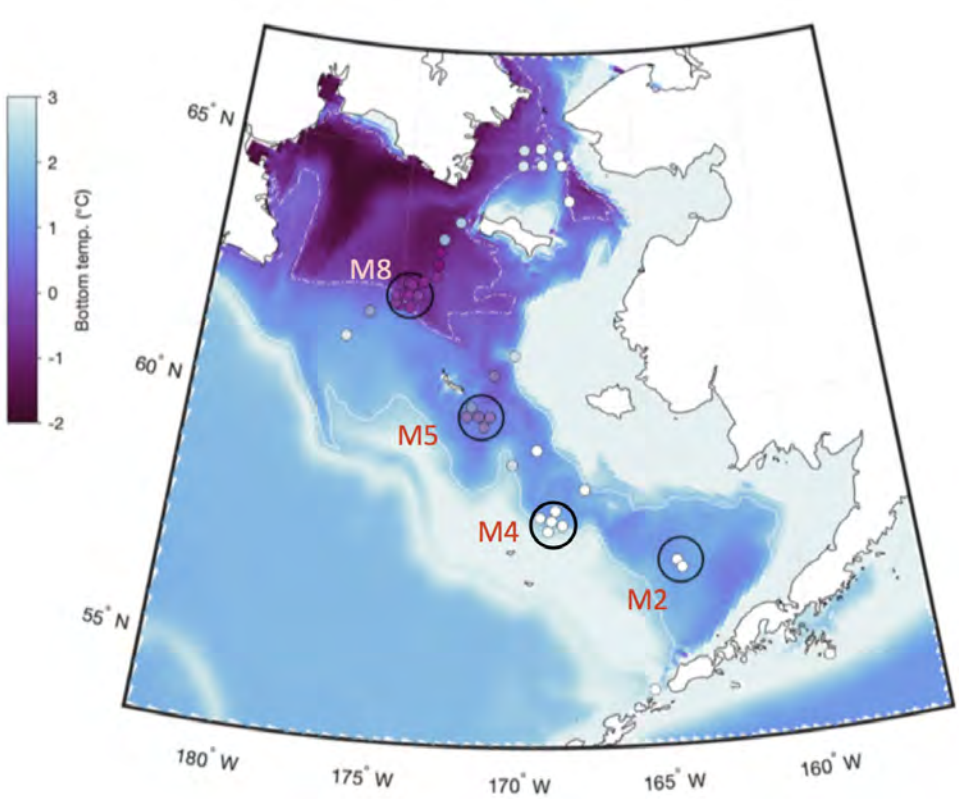

Figure 34: The background map is the Bering 10K ROMS hindcast for 15 August 2020. The small colored circles are the observed bottom temperatures measured on NOAA Ship *Oscar Dyson* during the first three weeks of September 2020.

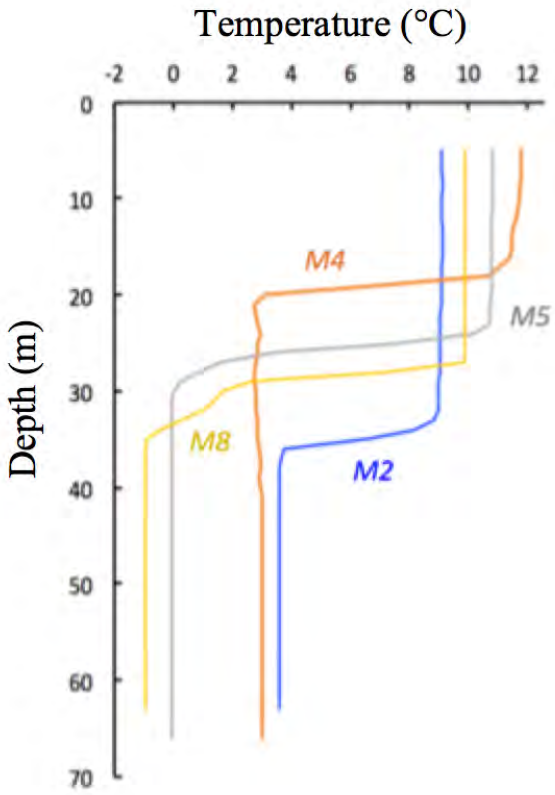

Figure 35: Vertical temperature profiles at four long-term mooring sites in September 2020. M4, M5 and M8 were sampled in early September and M2 in mid-September.

Habitat

There are no updates to Habitat indicators in this year's report. See the contribution archive for previous indicators at: `https://access.afsc.noaa.gov/REFM/REEM/ecoweb/`.

Primary Production

Spring Satellite Chlorophyll-a Concentrations in the Eastern Bering Sea

Contributed by Jens M. Nielsen[1], Lisa Eisner[2], Jordan Watson[2], Jeanette C. Gann[2], Calvin W. Mordy[3,4], Shaun W. Bell[3,4], Colleen Harpold[1], Deana Crouser[1], and Phyllis Stabeno[3]
[1]Resource Assessment and Conservation Engineering Division, Alaska Fisheries Science Center, NOAA Fisheries
[2]Auke Bay Laboratories, Alaska Fisheries Science Center, NOAA Fisheries
[3]Pacific Marine Environmental Laboratory, NOAA Research, Seattle, WA, USA
[4]Cooperative Institute for Climate, Ocean, and Ecosystem Studies (CICOES), University of Washington, Seattle, WA
Contact: jens.nielsen@noaa.gov
Last updated: October 2020

Description of indicator: In subarctic systems, such as the Bering Sea, the timing and magnitude of the spring bloom can have high and long-lasting effects on biological production which impact higher trophic level species including commercial fish stocks (Platt et al., 2003). The fate of the spring bloom, its timing, and species composition also impact benthic grazers in the Bering Sea (Hunt et al., 2002). Recent climatic changes in the Bering Sea have resulted in reduced sea ice and warming ocean temperatures (Stabeno and Bell, 2019), with consequent changes to the pelagic food web (Duffy-Anderson et al., 2019). Understanding annual changes in spring phytoplankton biomass and peak timing dynamics are thus important metrics for depicting ecosystem changes.

Here, we used ocean color satellite data from 2003–2020 available from MODIS at a 4x4 km resolution and aggregated as 8-day composites[10] to estimate: 1) average spring (Apr–Jun) chlorophyll-a concentrations (chl-a, an estimate of phytoplankton biomass), and 2) peak timing of the spring open water bloom for major regions in the eastern Bering Sea. In the southeastern Bering Sea, sustained observations at the M2 mooring (56.9°N, -164.1°W) provide good representation of the south middle shelf biophysical conditions. Thus, the long-term fluorescence mooring measurements were compared to the bloom peak timing estimates calculated from the satellite data.

We focus on the spring period as this is an important time for providing basal resources for zooplankton and thus energy for higher trophic level species. The April–June time-period was chosen as this period consistently include the pelagic spring bloom peak. We further divided the Bering Sea into 8 distinct regions split between approximately north and south of 60°N and defined by oceanographic fronts and water mass characteristics based on Ortiz et al. (2012) (Figure 36). There are several advantages of satellite data, including high spatial and temporal coverage. However, these products are also limited to measurements within the surface ocean and also have missing data due to ice and cloud cover, particularly in high latitude systems such as the Bering Sea. We used 8-day composite data to fill some of these data gaps but doing so also introduces an inherent uncertainty of 8 days in the timing of processes (e.g., peak timing).

Open water spring bloom peak timing was estimated for individual ADF&G groundfish statistical areas[11] (~0.5° lat x 1° lon) and then calculated the average and standard deviation of all estimated bloom peaks within a specific region, which allowed for calculation of variability for each of the 8 areas. ADF&G statistical areas are smaller than the 8 shelf regions so by using the ADF&G areas, we could better assess the range of bloom timing within each shelf region. ADF&G areas with less than 66% seasonal coverage were excluded.

Status and trends: There was a high degree of interannual variability in satellite chl-a from 2003–2020. Both the south inner and south middle shelf had below average values in 2020, similar to values in the period 2016–2019. Values in the south outer shelf region were above average in 2020, while being slightly below

[10] coastwatch.pfeg.noaa.gov/erddap/griddap/erdMBchla8day.html
[11] http://www.adfg.alaska.gov/index.cfm?adfg=fishingCommercialByFishery.statmaps

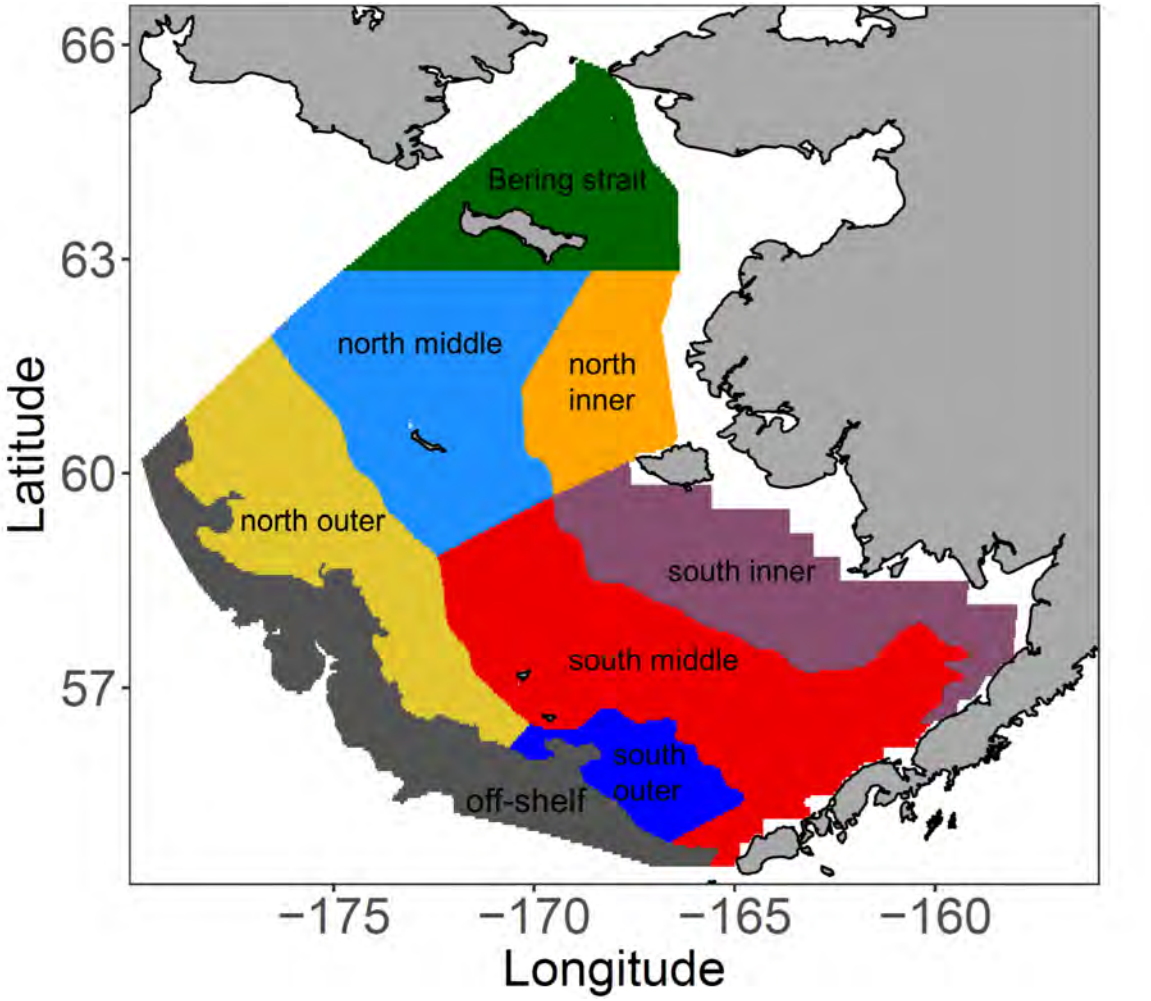

Figure 36: Map of the 8 shelf regions used for satellite chl-a analyses: south inner (purple), south middle (red), south outer (darkblue), off-shelf (darkgrey), north inner (orange), north middle (light blue), north outer (yellow), and the Bering Strait (darkgreen).

the long term average in both the north inner and north middle shelf region. Values along the shelf edge (off-shelf region) were low in 2020, continuing an apparent decreasing trend since 2014 (Figure 37). Data coverage in the southern regions was generally good across all years, however further north, in some years data from April were particularly scarce due to extended ice coverage (Figure 38). Consequently, averages in spring should be considered with caution during the years when coverage was limited.

Preliminary analyses of the pelagic spring bloom peak timing suggest that 2020 was similar to 2019 for the south inner and south middle shelf regions (Figure 39), and about a week earlier than the long-term average spring peak timing. For most regions the bloom peaks in 2020 were slightly earlier compared to the long-term average. This contrasts with 2018 which was among the latest in the time-period, while 2017 conversely was among the earliest for most regions. For the south middle shelf region, peak bloom timing estimated from the satellite data generally concurred well with estimates from the M2 mooring fluorescence data. One exception was 2016 during which the mooring data showed a much earlier peak than the average peak satellite chl-a timing. In the off-shelf region the bloom peak in 2020 was among the earliest recorded. However, the magnitude of off-shelf spring chlorophyll-a concentrations were low overall (Figure 39). Due to lack of consistent data coverage no bloom satellite peak estimates were done for the northern regions.

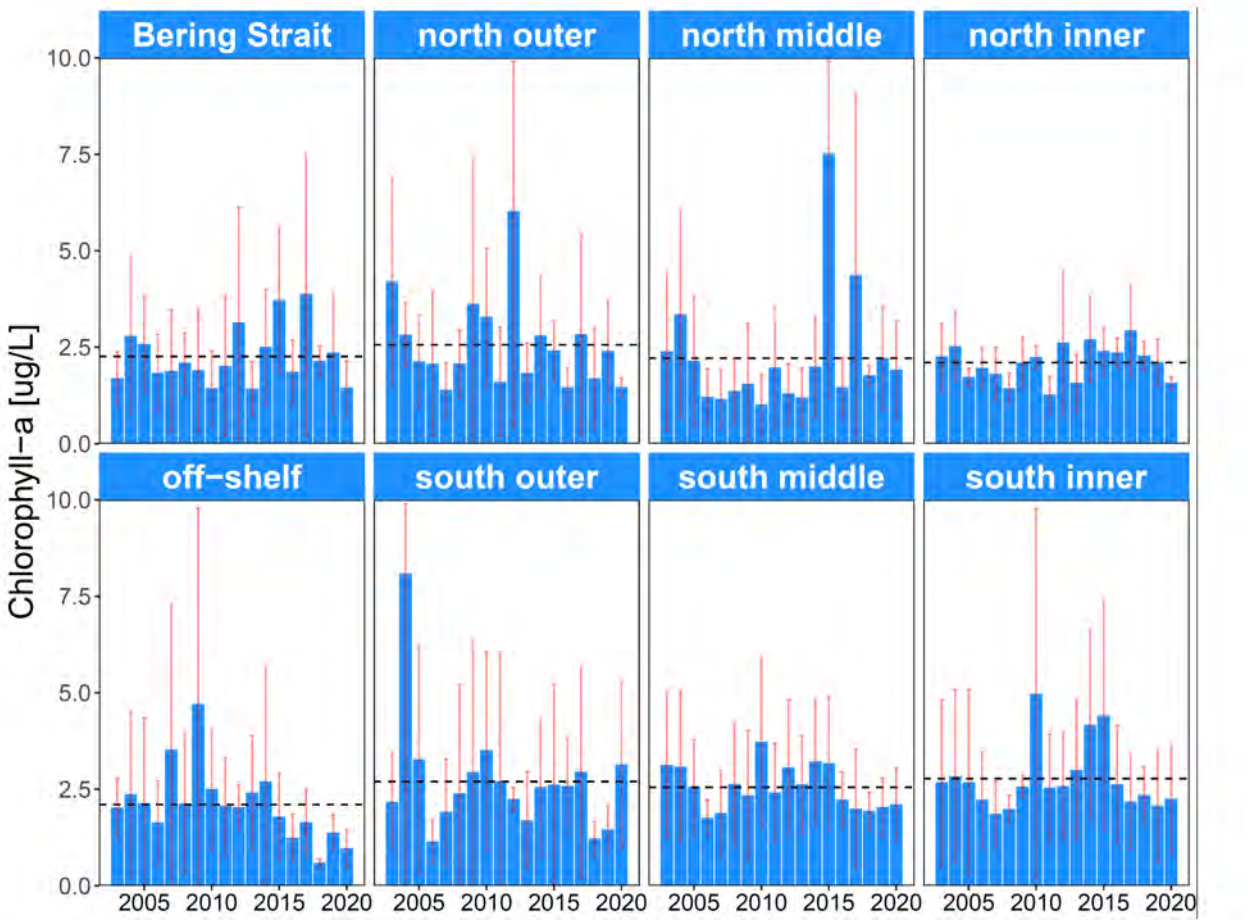

Figure 37: Average and standard deviation (SD) from spring (Apr–Jun) chlorophyll-a concentrations for 8 regions in the Bering Sea. Dotted black line denotes the long-term (2003–2020) average for each region. **Note:** For plotting purposes, the minimum error bar is set at 0.01 and the maximum at 9.99. Chl-a concentrations <0 do not make biological sense. In a few cases, the +standard deviation was >10 (south outer in 2004 was 18.9; north middle in 2015 was 13.8; south outer in 2012 was 11.6).

Factors influencing observed trends: Previous studies have highlighted the strong coupling between temperature and sea ice dynamics and bloom timing. For example, in the southern Bering Sea, ice present after mid-march commonly results in an early and prominent ice-associated bloom, while lack of ice normally results in a delayed open water bloom in mid- to late-May (Sigler et al., 2014). In the southern middle shelf, we observed an earlier spring bloom in the cold years of 2007–2012 (excluding 2009) and in the average temperature years of 2013 and 2017. However, spring bloom timing varied considerably in recent warm years (2018–2020), suggesting that the timing of the bloom was impacted by other factors besides ice. Nutrients on the shelf also influence the magnitude of the bloom (Stabeno et al., 2016) and it is unclear whether changed oceanographic patterns and thus potentially nutrient supply also played a regulating role on the spring bloom timing and magnitude during recent years with low ice coverage. For open water blooms, variations in springtime winds may impact the setup of stratification (e.g., higher winds can delay stratification, Stabeno et al. (2016)), which in turn impacts light availability and the timing of the spring phytoplankton bloom. Analysis of chl-a biomass, though informative in depicting bloom timing during spring, does not directly provide information of primary productivity (growth rates), though biomass levels in spring generally align well with the timing of production peak timing estimates. Since biomass is a balance between production and losses, lower biomass levels could also indicate enhanced grazing by microzooplankton and mesozooplankton.

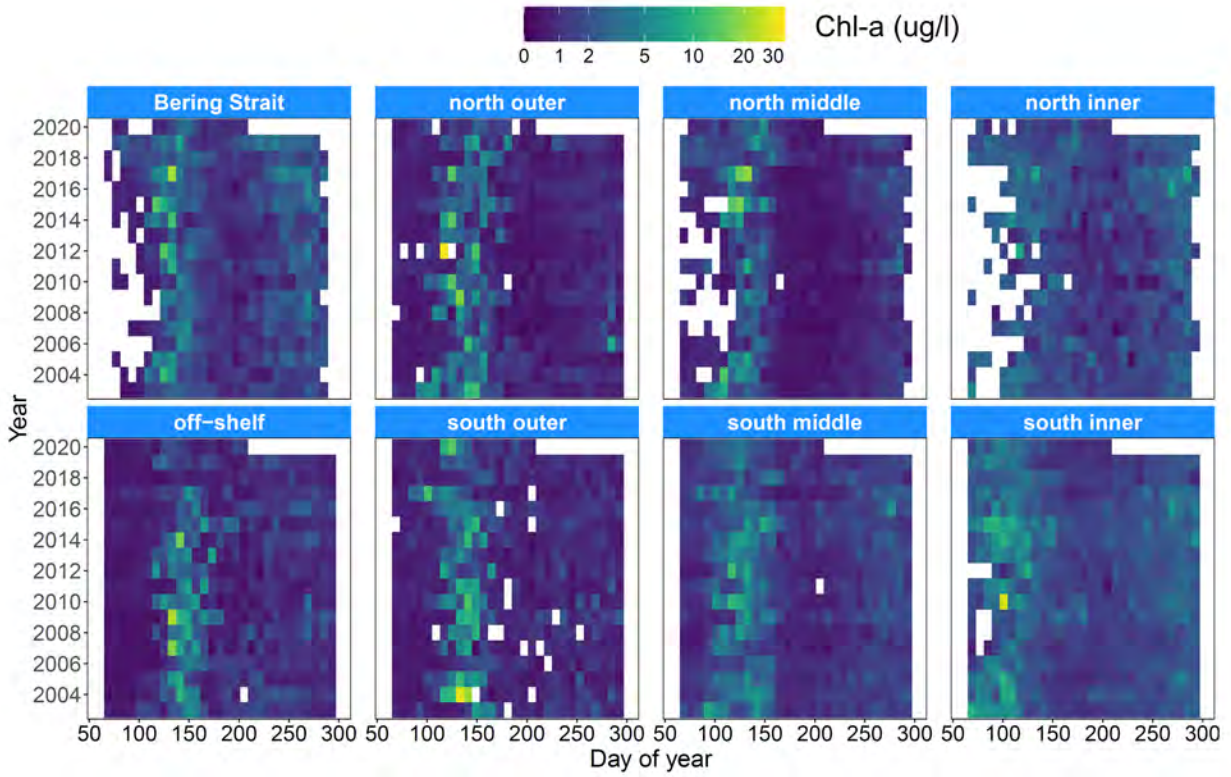

Figure 38: Heatmap of satellite 8-day composite chlorophyll-a concentrations for each year and region. Color scale is logged.

Implications: Primary producers provide fundamental energy and nutrients for zooplankton grazers and higher trophic level species. Understanding how climatic perturbations, and particularly the recent warm period, influence phytoplankton dynamics is a critical component in understanding ecosystem dynamics in the Bering Sea. Large, lipid-rich copepods, *Calanus* were in higher abundance in summer 2017 (see p. 82), a year with an early spring bloom (and average ice cover), which may have offered an early food resource for reproduction and survival. Our analyses also showed no significant long-term change in the bloom peak timing among low and high ice years combined. However if warming temperatures during winter and spring accelerate development rates of zooplankton (Coyle and Gibson, 2017) it may also reduce the duration of zooplankton diapause leading to earlier emergence (Pierson et al., 2013), thus the timing of the spring bloom still have important implications for consuming organisms such as zooplankton, and in turn their predators such as fish larvae. Reduction of sea ice, and thus lack of ice associated phytoplankton blooms also shifts the community composition in favor of pelagic phytoplankton species over of ice algae; changes that likely have strong impacts on benthic-pelagic energy fluxes (Hunt et al., 2002) and the nutritional composition of basal resources for consumers. The declining trends in chl-a biomass in the offshore region deserves further investigation. This area includes the "greenbelt", a known area of high production (Springer et al., 1996), and it will be important to understand the mechanism behind these apparent changes.

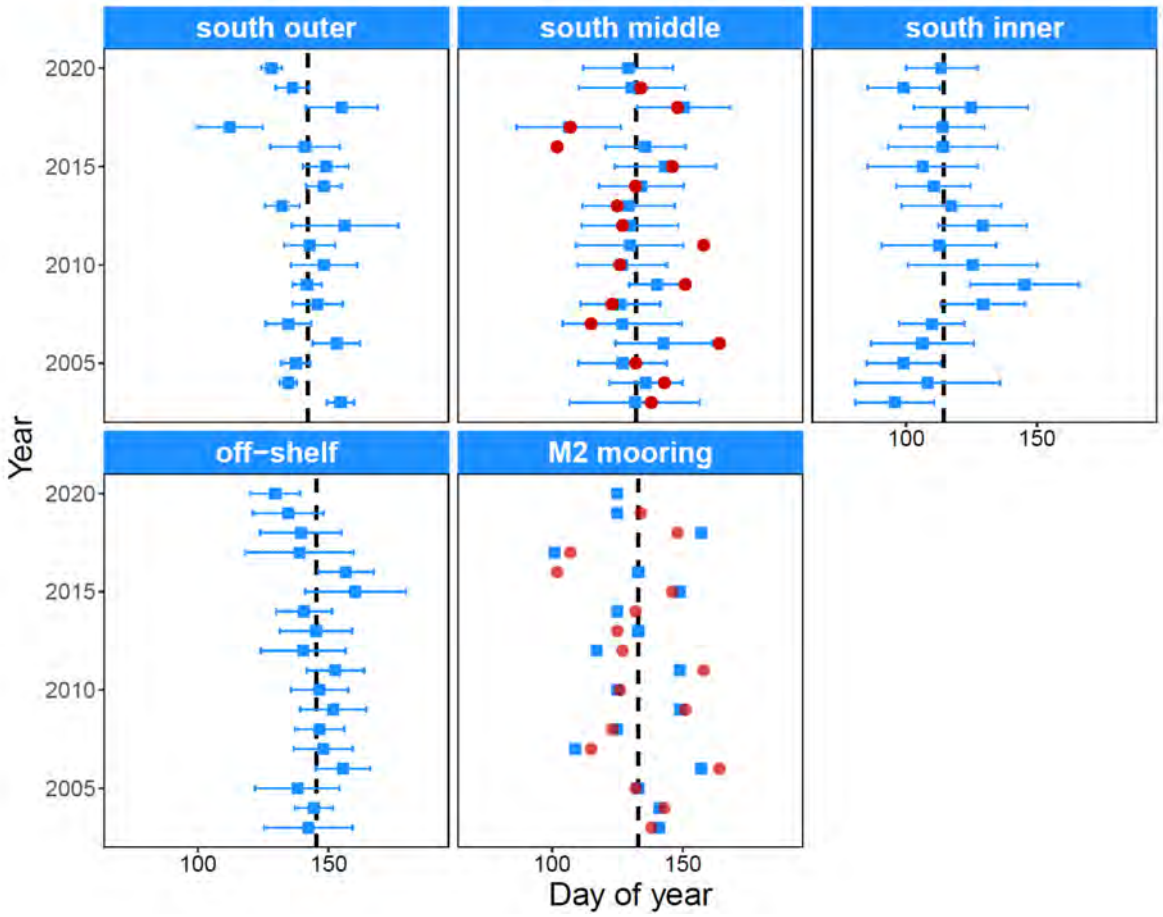

Figure 39: Average and SD of peak spring bloom timing estimated from individual ADF&G groundfish statistical areas within 4 southern regions in the Bering Sea. Red dots are the M2 mooring fluorescence peak timing estimates, which are compared to both the south middle shelf data and specifically to satellite data near M2 [1° lat x 1° lon].

Coccolithophores in the Bering Sea

Contributed by Carol Ladd[1] and Lisa Eisner[2]
[1]NOAA/PMEL, Building 3, 7600 Sand Point Way NE, Seattle, WA 98115-6349
[2]Auke Bay Laboratories, Alaska Fisheries Science Center, National Marine Fisheries Service, NOAA
Contact: carol.ladd@noaa.gov
Last updated: October 2020

Description of indicator: Blooms of coccolithophores, a unicellular calcium carbonate-producing phytoplanktonic organism, are easily observed by satellite ocean color instruments due to their high reflectivity. Coccolithophores produce calcium carbonate plates (coccoliths) that contribute to particulate inorganic carbon (PIC) in the ocean (Matson et al., 2019). Blooms are most commonly observed and cloud cover is typically lower during September than other months allowing for better quantification (Iida et al., 2012). An interannual index of the average area (km^2) covered by coccolithophores during the month of September is calculated with monthly average mapped PIC (Balch et al., 2005; Gordon et al., 2001) data from satellite. The indices calculated from MODIS-Aqua satellite data (2002–2019) and from the VIIRS-SNPP satellite (2012–2020) provided by NASA Goddard Space Flight Center, Ocean Ecology Laboratory (MODIS-Aqua, 2018) are highly correlated and both are presented here for continuity.

PIC >0.0011 mol/m^3 was used to estimate the location of the influence of coccolithophore blooms. This threshold was derived by Matson et al. (2019). Highly reflective waters in shallow water near the coast can be due to re-suspended diatom frustules rather than coccoliths (Broerse et al., 2003). Thus, the index is calculated from the region south of 60°N and deeper than 30m depth to avoid contamination by shallow regions around St. Matthew and St. Lawrence Islands and along the Alaskan coast, as well as sediment associated with the Yukon River. Because blooms are often largely confined to either the middle shelf or the inner shelf (Ladd et al., 2018), two indices are calculated: one for the middle shelf (50–100m depth) and one for the inner shelf (30–50m depth).

Note that the methodology for calculating the index has changed since the 2017 contribution. Because the index represents only a monthly estimate of spatial area influenced by coccolithophore blooms (and not more rigorous biomass or other biogeochemical estimates), it was determined that PIC provided the necessary information and is easily available data. Correlation with the previous index is R^2=0.98.

Before 1997, coccolithophore blooms in the eastern Bering Sea were rare. A large bloom (primarily *Emiliania huxleyi*) occurred in 1997 (Napp and Hunt, 2001; Stockwell et al., 2001)and for several years thereafter. During the 1997 bloom, the bloom was associated with a die-off of short-tailed shearwaters (*Puffinus tenuirostris*), a seabird commonly seen in these waters (Baduini et al., 2001). It was thought that the bloom may have made it difficult for the shearwaters to see their zooplankton prey from the air (Lovvorn et al., 2001). Since then, coccolithophore blooms in the eastern Bering Sea have become more common. Satellite ocean color data suggest that blooms are only found where water depths are between 20 and 100m. Blooms typically peak in September and interannual variability is related to both very weak and strong stratification (Iida et al., 2012; Ladd et al., 2018).

Status and trends: Annual images (Figure 40) show the spatial and temporal variability of coccolithophore blooms in September. Annual indices are obtained from satellite data by averaging spatially over the inner and middle shelf (Figure 41). Coccolithophore blooms were particularly large during the early part of the record, 1997–2000 (not shown). At the start of the MODIS-Aqua record, the index was low and remained low (<50,000 km^2) through 2006. In 2007, the index rose to almost double that observed in 2006 (∼102,000 km^2). A higher index (>50,000 km^2) was observed in 2007, 2009, 2011, 2014, 2016, and 2020 for the middle shelf and in 2011 and 2014 (>20,000 km^2) for the inner shelf. September 2017 exhibited the lowest index of the record. The bloom index remained below average in 2018 and 2019 but increased, particularly on the middle shelf, in 2020.

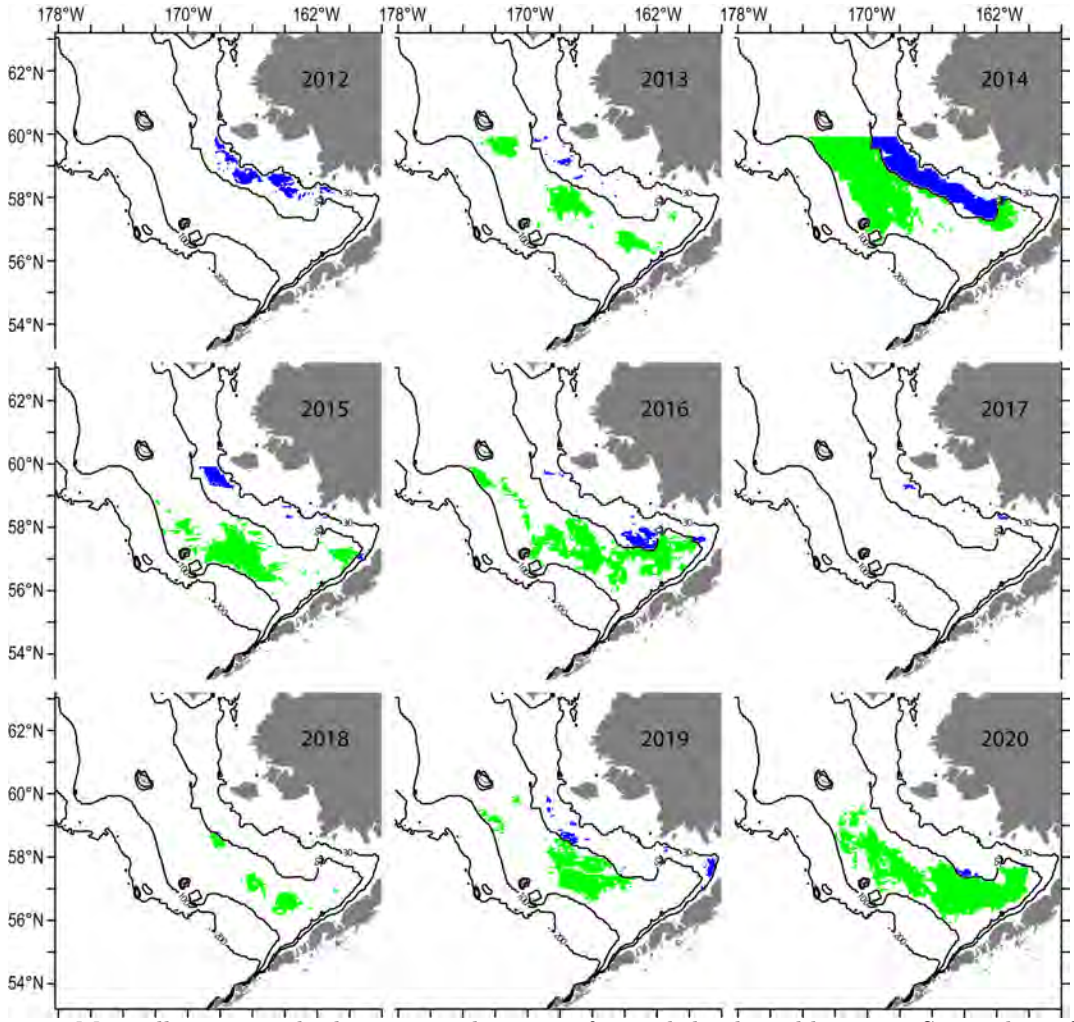

Figure 40: Maps illustrating the location and extent of coccolithophore blooms in September of each year from VIIRS-SNPP data. Color: satellite ocean color pixels exceeding the threshold indicating coccolithophore bloom conditions. Bloom conditions over the inner shelf are shown in blue; bloom conditions over the middle shelf are shown in green. These data are used to calculate the areal index in Figure 41.

Factors influencing observed trends: It has been suggested that the strength of density stratification is the key parameter controlling variability of coccolithophore blooms in the eastern Bering Sea (Iida et al., 2012; Ladd et al., 2018). Stratification influences nutrient supply to the surface layer. Stratification in this region is determined by the relative properties (both temperature and salinity) of two water masses formed in different seasons, the warm surface layer formed in summer and the cold bottom water influenced by ice distributions the previous winter. Thus, the strength of stratification is not solely determined by summer temperatures and warm years can have weak stratification and vice versa (Ladd and Stabeno, 2012).

Implications: Coccolithophore blooms can have important biogeochemical implications. The Bering Sea can be either a source or a sink of atmospheric CO_2, with the magnitude of coccolithophore blooms and the associated calcification playing a role (Iida et al., 2012)). In addition, variability in the dominant phytoplankton (diatoms vs. coccolithophores) is likely to influence trophic connections with the smaller coccolithophores resulting in longer trophic chains. Coccolithophores may be a less desirable food source for microzooplankton in this region (Olson and Strom, 2002). As noted previously, the striking milky aquamarine color of the water during a coccolithophore bloom can also reduce foraging success for visual predators.

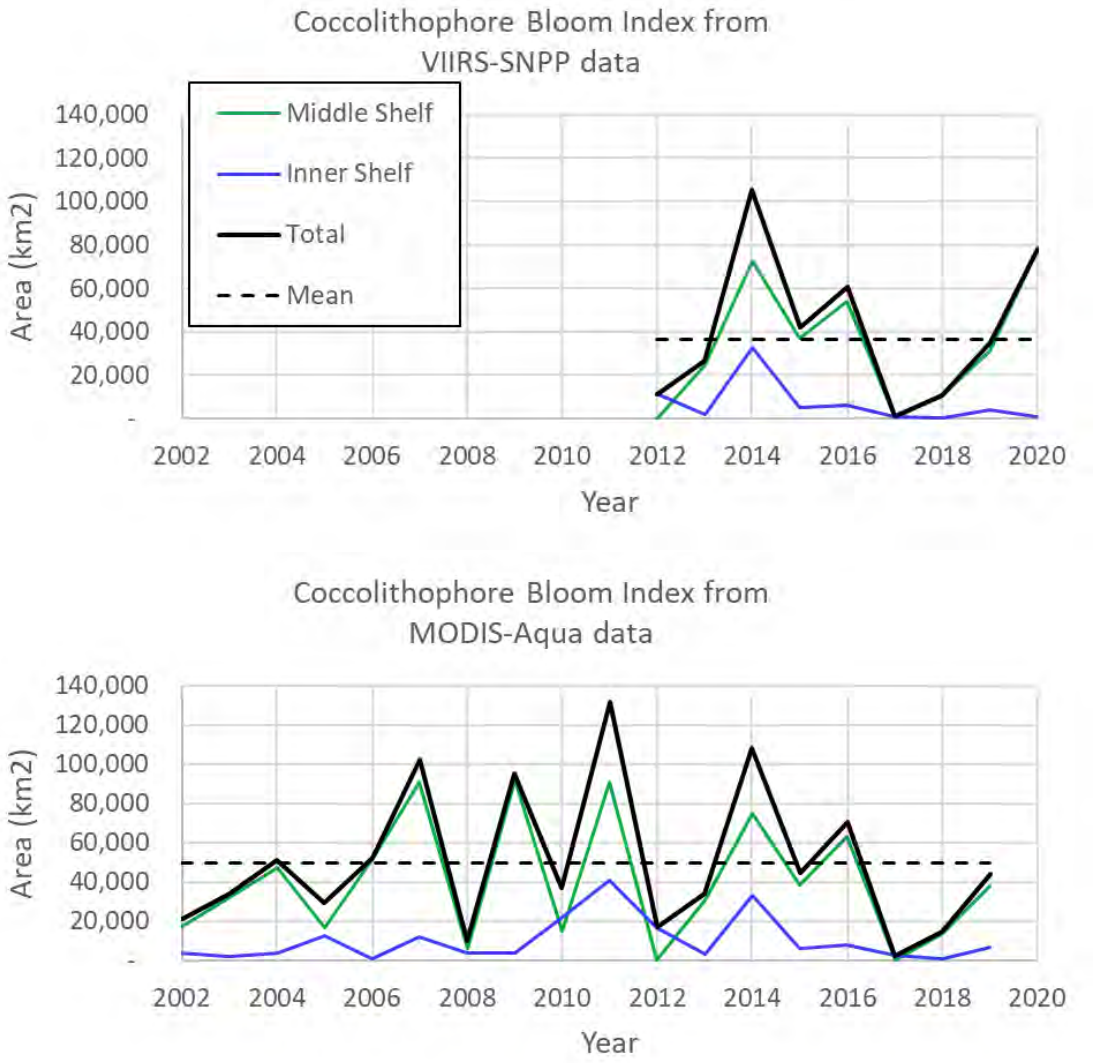

Figure 41: Coccolithophore index for the southeastern Bering Sea shelf (south of 60°N). Top panel shows index calculated from VIIRS-SNPP satellite; bottom panel shows index calculated from MODIS-Aqua satellite. Blue: average over the inner shelf (30–50 m depth), Green: average over the middle shelf (50–100 m depth), Black: Total. At the time of writing MODIS-Aqua data for 2020 were not yet available.

Zooplankton

Current and Historical Trends for Zooplankton in the Bering Sea

Contributed by David Kimmel[1], Lisa Eisner[2], Colleen Harpold[1], and Deana Crouser[1]
[1]Resource Assessment and Conservation Engineering Division, Alaska Fisheries Science Center, NOAA Fisheries
[2]Auke Bay Laboratories, Alaska Fisheries Science Center, NOAA Fisheries
Contact: david.kimmel@noaa.gov
Last updated: September 2020

Description of indicator: In 2015, AFSC implemented a method for an at-sea Rapid Zooplankton Assessment (RZA) to provide leading indicator information on zooplankton composition in Alaska's Large Marine Ecosystems. The rapid assessment, which is a rough count of zooplankton (from paired 20/60 cm oblique bongo tows from 10m from bottom or 300 m, whichever is shallower), provides preliminary estimates of zooplankton abundance and community structure. The method employed uses coarse categories and standard zooplankton sorting methods (Harris et al., 2000). The categories are small copepods (< 2 mm; example species: *Acartia* spp., *Pseudocalanus* spp., and *Oithona* spp.), large copepods (> 2mm; example species: *Calanus* spp. and *Neocalanus* spp.), and euphausiids (< 15 mm; example species: *Thysanoessa* spp.). Small copepods were counted from the 153 μm mesh, 20 cm bongo net. Large copepods and euphausiids were counted from the 505 μm mesh, 60 cm bongo net. Other, rarer zooplankton taxa were present but were not sampled effectively with the on-board sampling method.

RZA abundance estimates may not closely match historical estimates of abundance as methods differ between laboratory processing and ship-board RZA, particularly for euphausiids which are difficult to quantify accurately (Hunt et al., 2016). Rather, RZA abundances should be considered estimates of relative abundance trends overall. Detailed information on these taxa is provided after in-lab processing protocols have been followed (1 year post survey).

Here, we show updated long-term time series for the middle shelf of the southeastern Bering Sea for spring and summer, as well as a new time series developed for the northern Bering Sea. The mean abundance of each RZA category was plotted for the southern middle shelf of the Bering Sea (Ortiz et al., 2012) and represented primarily April and May in spring and August, September, and October in summer/fall as the months with the greatest sampling frequency. The northern Bering Sea time series was developed from samples collected in an area bounded by 60–63.5°N and 165–171°W and sampling occurred in late August/early September. Plots show the historical, archived abundance estimates from laboratory processed samples and on-board RZA estimates.

Status and trends:
Southeastern Bering Sea
No research surveys were conducted in 2020, therefore no RZA data were collected. Large copepods show considerable variability in abundance over time in the southeastern Bering Sea (Figure 42, a and b). This variability was less pronounced in the spring time series compared to summer/fall; however, the recent warming in the Bering Sea has resulted in lower overall abundances both in spring and summer/fall. This can be seen most prominently in the difference between the summer abundances during warm periods (2003–2006 and 2016–2018) compared to the colder period (2008–2011). Small copepods show very little interannual variability over time in either spring or fall (Figure 42, c and d). An increase in small copepod abundances can be seen after 2013 in the spring compared to historical values. Euphausiid abundances were higher and more variable in spring compared to summer (Figure 42, e and f).

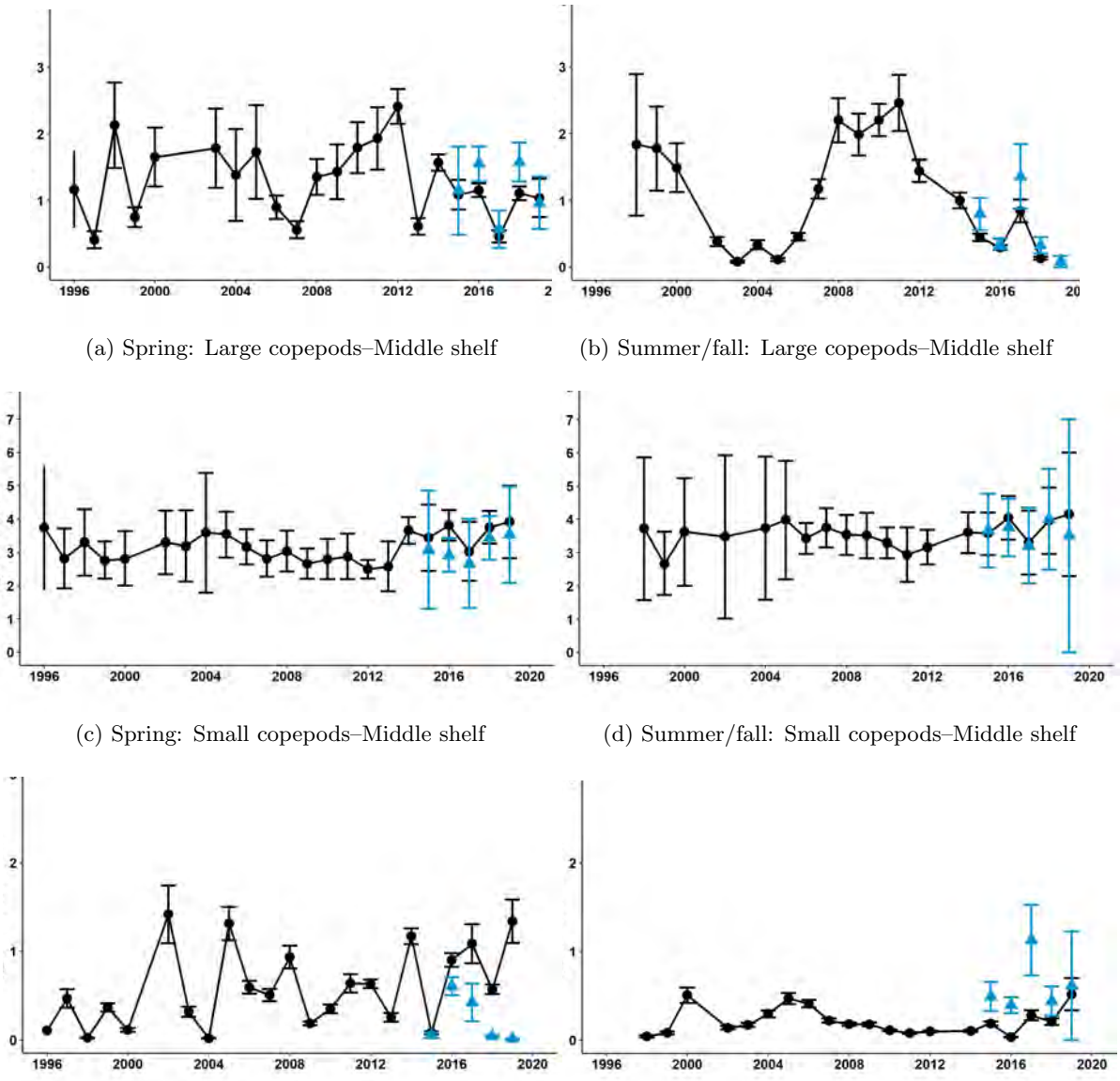

(a) Spring: Large copepods–Middle shelf

(b) Summer/fall: Large copepods–Middle shelf

(c) Spring: Small copepods–Middle shelf

(d) Summer/fall: Small copepods–Middle shelf

(e) Spring: Euphausiids–Middle shelf

(f) Summer/fall: Euphausiids–Middle shelf

Figure 42: Mean abundance of large copepods (> 2 mm), small copepods (< 2 mm), and euphausiids (< 15 mm) in the southeastern, middle shelf region of the Bering Sea (Ortiz et al., 2012). Black circles represent archived data, blue triangles represent RZA data. Left panels are the spring estimates and right panels the summer/fall estimates. Error bars represent the standard error of the mean. Note differences in scale.

Northern Bering Sea

Large copepod abundances in the northern Bering Sea are lower than those observed on the southeastern shelf (Figure 43a). Abundances did increase during the cold period, similar to the southeastern shelf, but to a lesser degree. Warm periods had very low abundances. Small copepods showed little interannual variability in the northern Bering Sea (Figure 43b). Euphausiid abundances were very low overall and showed variability that did not appear to correspond to warm and cold periods (Figure 43c).

Factors influencing observed trends: Large copepods (*Calanus* spp.) respond strongly to sea ice dynamics in the Bering Sea (Eisner et al., 2018; Kimmel et al., 2018). This is especially pronounced in the southeastern Bering Sea where the recent low ice years have resulted in reduced copepod abundances (Figure 42). Copepod development times are strongly linked to temperature, thus it is likely that *Calanus* spp. are developing to the copepodite stage faster during warm years and entering diapause earlier, thus are absent from the shelf during late summer and early fall (Figure 42). Variability was less evident in the northern Bering Sea where large copepod abundances were lower overall (Figure 43). In spring, there is a possibility that earlier stages of the large copepods may be counted as small copepods, as some life-history stages may be < 2 mm. A 2 mL Stempel pipet is used to estimate small copepods, as opposed to the larger 10 mL pipet used to subsample for large copepods. Therefore, we are much more likely to be counting smaller species such as *Oithona* spp. and *Pseudocalanus* spp. as opposed to members of the annual cohort of the large species, e.g. *Calanus* spp. It should be noted that the northern Bering Sea survey primarily samples the inner shelf and nearshore portion of the middle shelf, thus the lower abundances of *Calanus* spp. observed in this survey are to be expected due to recognized spatial differences in distribution (Cooney and Coyle, 1982).

Small copepods showed little interannual variability in either region of the Bering Sea (Figures 42 and 43). These small, continuously reproducing copepods experience faster growth rates compared to larger copepods when temperatures increase (Hirst and Lampitt, 1998). It is interesting to note that small copepods remain at historic high abundances relative to the long-term time series in both regions, suggesting that recent years with no ice seem to favor higher abundances of small copepods. It is likely that small copepod abundances will remain high if warming persists.

The more variable euphausiid abundances in spring reflect the ability of the bongo nets to capture early life-history stages that are more abundant in spring (Figure 42). Very low abundances of euphausiids are reported for summer/fall in both the southeastern and northern Bering Sea (Figures 42 and 43). This reflects the inability of the bongo nets to adequately capture older euphausiids. Furthermore, it should be noted that the RZA and processed estimates of abundances often differ. This is expected due to the patchy nature of euphausiid distribution and the difficulty in accurately estimating euphausiid abundances (Hunt et al., 2016).

Implications: Smaller copepods form the prey base for larval to early juvenile walleye pollock (*Gadus chalcogrammus*) during spring (Figures 42 and 43). The high abundances of small copepods indicate good forage for larval and juvenile pollock early in the year. The warm temperatures increase copepod secondary production rates and trophic transfer is generally favorable during warm springs (Kimmel et al., 2018). Low abundances of large copepods are less critical in the spring, but very important later in the year (Hunt et al., 2011; Eisner et al., 2020). Surveys consistently show that large copepod numbers are significantly lower during warm years. This may result in less lipid-rich large copepods available to age-0 fish about to overwinter. It has been suggested that euphausiids may compensate for a lack of copepods during fall (Duffy-Anderson et al., 2017); however, the inadequate estimates of euphausiids from the bongo nets makes testing this hypothesis difficult at present. We are exploring different gear deployment (Methot trawl) and acoustics on our surveys to increase our ability to estimate euphausiids. The lack of larger, lipid-rich copepods and euphausiids could affect the body condition and survival of overwintering groundfish within the region, which could become more pronounced if warming continues.

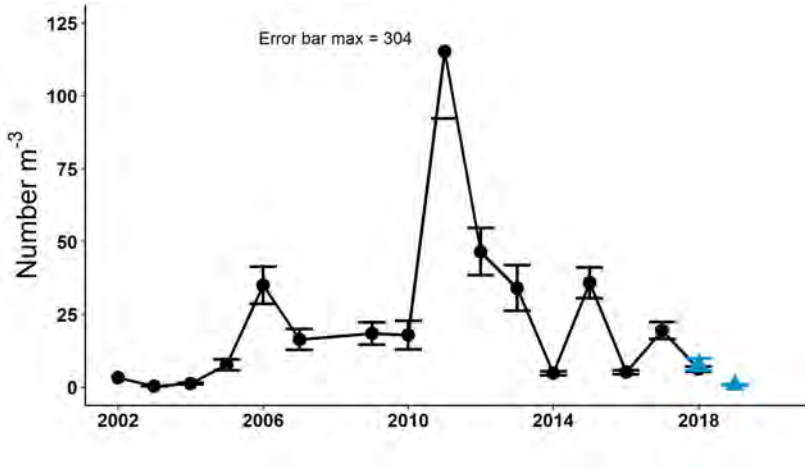

(a) Summer/fall: Large copepods

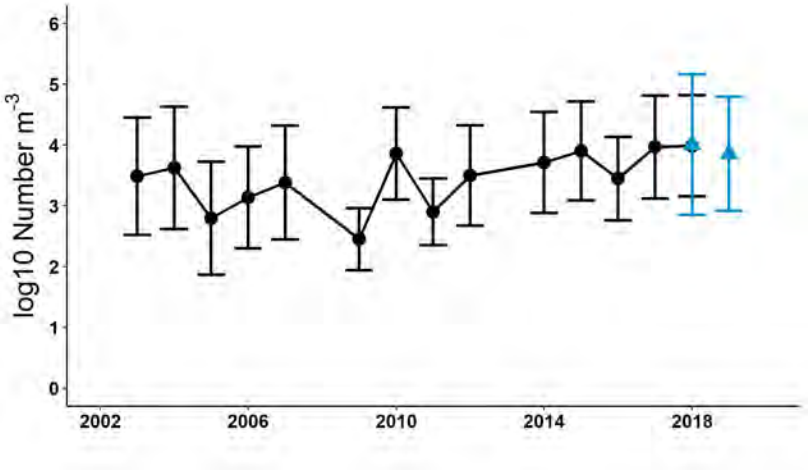

(b) Summer/fall: Small copepods

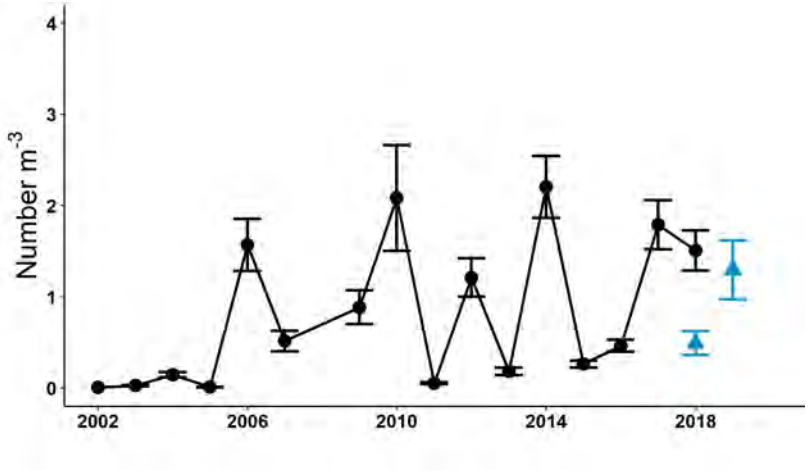

(c) Summer/fall: Euphausiids

Figure 43: Mean abundance of large copepods (> 2 mm), small copepods (< 2 mm), and euphausiids (< 15 mm) in the northern Bering Sea. Black circles represent archived data, blue triangles represent RZA data. Note differences in scale and that larger copepods and euphausiids are not on a logarithmic scale.

Jellyfish

There are no updates to Jellyfish indicators in this year's report. See the contribution archive for previous indicators at: `https://access.afsc.noaa.gov/REFM/REEM/ecoweb/`.

Ichthyoplankton

There are no updates to Ichthyoplankton indicators in this year's report. See the contribution archive for previous indicators at: `https://access.afsc.noaa.gov/REFM/REEM/ecoweb/`.

Forage Fish

There are no updates to Forage Fish indicators in this year's report. See the contribution archive for previous indicators at: `https://access.afsc.noaa.gov/REFM/REEM/ecoweb/`.

Herring

Togiak Herring Population Trends

Contributed by Greg Buck, Sherri Dressel, Sara Miller, and Caroline Brown
Alaska Department of Fish and Game
Contact: sherri.dressel@alaska.gov
Last updated: October 2020

Description of indicator: A time series of catch-at-age model estimates of mature Pacific herring (*Clupea pallasii*) biomass (1980–2019) spawning in the Togiak District of Bristol Bay serves as an index of mature population size. Togiak herring is an important prey species for piscivorous fish, seabirds, and marine mammals, and serve as an important resource for subsistence harvesters and commercial fisheries. The forecast size of the Togiak Bay herring spawning stock is used for the purpose of setting the State of Alaska commercial guideline harvest level for the following year's Togiak spring sac roe fishery and Dutch Harbor bait fishery. The forecast size of the Togiak Bay herring spawning stock, combined with the size of other eastern Bering Sea (EBS) herring stocks, serves as the basis for setting the annual prohibited species catch (PSC) limit for EBS groundfish fisheries per Amendment 16A of the Bering Sea/Aleutian Islands Groundfish Fishery Management Plan. The annual PSC limit is set at 1% of the annual biomass of mature EBS herring and is apportioned among trawl fishery categories. Attainment of any apportionment may trigger closure of Herring Savings Areas to that fishery. The Togiak Bay herring stock is the largest herring spawning stock in Alaskan waters and is thought to comprise approximately 70% of the EBS herring spawning biomass that occurs along the coastline from Port Heiden/Port Moller to Norton Sound. Due to reduced commercial market demands for herring and State of Alaska budget cuts, Togiak Bay herring is the only mature herring stock in the EBS area that is currently and consistently monitored, surveyed, and assessed for stock size on an annual basis.

The biomass of mature Pacific herring occurring in the Togiak District of Bristol Bay has been tracked through aerial surveys since the late 1970s using methods described by Lebida and Whitmore (1985). Generally, the peak aerial survey biomass estimate occurs while the commercial fishery is open. Typically, the harvest prior to the peak, along with the peak aerial survey biomass and an aerial survey biomass around the time commercial fishery ends, are combined to provide a survey estimate of mature herring biomass. A statistical catch-at-age model is then used to forecast Pacific herring biomass in the Togiak District of Bristol Bay (Funk et al., 1992; Funk and Rowell, 1995). The data used in the model includes aerial survey estimates of biomass weighted by a confidence score (confidence depends primarily on visibility conditions, aerial survey coverage, and number of surveys), age composition and weight-at-age information collected from the fishery, and harvest from the purse seine and gillnet fisheries. Recruitment of Togiak herring to the fishery begins around age-4 and fish are believed to be fully recruited into the fishery around age-8.

Status and trends: Mature Togiak herring biomass, as estimated by the model, increased from a low of 63,000 short tons in 1980 to over 400,000 short tons from 1985 to 1987 (Figure 44), due to large age-4 recruitments in 1981 and 1982 (Figure 45). The biomass then declined through the late-1990s and has remained stable since that time. The large annual biomasses estimated by the model during the late 1980s have considerable uncertainty due to the poor aerial survey conditions and confidence scores during that time.

The 2020 biomass forecast for Togiak was based on aerial survey estimates, annual age composition and weight-at-age data collected from the fishery, and harvest data. In 2019, for the first time in four years, a non-zero confidence rating was associated with the aerial survey biomass estimate (177,980 short tons) and used in the model. The forecast for 2020 (215,826 short tons) was lower than the 2019 forecast (217,548 short tons) but greater than the model hindcast for 2019 and the 2019 aerial survey estimate (Figure 44). The 2020 mature population was estimated to be predominantly age-6 and age-7 fish as the population continues to be supported by the 2013 and 2014 year classes (age-4 recruits in 2017 and 2018, Figure 45). While the

recruitment of age-4 fish to the spawning population in 2018 was still the largest estimated recruitment since 1982, the magnitude of that recruit class was estimated in the 2020-forecast model to be lower than was previously estimated.

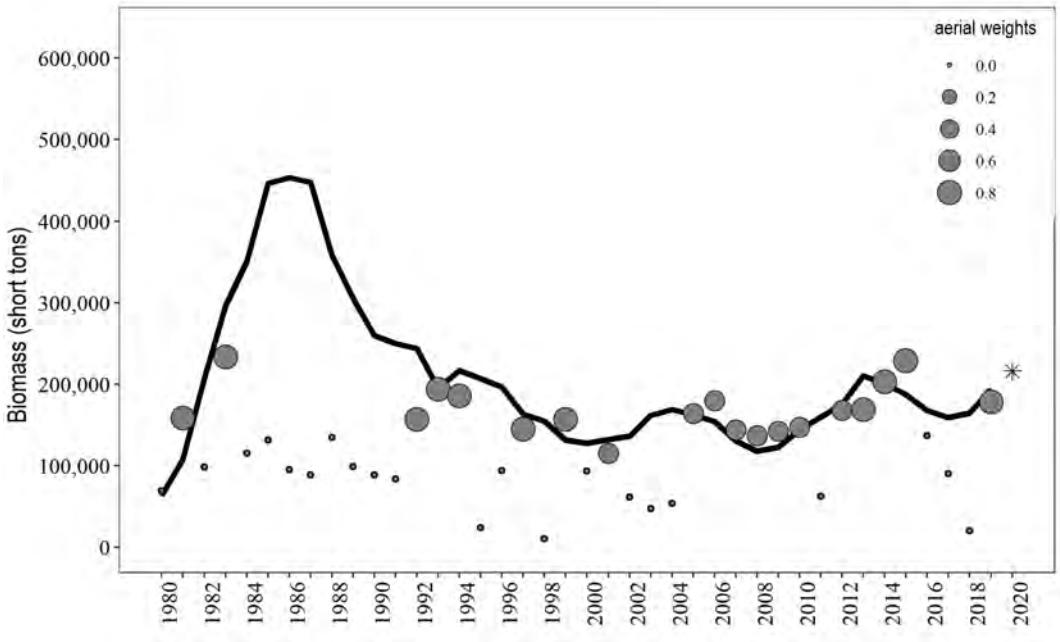

Figure 44: Aerial survey-estimated biomass plus pre-peak catch that were included in the model (gray points), model-estimated mature biomass (black solid line), and model-estimated mature biomass forecast (black asterisk). The size of the gray points reflects the confidence weighting of each aerial survey estimate in the model based on weather, number of surveys, quality of surveys, and timing of surveys relative to the spawn (ranging from 0=no confidence to 1=perfect confidence).

An active commercial sac roe fishery is conducted on this population with gillnet and purse seine gear. A small spawn on kelp quota is allowed but has not been utilized since 2003. The sac roe fishery has harvested an average of 21,416 tons annually over the last 10 years (2010–2019).

Residents of Togiak have related to Alaska Department of Fish and Game (ADF&G) staff that they do not participate in the Togiak herring commercial fishery as they once did primarily due to a concern about abundance of herring needed for subsistence uses, as well as competition with commercial fishers from outside the state. ADF&G has conducted two comprehensive subsistence surveys in Togiak: in 1999 (Coiley-Kenner et al., 2003) and 2008 (Fall et al., 2012). Harvests of herring and herring spawn on kelp were measured in both years. Comparing the two years, harvests of herring declined by 22% between 1999 and 2008 while the harvest of spawn on kelp increased by 146%, from 8 lbs per capita to 20 lbs per capita. However, during a 2017 study designed to address proposals coming before the Board of Fisheries, Togiak households reported harvesting only 3 lbs of spawn on kelp per capita. Many residents expressed concern about the herring stocks in 2008 and in 2017, especially about their ability to harvest spawn on kelp.

Factors influencing observed trends: Togiak herring biomass trends are dependent upon recruitment and are influenced by the environment. Pacific herring recruitment is both highly variable and cyclic with large recruitment events (age-4) occurring roughly every 8–10 years. Biomass trends are greatly influenced by recruitment, with the highest biomasses in 1985–1987 resulting from the largest age-4 recruitments in 1981 and 1982. The substantial recruitments in 2017 and 2018 continue to support a stable population at this time (Figure 44). Williams and Quinn (2000) demonstrate that Pacific herring populations in the North Pacific are closely linked to environmental conditions, particularly water temperature. Tojo et al. (2007) demonstrate how the complex reproductive migration of EBS herring is related to temperature and

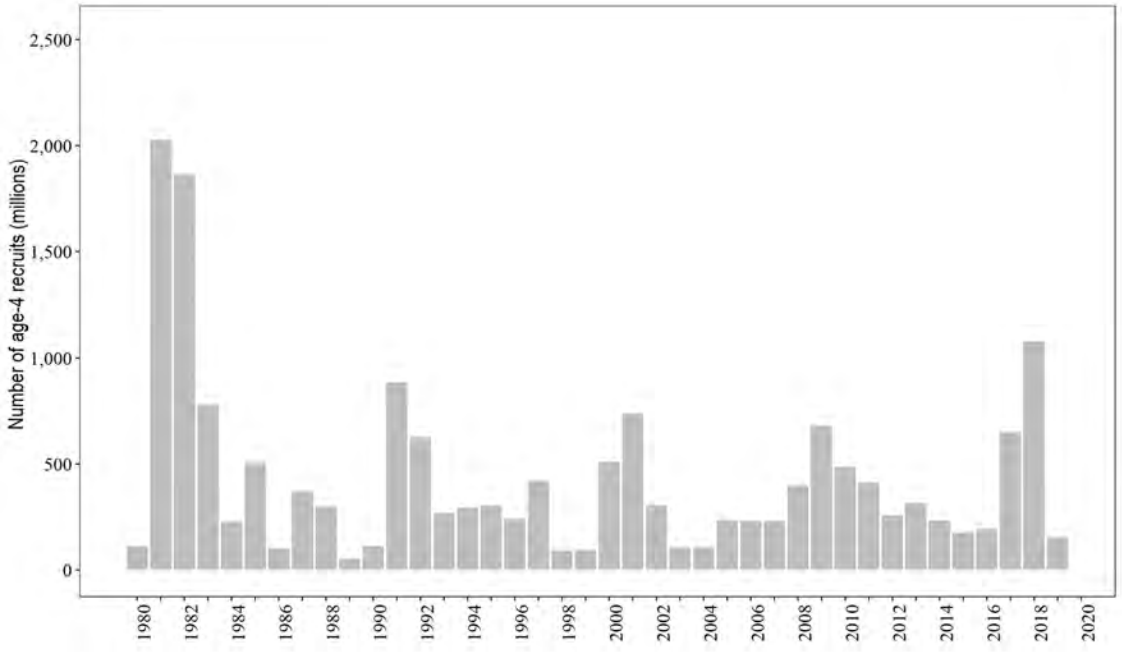

Figure 45: Model estimates of age-4 recruit strength (numbers of age-4 mature and immature fish).

the retreat of sea ice and how it has changed since the 1980s. Wespestad and Gunderson (1991) suggest that recruitment variation in the EBS relates to the degree of larval retention in near-coastal nursery areas where temperatures and feeding conditions are optimal for rapid growth. Specifically, they indicate that above average year-classes occur in years with warm sea surface temperatures when the direction of transport is north to northeast (onshore) and wind-driven transport velocity is low, whereas weak year classes occur in years when sea-surface temperature is cold, wind-driven transport is west to northwest (offshore), and wind-driven transport velocity is high. Closer examination of environmental conditions such as sea surface temperature, air temperature, surface winds, and EBS ice coverage may increase our understanding of the recruitment processes at play in this population.

Elders and Togiak residents have expressed concern that commercial purse seine fishing for sac roe has influenced Togiak herring biomass trends. They describe changes in the density and spatial extent of herring spawn and decreases in herring abundance since approximately the 1990s. As is beginning to be explored for other herring stocks in the North Pacific, closer examination of the spatial distribution of herring spawn and the spatial distribution of commercial fishing effort may increase our understanding of the potential impacts of commercial fishing on herring spawning populations and subsistence harvest.

Implications: Togiak herring are an important prey species for piscivorous fish, seabirds, and marine mammals. Togiak herring are also an important resource for subsistence harvesters, as well as the basis for a directed Togiak commercial herring sac roe fishery and a directed commercial Dutch Harbor bait fishery, as well as being PSC in the EBS groundfish fisheries. The cyclic nature of recruitment into this population has implications for predators and prey of Pacific herring as well as fisheries. The stable trend of this stock since the mid-1990's, despite cyclic recruitment, has allowed for directed commercial fisheries to open and has contributed to approximately stable PSC levels for EBS groundfish fisheries since 1992. However, Togiak residents express considerable concern about declines in the subsistence fishery since the early 1990s. Elders recall much larger amounts of herring returning in the past and subsistence survey respondents note the diminished densities of spawn on kelp. Therefore, despite the estimated stability of the Togiak herring stock over the past 25 years, past declines have impacted subsistence harvesters.

Salmon

Historical and Current Alaska Salmon Trends – Bering Sea

Contributed by George A. Whitehouse
Cooperative Institute for Climate, Ocean, and Ecosystem Studies (CICOES), University of Washington, Seattle, WA
Contact: andy.whitehouse@noaa.gov
Last updated: September 2020

Description of indicator: This contribution provides historic and current commercial catch information for salmon of the Bering Sea. This contribution summarizes available data and information that is included in current Alaska Department of Fish and Game (ADF&G) agency reports (e.g., Brenner et al. (2020)) and on their website[12].

Pacific salmon in Alaska are managed in four regions based on freshwater drainage basins[13]: Southeast/Yakutat, Central (encompassing Prince William Sound, Cook Inlet, and Bristol Bay), Arctic-Yukon-Kuskokwim, and Westward (Kodiak, Chignik, and Alaska peninsula). ADF&G prepares harvest projections for all areas rather than conducting run size forecasts for each salmon run. There are five Pacific salmon species with directed commercial fisheries in Alaska; they are sockeye salmon (*Oncorhynchus nerka*), pink salmon (*O. gorbuscha*), chum salmon (*O. keta*), Chinook salmon (*O. tshawytscha*), and coho salmon (*O. kisutch*).

Status and trends:
Statewide
Catches from directed fisheries on the five salmon species have fluctuated over recent decades but in total have been generally strong (Figure 46). According to ADF&G, total salmon commercial harvests from 2019 totaled 207.9 million fish, which was about 5.3 million less than the preseason forecast of 213.2 million. The total statewide salmon harvest increased more than 92 million from 2018 to 2019 and was bolstered in 2019 by the catch of 128.6 million pink salmon. In 2020 ADF&G is projecting a decrease in the total commercial salmon catch to 132.7 million fish due to expected decreases in the number of pink and sockeye salmon. While the 2020 commercial salmon harvest data are not yet final, preliminary data from ADF&G for 2020 indicates that statewide total commercial salmon harvests are about 113.4 million (as of 22 September), which is below the preseason forecast but nearing the 2018 total harvest of 115.7 million fish.

Bering Sea
Chinook salmon abundance in the Arctic-Yukon-Kuskokwim region has been low since the mid-2000s and generally remains low. There has been some indication of a Chinook rebound in the Yukon area since 2016 (Murphy et al., 2017; Estensen et al., 2018). However, for the 12th consecutive year no commercial periods targeting summer season Chinook salmon were allowed in 2019 in the Yukon Management Area. Additionally, the estimated escapement of 42,052 Yukon Chinook salmon into Canada was just short of the lower end of the escapement goal range of 42,500 (JTC, 2020). In Norton Sound, one of two Chinook salmon escapement goals were met, but commercial fishing targeting Chinook salmon was not allowed. In Bristol Bay, the total 2019 Chinook salmon commercial harvest of 33,318 was approximately 23% below the recent 20-year average.

The 2019 commercial catch of 80,997 coho salmon in Bristol Bay is below the recent 20-year average of 93,339. Coho abundance in the Arctic-Yukon-Kuskokwim region in 2019 was healthy, and the harvest of 139,837 in the Norton Sound area was the 4th highest catch on record.

The chum salmon harvest of 157,838 in Norton Sound was less than the forecast harvest range. The harvest of 1.4 million chum salmon in Bristol Bay was above the recent 20-year average of 1.1 million fish.

[12] https://www.adfg.alaska.gov/
[13] https://www.adfg.alaska.gov/index.cfm?adfg=commercialbyfisherysalmon.salmonareas

The 2019 Bristol Bay sockeye salmon run of 56.5 million is the 4th largest ever, and the harvest of 43 million was the 2nd highest ever. Escapement goals for sockeye salmon were met or exceeded in every drainage in Bristol Bay where escapement was defined. Historically, total runs to Bristol Bay have been highly variable, but in recent years (2014–2019), sockeye salmon runs have been above the recent 20-year mean of 39 million. Preliminary data from ADF&G for 2020 indicates that the commercial harvest of Bristol Bay sockeye salmon is strong again, exceeding 39 million fish (see p. 92).

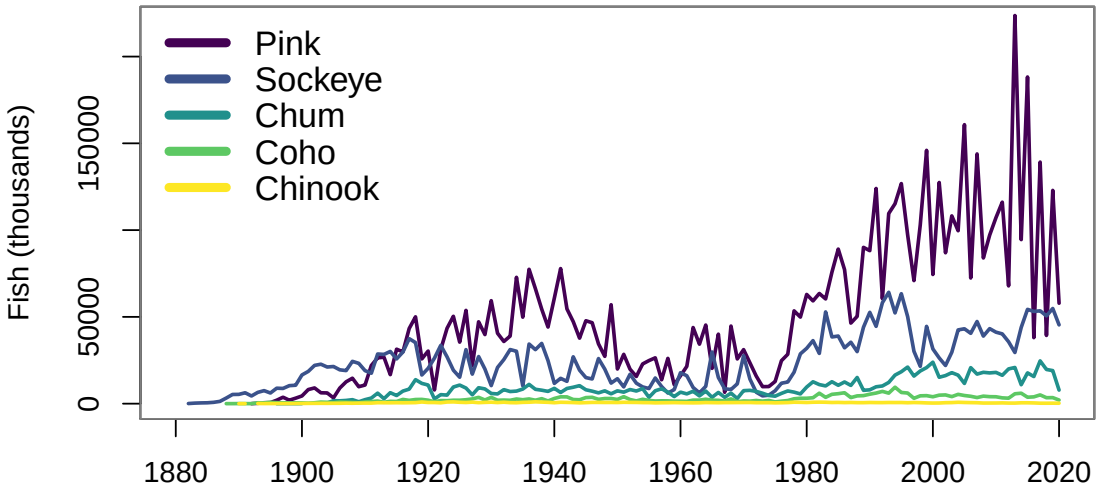

Figure 46: Alaska historical commercial salmon catches, 2020 values are preliminary. Source: ADF&G, `http://www.adfg.alaska.gov`. ADF&G not responsible for the reproduction of data.

Factors influencing observed trends: Salmon have complex life histories and are subject to stressors in the freshwater and marine environments, as well as anthropogenic pressures. These forces do not affect all species and stocks equally or in the same direction, and resolving what is driving the population dynamics of a particular stock is challenging (Rogers and Schindler, 2011). Interannual variation in Alaska statewide total salmon abundance is partly due to the even-year, odd-year cycle in pink salmon, particularly production from the Prince William Sound stock of pink salmon, which typically have larger runs in odd years. Chinook runs have been declining statewide since 2007. Size-dependent mortality during the first year in the marine environment is thought to be a leading contributor to low Chinook run sizes (Beamish and Mahnken, 2001; Graham et al., 2019).

In the Bering Sea, sockeye salmon are the most abundant salmonid, and since the early 2000s, they have had consistently strong runs which have supported large harvests. Bristol Bay sockeye salmon display a variety of life history types. For example, their spawning habitat is highly variable and demonstrates the adaptive and diverse nature of sockeye salmon in this area (Hilborn et al., 2003). Therefore, productivity within these various habitats may be affected differently depending upon varying conditions, such as climate (Mantua et al., 1997), so more diverse sets of populations provide greater overall stability (Schindler et al., 2010). The abundance of Bristol Bay sockeye salmon may also vary over centennial time scales, with brief periods of high abundance separated by extended periods of low abundance (Schindler et al., 2006).

Implications: Salmon have important influences on Alaska marine ecosystems through interactions with marine food webs as predators on lower trophic levels and as prey for other species such as Steller sea lions. In years of great abundance, salmon may exploit prey resources more efficiently than their competitors. A negative relationship between seabird reproductive success and years of high pink salmon abundance has been demonstrated (S et al., 2013; Springer and van Vliet, 2014). Directed salmon fisheries are economically important for the state of Alaska. The trend in total salmon catch in recent decades has been for generally strong harvests, despite annual fluctuations.

Temporal Trend in the Annual Inshore Run Size of Bristol Bay Sockeye Salmon (*Oncorhynchus nerka*)

Contributed by Curry J. Cunningham[1], Gregory Buck[2], Stacy Vega[2], and Jordan Head[2]
[1]College of Fisheries and Ocean Sciences, University of Alaska Fairbanks, Juneau, Alaska
[2]Alaska Department of Fish and Game, Anchorage, Alaska
Contact: cjcunningham@alaska.edu
Last updated: September 2020

Description of indicator: The annual abundance of adult sockeye salmon (*Oncorhynchus nerka*) returning to Bristol Bay, Alaska is enumerated by the Alaska Department of Fish and Game (ADF&G). The total inshore run in a given year is the sum of catches in five terminal fishing districts plus the escapement of sockeye to nine major river systems. Total catch is estimated based on the mass of fishery offloads and the average weight of individual sockeye within time and area strata. Escapement is the number of fish successfully avoiding fishery capture and enumerated during upriver migration toward the spawning grounds, or through post-season aerial surveys of the spawning grounds (Elison et al., 2018). Although there have been slight changes in the location and operation of escapement enumeration projects and methods over time, these data provide a consistent index of the inshore return abundance of sockeye salmon to Bristol Bay since 1963.

Status and trends: The 2020 Bristol Bay salmon inshore run of 58.2 million sockeye is the 5th largest on record since 1963 and is 28.0% higher than the recent 10-year average of 45.5 million sockeye, and 74.5% higher than the 1963–2019 average of 33.3 million sockeye. The temporal trend in Bristol Bay sockeye salmon indicates a large increase during the recent 6-year period, with inshore run sizes in 2015–2020 all exceeding 50 million salmon and above recent and long-term averages. The current period of high Bristol Bay sockeye salmon production now exceeds the previous high production stanza that occurred 1989–1995. Also of note, following record high inshore runs to the Nushagak District (2017–2019), inshore runs to the Egegik District in 2019 (17.0 million) and 2020 (15.8 million) are the 3rd and 4th highest runs on record to this fishing district since 1963.
Note: At this time 2020 Bristol Bay inshore run size numbers are preliminary and subject to change.

Factors influencing observed trends: The return abundance of Bristol Bay sockeye salmon is positively correlated with the Pacific Decadal Oscillation (Hare et al., 1999), specifically with Egegik and Ugashik district run sizes increasing after the 1976/1977 regime shift. However, recent research has highlighted that relationships between salmon population dynamics and the PDO may not be as consistent as once thought, and may in fact vary over time (Litzow et al., 2020*a*,*b*). The abundance and growth of Bristol Bay sockeye salmon has also been linked to the abundance of pink salmon (*Oncorhynchus gorbuscha*) in the North Pacific (Ruggerone and Nielsen, 2004; Ruggerone et al., 2016).

Implications: The high inshore run of Bristol Bay sockeye salmon in 2020 and the preceding 5-year period indicate positive survival conditions for these stocks while in the ocean. Given evidence that the critical period for sockeye salmon survival occurs during the first summer and winter at sea (Beamish and Mahnken, 2001; Farley et al., 2007, 2011) and the predominant age classes observed for Bristol Bay stocks are 1.2, 1.3, 2.2, and 2.3 (European designation: years in freshwater–years in the ocean), the large 2020 Bristol Bay sockeye salmon inshore run suggests these stocks experienced positive conditions at entry into the Eastern Bering Sea in the summers of 2017 and 2018, and winters of 2017–2018 and 2018–2019.

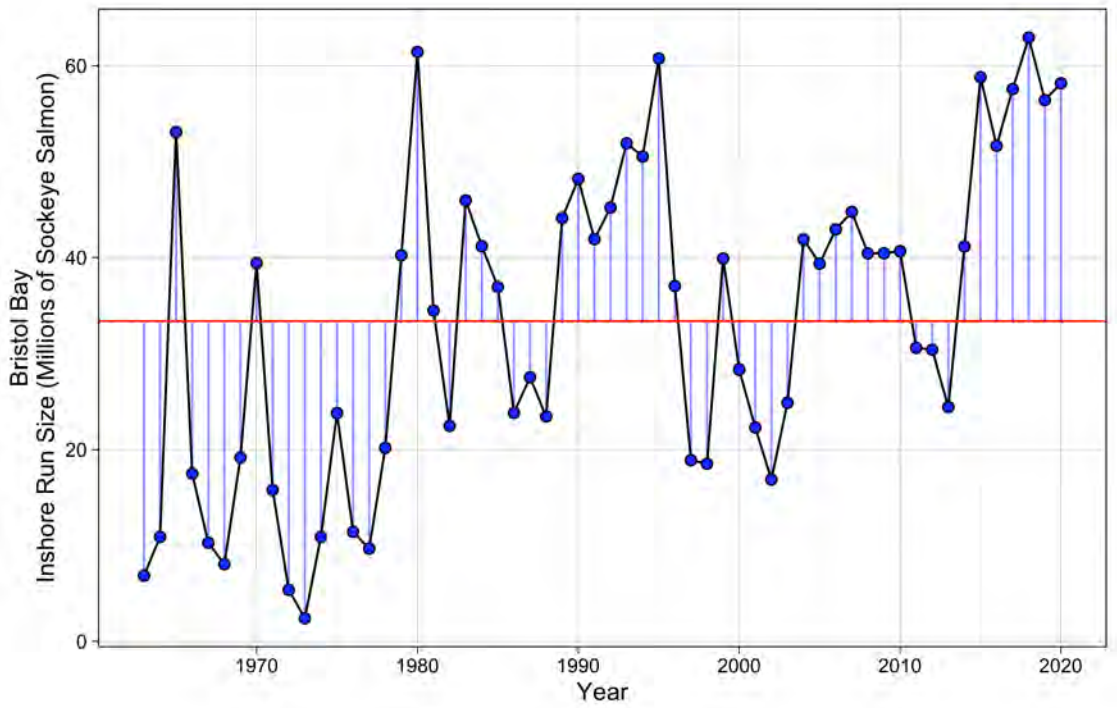

Figure 47: Annual Bristol Bay sockeye salmon inshore run size 1963–2020. Red line is the time series average of 33.3 million sockeye.

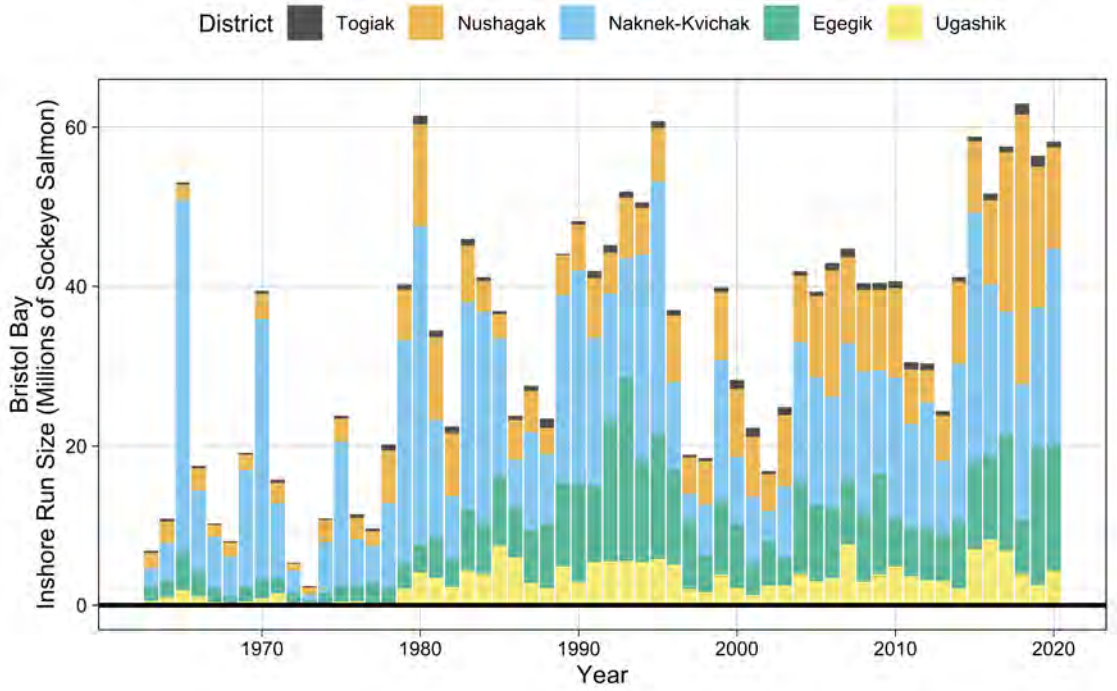

Figure 48: Annual Bristol Bay sockeye salmon inshore run size 1963-2020 by commercial fishing district.

Groundfish

Eastern Bering Sea Adult Pacific Cod Food Habits

Contributed by Kerim Aydin
Resource Ecology and Ecosystem Modeling Program, Alaska Fisheries Science Center, National Marine Fisheries Service, NOAA
Contact: kerim.aydin@noaa.gov
Last updated: October 2020

Description of indicator: As part of its annual eastern Bering Sea (EBS) bottom-trawl survey (BTS) program, the Alaska Fisheries Science Center has been collecting and analyzing the stomach contents of groundfish predators since 1985. Fish are caught in bottom trawl hauls that typically vary from 15 to 30 min in duration. Individual fish are selected from the catch and their stomachs are removed for analysis and preserved in a 10% formalin solution for laboratory analysis. Laboratory analysis includes: total stomach content weight recorded to the decagram (0.01 g), exact prey count, weight (0.001 g) and size (mm) when feasible for all crab and fish, and species identification of all fish and crab prey (Livingston et al., 2017). The indicator presented here is %weight by prey type; fish within a particular species, size class, and oceanographic stratum are pooled, and the prey weight of each stomach is corrected for predator size before summing to determine % by weight diet composition for all fish. For this contribution, the focus is on the diet of Pacific cod (*Gadus macrocephalus*) with fork lengths of 60cm or greater.

Status and trends: In the eastern Bering Sea, Pacific cod feed on zooplankton until reaching approximately 20cm fork length, then feed primarily on benthic epifauna between 20–60cm fork length, and at larger sizes (60cm+) switch to feeding on fish, crustaceans, and other large invertebrates, in particular Walleye pollock (*G. chalcogrammus*) and *Chionoecetes* spp. of crab (snow crab and tanner crab). Diet proportions by weight for three key EBS strata are shown: the southeast middle domain, the northwest outer domain, and the northern Bering Sea (Figure 49).

In the southeast middle domain, pollock were the dominant prey in most years, but were extremely low from 2008–2012 when they were replaced with a mix of *Chionoecetes* spp. and flatfish, in particular. In the northwest outer domain, pollock were the dominant prey except for the periods 1996–1997, 2008–2009, and 2016–2019. In that most recent period, both *Chionoecetes* spp. and octopus were seen at increased levels. During 2009–2012 in the northwest outer domain, Pandalid shrimp were also higher in the cod diets.

There have been limited surveys in the northern Bering Sea; of the years surveyed, for most years *Chionoecetes* spp. (primarily identified as snow crab) were the largest portion of cod diet, except for 2010 in which both flatfish and forage fish were the main prey items.

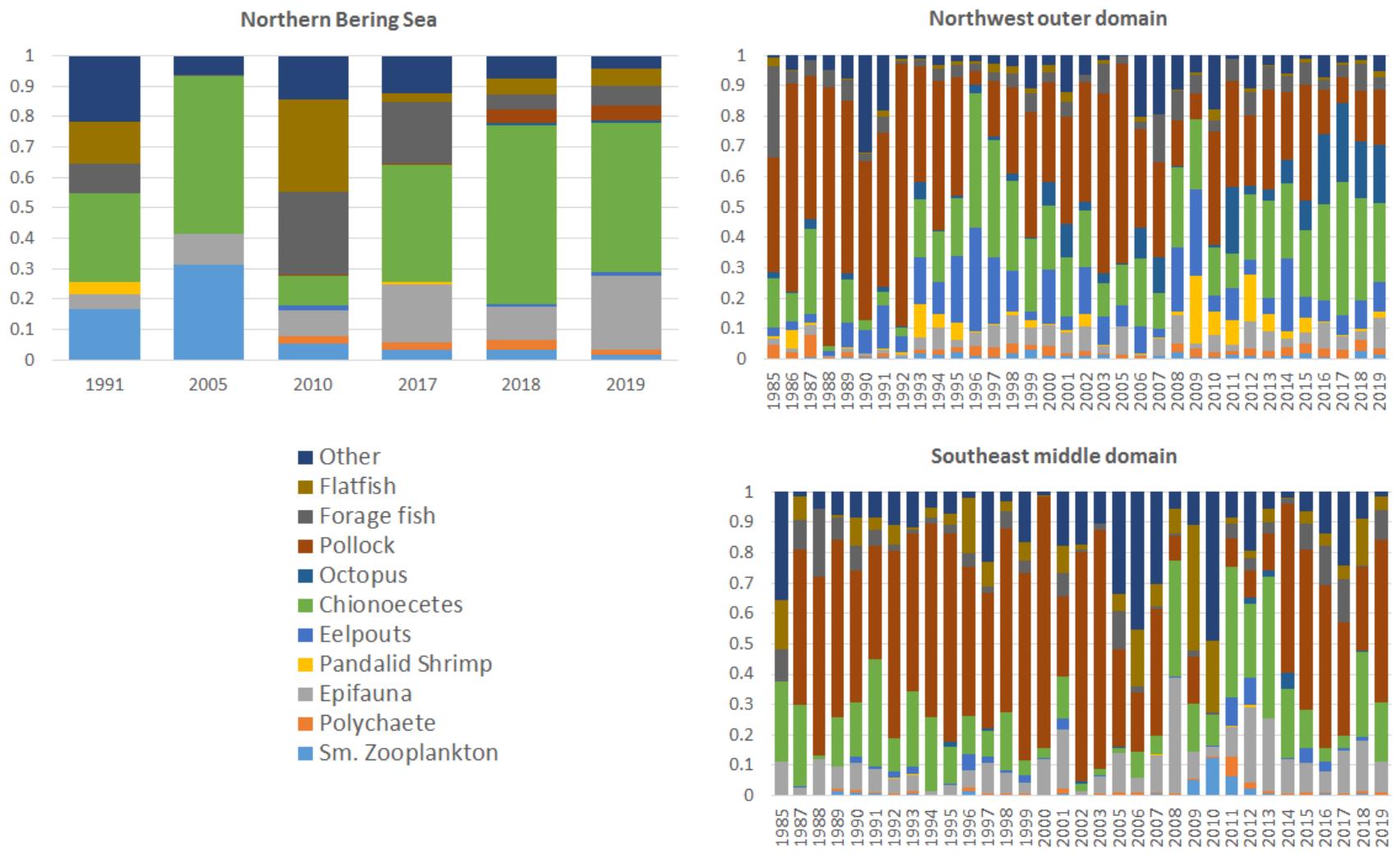

Figure 49: Diet proportions (proportion by weight) of eastern Bering Sea Pacific cod (*Gadus macrocephalus*) with fork lengths of 60cm+, by survey stratum, as sampled from Alaska Fisheries Science Center summer bottom-trawl surveys.

Factors influencing observed trends: Pacific cod are generalist predators and able to switch between benthic and demersal foraging based on prey availability. The trends show the influence of the Bering Sea cold pool: years with a large cold pool extent show a decrease of pollock in Pacific cod prey and an increase in a range of other prey items. In recent years however (2015–2019), pollock have remained relatively low in diets in spite of a decreased cold pool, particularly on the northwest outer shelf, with octopus increasing. This may represent a trend of increasing octopus in the region.

Implications: The decrease in pollock in diets between 2015–2019 does not correspond to low pollock recruitment; it may be related to the increase of other prey types (in particular octopus) that may be the result of sustained warmth in the region.

Eastern and Northern Bering Sea Groundfish Condition

Contributed by Sean Rohan and Ned Laman
Resource Assessment and Conservation Engineering Division, Alaska Fisheries Science Center, National Marine Fisheries Service, NOAA
Contact: sean.rohan@noaa.gov
Last updated: September 2020

Description of indicator: Length-weight residuals represent how heavy a fish is per unit body length and are an indicator of somatic growth variability (Brodeur et al., 2004). Therefore, length-weight residuals can be considered an indicator of prey availability and growth conditions. Positive length-weight residuals indicate better condition (i.e., heavier per unit length) and negative residuals indicate poorer condition (i.e., lighter per unit length). Fish condition calculated in this way reflects fish growth trajectories which can have implications for biological productivity due to growth, reproduction, and mortality (Paul and Paul, 1999; Boldt and Haldorson, 2004).

Paired fork lengths (mm) and weights (g) of individual fishes were collected from the Alaska Fisheries Science Center's Resource Assessment and Conservation Engineering (AFSC/RACE) - Groundfish Assessment Program's (GAP) bottom trawl surveys of the eastern Bering Sea (EBS) shelf and northern Bering Sea (NBS). Fish condition analyses were applied to walleye pollock (*Gadus chalcogrammus*), Pacific cod (*G. macrocephalus*), arrowtooth flounder (*Atheresthes stomias*), yellowfin sole (*Limanda aspera*), flathead sole (*Hippoglossoides elassodon*), northern rock sole (*Lepidopsetta polyxystra*), and Alaska plaice (*Pleuronectes quadrituberculatus*) collected in bottom trawls at standard stations (Figure 50). For these analyses and results, survey strata 31 and 32 were combined as stratum 30; strata 41, 42, and 43 were combined as stratum 40; and strata 61 and 62 were combined as stratum 60. Corner stations and non-standard survey strata 82 and 90 were excluded from these analyses.

Length-weight relationships were estimated using a linear regression based on a log-transformation of the exponential growth relationship, $W=aL^b$, where W is weight (g) and L is fork length (mm) for all areas for the period 1997–2019 (EBS: 1997–2019, NBS: 2010, 2017–2019). A different slope (b) was estimated for each stratum to account for spatial-temporal variation in growth and bottom trawl survey sampling. Length-weight relationships for 100–250 mm pollock (corresponding with ages 1–2 years) were calculated independently. Bias-corrected weights-at-length (log scale) were estimated from the model and subtracted from observed weights to compute individual residuals per fish. Length-weight residuals were averaged for each stratum and weighted in proportion to total biomass in the region based on stratum-level area-swept expansion of bottom-trawl survey catch per unit effort (CPUE). Average length-weight residuals were compared by stratum and year on the EBS shelf to evaluate spatial variation in fish condition. The NBS was treated as a single stratum and used a different length-weight regression than the EBS. Combinations of stratum and year with sample size <10 were used for length-weight calculations but excluded from calculation of length-weight residuals.

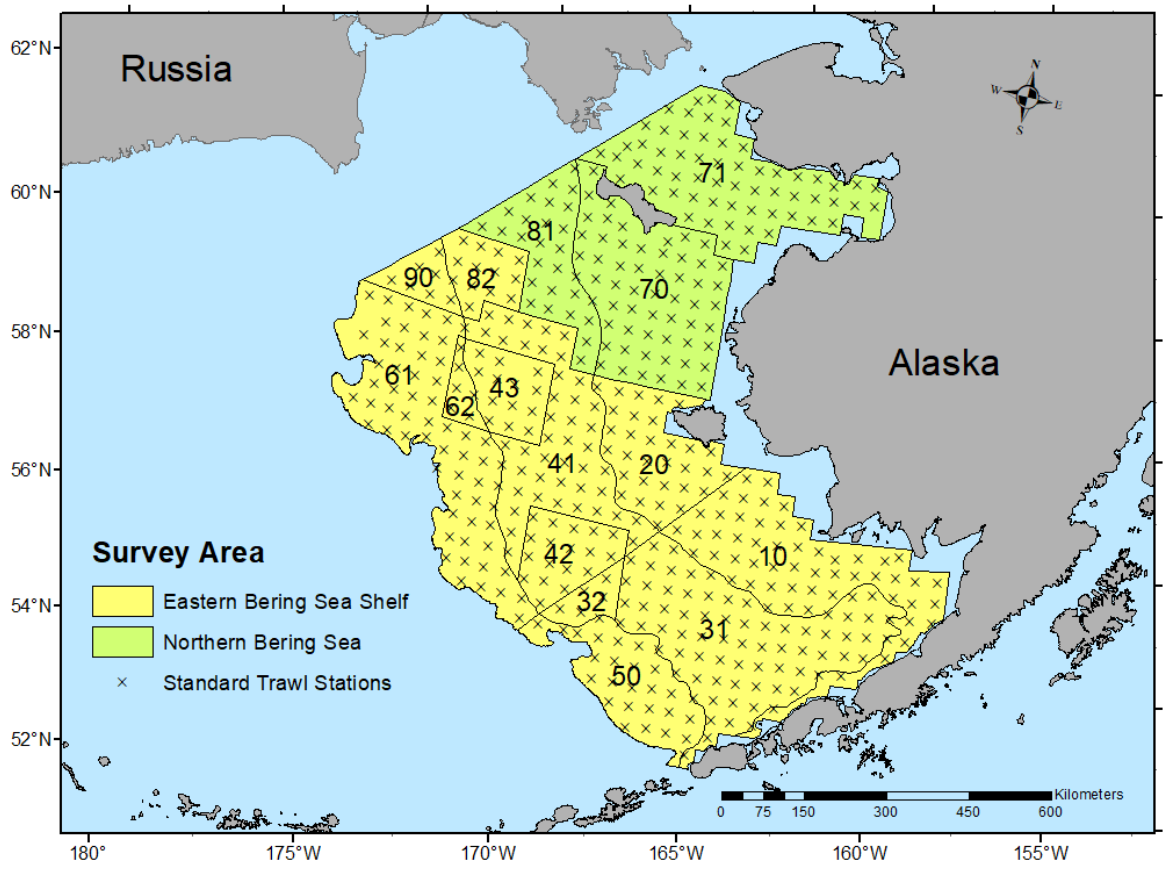

Figure 50: AFSC/RACE GAP summer bottom trawl survey strata (10–90) and station locations (x) on the eastern Bering Sea Shelf and in the northern Bering Sea.

Methodological changes: The method used to calculate groundfish condition this year (2020) differs from previous years in that: 1) different regression slopes were estimated for each stratum, 2) a bias-correction was applied to predict weights prior to calculating residuals, 3) stratum mean residuals were weighted in proportion to stratum biomass, 4) stratum-year combinations with sample size <10 were not used in indicator calculations, and 5) the NBS had its own length-weight regression. As in previous years, confidence intervals for the condition indicator reflect uncertainty based on length-weight residuals, but are larger due to differences in sample sizes and stratum biomasses among years. Confidence intervals do not account for uncertainty in stratum biomass estimates.

Status and trends: Fish condition, indicated by length-weight residuals, has varied over time for all species examined (Figures 51 and 52). The updated method for calculating groundfish condition has resulted in changes compared to last year's condition indicator. Notably, the magnitude of length-weight residuals was much lower using the new method, in part because the new method reduces the influence of spatial variation in length-weight relationships and spatial-temporal variation in sampling effort on length-weight residuals. Last year, it was reported for the EBS that: "with the exception of [100–250 mm pollock], length-weight residuals in 2019 were positive or have continued an upward trend that began in 2017 or 2018." Based on the new method, an upward trend was still evident for most species relative to 2017–2018 and weighted length-weight residuals were positive relative to historical averages for pollock (>250 mm), northern rock sole, yellowfin sole, arrowtooth flounder, and Alaska plaice in 2019 (Figure 51). Length-weight residuals were near historical averages for age 1–2 pollock (100–250 mm), Pacific cod, and flathead sole.

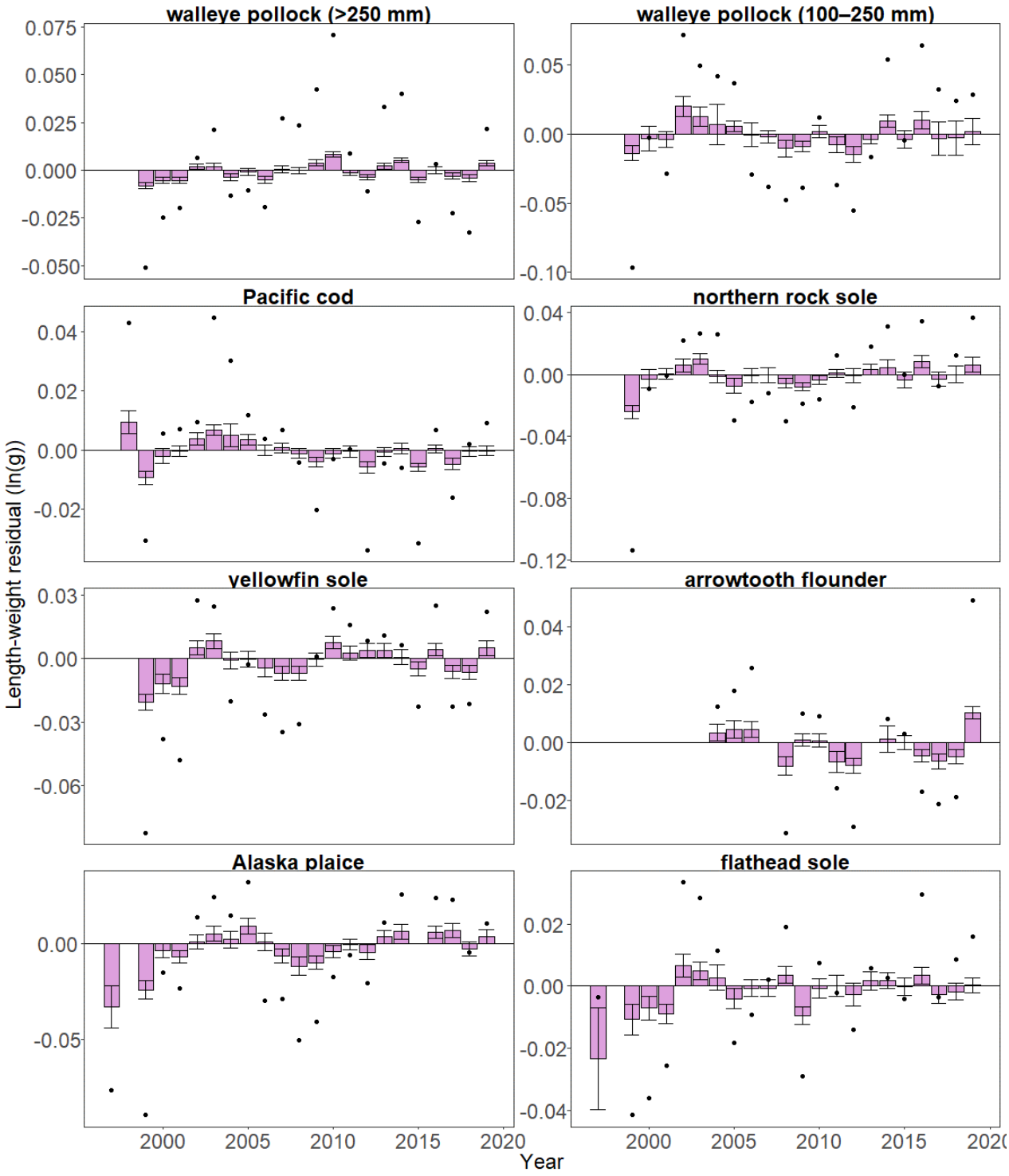

Figure 51: Weighted length-weight residuals for seven groundfish species and age 1–2 pollock (100–250 mm) collected during AFSC/RACE GAP standard summer bottom trawl surveys of the eastern Bering Sea shelf, 1997–2019. Filled bars denote weighted length-weight residuals using this year's indicator calculation, error bars denote two standard errors, points denote the mean of the unweighted length-weight residual from the 2019 calculations.

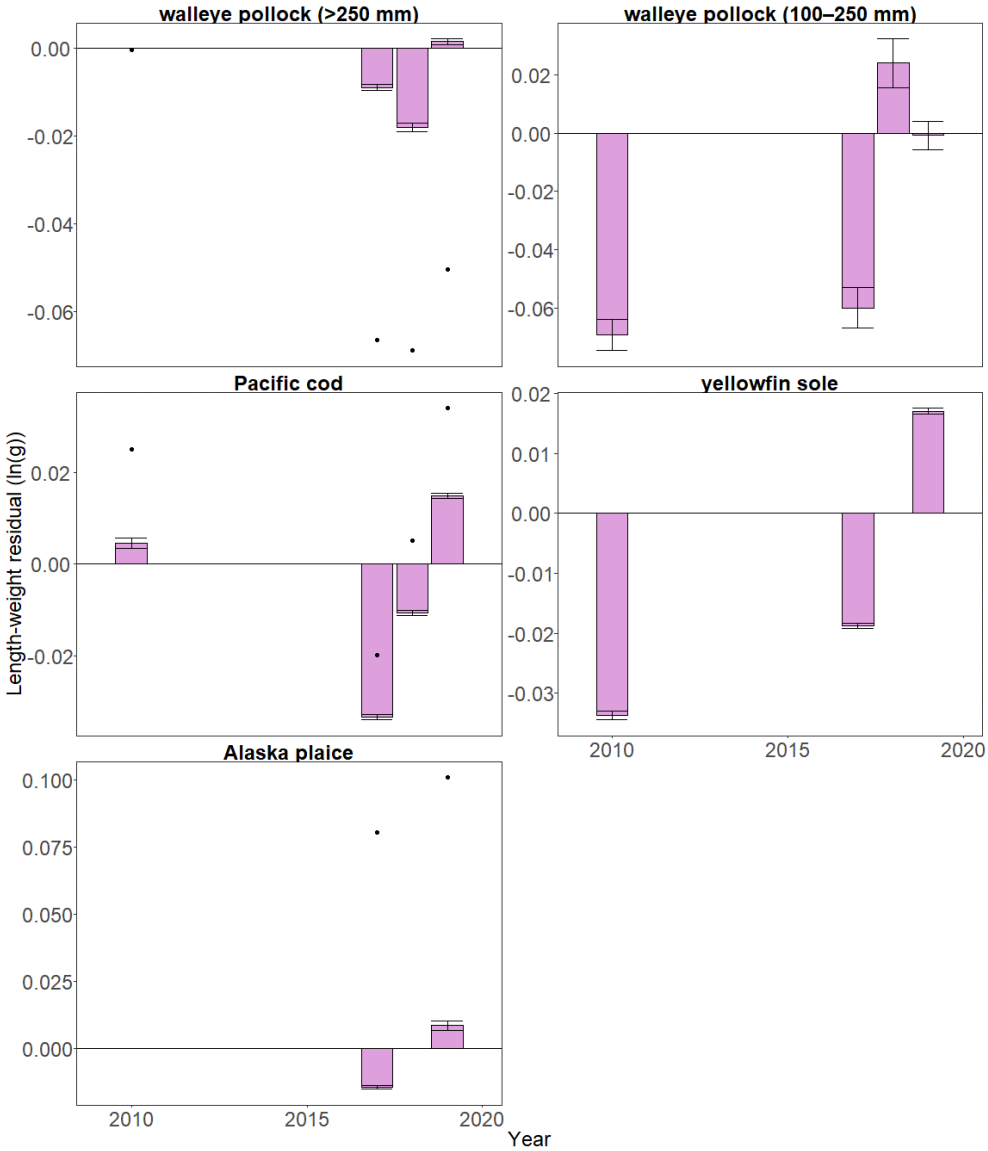

Figure 52: Length-weight residuals for groundfish species and age 1–2 pollock (100–250 mm) collected during AFSC/RACE GAP summer bottom trawl surveys of the northern Bering Sea, 2010 and 2017–2019. Filled bars denote length-weight residuals using this year's indicator calculation, error bars denote two standard errors, points denote the mean of length-weight residual from the 2019 calculations.

Last year, it was reported that: "trends in fish condition [for the NBS] are similar to those on the EBS shelf with length-weight residuals becoming more positive for adult pollock and Pacific cod, although length-weight residuals overall for adult pollock were negative." (Figure 52). Based on this year's method with a separate length-weight regression for the NBS, positive residuals were observed in 2019 for pollock (>250 mm), Pacific cod, yellowfin sole, and Alaska plaice. Residuals for pollock (100–250 mm) were neutral.

In previous years, stratum length-weight residuals were strongly influenced by the spatial and temporal distribution of samples. This is because the bottom trawl progresses from the southeast inner shelf towards the northwest outer shelf, resulting in a cross-shelf gradient in somatic growth that has accumulated by the time a length-weight sample is collected.

Last year, it was noted that: "spatial patterns of length-weight residuals over the EBS shelf were apparent for most species" and that "fish were in better condition on the outer shelf (strata 50 and 60) and length-weight residuals were positive for nearly all species in the last 3–5 survey years; gadids tended toward having negative residuals on the inner shelf (strata 10 and 20)."

With this year's methodological change, all species and strata now show switches between positive and negative residuals over time (Figure 53). Pacific cod condition was generally negative on the outer and northern shelf (Strata 40, 50, and 60) from 2010–2019 and positive from 2001–2005. Large pollock (>250 mm) condition was negative on the inner shelf (strata 10 and 20) from 2015–2019 and positive from 2006–2014. Small pollock (100–250 mm) condition was generally positive on the inner shelf from 2014–2019 and negative from 2006–2013. In 2019, positive residuals occurred in all strata for northern rock sole, yellowfin sole, and arrowtooth flounder. Other species had a mix of positive and negative residuals among strata.

Factors influencing observed trends: There are several factors that may influence the observed temporal and spatial patterns in fish condition over the EBS and NBS shelf. Water temperature could explain some of the spatial and temporal variability in length-weight residuals. Water temperatures during the 1999 survey were particularly cold in the Bering Sea and this corresponded to a year of negative length-weight residuals for all groundfish examined where data existed. Despite the abundant large crustacean zooplankton and relatively high microzooplankton productivity present in 1999 (Hunt et al., 2008), temperature-dependent groundfish spatial distributions may have affected the spatial overlap of fish and their prey thereby impacting fish growth and condition in that year. Cold temperatures may have also affected fish energy requirements in that year. Conversely, recent and continuing warm temperatures across the Bering Sea shelf since the "Warm Blob" (Bond et al., 2015; Stabeno and Bell, 2019) may be influencing the present positive trend in fish condition for the species examined.

Other factors that could affect length-weight residuals include survey timing, stomach fullness, and fish movement patterns. The starting date of length-weight data collections has varied annually from late May to early June (except 1998, where the first data available were collected in late July). Variation in condition could relate to the timing of collection within stratum. Another consideration that cannot be addressed with the present data set is that the fish weights used in these analyses are typically inclusive of stomach weights so that gut fullness could influence the length-weight residuals. Since feeding conditions likely change over space and time, how much the fish ate at its last meal and the proportion of its total body weight attributable to the gut weight could be an important factor influencing the length-weight residuals. We can also expect some fish to exhibit seasonal or ontogenetic movement patterns during the survey months. For example, seasonal migrations of pollock occur from overwintering areas along the outer shelf to shallow waters (90–140 m) for spawning; Pacific cod concentrate on the shelf edge and upper slope (100–250 m) in the winter and move to shallower waters (generally <100 m) in the summer; and arrowtooth flounder are distributed throughout the continental shelf until age 4, when, at older ages, they disperse to occupy both the shelf and the slope (Witherell, 2000). It is important to note that the data and analyses reported here depict spatial and temporal variation of length-weight residuals for a small subset of the fish species collected in the AFSC/RACE GAP summer bottom trawl surveys of the EBS and NBS and that they do not inform the mechanisms or processes behind the observed patterns.

Implications: Fish condition can be considered an indicator of ecosystem productivity with implications for fish survival. In Prince William Sound, the condition of herring prior to the winter may determine their subsequent survival (Paul and Paul, 1999). Thus, the condition of EBS and NBS groundfishes may provide us with insight into ecosystem productivity as well as fish survival and population health. However, survivorship is likely affected by many factors not examined here. We also must consider that, in these analyses, fish condition was computed for all sizes of fishes combined, except in the case of pollock. Examining condition of early juvenile stage fishes not yet recruited to the fishery, or the condition of adult fishes separately, could provide greater insight into the value of length-weight residuals as an indicator of individual health or survivorship.

The positive trend in fish condition observed over the last two to three AFSC/RACE GAP EBS and NBS bottom trawl surveys (i.e., increasingly positive length-weight residuals) could be related to concurrent trends

in other ecosystem covariates and needs to be examined further. Trends such as warmer water temperatures following the "Warm Blob" event of 2014–2015 (Bond et al., 2015) and reduced sea ice and cold pool areal extent in the eastern Bering Sea (Stabeno and Bell, 2019) may affect fish condition here in ways that are yet to be determined. As we continue to add years of fish condition indices to the record and expand on our knowledge of the relationships between condition, growth, production, survival, and the ecosystem, these data may increase our insight into the health of fish populations in the EBS and NBS.

Research priorities: Efforts are underway to redevelop the groundfish condition indicator for next year's (2021) Ecosystem Status Report using a spatio-temporal model with spatial random effects (VAST). The change is expected to allow more precise biomass expansion, improve estimates of uncertainty, and better account for spatial-temporal variation in length-weight samples from bottom trawl surveys due to methodological changes in sampling (e.g., transition from sex-and-length stratified sampling to random sampling). For 2021, revised indicators will be presented alongside a retrospective analysis that compares the historical and revised condition indicator. Currently, research is being planned across multiple AFSC programs to explore standardization of statistical methods for calculating condition indicators, and to examine relationships among morphometric condition indicators, bioenergetic indicators, and physiological measures of fish condition.

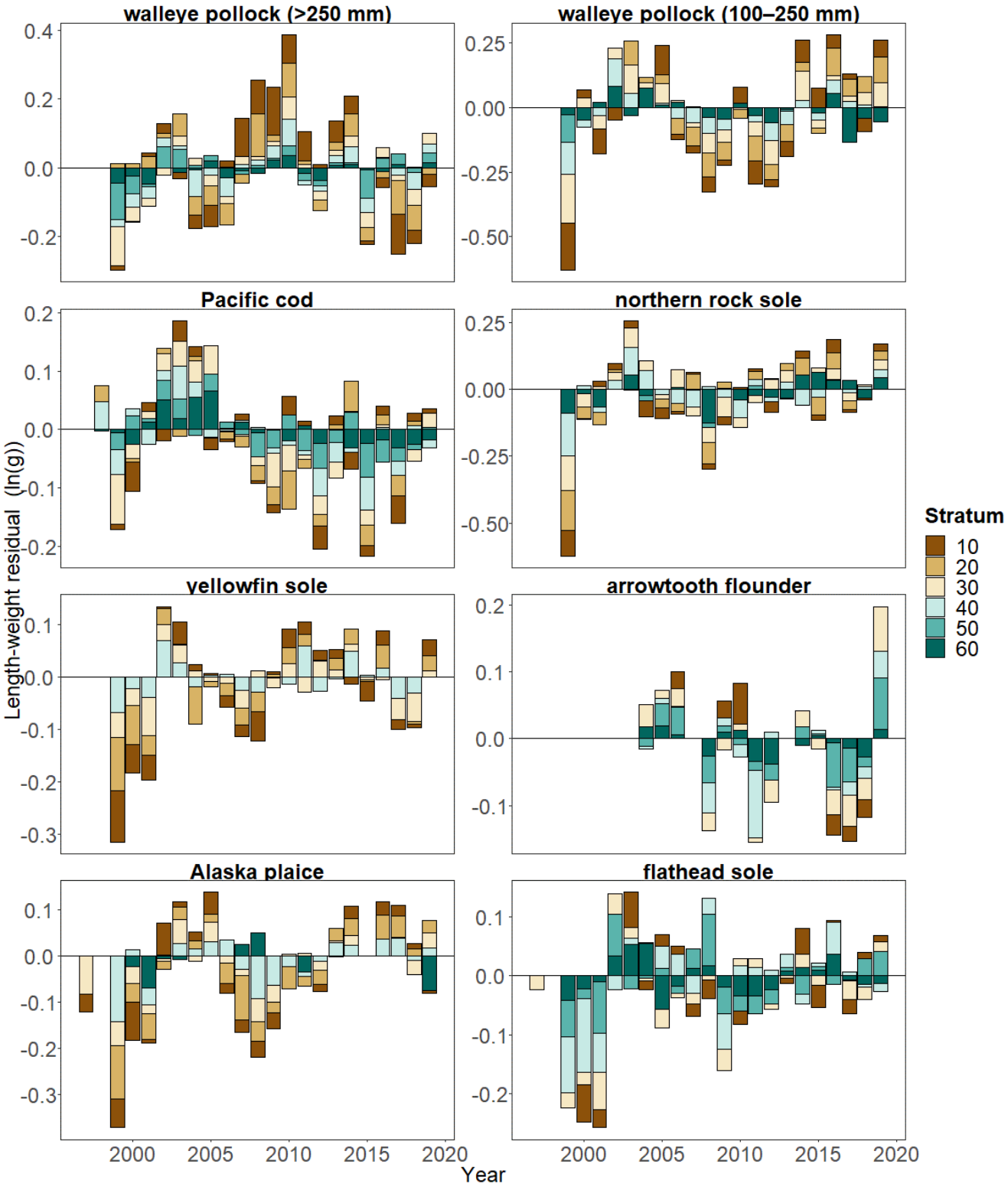

Figure 53: Length-weight residuals by survey stratum (10–60) for seven eastern Bering Sea shelf groundfish species and age 1–2 pollock (100–250 mm) sampled in the AFSC/RACE GAP standard summer bottom trawl survey, 1997–2019. Length-weight residuals are not weighted by stratum biomass.

Multispecies Model Estimates of Time-varying Natural Mortality

Contributed by Kirstin K. Holsman[1], Jim Ianelli[1], Kerim Aydin[1], Kalei Shotwell[1], Grant Thompson[1], Kelly Kearney[2], and Ingrid Spies[1]
[1]Resource Ecology and Fishery Management Division, Alaska Fisheries Science Center, National Marine Fisheries Service, NOAA
[2]University of Washington, Cooperative Institute for Climate, Ocean, and Ecosystem Studies [CICOES] and NOAA Fisheries, Alaska Fisheries Science Center

Contact: kirstin.holsman@noaa.gov
Last updated: November 2020

Description of indicator: We report trends in age-1 total mortality for walleye pollock (*Gadus chalcogrammus*), Pacific cod (*Gadus macrocephalus*), and arrowtooth flounder (*Atheresthes stomias*) from the eastern Bering Sea. Total mortality rates are based on residual mortality inputs (M1) and model estimates of annual predation mortality (M2) produced from the multi-species statistical catch-at-age assessment model (known as CEATTLE; Climate-Enhanced, Age-based model with Temperature-specific Trophic Linkages and Energetics). See Appendix 1 of the BSAI pollock stock assessment for 2020, Holsman et al. (2016), Holsman and Aydin (2015), Ianelli et al. (2016), and Jurado-Molina et al. (2005) for more information.

Status and trends: Estimated age-1 natural mortality (i.e., M1+M2) for pollock, Pacific cod, and arrowtooth flounder peaked in 2016. At 1.55 yr^{-1}, age-1 mortality estimated by the model was greatest for pollock and lower for Pacific cod and arrowtooth, with total age 1 natural mortality at around 0.69 and 0.65 yr^{-1}, respectively. 2020 natural mortality across species is 19% to 34% lower than in 2016 and is no longer above average for pollock (relative to the long-term mean) (Figure 54), while Pacific cod and arrowtooth mortality continue to decline and are well below the long-term mean.

The total biomass of each species consumed by the predators in the model reflects patterns in age-1 natural mortality. In 2020, the total biomass of pollock consumed by all three predators in the model (typically 1–3 yr old fish) dropped slightly below the long-term mean. Meanwhile, Pacific cod and arrowtooth biomass consumed was well below and near the long-term means, respectively (Figure 55).

Factors influencing observed trends: Temporal patterns in natural mortality reflect annually varying changes in predation mortality that primarily impact age-1 fish (and to a lesser degree impact ages 2 and 3 fish in the model). Pollock are primarily consumed by older conspecifics, and pollock cannibalism accounts for 58% (on average) of total age-1 predation mortality on average, with the exception of the years 2006–2008 when predation by arrowtooth exceeded cannibalism as the largest source of predation mortality of age-1 pollock (Figure 56). The relative proportion of pollock consumed by Pacific cod predators declined in 2020.

Combined annual predation demand (annual ration) of pollock, Pacific cod, and arrowtooth flounder in 2020 was 5.94 million tons, down slightly from the 6.98 million t annual average during the warm years of 2014–2016. Pollock represent approximately 79% of the model estimates of combined prey consumed with a long term average of 5.29 million tons of pollock consumed annually by all three predators in the model. Individual annual rations continue to increase and are well above average for all three predator species, driven by maturing adult biomass combined with anomalously warm water temperatures in the Bering Sea during recent years (Figure 57).

Implications: We find evidence of continued decline in predation mortality on age-1 pollock, Pacific cod, and arrowtooth flounder. While warm temperatures continue to lead to high metabolic (and energetic) demand of predators, declines in total predator biomass are contributing to an overall decline in total consumption and therefore reduced predation rates and mortality. This pattern may also explain recent increases in recruitment of EBS pollock over 2018–2020 and Pacific cod in 2020.

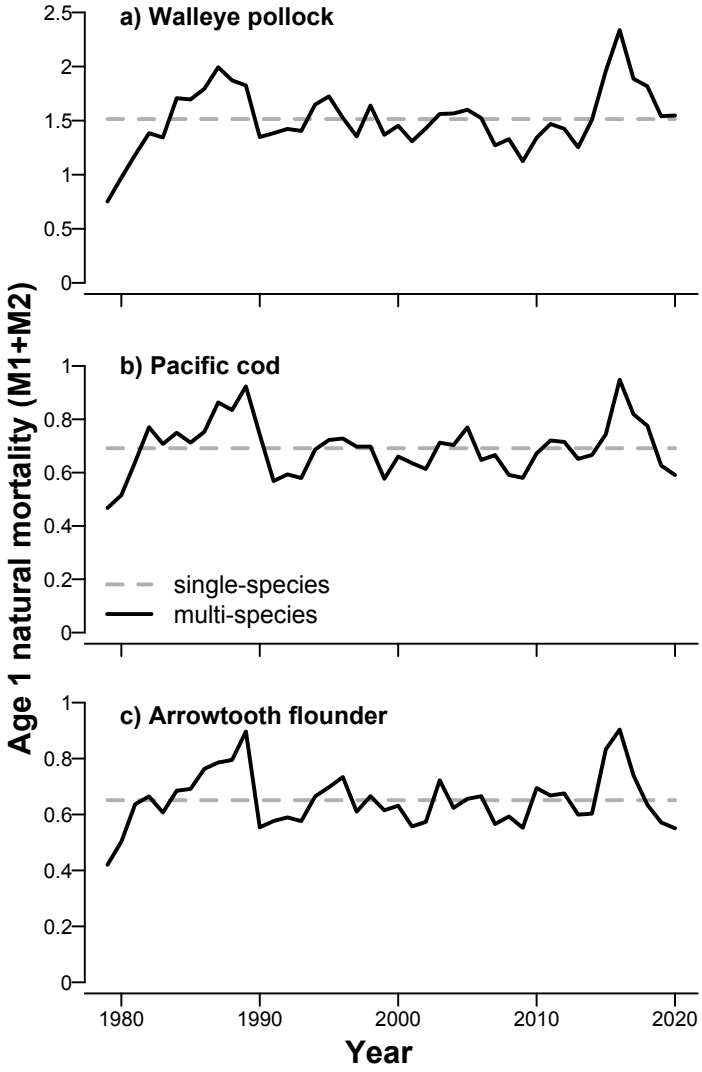

Figure 54: Annual variation in total mortality ($M1_{i1} + M2_{i1,y}$) for (a) age-1 pollock, (b) Pacific cod, and (c) arrowtooth flounder from the single-species models (dashed gray line) and the multi-species models with temperature (black line). Updated from Holsman et al. (2016); more model detail can be found in Appendix 1 of the BSAI pollock stock assessment for 2020.

Between 1980 and 1993, relatively high natural mortality rates reflect patterns in combined annual demand for prey by all three predators that was highest in the mid 1980's (collectively 8.34 million t per year) and in recent years (collectively 6.72 million t per year). The peak in predation mortality of age-1 pollock in 2006 corresponds to the maturation of a large age class of 5–7 year old pollock and 2 year old Pacific cod that dominated the age composition of the two species in 2006. Similarly, the recent peaks in mortality in 2016 reflect anomalously warm water temperatures combined with the maturation of the large 2010–2012 year class of pollock.

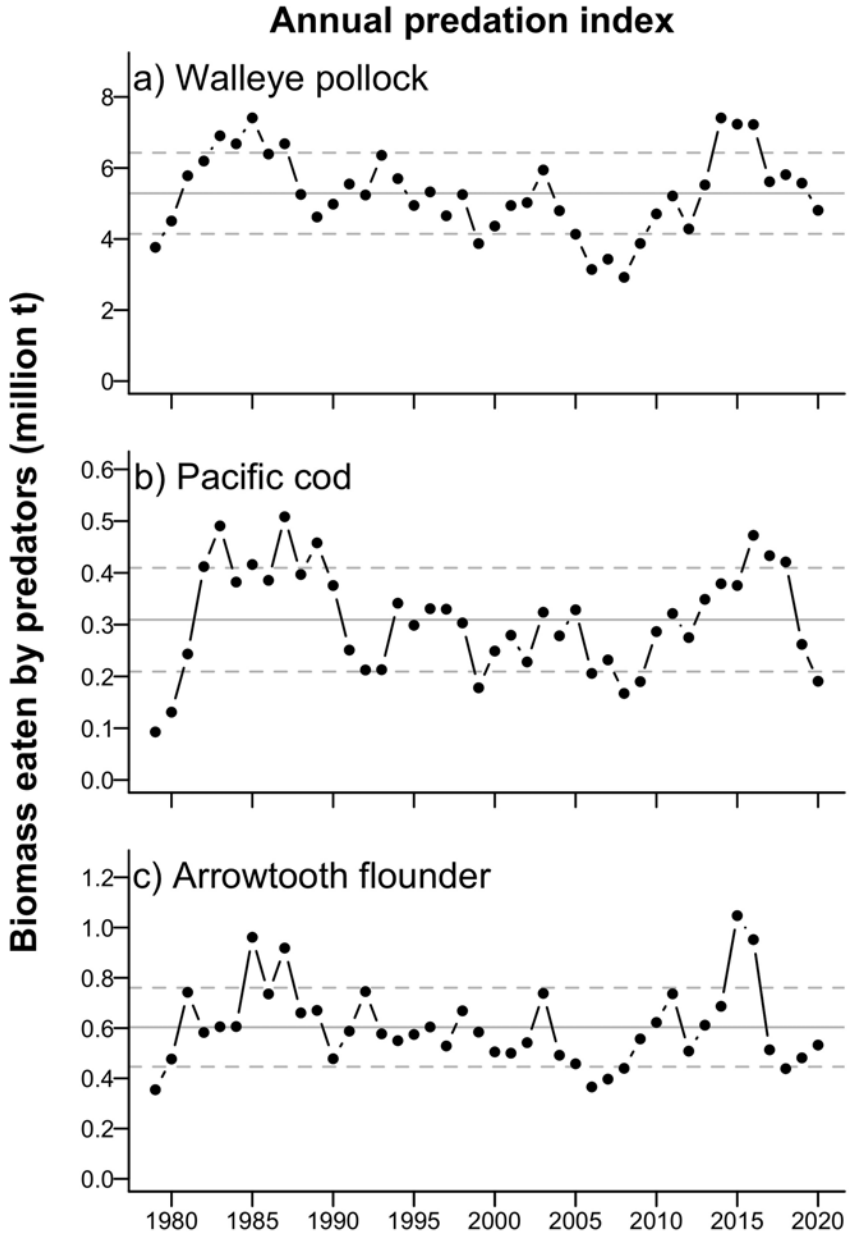

Figure 55: Multispecies estimates of prey species biomass consumed by all predators in the model: a) total biomass of pollock consumed by predators annually, b) total biomass of Pacific cod consumed by predators annually, c) total biomass of arrowtooth flounder consumed by predators annually. Gray lines indicate 1979–2020 mean estimates for each species.

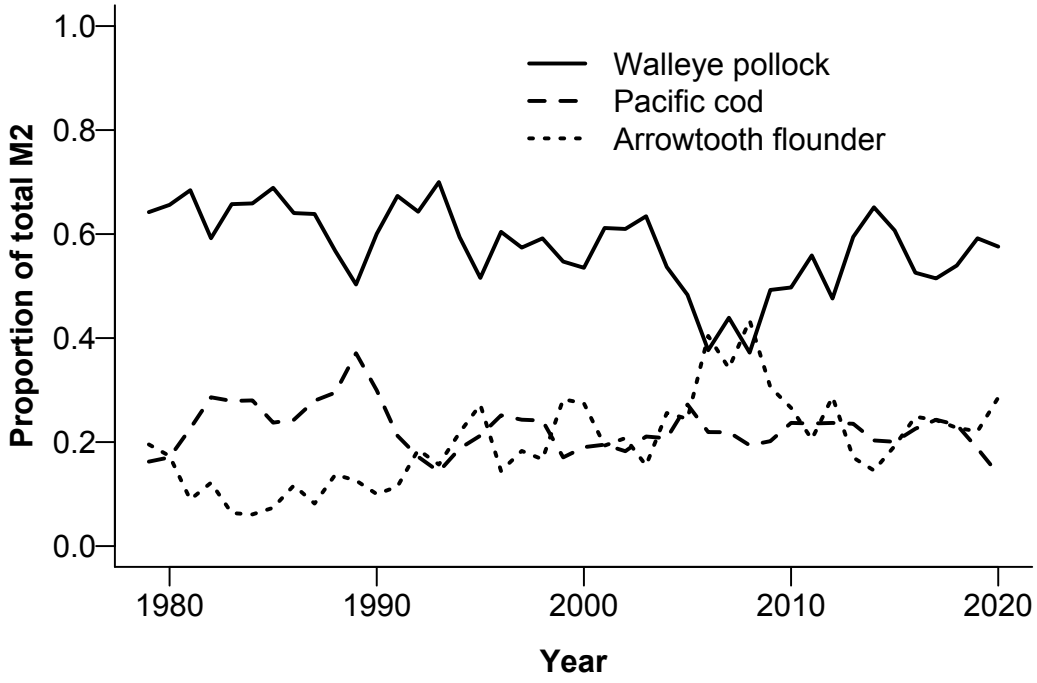

Figure 56: Proportion of total predation mortality for age-1 pollock from pollock (solid), Pacific cod (dashed), and arrowtooth flounder (dotted) predators across years. Updated from Holsman et al. (2016); more model detail can be found in Appendix 1 of the BSAI pollock stock assessment for 2020.

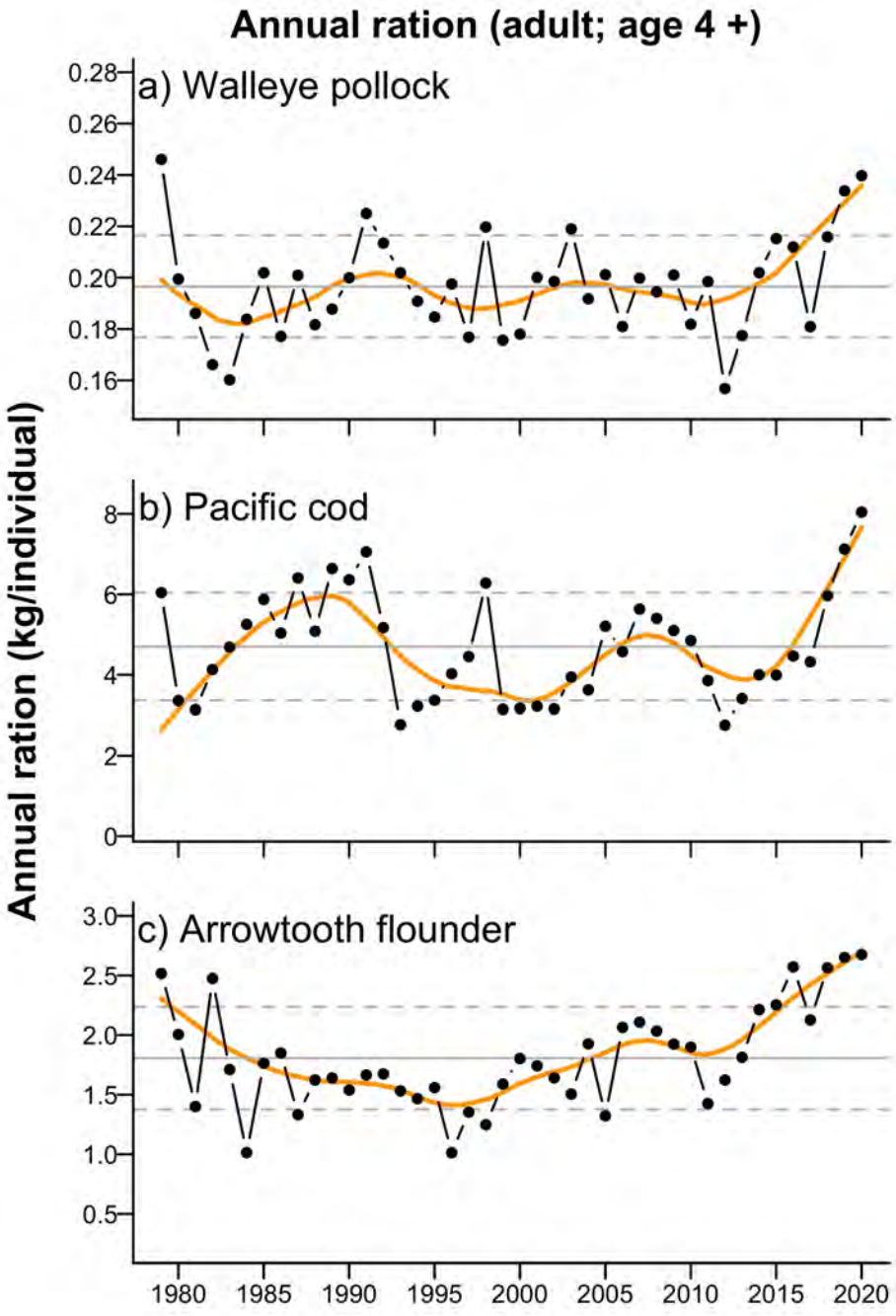

Figure 57: Multispecies estimates of annual ration (kg consumed per individual per year) for adult (age 4+) predators: a) pollock, b) Pacific cod, and c) arrowtooth flounder. Gray lines indicate 1979–2020 mean estimates and 1 SD for each species; orange line is a 10-y (symmetric) loess polynomial smoother indicating trends in ration over time.

Groundfish Recruitment Predictions

Temperature Change Index and the Recruitment of Bering Sea Pollock

Contributed by Ellen Yasumiishi
Auke Bay Laboratories, Alaska Fisheries Science Center, National Marine Fisheries Service, NOAA
Contact: ellen.yasumiishi@noaa.gov
Last updated: August 2020

Description of indicator: The temperature change (TC) index is a composite index for the pre- and post-winter thermal conditions experienced by walleye pollock (*Gadus chalcogrammus*) from age-0 to age-1 in the southeastern Bering Sea (Martinson et al., 2012). The TC index (year t) is calculated as the difference in the average monthly sea surface temperature in June (t+1) and August (t) (Figure 58) in an area of the southern region of the eastern Bering Sea (56.2°N to 58.1°N by 166.9°W to 161.2°W). Time series of average monthly sea surface temperatures were obtained from the NOAA Earth System Research Laboratory Physical Sciences Division website. Sea surface temperatures were based on NCEP/NCAR gridded reanalysis data (Kalnay et al. (1996), data obtained from `http://www.esrl.noaa.gov/psd/cgi-bin/data/timeseries/timeseries1.pl`). Less negative values represent a cool late summer during the age-0 phase followed by a warm spring during the age-1 phase for pollock.

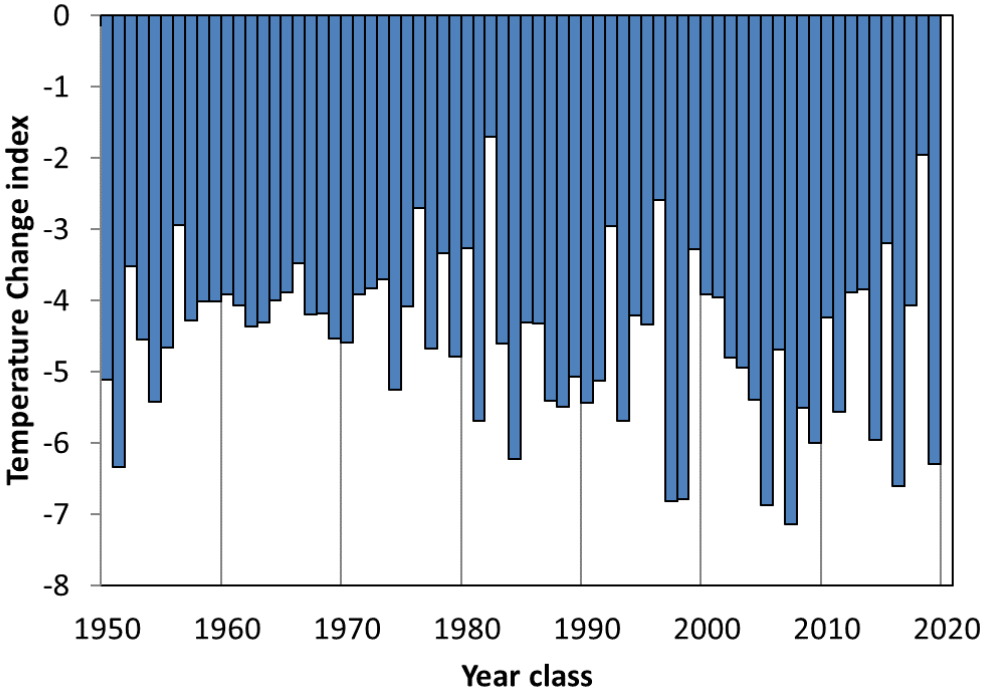

Figure 58: The temperature change index values for the 1950–2019 pollock year classes. Values represent the difference in sea temperatures on the southeastern Bering Sea shelf experienced by the 1950–2019 year classes. Less favorable conditions (more negative values) represent a warm late summer during the age-0 life stage followed by a relatively cool spring during the age-1 life stage. More favorable conditions (less negative values) represent a cool late summer during the age-0 life stage followed by a relatively warm spring during the age-1 life stage.

Status and trends: The 2020 TC index is -6.30, higher than the 2019 TC index of -1.96, indicating below average conditions for pollock survival from age-0 and age-1 from 2019 to 2020. The decrease in expected survival is due to the larger difference in sea temperature from late summer to the following spring. The late summer sea surface temperature in August 2019 was 13.3°C (higher the long-term average of 9.8°C) and spring sea surface temperature in June 2020 was 7.0° (higher than the long-term average of 5.2°C). The TC index was positively correlated with recruitment of pollock to age-1 through age-6 for the 1964–2019 and 1977–2019 year classes, significantly correlated for age-5 and age-6 for the 1996–2019 year classes, but not significantly correlated for the shorter period for age-1 through age-4 year classes in 1996–2019) (Table 3).

Table 3: Pearson's correlation coefficient relating the temperature change index to subsequent estimated pollock year class strength. Bold values are statistically significant ($p<0.05$).

	Correlations					
	Age-1	Age-2	Age-3	Age-4	Age-5	Age-6
1964–2019	**0.34**	**0.37**	**0.36**	**0.31**	**0.31**	**0.30**
1977–2019	**0.41**	**0.45**	**0.46**	**0.45**	**0.52**	**0.52**
1996–2019	0.32	0.38	0.40	0.38	**0.48**	**0.44**

Factors influencing observed trends: According to the original Oscillating Control Hypothesis (OCH), warmer spring temperatures and earlier ice retreat lead to a later oceanic and pelagic phytoplankton bloom and more food in the pelagic waters at an optimal time for use by pelagic species (Hunt et al., 2002). The revised OCH indicated that age-0 pollock were more energy-rich and have higher over wintering survival to age-1 in a year with a cooler late summer (Coyle et al., 2011; Hunt et al., 2011; Heintz et al., 2013). Therefore, the warmer late summer conditions during the age-0 phase followed by warmer spring temperatures during the age-1 phase are assumed unfavorable for the survival of pollock from age-0 to age-1. The 2019 year class of pollock experienced above average late summer temperatures during the age-0 stage and warm spring conditions in 2020 during the age-1 stage, indicating below average conditions for over wintering survival from age-0 to age-1.

Implications: The TC index for the 2016 year class would indicate poor recruitment of pollock to age-4 in 2020. The 2020 TC index value of -6.30 was below the long-term average of -4.58, therefore we expect below average recruitment of pollock to age-4 in 2023 from the 2019 year class (Figure 59).

Large Copepod Abundance (Sample-Based and Modeled) as an Indicator of Pollock Recruitment to Age-3 in the Southeastern Bering Sea

Contributed by Ellen Yasumiishi[1], Lisa Eisner[1], and David Kimmel[2]
[1]Auke Bay Laboratories, Alaska Fisheries Science Center, NOAA Fisheries
[2]Resource Assessment and Conservation Engineering Division, Alaska Fisheries Science Center, NOAA Fisheries
Contact: Ellen.Yasumiishi@noaa.gov
Last updated: August 2020

Description of indicator: Interannual variations in large copepod abundance during the age-0 life stage were compared to age-3 walleye pollock (*Gadus chalcogrammus*) abundance (billions of fish) for the 2002–2018 year classes on the southeastern Bering Sea shelf (south of 60°N, < 200 m bathymetry) (Eisner et al., 2020). The large copepod index sums the abundances of *Calanus marshallae/glacialis* (copepodite stage 3 (C3)–adult), *Neocalanus* spp. (C3–adult), and *Metridia pacifica* (C4–adult), taxa typically important in age-0 pollock diets (Coyle et al., 2011). Zooplankton samples were collected with oblique bongo tows over

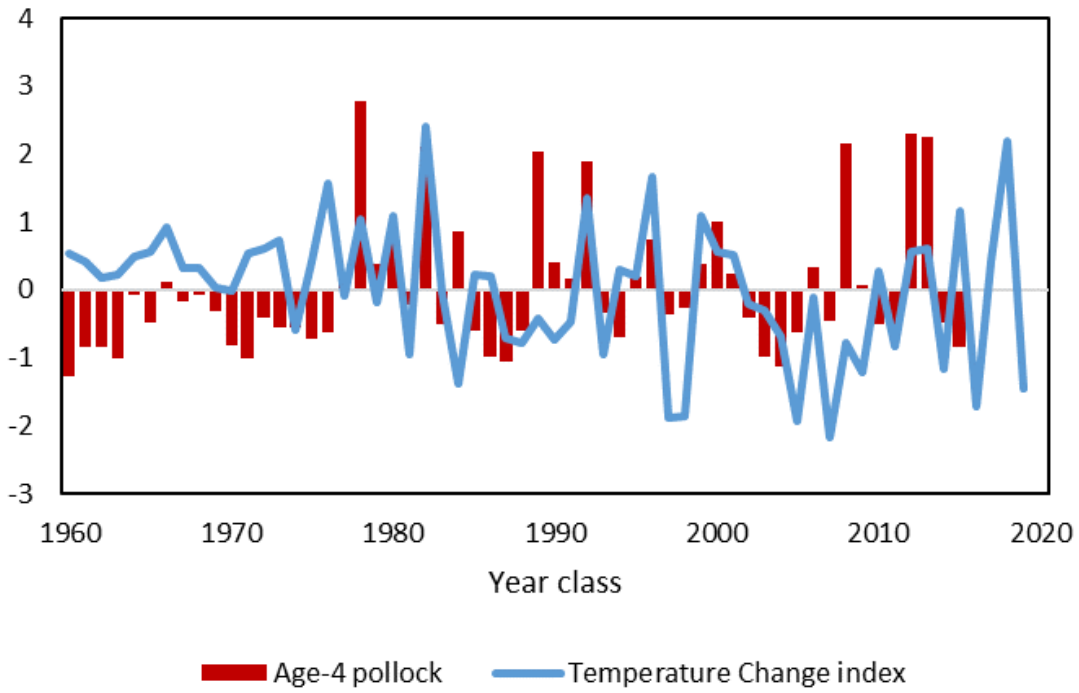

Figure 59: Normalized time series values of the temperature change index indicating conditions experienced by the 1960–2019 pollock year classes during the late summer age-0 and spring age-1 life stages. Normalized values of the estimated abundance of age-4 pollock from 1964–2019 for the 1960–2015 year classes are shown. Age-4 pollock estimates are from Table 30 in Ianelli et al. 2019.

the water column using 60 cm, 505 μm mesh nets for 2002–2011, and 20 cm, 153 μm mesh or 60 cm, 505 μm nets, depending on taxa and stage for 2012–2018.

Data were collected on the Bering Arctic Subarctic Integrated Survey (BASIS) fishery oceanography surveys and along the 70 m isobath during mid-August to late September, for four warm years (2002–2005) followed by one average (2006), six cold (2007–2012), four warm (2014–2016, 2018), and an average year (2017, 70 m isobath only) using methods in Eisner et al. (2014). Zooplankton data were not available for 2013. Age-3 pollock abundance was obtained from the stock assessment report for the 2002–2016 year classes (Ianelli et al., 2019). Two estimates of large copepod abundances were calculated, the first using means among stations (sample-based), and the second using the means estimated from the geostatistical model, Vector Autoregressive Spatial Temporal (VAST) package version 9.4.0 (Thorson et al., 2016*a*,*b*; Thorson and Barnett, 2017). We specified 30 knots, a log normal distribution, and the delta link function between probability of encounter and positive catch rate in VAST.

Status and trends: Positive significant linear relationships were found between BASIS sample-based mean abundances, BASIS VAST-modeled mean abundances, and sample-based mean abundances from the 70 m isobath surveys of large copepods collected during the age-0 stage of pollock and stock assessment estimates of age-3 pollock for the 2002–2016 year classes (Figure 60). For the BASIS survey stations, the stronger relationship of age-3 pollock with the large copepod index using the VAST model compared to observed means among stations (R^2=0.72 vs R^2=0.43) appeared to be partially due to the VAST model filling in data for survey areas missed in some years (e.g., 2008).

Fitted means and standard errors of the age-3 pollock abundances were estimated from the linear regression model using large copepod estimates from the BASIS VAST model and compared to the pollock stock

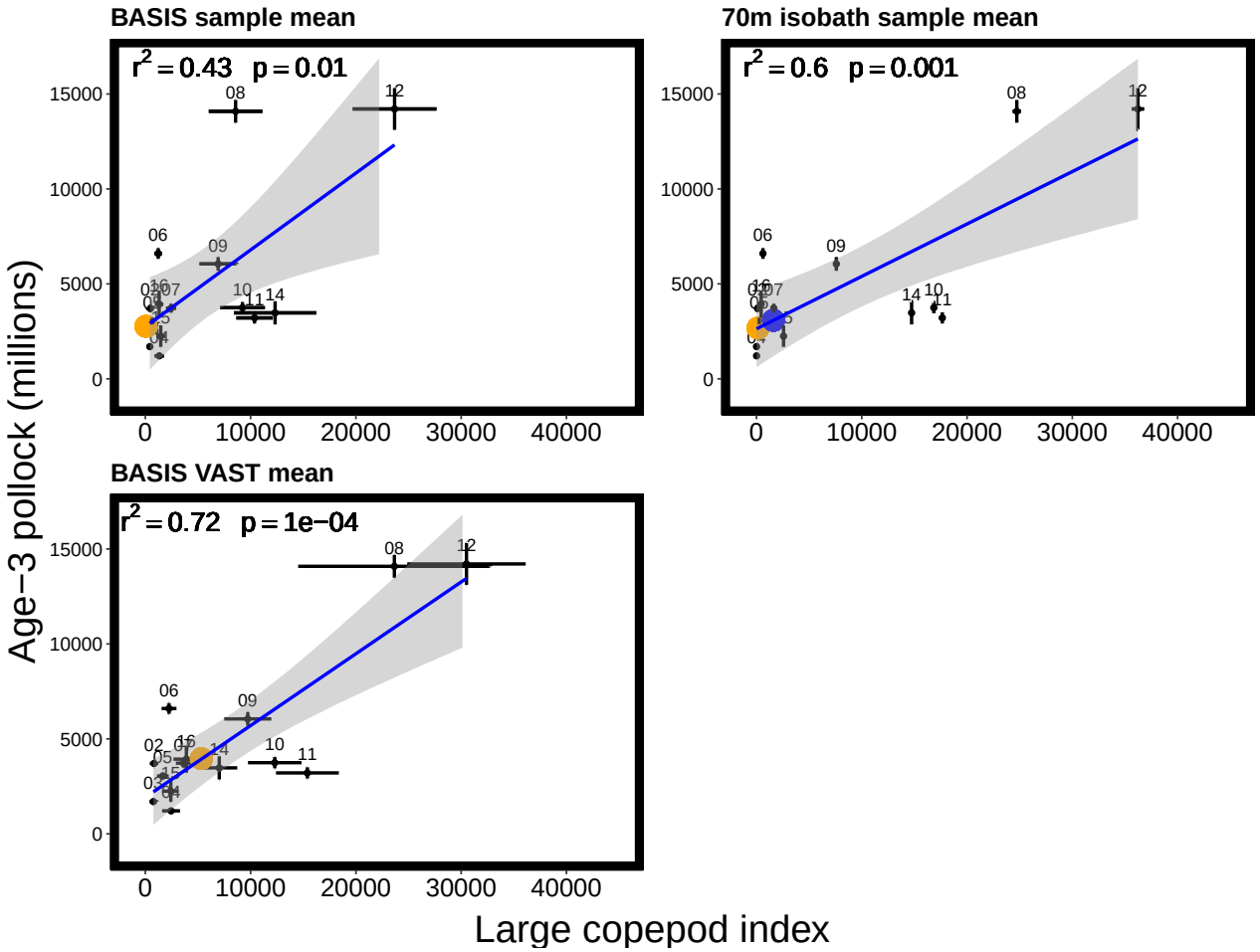

Figure 60: Linear relationships between sample-based (top) from the BASIS and 70 m isobaths surveys and VAST-model (bottom; from BASIS) estimated mean abundance of large copepods (C+MN, sum of *Calanus marshallae/glacialis*, *Metridia pacifica*, and *Neocalanus* spp.) during the age-0 life stage of pollock, and the estimated abundance (millions) of age-3 pollock from Ianelli et al. (2019) for 2002–2016 year classes. No zooplankton data were available for 2013. The blue dot is the age-3 pollock estimate from the 2017 large copepod index and the orange dots are the estimates from the 2018 copepod indices.

assessment estimates from Ianelli et al. (2019) (Figure 61). Using the linear regression model relating copepods to age-3 pollock for the 2002–2016 year classes, the VAST copepod estimates in 2018 (5,321 /m^2) predicts below average abundance of age-3 pollock in 2021 (3,959 million, SE=642 million) for the 2018 year class. For data collected from the 70 m isobath, the large copepod index from 2017 predicts relatively higher recruitment of pollock to age-3 in 2020 than from the 2018 year class that will recruit to age-3 in 2021. However, the low values of the copepod indices predict relatively low recruitment to age-3 for the 2017 and 2018 year classes of pollock.

Factors influencing observed trends: Increases in sea ice extent and duration were associated with increases in large zooplankton abundances on the southeastern shelf (Eisner et al., 2014, 2015, 2020), increases in large copepods and euphausiids in pollock diets (Coyle et al., 2011; Hunt et al., 2011), and increases in age-0 pollock lipid content (Heintz et al., 2013). The increases in sea ice and associated ice algae and phytoplankton may provide an early food source for large crustacean zooplankton reproduction and growth (Baier and Napp, 2003; Hunt et al., 2011). These large zooplankton taxa contain high lipid concentrations (especially in cold,

high ice years) which in turn increases the lipid content in their predators such as age-0 pollock and other fish that forage on these taxa. Increases in energy density (lipids) in age-0 pollock allow them to survive their first winter (a time of high mortality) and eventually recruit into the fishery. Accordingly, a strong relationship has been shown for energy density in age-0 fish and age-1 pollock abundance (Heintz et al., 2013).

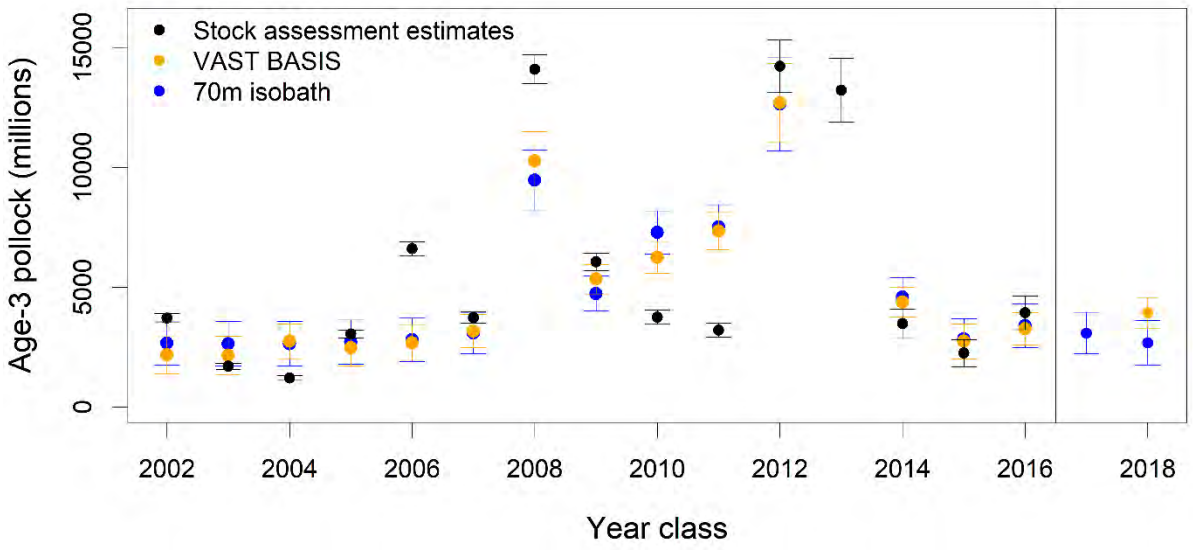

Figure 61: Mean abundance of age-3 pollock estimated from regression models using estimates of large copepods from VAST (orange), sample mean abundance at the 70m isobaths stations (blue), and means from the pollock stock assessment estimates (black) from Ianelli et al. (2019). Predicted estimates of age-3 pollock are shown for the 2017 and 2018 year classes.

Implications: Our results suggest low availability of large copepod prey for age-0 pollock during the first year of life in 2017 and 2018. These conditions may not be favorable for age-0 pollock overwinter survival and recruitment to age-3. Information from the 70 m isobath survey may be useful in years of no BASIS survey in the southeastern Bering Sea. If the relationship between large copepods and age-3 pollock remains significant in our analysis, the index can be used to predict the recruitment of pollock three years in advance of recruiting to age-3, from zooplankton data collected three years prior. This relationship also provides further support for the revised oscillating control hypothesis that suggests that as the climate warms, reductions in the extent and duration of sea ice could be detrimental to large crustacean zooplankton and subsequently to the pollock fishery in the southeastern Bering Sea (Hunt et al., 2011).

Benthic Communities and Non-Target Fish Species

There are no updates to Benthic Communities and Non-Target Fish Species indicators in this year's report. See the contribution archive for previous indicators at: `https://access.afsc.noaa.gov/REFM/REEM/ecoweb/`.

Seabirds

Integrated Seabird Information

This integration is in response to ongoing collaborative efforts within the seabird community and contains contributions from (in alphabetical order):

Lauren Divine (Ecosystem Conservation Office at Aleut Community of St. Paul Island)
Serafima Edelen (Community member, St. Paul Island)
Tim Jones (University of Washington, Coastal Observation and Seabird Survey Team (COASST), Seattle, WA)
Robb Kaler (U.S. Fish and Wildlife Service, Migratory Bird Management, Anchorage, AK)
Alexander Kitaysky (University of Alaska Fairbanks, Institute of Arctic Biology, Fairbanks, AK)
Kathy Kuletz (U.S. Fish and Wildlife Service, Migratory Bird Management, Anchorage, AK)
Elizabeth Labunski (U.S. Fish and Wildlife Service, Migratory Bird Management, Anchorage, AK)
Dennis Lekanof (Community member, Island Sentinel, St. George Island)
Aaron Lestenkof (Community member, Island Sentinel, St. Paul Island)
Jackie Lindsey (University of Washington, Coastal Observation and Seabird Survey Team (COASST), Seattle, WA)
Paul Melovidov (Community member, Island Sentinel, St. Paul Island)
Elena Oaks (Community member, Hooper Bay)
Marc Romano (U.S. Fish and Wildlife Service, Alaska Maritime National Wildlife Refuge, Homer, AK)
Gay Sheffield (University of Alaska Fairbanks, Alaska Sea Grant, Nome, AK)
Punguk Shoogukwruk (Community member, Savoonga, AK)
Alexis Will (University of Alaska Fairbanks, Institute of Arctic Biology, Fairbanks, AK)

Last updated: October 2020

Summary Statement
During 2020, the U.S. Fish and Wildlife Service was unable to conduct field research in the eastern and northern Bering Sea due to COVID-19 travel restrictions. Coastal community members, tribal governments, and state/university partners provided information on seabird dynamics; the U.S. Fish and Wildlife Service biologists helped to synthesize this information. At the Pribilof Islands, seabird attendance appeared generally similar to recent years, though some species may have begun attending the colony later than usual. Least auklet attendance at the colonies and abundance in the waters around the island has declined in recent years and this continues to be of concern to the St. Paul Island community. Community members of St. George Island reported that birds returned to the island at the usual time and in typical abundance with good colony attendance throughout the summer. In the northern Bering Sea, on St. Lawrence Island, reproductive success and colony attendance differed among fish-eating and planktivorous seabirds suggesting foraging impacts across trophic levels. In the Bering Strait region, emaciation and starvation were observed in some individuals throughout the summer and beach-cast carcasses of several species were observed on the eastern and western sides of the Bering Strait (for more information on this, see the USFWS B Report). Seabird mortality events observed in the northern Bering Sea in 2020 were unusual owing to the magnitude, geographic range, and their duration.

Introduction
Seabirds are upper-trophic level predators and as such are indicators of marine ecosystem changes. Population-level responses in vital rates (e.g., reproductive success, adult survival, population growth) can signal shifts in prey availability that also affect commercial fish populations. In this Integrated Seabird Information section, we synthesize information from tribal members, community members, and researchers to provide an overview of environmental impacts to seabirds and what that may indicate for ecosystem productivity

as it pertains to fisheries management. We merge across information sources to derive regional summaries within the southeastern and northern Bering Sea and interpret changes in seabird dynamics with respect to understanding ecosystem productivity.

Approach
We focused on three observable parameters of seabird ecology that serve as broader ecosystem indicators important to fisheries managers:

Reproductive success reflects feeding conditions in the environment for breeding birds and has implications on seabird population trajectories, subsistence egging practices, and food security. Timing of seabird reproductive stages (phenology) at colonies can reflect ecosystem conditions encountered by birds during the months preceding the breeding season. Long-lived seabirds may defer or delay breeding if foraging conditions limit their ability to build up energy reserves to support energetic demands during the breeding season. Widespread reproductive failure during the breeding season, such as abandonment of nest sites, may indicate that foraging conditions deteriorated rapidly or the presence of disturbance at the colony such as from land-based predators. Reproductive success within a season can differ among planktivorous (primarily zooplankton-feeding), piscivorous (primarily forage fish-feeding), and mixed planktivorous/piscivorous species, which may reflect differences among availability of prey resources including differences in abundance, distribution, and nutritional quality.

Colony attendance (timing and numbers) reflects differences in the proportion of birds attempting to breed or may reflect survival trends. Non-breeders also attend the colony (e.g., murres), even in poor years, so attendance patterns must be interpreted with caution. Changes in colony attendance can represent the conditions birds experienced prior to breeding and/or more variability in the cyclic and seasonal patterns in the marine environment. Earlier colony attendance may indicate that foraging conditions were favorable, such that birds were able to build enough energy reserves to prepare them for the breeding season. Later and/or lower numbers of birds arriving at colonies may reflect poor winter foraging conditions or a mismatch in bloom timing and subsequent ocean productivity.

Mortality events indicate broader ecosystem concerns such as changes in prey abundance, distribution, or nutritional quality, as well as harmful algal bloom (HAB) events. Birds in poor physical condition due to lack of food or low food quality may be more susceptible to disease or severe storm events. Seabird mortality events in the northern Bering Sea are unusual owing to the magnitude, geographic range, and their duration.

Status and Trends
Southeastern Bering Sea (Pribilof Islands)
Reproductive Success
No observations on reproductive success were collected in 2020 due to COVID-19-related survey cancellations.

Colony Attendance
At St. Paul Island least, crested, and parakeet **auklets** have been declining in abundance for several years, but for the first time, no parakeet auklets were observed in 2020. **Red-faced cormorant** populations appeared lower this year; in fact, cormorants were virtually absent from nesting sites close to town on St. Paul Island. **Kittiwakes** and **murres** arrived at St. Paul Island at the typical time, but abundances seemed lower than recent years. That said, subsistence egging of murre eggs occurred and the season was more successful this year than in 2019. Tufted and horned **puffins** were "lower in abundance, as they have been the last 2–3 years".

At St. George Island, red-legged **kittiwakes** and least **auklets** returned to the island at the usual time and in typical abundances with good colony attendance throughout the summer.

Mortality Events
Monitoring by the Coastal Observation and Seabird Survey Team (COASST) and regional partners provides a standardized measure of relative beached bird abundance for the Pribilof Islands from 2006 to present. Time series of month-averaged beached bird abundance for the Pribilof Islands show several of the recent mortality

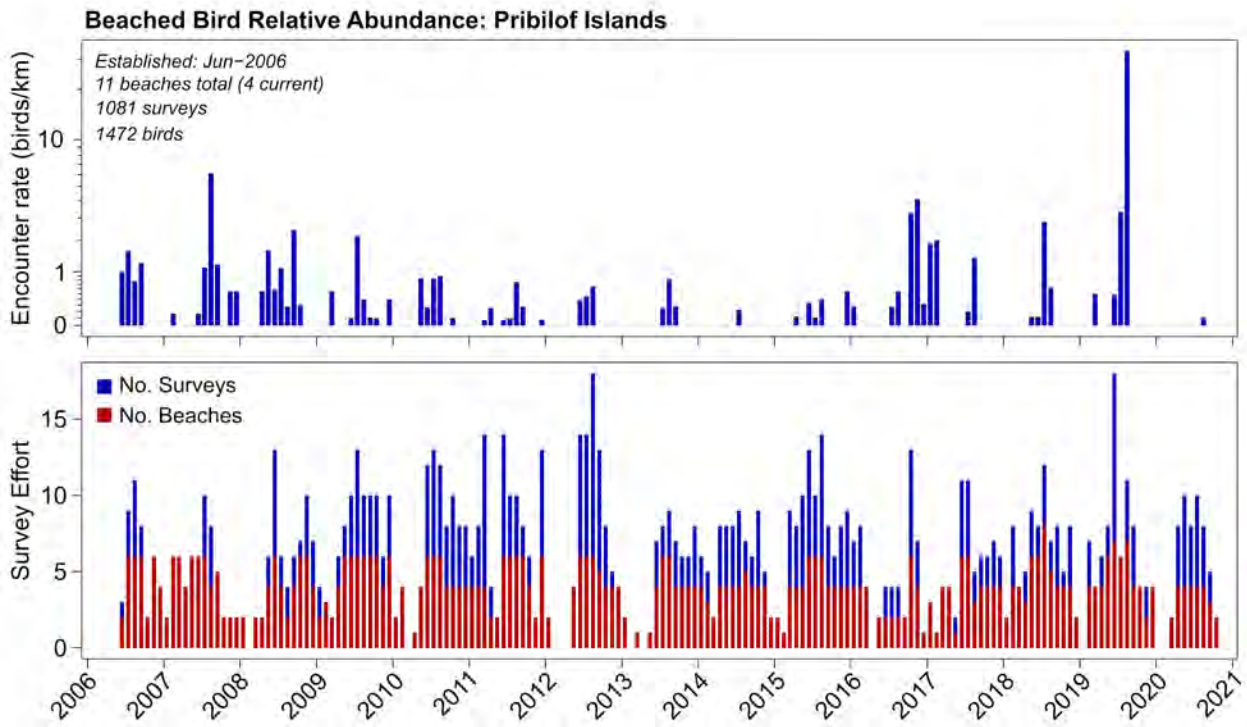

Figure 62: Month-averaged beached bird abundance, standardized per km of survey effort, for the Pribilof Islands. The top panel shows the month-averaged encounter rate (ER: birds per km). The bottom panel shows survey effort at the monthly scale.

events that have affected the Bering Sea. In 2020, monthly beach survey effort was decreased compared to previous years, both in number of surveys conducted and number of beaches surveyed – notably beaches on St. George Island were not surveyed in 2020 (Figure 62). However, fewer birds were found in the Pribilof Islands in 2020 (a single Shearwater was reported); 2020 was among the lowest encounter rate recorded for the Pribilof Islands.

Northern Bering Sea (including St. Lawrence Island and the Bering Strait region)

Reproductive Success

Saint Lawrence Island:

Reproductive success for least and crested **auklets** is calculated as the number of chicks potentially fledged from the number of active nests observed on the first nest check of the season (in 2020 nest checks started approximately 2 weeks later than in previous years). Least and crested auklets at the Kitnik colony hatched chicks about a week earlier than usual (Figure 63).

Least auklet reproductive success was low (0.18 chicks per active nest) and was characterized by an unusual early mass fledging event in which chicks left their nests and wandered inland, to nearby ponds, and in a few cases to the ocean. These events occur when chicks begin to starve later in the chick-rearing period. Crested auklet reproductive success was comparable to 2016 and 2017 (0.52 chicks per active nest) after two years of complete reproductive failure in 2018 and 2019. A resident of the Native Village of Savoonga reported that crested auklets were present, but fewer than normally seen.

Reproductive success for common and thick-billed **murres** is based on the number of chicks estimated and counted on study plots. At Kevipak colony, common murres experienced similar reproductive success in 2020 to 2019, but lower than 2017. Thick-billed murres had slightly lower reproductive success in 2020 than in 2019, and much lower than in 2017.

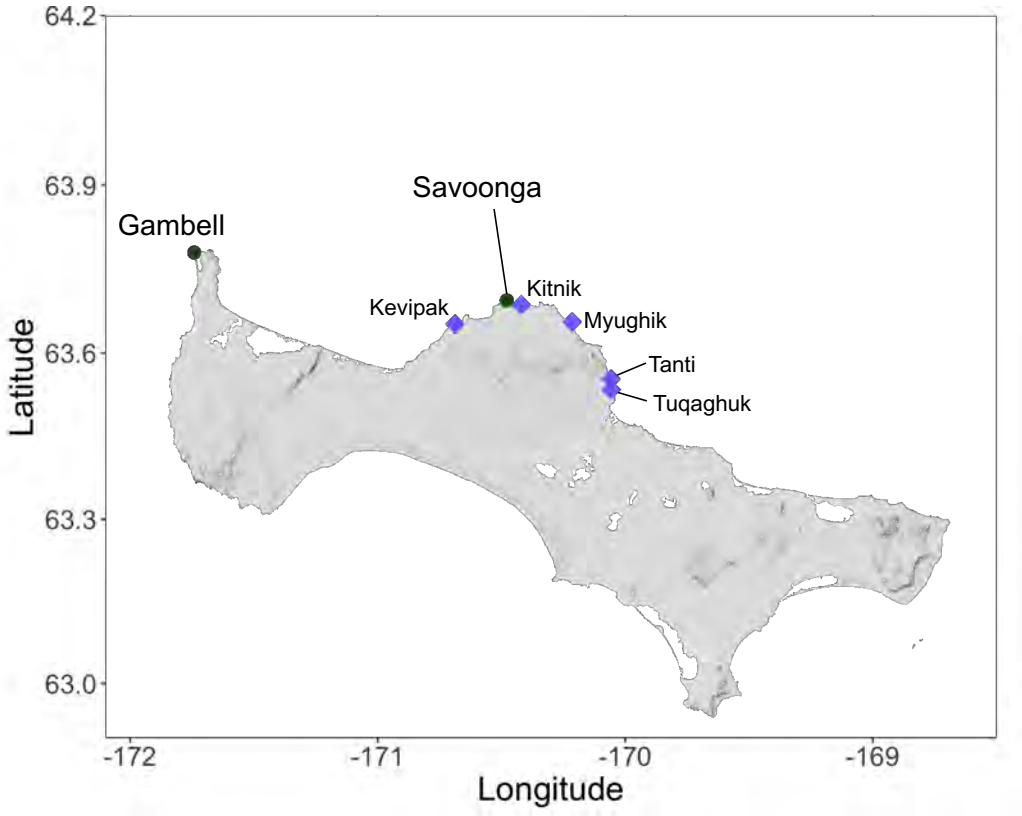

Figure 63: Map of St. Lawrence Island showing seabird colonies (purple diamonds) surveyed by community members in 2020. The Native Village of Gambell and Native Village of Savoonga are denoted by green circles.

The subsistence murre egg harvest in Savoonga began 21 June, which is the average harvest date. Murres were breeding at colonies near the Native Village of Gambell until late July (about one month later than usual). Residents at Gambell were able to harvest murre eggs at this time.

Reproductive success for black-legged **kittiwakes** is calculated as the number of large chicks observed per the number of active nests counted earlier in the season. At Kevipak colony, black-legged kittiwakes have had relatively stable, although low, reproductive success 2017–2019 (approximately 0.3 chicks per active nest). In 2020, they experienced much lower reproductive success (0.09). At other colonies (Myughi, Tanti, Tuqaghuk), black-legged kittiwakes were observed to experience complete (Myughi) or near complete reproductive failure. Nest counts were not made at the other study locations.

Colony Attendance

The number of common **murres** attending the study plots at Kevipak colony was similar in 2020 compared to 2016, 2017, and 2019. Thick-billed murre numbers declined for a second year in a row, and were half the number observed prior to the 2018 die-off event.

Mortality Events

COASST and regional partners provide a standardized measure of relative beached bird abundance for the Bering Strait/southern Chukchi Sea from 2009 to present. Time series of month-averaged beached bird abundance for the Chukchi Sea show several of the recent mortality events that have affected the Bering Strait/southeastern Chukchi Sea region. In 2020, survey effort was similar to previous years, though the number of carcasses reported was closer to pre-2017 data (Figure 64). Birds reported included murres,

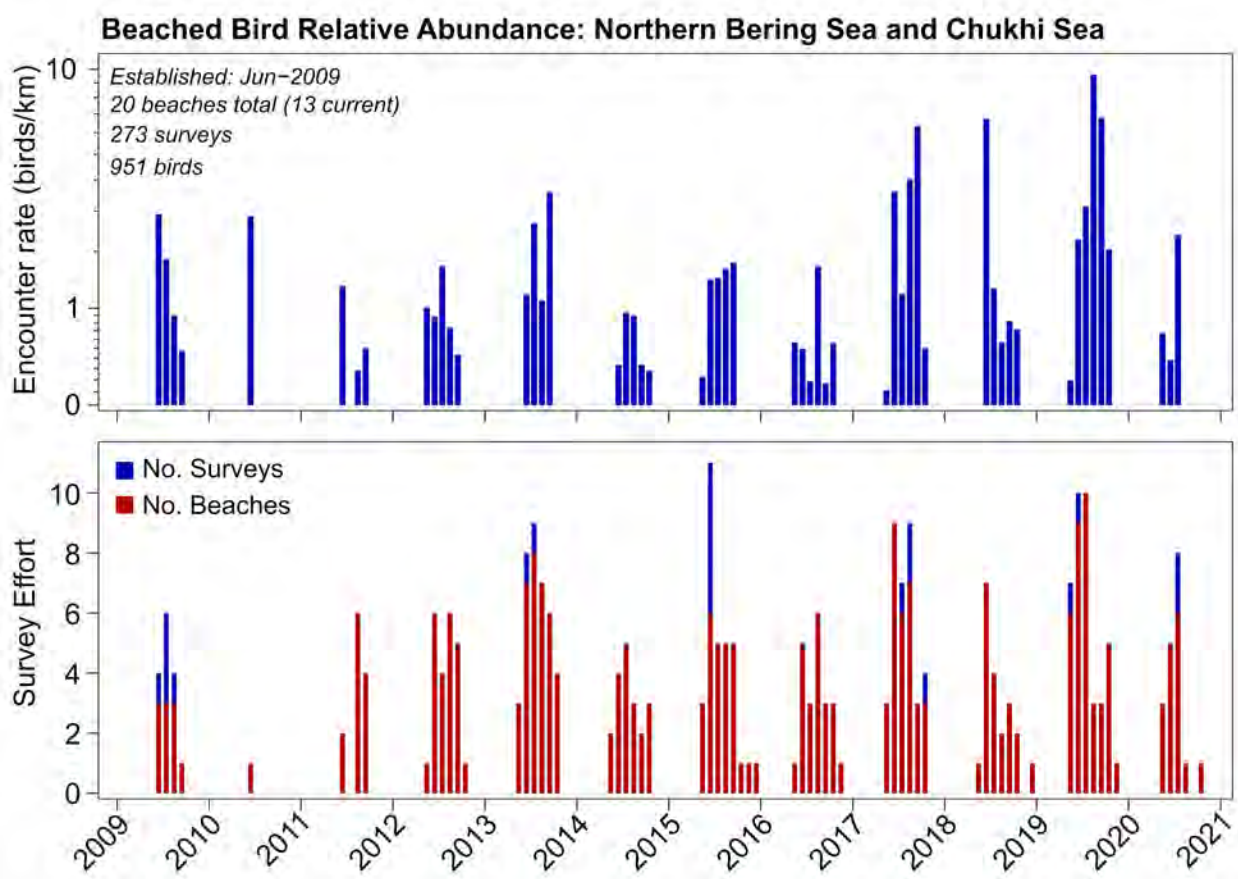

Figure 64: Month-averaged beached bird abundance, standardized per km of survey effort, for the Bering Strait/Chukchi Sea. The top panel shows the month-averaged encounter rate (ER: birds per km). The bottom panel shows survey effort at the monthly scale.

horned puffins, and shearwaters. Surveyed beached bird abundance peaked in July, the majority of which were puffins that are generalist piscivores. In addition to puffins, June and July surveys noted murres, matching species composition from local reports of beached birds in the northern Bering/Chukchi region in June/July (Figure 65).

In the Bering Strait region, reports of dead seabirds were received by the Alaska Sea Grant office (Nome) from June to September 2020 from regional coastal communities. Seabird carcasses (n=32) were received from Nome, Savoonga, and Shishmaref and sent to the U.S. Fish and Wildlife Service Migratory Bird Management program in Anchorage for analysis at the U.S. Geological Service National Wildlife Health Center in Madison, WI. Carcasses included horned puffins (n=10), shearwaters (n=10), murres (n=7), crested auklets (n=2), and one each of black guillemot, tufted puffin, and northern fulmar.

Seabird mortalities were observed throughout the summer 2020 across the northern Bering Sea and Bering Strait region. While the magnitude across species was much less than that observed for short-tailed shearwaters in 2019, the seabird mortalities involved multiple species, occurred broadly across the region, and for a prolonged duration. The multiple species represented different foraging guilds that could indicate changes or shifts in the prey base.

In Nome, mortalities were observed for murres, horned puffins, black-legged kittiwakes, and shearwaters. On August 24, a Nome resident traveling from Nome to Sinuk River reported approximately 100 dead seabirds including shearwaters, puffins, murres, and glaucous gulls. Murre mortalities occurred in Shishmaref and

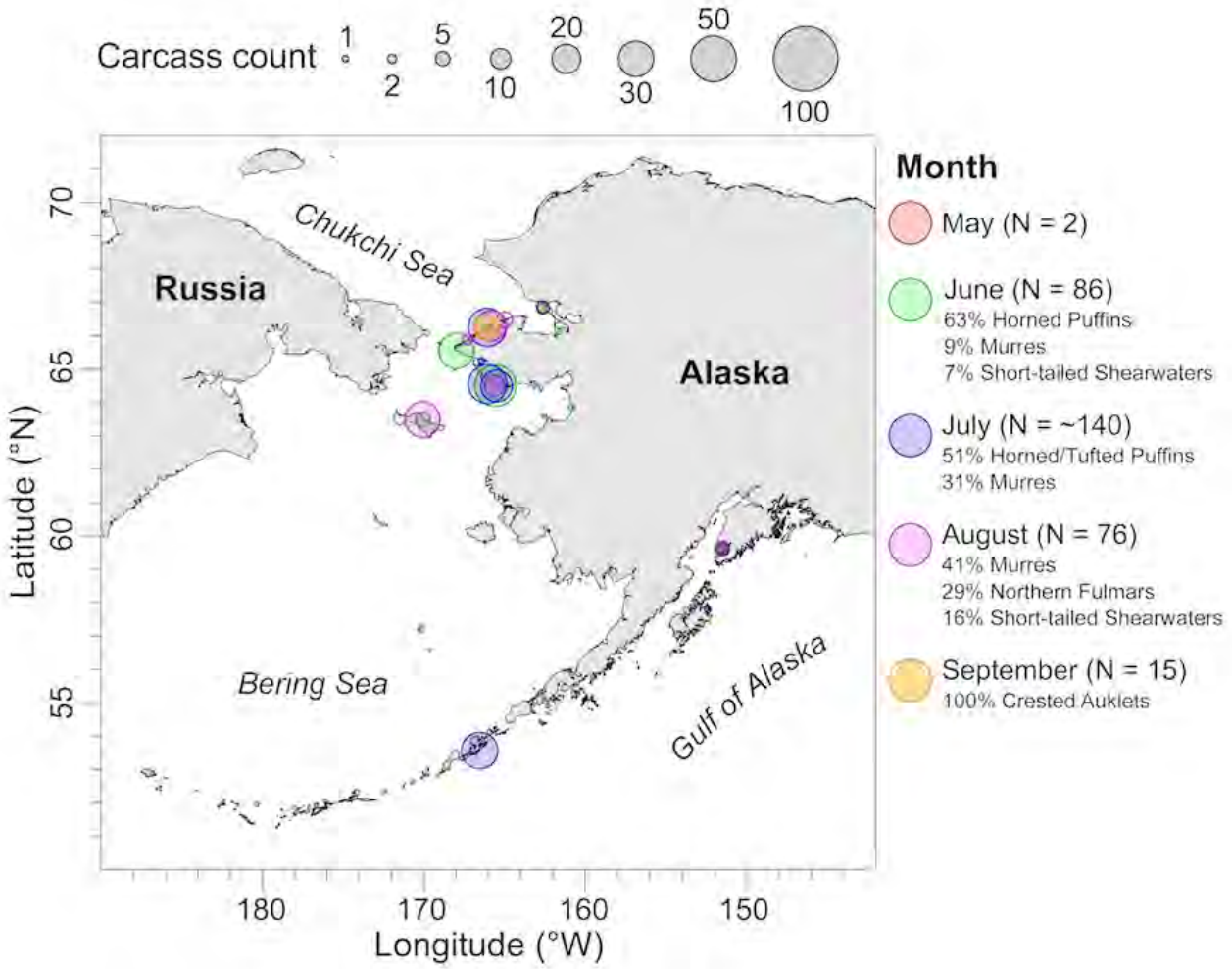

Figure 65: Seabird die-off map for Alaska during May–September 2020. Data provided by Coastal Observation and Seabird Survey Team (COASST) participants and National Park Service staff, and coastal community members reporting to ADF&G, USFWS, UAF-Alaska Sea Grant, and Kawerak, Inc. Map is courtesy of COASST.

Savoonga, as well as on the western side of the Bering Strait. Puffin carcasses were reported from the villages of Shishmaref and Wales. Earlier in the summer, "sick" horned puffins were reported from Hooper Bay.

In addition to impacts of starvation, an oil-fouling event occurred in mid-June east of Savoonga. The oil was determined to be non petroleum-based, but rather a biogenic oil of unknown origin. The USGS-NWHC determined that, among birds impacted, eight short-tailed shearwaters were determined to have aspirated the biogenic material, contributing to their death. The U.S. Geological Service National Wildlife Health Center also noted that the oil-fouling of feathers contributed to a loss of thermal insulation which aided in the death.

Implications
Seabirds are indicators of potential foraging condition therefore they might shift their distribution accordingly in response to the prey base that is important for both birds and groundfish species.

Fish-eating, surface feeding seabirds include black-legged kittiwakes, which feed on small schooling fish that are available at the surface (e.g., sandlance, capelin, juvenile herring), making them potential indicators of processes affecting juvenile groundfish that migrate to the surface to feed. Fish eating, diving seabirds include common murres that feed on small, schooling fish (e.g., age-0 or age-1 pollock) to depths up to 90 m, thus they have access to fish throughout the water column and to the ocean bottom in shallow areas.

Planktivorous seabirds include least and crested auklets, which feed primarily on copepods and euphausiids. Shearwaters and thick-billed murres also consume euphausiids, along with larvae and small fish. All of these species are indicators of feeding conditions for planktivorous groundfish species, including the larvae and juveniles of fish-eating species.

In 2020, over 330 seabird carcasses were reported from the Bering Sea, with most reported from the Bering Strait region. Fifteen carcasses were collected and submitted for examination, disease testing, and determination of the presence of harmful algal bloom (HAB) biotoxins. The cause of death of nearly all birds submitted was emaciation, and birds were negative for Avian Influenza. Results from biotoxin tests are pending.

While most of the species recorded in the 2020 seabird die-offs were fish-eating birds, plankton-eating birds were also affected, suggesting some impact across trophic levels, albeit less severe than in 2018 and 2019.

Although data was limited from the 2020 breeding season in the Pribilof Islands, available observations suggest that it was an average, to slightly below average, year for most fish-eating seabird species observed (e.g., kittiwakes, murres). Reproductive success and colony attendance have been variable, though generally below long-term means in recent years.

Planktivorous species (i.e., auklets) have been declining in the Pribilof Islands in recent years and 2020 appears to be a continuation of the decline, at least for St. Paul Island. Warmer water temperatures from 2014–2019 seem to have negatively affected least auklets, and likely parakeet auklets, as evidenced by declines in reproductive success and colony attendance. The complete lack of parakeet auklet observations from St. Paul Island in 2020 is troubling, considering that this population has been estimated in the past as >30,000 birds and parakeet auklets have been the most abundant auklet species on St. Paul Island since the late 1970s when annual seabird monitoring began in the Pribilof Islands.

Only a single beach-cast carcass was observed from COASST surveys on St. Paul Island in 2020. This resulted in the lowest carcass encounter rate for St. Paul since monitoring began in 2006. St. Paul has been the site of large seabird die-offs in the past, most recently in 2015–2016 (Jones et al., 2019).

Marine Mammals

There are no updates to Marine Mammal indicators in this year's report. See the contribution archive for previous indicators at: `https://access.afsc.noaa.gov/REFM/REEM/ecoweb/`.
Please see p. 48 for an update on the gray whale Unusual Mortality Event (UME).

Ecosystem or Community Indicators

Aggregated Catch-Per-Unit-Effort of Fish and Invertebrates in Bottom Trawl Surveys on the Eastern Bering Sea Shelf, 1982–2019

Contributed by Franz Mueter[1] and Lyle Britt[2]
[1]University of Alaska Fairbanks, 17101 Point Lena Loop Road, Juneau, AK 99801
[2]Resource Ecology and Fisheries Management Division, Alaska Fisheries Science Center, NOAA Fisheries
Contact: fmueter@alaska.edu
Last updated: October 2020

Description of indicator: The index provides a measure of the overall biomass of demersal and benthic fish and invertebrate species. We obtained catch-per-unit-effort (CPUE in kg ha) of fish and major invertebrate taxa for each successful haul completed during standardized bottom trawl surveys on the eastern Bering Sea shelf (EBS), 1982–2019. Total CPUE for each haul was computed as the sum of the CPUEs of all fish and major invertebrate taxa. To obtain an index of average CPUE by year across the survey region, we modeled log-transformed total CPUE (N=14,090 hauls) as a smooth function of depth, Julian Day, and location (latitude/longitude) with year-specific intercepts using Generalized Additive Models following Mueter and Norcross (2002). Hauls were weighted based on the area represented by each station. The CPUE index does not account for gear or vessel differences, which are confounded with interannual differences and may affect results prior to 1988.

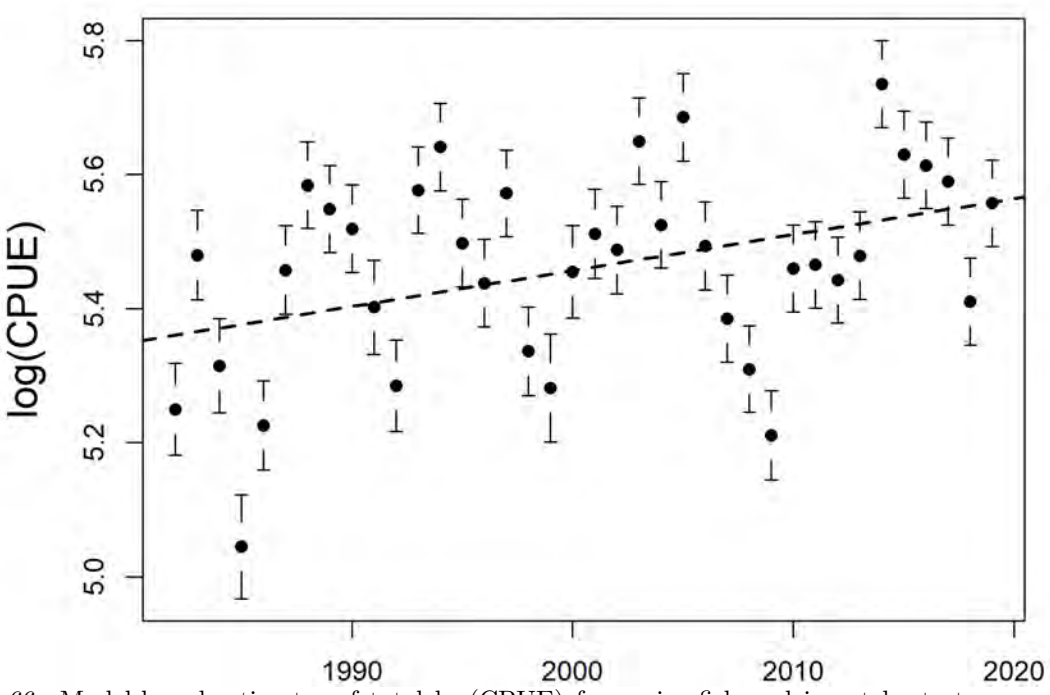

Figure 66: Model-based estimates of total log(CPUE) for major fish and invertebrate taxa captured in bottom trawl surveys from 1982–2019 in the eastern Bering Sea with approximate pointwise 95% confidence intervals and linear time trend. Estimates were adjusted for differences in depth, day of sampling, and sampling locations among years. Gear differences prior to 1988 were not accounted for. The linear time trend based on generalized least squares regression assuming 1st order auto-correlated residuals was not statistically significant at the 95% significance level (t=1.626, p=0.113).

Status and trends: Total log(CPUE) in the EBS shows an increase over the entire time series that was not statistically significant when adjusted for temporal autocorrelation (Figure 66, t = 1.626, p = 0.113). The highest observed value in the time series occurred in 2014 and total CPUE declined thereafter with a sharp and significant drop between 2017 and 2018. Total CPUE increased again in 2019. Estimated means prior to 1988 may be biased due to unknown gear effects and because annual differences are confounded with changes in mean sampling date, which varied from as early as June 15 in 1999 to as late as July 16 in 1985. On average, sampling occurred about a week earlier since the 2000s compared to the 1980s.

Factors influencing observed trends: Commercially harvested species accounted for approximately 95% of survey catches. Fishing is expected to be a major factor determining trends in survey CPUE, but environmental variability is likely to account for a substantial proportion of the observed variability in CPUE through variations in recruitment, growth, and distribution. The increase in survey CPUE in the early 2000s primarily resulted from increased abundances of walleye pollock (*Gadus chalcogrammus*) and a number of flatfish species (arrowtooth flounder, *Atheresthes stomias*; yellowfin sole, *Limanda aspera*; rock sole, *Lepidopsetta bilineata*; and Alaska plaice, *Pleuronectes quadritubercularus*) due to strong recruitments in the 1990s. Decreases in 2006–2009 and subsequent increases are largely a result of fluctuations in pollock recruitment and abundance.

Models including bottom temperature suggest that, in the EBS, CPUE is greatly reduced at low temperatures ($< 1^{\circ}$C) as evident in reduced CPUEs in 1999 and 2006–2009, when the cold pool covered a substantial portion of the shelf. Overall, there is a moderate positive relationship between average bottom temperatures and CPUE in the same year (r=0.49, p=0.0016), but not in the following years. The reduction in CPUE during cold periods is likely due to a combination of actual changes in abundance, temperature-dependent changes in catchability of certain species (e.g., flatfish, crab), and changes in distribution as a result of the extensive cold pool displacing species into shallower (e.g., red king crab) or deeper (e.g., arrowtooth flounder) waters. The large decrease in 2018 was primarily due to a decrease in the CPUE of pollock, as well as that of Pacific cod and most flatfish species, except arrowtooth flounder (which increased). The subsequent increase in 2019 was primarily due to a large increase in pollock catches.

Implications: This indicator can help address concerns about maintaining adequate prey for upper trophic level species and other ecosystem components. Relatively stable or increasing trends in the total biomass of demersal fish and invertebrates, together with a relatively constant size composition of commercial species, suggest that the prey base has remained stable over recent decades, but displays substantial fluctuations over time, largely as a result of variability in pollock biomass.

Average Local Species Richness and Diversity of the Eastern Bering Sea Groundfish Community

Contributed by Franz Mueter[1] and Lyle Britt[2]
[1]University of Alaska Fairbanks, 17101 Point Lena Loop Road, Juneau, AK 99801
[2]Resource Ecology and Fisheries Management Division, Alaska Fisheries Science Center, NOAA Fisheries
Contact: fmueter@alaska.edu
Last updated: October 2020

Description of indicator: Indices of local species richness and diversity are based on standard bottom trawl surveys in the eastern Bering Sea (EBS). We computed the average number of fish and major invertebrate taxa per haul (richness) and the average Shannon index of diversity (Magurran, 1988) by haul based on CPUE (by weight) of each taxon. Indices for the EBS were based on 45 fish and invertebrate taxa that were consistently identified throughout all surveys since 1982 (Table 1 in Mueter and Litzow (2008), excluding Arctic cod *Boreogadus saida* because of unreliable identification in early years). Indices were computed following Mueter and Norcross (2002). Annual average indices of local richness and diversity were estimated by first computing each index on a per-haul basis, then estimating annual averages with confidence intervals

across the survey area using a Generalized Additive Model that accounted for the effects of variability in sampling locations (latitude/longitude), depth, and date of sampling. In addition to trends over time, we mapped average spatial patterns for each index across the survey region.

Status and trends: Species richness and diversity on the EBS shelf have undergone significant variations from 1982 to 2019 (Figure 67). The average number of species per haul increased by one to two species per haul from 1995 to 2004, remained relatively high through 2011 and both richness and diversity decreased through 2014, followed by a return to relatively high levels, with an unusually high Shannon diversity observed in 2018. Richness tends to be highest along the 100m isobaths, while diversity tends to be highest on the middle shelf (Figure 68). Local richness is lowest along the slope and in the northern part of the survey region, while diversity is lowest in the inner domain.

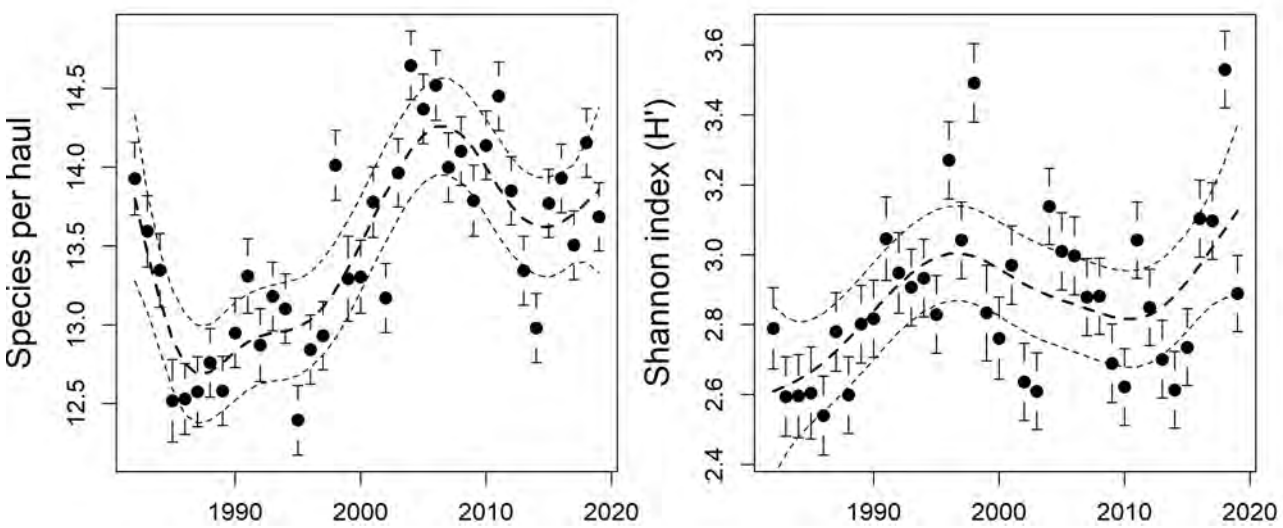

Figure 67: Model-based annual averages of local species richness (left, average number of species per haul) and species diversity (Shannon index, right) in the eastern Bering Sea, 1982–2018, based on 45 fish and invertebrate taxa collected by standard bottom trawl surveys with pointwise 95% confidence intervals (bars) and loess smoother with 95% confidence band (dashed/dotted lines). Model means were adjusted for differences in depth, date of sampling, and geographic location.

Factors influencing observed trends: Local richness and diversity reflect changes in the spatial distribution, abundance, and species composition that may be caused by fishing, environmental variability, or climate change. If species are, on average, more widely distributed in the sampling area the number of species per haul increases. Spatial shifts in distribution from year to year can cause high variability in local species richness in certain areas, for example along the 100m contour. These shifts appear to be the primary drivers of changes in species richness over time. Local species diversity is a function both of how many species are caught in a haul and how evenly CPUE is distributed among these species, hence time trends (Figure 67) and spatial patterns (Figure 68) in species diversity differ from those in species richness. The large increase in diversity in 2018 was associated with a moderate increase in species richness and a decrease in the dominance of pollock, which made up 38–49% of total biomass in recent years, but only 30% in 2018 (46% in 2019).

Implications: There is evidence from many systems that diversity is associated with ecosystem stability, which depends on differential responses to environmental variability by different species or functional groups (e.g., McCann, 2000). To our knowledge, such a link has not been established for marine fish communities. In the EBS, local species richness may be particularly sensitive to long-term trends in bottom temperature as the cold pool extent changes (Mueter and Litzow, 2008) and provides a useful index for monitoring responses of the groundfish community to projected climate warming (Alabia et al., 2020).

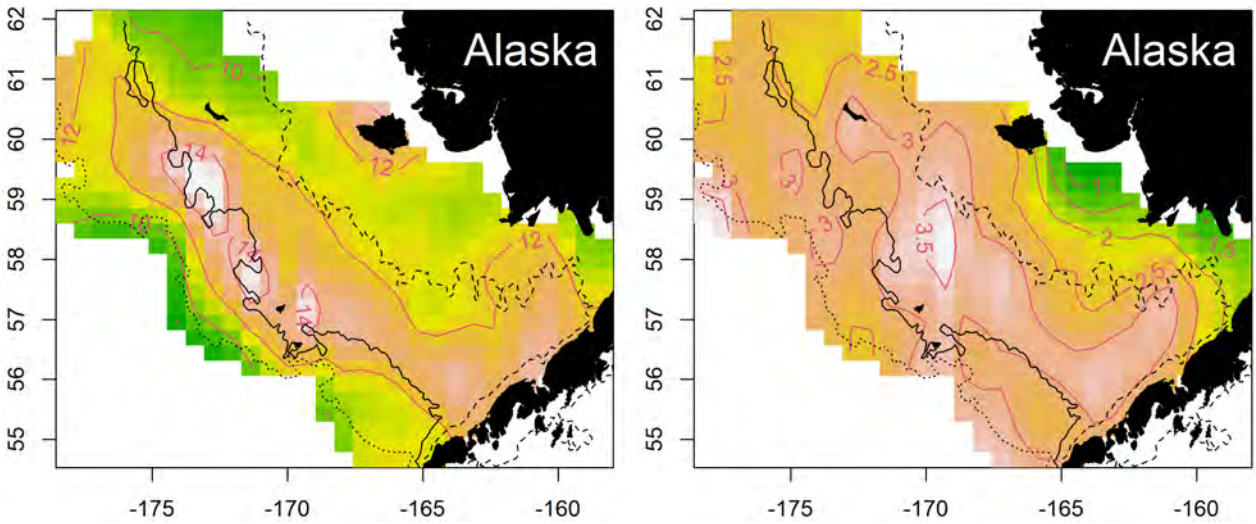

Figure 68: Average spatial patterns in local species richness (left, number of taxa per haul) and Shannon diversity in the eastern Bering Sea. The 50m (dashed), 100m (solid), and 200 m (dotted) depth contours are shown. Note highest richness along 100m contour, highest diversity on middle shelf.

Spatial Distribution of Groundfish Stocks in the Bering Sea

Contributed by Franz Mueter[1] and Lyle Britt[2]
[1]University of Alaska Fairbanks, 17101 Point Lena Loop Road, Juneau, AK 99801
[2]Resource Assessment and Conservation Engineering Division, Alaska Fisheries Science Center, NOAA Fisheries
Contact: fmueter@alaska.edu
Last updated: October 2020

Description of indicator: We provide indices of changes in the spatial distribution of groundfish on the eastern Bering Sea shelf. The first index provides a simple measure of the average North-South displacement of major fish and invertebrate taxa from their respective centers of gravity (e.g., Woillez et al., 2009) based on AFSC-RACE bottom trawl surveys for the 1982–2019 period. Annual centers of gravity for each taxon were computed as the CPUE-weighted mean latitude across 285 standard survey stations that were sampled each year and an additional 58 stations sampled in all but one survey year. Each station (N=343) was also weighted by the approximate area that it represents. Initially, we selected 46 taxa as in Table 1 of Mueter and Litzow (2008). Taxa that were not caught at any of the selected stations in one or more years were not included, resulting in a total of 39 taxa for analysis. In addition to quantifying N-S shifts in distribution, we computed CPUE and area-weighted averages of depth to quantify changes in depth distribution. Because much of the variability in distribution is likely to be directly related to temperature variability, we removed linear relationships between changes in distribution and temperature by regressing distributional shifts on annual mean bottom temperatures. Residuals from these regressions are provided as an index of temperature-adjusted shifts in distribution.

Status and trends: Both the latitudinal and depth distribution of the demersal community on the eastern Bering Sea shelf show strong directional trends over the last four decades, indicating significant distributional shifts to the north and into shallower waters (Figure 69). The distribution shifted slightly to the south and deeper in recent cold years (2006–2013) and has shifted back to the north and shallower since 2014 with a substantial shift to the northwest (along the main axis of the shelf) in 2016. The distribution temporarily shifted back towards the south in 2017 but has been shifting northward again since then and remained further

north than in any other year besides 2016. Strong shifts in distribution remain evident even after adjusting for linear temperature effects (Figure 69). The center of gravity of most individual species shifted to the northwest along the shelf and/or to the northeast onto the shelf in 2016, the warmest year in the survey time series (Figure 70). Cooler temperatures in 2017 appeared to result in an immediate and substantial southeastward shift, in contrast to a more moderate response to similar cooling in 2006. Following the return to higher bottom temperatures in 2018 and 2019, the overall center of gravity shifted slightly to the northwest. However, northern Bering Sea surveys in 2017, 2018, and 2019 suggest that much of the biomass of fishes in recent years occurred in the northern Bering Sea, with the depth-adjusted latitudinal gradient in density reversing from 2010 to 2019 and higher estimated densities near Bering Strait than off the Alaska Peninsula (Figure 71). These patterns are primarily driven by changes in the distribution of pollock and Pacific cod (Figure 72, see also Stevenson and Lauth (2012); Thorson et al. (2020)). Therefore, the true center of gravity for many species likely shifted further to the north then indicated by the distributional indices, which is based on stations sampled in the standard survey area on the southeastern shelf.

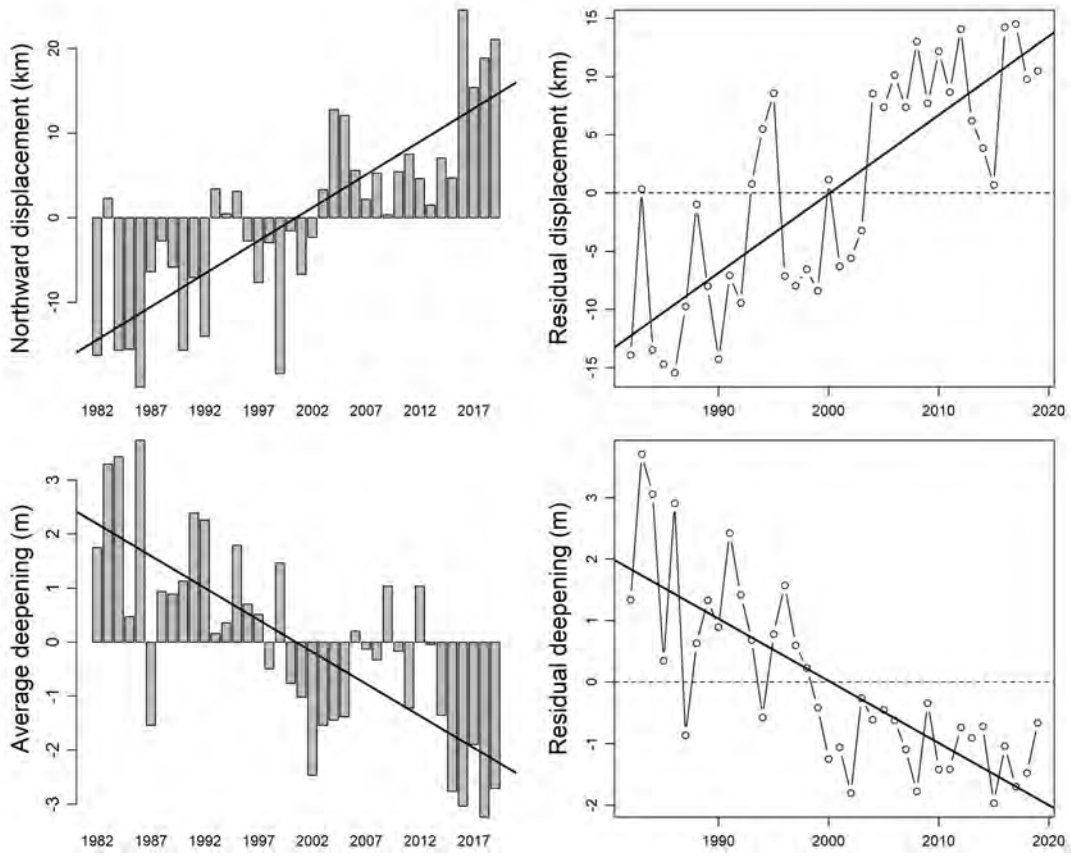

Figure 69: Left: Distributional shifts in latitude (average northward displacement in km from species-specific mean latitudes) and shifts in depth distribution (average vertical displacement in m from species-specific mean depth, positive indices indicate deeper distribution). Right: Residual displacement from species-specific mean latitude (top) and species-specific mean depth (bottom) after adjusting the indices on the left for linear effects of mean annual bottom temperature on distribution. Residuals were obtained by linear regression of the displacement indices on annual average temperature (northward displacement: R^2=0.23, t=4.74, p<0.001; deepening: R^2=0.31, t=-5.01, p<0.001). Solid trend lines denote linear regressions over time (northward displacement: R^2=0.61, t=6.20, p<0.001; residual northward displacement: R^2=0.63, t=5.41, p<0.001; deepening: R^2=0.83, t=-5.33, p<0.001; residual deepening: R^2=0.60, t=-7.39, p<0.001).

Factors influencing observed trends: Many populations shift their distribution in response to temperature variability. Such shifts may be the most obvious response of animal populations to global warming (Parmesan and Yohe, 2003). However, distributional shifts of demersal populations in the Bering Sea are not a simple linear response to temperature variability (Mueter and Litzow (2008); Figure 69). The reasons for strong residual shifts in distribution that are not related to temperature changes remain unclear but could be related to density-dependent responses (Spencer, 2008) in combination with internal community dynamics (Mueter and Litzow, 2008). Unlike groundfish in the North Sea, which shift to deeper waters in response to warming (Dulvy et al., 2008), the Bering Sea groundfish community shifted to shallower waters during warm periods (Figure 69) because of the retreat of the cold pool from the middle shelf that allows subarctic species to expand from the outer shelf into shallower shelf regions.

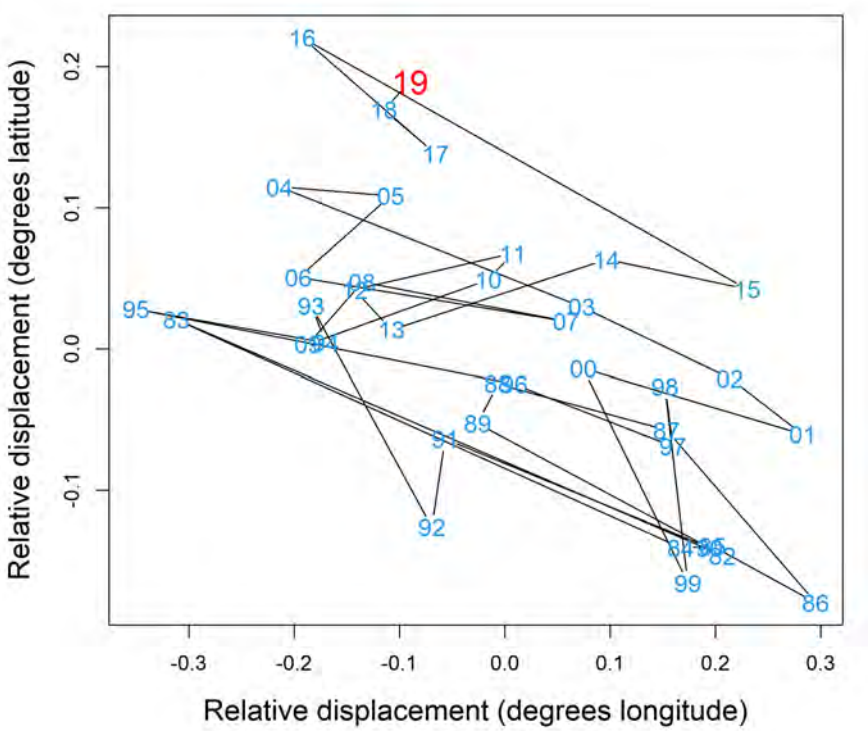

Figure 70: Average North-South and East-West displacement across 39 taxa on the eastern Bering Sea shelf relative to species-specific centers of distribution.

Implications: Changes in distribution have important implications for the entire demersal community, for other populations dependent on these communities, for the fishing industry, and for stock assessments. The demersal community is affected because distributional shifts change the relative spatial overlap of different species, thereby affecting trophic interactions among species (Hunsicker et al., 2013; Spencer et al., 2016) and, ultimately, the relative abundances of different species. Upper trophic level predators, for example fur seals and seabirds on the Pribilof Islands and at other fixed locations, are affected because the distribution and hence availability of their prey changes. Fisheries are directly affected by changes in the distribution of commercial species, which alters the economics of harvesting because fishing success within established fishing grounds may decline and travel distances to new fishing grounds may increase (Haynie and Pfeiffer, 2013). Finally, stock assessments are affected by shifts outside the standard survey area, such as the substantial redistribution of Pacific cod into the northern Bering Sea in 2018 and the apparent redistribution of much of the overall biomass in the Bering Sea to the northern Bering Sea shelf as evident in decreasing densities in the south and increasing densities in the north (Figure 71).

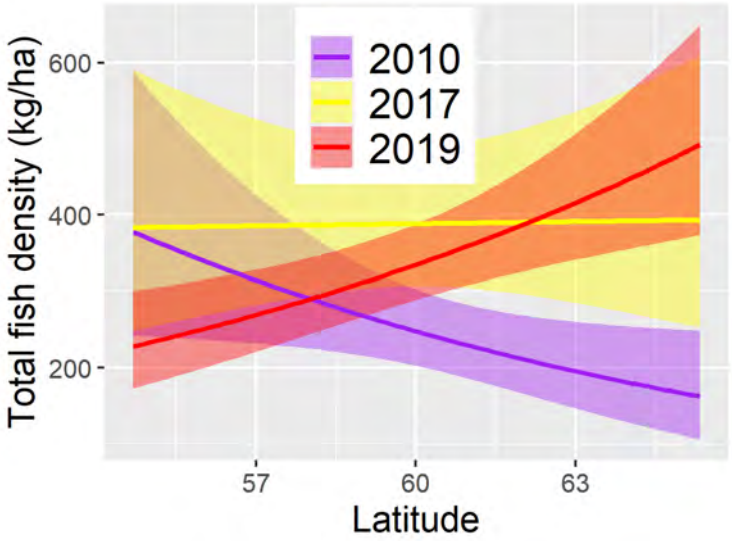

Figure 71: Estimated latitudinal trends in average fish density for all major fish taxa combined along the 50m isobath for three years, from the Alaska Peninsula in the south to the Bering Strait in the North. Estimates are based on generalized additive models of log(catch-per-unit-effort) as a function of latitude and depth by year with an exponential spatial autocorrelation structure.

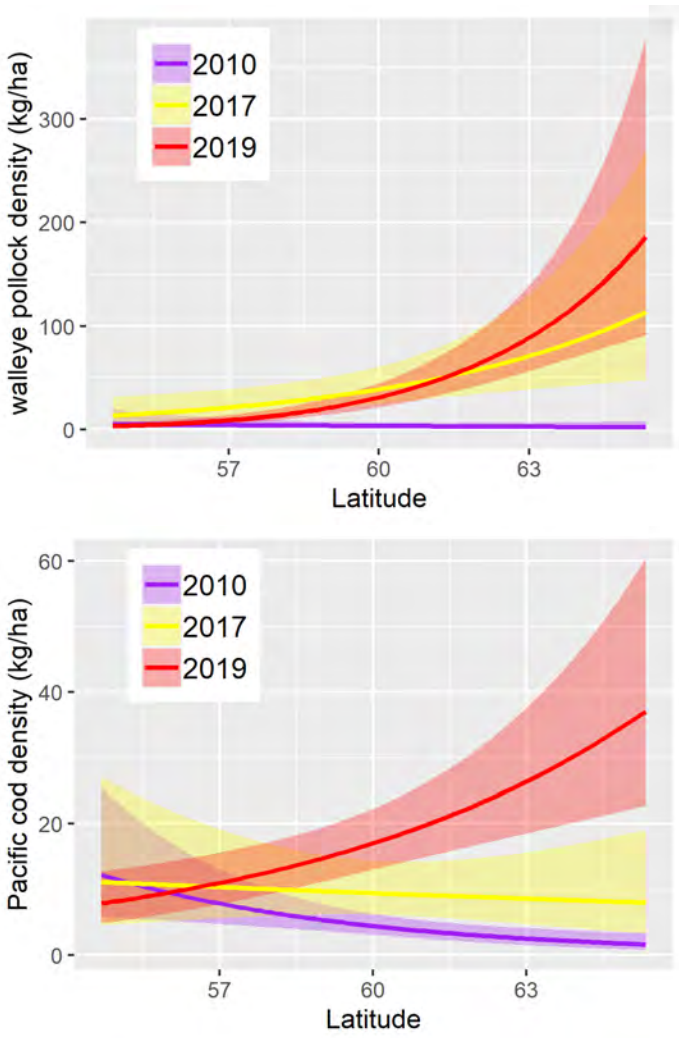

Figure 72: Estimated latitudinal trends in average fish density along the 50 m isobath for pollock (left) and Pacific cod (right) for three years, from the Alaska Peninsula in the south to the Bering Strait in the North. Estimates are based on generalized additive models of log(catch per unit effort) as a function of latitude and depth by year with an exponential spatial autocorrelation structure.

Mean Lifespan of the Fish Community

Contributed by George A. Whitehouse[1] and Geoffrey M. Lang[2]
[1]Cooperative Institute for Climate, Ocean, and Ecosystem Studies (CICOES), University of Washington, Seattle WA
[2]Resource Ecology and Fisheries Management Division, Alaska Fisheries Science Center, National Marine Fisheries Service, NOAA
Contact: andy.whitehouse@noaa.gov
Last updated: August 2020

Description of indicator: The mean lifespan of the community is defined by Shin et al. (2010) as "a proxy for the mean turnover rate of species and communities" and is intended to reflect "ecosystem stability and resistance to perturbations." The indicator for mean lifespan of the groundfish community is modeled after the method for mean lifespan presented in Shin et al. (2010). Lifespan estimates of groundfish species regularly encountered during the NMFS/AFSC annual summer bottom-trawl survey of the southeastern Bering Sea were retrieved from the AFSC Life History Database[14]. The groundfish community mean lifespan is weighted by biomass indices calculated from the bottom-trawl survey catch data.

This indicator specifically applies to the portion of the demersal groundfish community that is efficiently sampled by the trawling gear used by NMFS during this survey at the standard survey sample stations (for survey details see Conner and Lauth (2016)). Species that are infrequently encountered or not efficiently caught by the bottom-trawling gear are excluded from this indicator (e.g., sharks, grenadiers, myctophids, pelagic smelts).

Walleye pollock is a biomass dominant species in the eastern Bering Sea and may drive the value of community indicators. Therefore, we have produced this indicator in two time series, one that includes and one that excludes pollock.

Status and trends: *With pollock included* The mean lifespan of the southeastern Bering Sea demersal fish community in 2019 is 30.2 years, and is the second highest over the time series (Figure 73, gray circles). This is up from 27.6 years in 2018 and above the long-term mean of 28.2 years. Mean groundfish lifespan has generally been stable over the 38-year time series with only a small amount of year-to-year variation, and shows no indication of a long-term trend.

Without pollock The mean lifespan of the southeastern Bering Sea groundfish community without pollock is slightly less than when pollock is included. Over the time series, the patterns and trends are similar between the two series with the values being slightly lower for the series without pollock. The exception to this pattern was 1985 when the mean lifespan was 32.0 with pollock included and 32.9 without pollock.

Factors influencing observed trends: Fishing can affect the mean lifespan of the groundfish community by preferentially targeting larger, older fishes, leading to decreased abundance of longer-lived species and increased abundance of shorter-lived species (Pauly et al., 1998). Interannual variation in mean lifespan can be influenced by the spatial distribution of species and the differential selectivity of species and age classes to the trawling gear used in the survey. Strong recruitment events or periods of weak recruitment could also influence the mean community lifespan by altering the relative abundance of age classes and species. For example, the low value observed in 1993 reflects a year of peak biomass index for capelin, a shorter-lived species. The peak mean lifespan for both series in 1985 was in part elevated by high biomass indices for long-lived species, such as sablefish. The lifespan of pollock is slightly higher than the mean groundfish lifespan without pollock. When pollock are removed from this indicator, there is a small decrease in value but the same overall trend is followed.

[14]`https://access.afsc.noaa.gov/reem/LHWeb/Index.php`

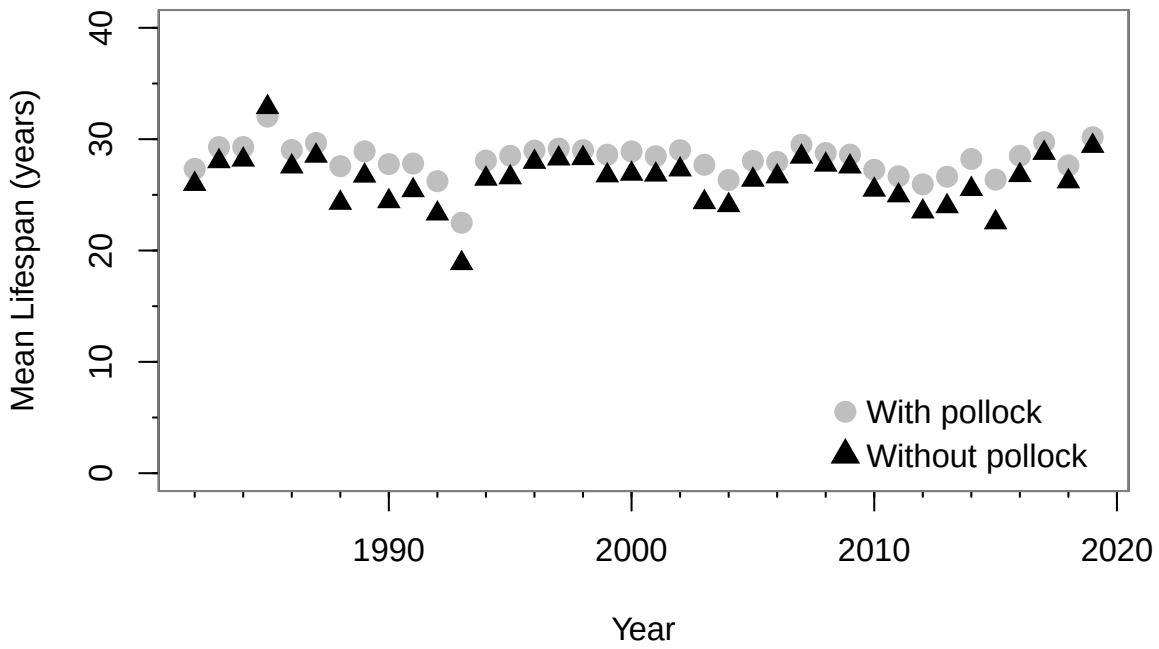

Figure 73: The mean lifespan of the southeastern Bering Sea demersal fish community, weighted by biomass indices calculated from the NMFS/AFSC annual summer bottom-trawl survey. The gray circles are the series with pollock included and the black triangles are the series without pollock included.

Implications: The groundfish mean lifespan has been stable over the time series of the summer bottom-trawl survey. There is no indication longer-lived species have decreased in relative abundance or are otherwise being replaced by shorter lived-species. Species that are short-lived are generally smaller and more sensitive to environmental variation than larger, longer-lived species (Winemiller, 2005). Longer-lived species help to dampen the effects of environmental variability, allowing populations to persist through periods of unfavorable conditions and to take advantage when favorable conditions return (Berkeley et al., 2004; Hsieh et al., 2006).

Mean Length of the Fish Community

Contributed by George A. Whitehouse[1] and Geoffrey M. Lang[2]
[1]Cooperative Institute for Climate, Ocean, and Ecosystem Studies (CICOES), University of Washington, Seattle WA
[2]Resource Ecology and Fisheries Management Division, Alaska Fisheries Science Center, National Marine Fisheries Service, NOAA
Contact: andy.whitehouse@noaa.gov
Last updated: August 2020

Description of indicator: The mean length of the groundfish community tracks fluctuations in the size of groundfish over time. This size-based indicator is thought to be sensitive to the effects of commercial fisheries because larger predatory fish are often targeted by fisheries and their selective removal would reduce mean size (Shin et al., 2005). This indicator is also sensitive to shifting community composition of species with different mean sizes. Fish lengths are routinely recorded during the NMFS bottom trawl survey of the southeastern Bering Sea, which has occurred each year from 1982 to 2019. Mean lengths are calculated for groundfish species (or functional groups of multiple species; e.g., eelpouts) from the length measurements

collected during the trawl survey. The mean length for the groundfish community is calculated with the species mean lengths, weighted by biomass indices (Shin et al., 2010) calculated from the bottom-trawl survey catch data.

This indicator specifically applies to the portion of the demersal groundfish community that is efficiently sampled with the trawling gear used by NMFS during the summer bottom-trawl survey of the southeastern Bering Sea at the standard survey sample stations (for survey details see Conner and Lauth (2016)). Species that are infrequently encountered or not efficiently caught by the bottom-trawling gear are excluded from this indicator (e.g., sharks, grenadiers, myctophids, pelagic smelts).

Species (or functional groups) infrequently sampled for lengths (less than five times over the time series) are excluded from this indicator (e.g., capelin, eulachon, greenlings). Twenty-two species are included in this indicator. Eleven species had their lengths sampled in all 38 years of the time series. Another eleven species were sampled between 11 and 35 times over the time series. In those years where lengths were not sampled for a species, we instead used a long-term mean for that species.

Walleye pollock is a biomass dominant species in the eastern Bering Sea and may drive the value of community indicators. Therefore, we have produced this indicator in two time series, one that includes and one that excludes pollock.

Status and trends: *With pollock included* The mean length of the southeastern Bering Sea groundfish community in 2019 is 37.2 cm, which is only slightly less than the peak value of 37.6 cm in 2018. Since 1982, the mean length has shown variation from year to year, and has been trending upward since 2012 (Figure 74, gray circles).

Without pollock The mean length of the southeastern Bering Sea groundfish community without pollock peaked at 38.0 cm in 2018 and dropped to 34.4 cm in 2019 (Figure 74, black triangles). This series gradually declined from 1996–2012, then trended upward to 2018.

Factors influencing observed trends: This indicator is specific to the fishes that are routinely caught and sampled during the NMFS summer bottom-trawl survey. The estimated mean length can be biased if specific species-size classes are sampled more or less than others, and is sensitive to spatial variation in the size distribution of species. Changes in fisheries management or fishing effort could also affect the mean length of the groundfish community. Modifications to fishing gear, fishing effort, and targeted species could affect the mean length of the groundfish community if different size classes and species are subject to changing levels of fishing mortality. The mean length of groundfish could also be influenced by fluctuations in recruitment, where a large cohort of small forage species could reduce mean length of the community. Environmental factors could also influence fish growth and mean length by affecting the availability and quality of food, or by direct temperature effects on growth rate.

Walleye pollock is a biomass dominant component of this ecosystem and year-to-year fluctuations in their mean size and biomass have a noticeable effect on this indicator. In 1993, their biomass index was above average but their mean size was the fifth lowest of the time series. Additionally, 1993 was a pronounced peak in the biomass index of capelin. This reduced the proportional contribution of other species to total groundfish biomass index, thus reducing the indicator value (i.e., mean length) in 1993. Years where this indicator attained its highest values (1987, 2016–2019) generally correspond to years of above average mean size and/or biomass index for pollock, except 2018 where pollock mean size was average but their biomass index was below average. The groundfish mean size in 2019 was buoyed by other prominent groundfish such as Alaska skate, arrowtooth flounder, and yellowfin sole, which had above average mean length.

The series without pollock mirrored the overall trends in the series with pollock included, but was generally lower. This was because the mean length of pollock was generally a few centimeters greater than the mean length of the rest of the groundfish community. Exceptions occurred in 1983, 1985, and 2018 when the mean length of pollock was less than the mean of the rest of the groundfish community. In these three instances, the indicator value was higher for the series without pollock.

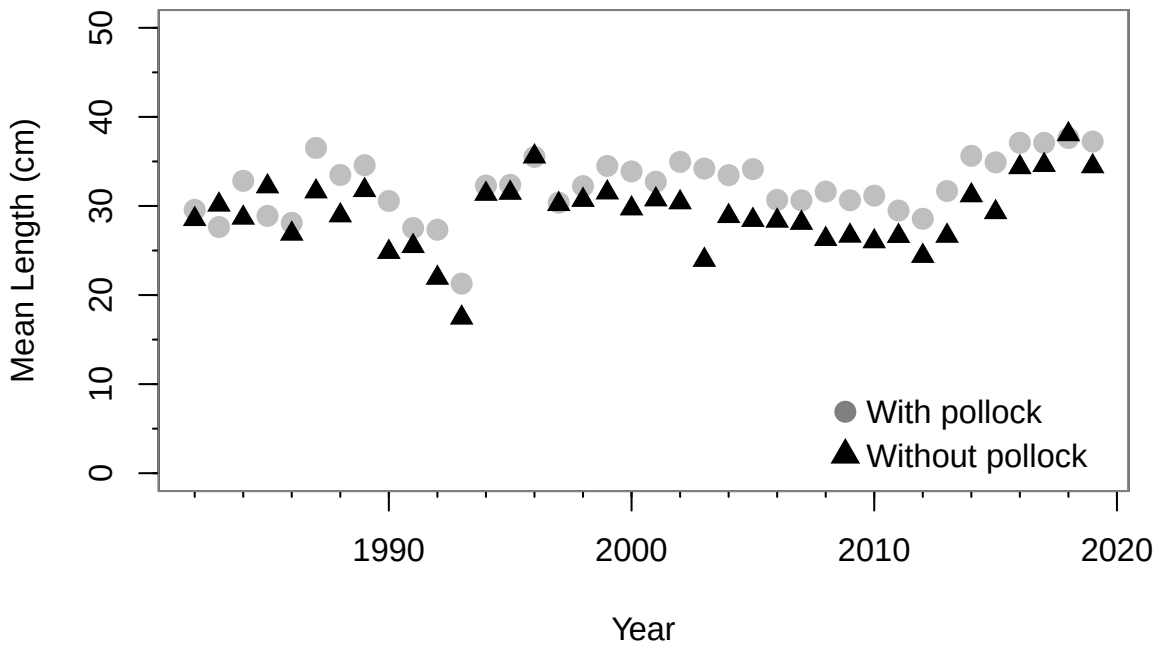

Figure 74: Mean length of the groundfish community sampled during the NMFS/AFSC annual summer bottom-trawl survey of the southeastern Bering Sea (1982–2019). The groundfish community mean length is weighted by the relative biomass of the sampled species. The gray circles are the mean length with pollock included and the black triangles are the series without pollock included.

Implications: The mean length of the groundfish community in the southeastern Bering Sea has been stable over the bottom-trawl time series (1982–2019) with some interannual variation. The collective stability of the combined biomass of relatively larger groundfish species has helped to maintain this indicator at its recent high values. Previous dips in this indicator were in part attributable to spikes in abundance of smaller forage species (e.g., capelin) as opposed to a sustained shift in community composition or reductions in species mean length.

Stability of Groundfish Biomass

Contributed by George A. Whitehouse
Cooperative Institute for Climate, Ocean, and Ecosystem Studies (CICOES), University of Washington, Seattle WA
Contact: andy.whitehouse@noaa.gov
Last updated: August 2020

Description of indicator: The stability of the groundfish community total biomass is measured with the inverse biomass coefficient of variation (1 divided by the coefficient of variation of total groundfish biomass (1/CV[B])). This indicator provides a measure of the stability of the ecosystem and its resistance to perturbations. The variability of total community biomass is thought to be sensitive to fishing and is expected to increase with increasing fishing pressure (Blanchard and Boucher, 2001). This metric is calculated following the methods presented in Shin et al. (2010). The CV is calculated as the standard deviation of the groundfish biomass index over the previous 10 years divided by the mean over the same time span. The biomass index for groundfish species was calculated from the catch of the NMFS/AFSC annual summer bottom-trawl survey of the southeastern Bering Sea. Since 10 years of data are required to calculate this

metric, the indicator values start in 1991, the tenth year in the trawl survey time series (1982–2019). This metric is presented as an inverse, so as the CV increases the value of this indicator decreases, and if the CV decreases the value of this indicator increases.

This indicator specifically applies to the portion of the demersal groundfish community that is efficiently sampled by the trawling gear used by NMFS during the annual summer survey at the standard survey sample stations (for survey details see Conner and Lauth (2016)). Species that are infrequently encountered or not efficiently caught by the bottom-trawling gear are excluded from this indicator (e.g., sharks, grenadiers, myctophids, pelagic smelts).

Walleye pollock is a biomass dominant species in the eastern Bering Sea and may drive the value of community indicators. Therefore, we have produced this indicator in two time series, one that includes and one that excludes pollock.

Status and trends: *With pollock included* The state of this indicator in 2019 is 7.68, which is up from 5.5 in 2017, and is the highest over the time series (Figure 75, gray circles). The previous high of 7.63 was observed in 1992, which was followed by a steady decrease to a low of 3.9 in 2002. Since then it gradually increased to a value of 5.5 in 2018 before sharply increasing to its new high in 2019. In between the high values at the start of this time series and in 2019, this indicator has remained generally stable and does not exhibit a clear trend. Since 1991, the mean value for this metric is 5.2.

Without pollock This indicator reached a high value of 9.79 in 2019, which is up from the previous high of 8.48 in 2018 (Figure 75, black triangles). This indicator dropped sharply from 7.61 in 1992 to 3.48 in 1993, and remained below 4.0 until 2003, where the value increased to 5.21. The indicator value remained relatively stable until 2010, when the indicator began a steady upward trend up through the series high value in 2019.

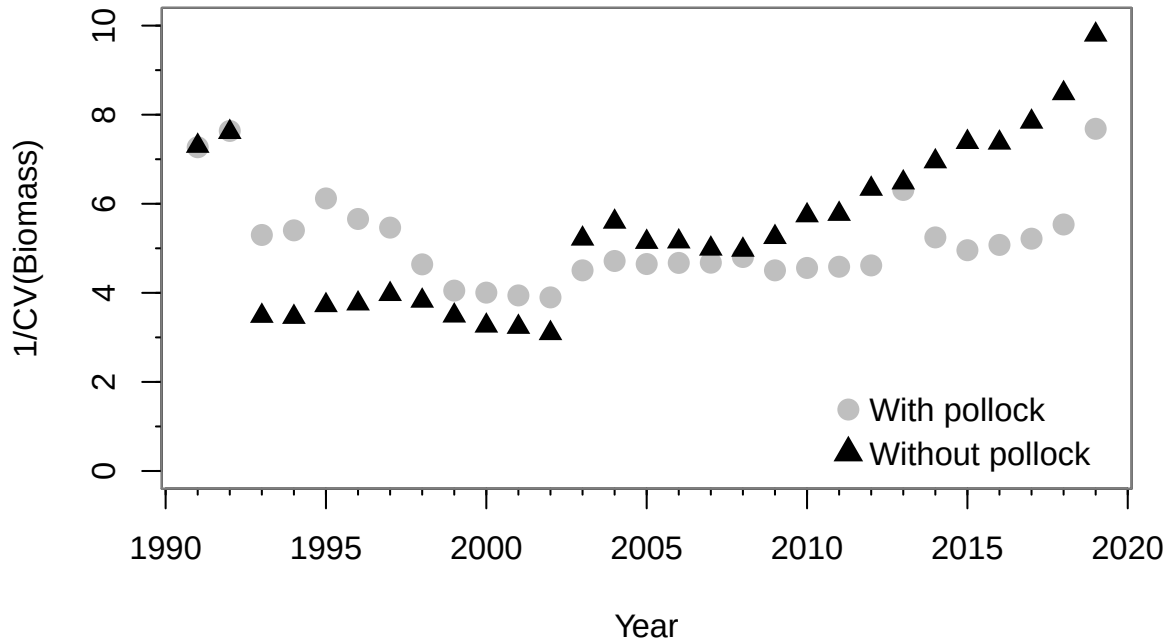

Figure 75: The stability of groundfish in the southeastern Bering Sea represented with the inverse biomass coefficient of variation of total groundfish biomass (1/CV[B]). Ten years of data are required to calculate this metric, so this time series begins in 1991 after the tenth year of the NMFS/AFSC annual summer bottom-trawl survey. The gray circles are the series with pollock included and the black triangles are the series without pollock included.

Factors influencing observed trends: Fishing is expected to influence this metric as fisheries can selectively target and remove larger, long-lived species effecting population age structure (Berkeley et al., 2004; Hsieh et al., 2006). Larger, longer-lived species can become less abundant and be replaced by smaller shorter-lived species (Pauly et al., 1998). Larger, longer-lived individuals help populations to endure prolonged periods of unfavorable environmental conditions and can take advantage of favorable conditions when they return (Berkeley et al., 2004). A truncated age-structure could lead to higher population variability (CV) due to increased sensitivity to environmental dynamics (Hsieh et al., 2006). Interannual variation in this metric could also be influenced by interannual variation in species abundance in the trawl survey catch, and patchy spatial distribution for some species. This metric, as calculated here with trawl survey data, reflects the stability of the portion of the groundfish community that is represented in the catch data of the annual summer bottom-trawl survey. Both, sharp increases or decreases in species index values can increase variability and reduce the indicator value.

The high values for this indicator in 2019 and at the start of the time series are indicative of stable groundfish biomass with a relatively low CV during the previous ten years. Both series (with and without pollock) drop sharply from 1992 to 1993. This is because the index for capelin in 1993 was anomalously high which increased variability and reduced the indicator value. In 2003, both series increase, which is in part due to the 1993 increase in capelin no longer being a part of the most recent 10 years.

In 2009, the series without pollock begins a steady increase towards its high value in 2019. The series with pollock included has a more modest positive trend over the same span, with high values in 2013 and 2019. Pollock is a biomass dominant species in the eastern Bering Sea and interannual fluctuations in their biomass are sufficient to increase variability for the total groundfish community and thus, reduce the indicator value for the series that includes pollock. Additionally, the indicator series without pollock is more sensitive to fluctuations of other species, such as capelin. The sharp increase in the capelin index in 1993 kept this series lower than the series with pollock included from 1993–2002.

Implications: The measure 1/CV[B] indicates that the southeastern Bering Sea groundfish community is stable over the time period examined here. For the duration of the trawl-survey time series this indicator is generally stable and has a positive trend in recent years.

Disease & Toxins Indicators

Harmful Algal Blooms in the Eastern Bering Sea

Contributed by Darcy Dugan[1], Rosie Masui[2], Ginny Eckert[3], Kris Holderied[4], Andie Wall[5], Kari Lanphier[6], Chandra Poe[7], Gay Sheffield[3], Kathi Lefebvre[8], Don Anderson[9]
[1] Alaska Ocean Observing System, Anchorage, AK
[2] Kachemak Bay National Estuarine Research Reserve, Homer, AK
[3] University of Alaska Fairbanks, Alaska Sea Grant, Juneau, AK
[4] NOAA NOS Kasitsna Bay Lab, Seldovia, AK
[5] Kodiak Area Native Association, Kodiak, AK 99615
[6] Sitka Tribe of Alaska, Sitka, AK
[7] Qawalangin Tribe of Unalaska, Unalaska, AK
[8] NOAA Northwest Fisheries Science Center, Seattle, WA
[9] Woods Hole Oceanographic Institution, Woods Hole, MA
Contact: dugan@aoos.org
Last updated: September 2020

Sampling Partners:

Alaska Ocean Observing System
UAF-Alaska Sea Grant
Alaska Veterinary Pathologists
Aleutian Pribilof Island Association
Central Council of Tlingit and Haida*
Chilkoot Indian Association*
Craig Tribal Association*
Hoonah Indian Association*
Hydaburg Cooperative Association*
Kachemak Bay NERR
Ketchikan Indian Association*
Klawock Cooperative Association*
Knik Tribe of Alaska
Kodiak Area Native Association
Metlakatla Indian Community*
NOAA Kasitsna Bay Lab
NOAA WRRN-West
North Slope Borough
Organized Village of Kake*
Organized Village of Kasaan*
Petersburg Indian Association*
Qawalangin Tribe of Unalaska
Sitka Tribe of Alaska*
Skagway Traditional Council*
Southeast Alaska Tribal Ocean Research
Sun'aq Tribe of Kodiak*
Woods Hole Oceanographic Institution
Wrangell Cooperative Association*
Yakutat Tlingit Tribe*

**Partners of Southeast Alaska Tribal Ocean Research (SEATOR)*

Description of indicator: Alaska's most well-known and toxic harmful algal blooms (HABs) are caused by *Alexandrium* spp. and *Pseudo-nitzschia* spp. *Alexandrium* produces saxitoxin which can cause paralytic shellfish poisoning (PSP) and has been responsible for five deaths and over 100 cases of PSP in Alaska since 1993 (see DHSS fatality report[15]). Analyses of paralytic shellfish toxins are commonly reported as of toxin/100 g of tissue, where the FDA regulatory limit is 80/100g. Toxin levels between 80–1000/100 g are considered to potentially cause non-fatal symptoms, whereas levels above 1000/100g ($\sim$ 12x) are considered potentially fatal.

Pseudo-nitzschia produces domoic acid which can cause amnesic shellfish poisoning and inflict permanent brain damage. *Pseudo-nitzschia* has been detected in 13 marine mammal species and has the potential to impact the health of marine mammals and birds in Alaska.

[15] `http://www.dhss.alaska.gov/News/Documents/press/2020/DHSS_PressRelease_PSPFatality_20200715.pdf`

The State of Alaska tests all commercial shellfish harvest, however there is no state-run shellfish testing program for recreational and subsistence shellfish harvest. Regional programs, run by Tribal, agency, and university entities, have expanded over the past five years to provide test results to inform harvesters and researchers and reduce human health risk (Figure 76). All of these entities are partners in the Alaska Harmful Algal Bloom Network which was formed in 2017 to provide a statewide approach to HAB awareness, research, monitoring, and response in Alaska. More information on methods can be found on the Alaska HAB Network website[16] or through the sampling partners listed above.

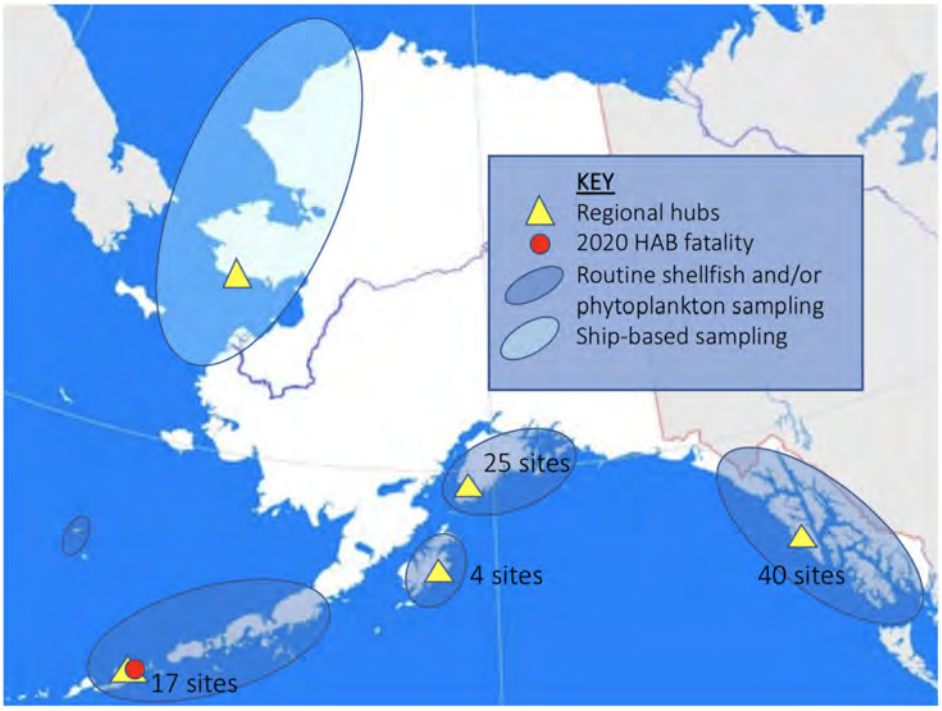

Figure 76: Map of 2020 sampling efforts conducted by partners of the Alaska Harmful Algal Bloom Network (AHAB). Opportunistic sampling of marine mammal tissue and other marine species occurs statewide and is not shown here. A more detailed view of ship-based sampling will be available after the 2020 fall field season.

Status and trends:
Alaska Region: Results from shellfish and phytoplankton monitoring showed a consistent presence of harmful algal blooms (HABs) throughout all regions of Alaska in 2020. Bivalve shellfish from areas that are well known for having PSP levels above the regulatory limit, including Southeast Alaska and Kodiak, continued to test above the regulatory limit, while shellfish in other areas, which have not traditionally seen high levels, had unprecedented levels, including in the Aleutian region.

Northern Bering Sea: In the northern Bering Sea and Bering Strait area, samples were collected from more than 70 animals including marine mammals, fish, clams, birds, and krill. Results are not yet available. Although most Arctic research cruises for 2020 were canceled due to COVID, there are still a few cruises that are, in addition to their main objective, scheduled to collect samples of phytoplankton, cysts, clams, and worms for saxitoxin and domoic acid analyses at several locations in the Bering and Chukchi seas.

Factors influencing observed trends: HABs are likely to increase in intensity and geographic distribution in Alaska waters with warming water temperatures. Observations in Southeast and Southcentral Alaska suggest *Alexandrium* blooms occur at temperatures above 10°C and salinities above 20 (Vandersea et al.,

[16] `https://aoos.org/alaska-hab-network/`

2018; Tobin et al., 2019; Harley et al., 2020). As waters warm throughout Alaska, blooms may increase in frequency and geographic extent.

Implications: HABs pose a risk to human health when present in wildlife species that people consume, including shellfish, birds, and marine mammals. Research across the state is attempting to better understand the presence and circulation of HABs in the food web. HAB toxins have been detected in stranded and harvested marine mammals from all regions of Alaska in past years (Lefebvre et al., 2016) (Figure 77). A multi-disciplinary statewide study funded by NOAA's ECOHAB program is underway and encompasses ship-based sampling of sediments, water, zooplankton, krill, copepods, multiple fish species, bivalves, and the continuation of sampling subsistence-harvested and dead stranded marine mammals.

Figure 77: Algal toxins detected in stranded and harvested marine mammals suggest widespread prevalence of HABs throughout the food web in all regions of Alaska (Lefebvre et al., 2016). Updates to HAB toxin levels in Arctic/subarctic marine mammals are currently in progress.

Fishing and Human Dimensions Indicators

Indicators presented in this section are intended to provide a summary of the status of several ecosystem-scale indicators related to fishing and human economic and social well-being. These indicators are organized around objective categories derived from U.S. legislation and current management practices (see Table 1 for a full list of objective categories and resulting indicators):

- Maintaining diversity
- Maintaining and restoring fish habitats
- Sustainability (for consumptive and non-consumptive uses)
- Seafood production
- Profits
- Recreation
- Employment
- Socio-cultural dimensions

The indicators presented are meant to represent trends in different aspects of the general management objective, but some indicators are better proxies than others. For example, seafood production is a fairly good proxy for the production of seafood to regional, national, and international markets but ex-vessel and wholesale value are imperfect proxies for harvesting and processing sector profits. This suite of indicators will continue to be revised and updated to provide a more holistic representation of human/environment interactions and dependencies.

Maintaining Diversity: Discards and Non-Target Catch

Time Trends in Groundfish Discards

Contributed by Jean Lee
Resource Ecology and Fisheries Management Division, Alaska Fisheries Science Center, NOAA Fisheries
Alaska Fisheries Information Network, Pacific States Marine Fisheries Commission
Contact: jean.lee@noaa.gov
Last updated: September 2020

Description of indicator: Estimates of groundfish discards for 1993–2002 are sourced from NMFS Alaska Region's blend data, while estimates for 2003 and later come from the Alaska Region's Catch Accounting System. These sources, which are based on observer data in combination with industry landing and production reports, provide the best available estimates of groundfish discards in the North Pacific. Discard rates as shown in Figure 78 below are calculated as the weight of groundfish discards divided by the total (i.e., retained and discarded) catch weight for the relevant area-gear-target sector. Where rates are described below for species or species groups, they represent the total discarded weight of the species/species group divided by the total catch weight of the species/species group for the relevant area-gear-target sector. These estimates include only catch of FMP-managed groundfish species within the FMP groundfish fisheries. Discards of groundfish in the halibut fishery and discards of forage fish and species managed under prohibited species catch limits, such as halibut, are not included.

Status and trends: Since 1993, discard rates of groundfish in federally-managed Alaskan groundfish fisheries have generally declined in the trawl pollock and non-pollock trawl fisheries in the eastern Bering Sea

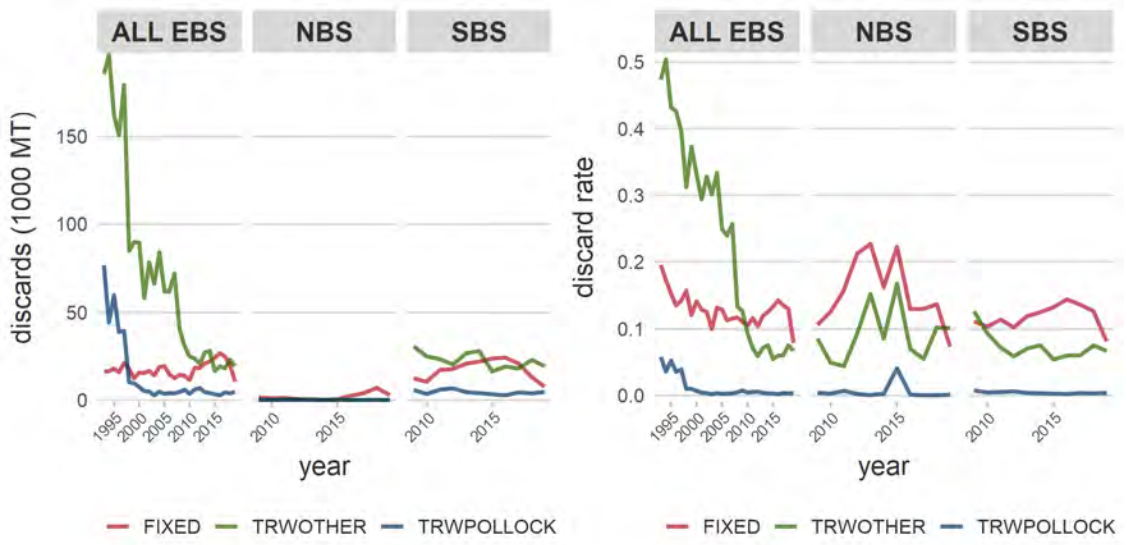

Figure 78: Total biomass and percent of total catch biomass of FMP groundfish discarded in the fixed gear (FIXED), pollock trawl (TRWPOLLOCK), and non-pollock trawl sectors (TRWOTHER) for the eastern Bering Sea (ALL EBS) region, 1993–2019; and for northern (NBS) and southern (SBS) subregions, 2009–2019. Discard rates are calculated as total discard weight of FMP groundfish divided by total retained and discarded weight of FMP groundfish for the sector (includes only catch counted against federal TACs).

(EBS) (Figure 78). Annual discard rates in the EBS pollock trawl sector declined from 20% to about 1% in 1998 and have continued to remain at or below this level. Rates in the non-pollock trawl sector have declined from a high of 50% in 1994 and have remained below 8% since 2011. Discard rates and volumes in the fixed gear (hook-and-line and pot) sector trended upward from 2010 to 2016, reaching the highest annual discard biomass (26.7K metric tons) over the entire time series before declining from 2017 to 2019. Fixed gear discards in the northern Bering Sea trended upward from 2016 to 2018 as some vessels targeting Pacific cod moved their fishing activity northward, but these increases were offset by declines in discard biomass in the southern subregion. Through week 36 of 2020, discard biomass across the entire EBS is consistent with the 2015–2019 period for the trawl non-pollock sector (Figure 79). Trawl pollock discards to date in 2020 are trending slightly higher than the 2015–2019 period, while fixed gear discards are trending lower.

Factors influencing observed trends: Fishery discards may occur for economic or regulatory reasons. Economic discards include discarding of lower value and unmarketable fish, while regulatory discards are those required by regulation (e.g., upon reaching an allowable catch limit for a species). Minimizing discards is recognized as an ecological, economic, and moral imperative in various multilateral initiatives and in National Standard 9 of the Magnuson-Stevens Fishery Conservation and Management Act (Alverson et al., 1994; FAO, 1995; Karp et al., 2011). In the North Pacific groundfish fisheries, mechanisms to reduce discards include:

- Limited access privilege programs (LAPPs), which allocate catch quotas and may reduce economic discards by slowing down the pace of fishing
- In-season closure of fisheries once target or bycatch species quotas are attained
- Minimum retention and utilization standards for certain fisheries
- Maximum retainable amounts (MRAs), which allow for limited retention of species harvested incidentally in directed fisheries.

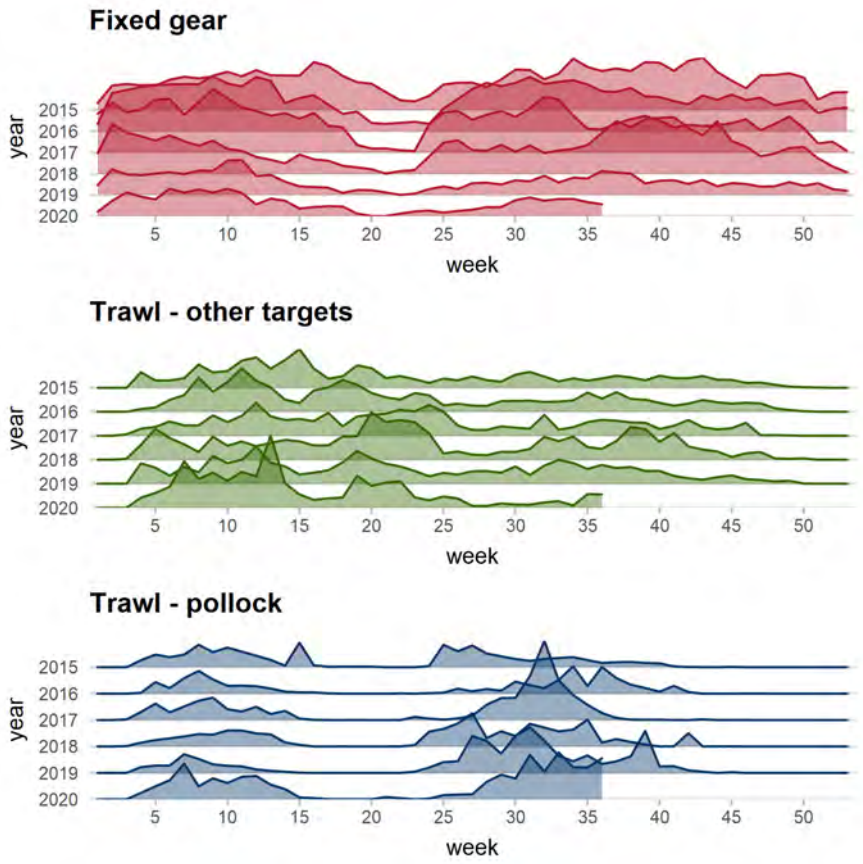

Figure 79: Total biomass of FMP groundfish discarded in the eastern Bering Sea region by sector and week, 2014–2020 (data for 2020 is shown through week 36). Plotted heights are not comparable across sectors.

In the EBS, management and conservation measures aimed at reducing bycatch have contributed to an overall decline in groundfish discards since the early 1990s (NPFMC, 2016, 2017). Pollock roe stripping, wherein harvesters discard all but the the highest value pollock product, was prohibited in 1991 (56 Federal Register 492). Throughout the 1990s, declines in total catch and discard of non-pollock groundfish in the pollock fishery coincided with the phasing out of bottom trawl gear in favor of pelagic gear, which allows for cleaner pollock catches (Graham et al., 2007). Full retention requirements for pollock and Pacific cod were implemented in 1998 for federally-permitted vessels fishing for groundfish (62 Federal Register 63880). Between 1997 and 1998 annual discard rates for cod fell from 13% to 1% in the non-pollock trawl sector and from 50% to 3% in the trawl pollock sector; pollock discards also declined significantly across both trawl gear sectors. In the trawl pollock fishery, discards of pollock have remained at nominal levels since passage of the American Fisheries Act, which established a sector-based LAPP and implemented more comprehensive observer requirements for the fishery in 2000.

Low retention rates in the non-AFA trawl catcher processor (head and gut) fleet prompted Amendments 79 and 80 to the BSAI Groundfish FMP in 2008 (NPFMC, 2016). Amendment 79 established a Groundfish Retention Standard (GRS) Program with minimum retention and utilization requirements for vessels at least 125 feet LOA; industry-internal monitoring of retention rates has since replaced the program. Amendment 80 expanded the GRS program to all vessels in the fleet and established a cooperative-based LAPP with fixed allocations of certain non-pollock groundfish species. In combination with the GRS program, these allocations are intended to remove the economic incentive to discard less valuable species caught incidentally in the multi-species fishery. In 2013, NMFS revised MRAs for groundfish caught in the BSAI arrowtooth

flounder fishery, including an increase from 0 to 20 percent for pollock, cod, and flatfish (78 Federal Register 29248). Groundfish discard rates in the trawl flatfish fishery fell from 23% to 12% between 2007 and 2008 and have continued on a gradual decline since then.

Since 2003 across all Bering Sea sectors combined, discard rates for species groups historically managed together as the "other groundfish" assemblage (skate, sculpin, shark, squid, and octopus) have ranged from 65% to 80%, with skates representing the majority of discards by weight. In the fixed gear sector other groundfish typically account for at least 70% of total groundfish discards annually. Fluctuations in discard volumes and rates for these species may be driven by changes in market conditions and in fishing behavior within the directed fisheries in which these species are incidentally caught. For example, low octopus catch from 2007–2010 may be attributable to lower processor demand for food-grade octopus and decreases in cod pot-fishing effort stemming from declines in cod prices (Conners et al., 2016).

Implications: Fishery bycatch adds to the total human impact on biomass without providing a benefit to the Nation and as such is perceived as "contrary to responsible stewardship and sustainable utilization of marine resources" (Kelleher, 2005). Bycatch may constrain the utilization of target species and increases the uncertainty around total fishing-related mortality, making it more difficult to assess stocks, define overfishing levels, and monitor fisheries for overfishing (Alverson et al., 1994; Clucas, 1997; Karp et al., 2011). Although ecosystem effects of discards are not fully understood, discards of whole fish and offal have the potential to alter energy flow within ecosystems and have been observed to result in changes to habitat (e.g., oxygen depletion in the benthic environment) and community structure (e.g., increases in scavenger populations) (Queirolo et al., 1995; Alverson et al., 1994; Catchpole et al., 2006; Zador and Fitzgerald, 2008). Monitoring discards and discard rates provides a means of assessing the efficacy of measures intended to reduce discards and increase groundfish retention and utilization.

Time Trends in Non-Target Species Catch

Contributed by George A. Whitehouse[1] and Sarah Gaichas[2]
[1]Cooperative Institute for Climate, Ocean, and Ecosystem Studies (CICOES), University of Washington, Seattle WA
[2]Ecosystem Assessment Program, Northeast Fisheries Science Center, National Marine Fisheries Service, NOAA, Woods Hole MA
Contact: andy.whitehouse@noaa.gov
Last updated: August 2020

Description of indicator: We monitor the catch of non-target species in groundfish fisheries in the eastern Bering Sea. In previous years we included the catch of "other" species, "non-specified" species, and forage fish in this contribution. However, stock assessments have now been developed or are under development for all groups in the "other species" category (sculpins, unidentified sharks, salmon sharks, dogfish, sleeper sharks, skates, octopus), some of the species in the "non-specified" group (giant grenadier, other grenadiers), and forage fish (e.g., capelin, eulachon, Pacific sand lance, etc.), therefore we no longer include trends for these species/groups here[17]. Invertebrate species associated with habitat areas of particular concern, previously known as HAPC biota (seapens/whips, sponges, anemones, corals, and tunicates) are now referred to as structural epifauna. Starting with the 2013 Ecosystem Status Report, the three categories of non-target species we continue to track here are:

[17]See AFSC stock assessment website at `https://www.fisheries.noaa.gov/alaska/population-assessments/north-pacific-groundfish-stock-assessments-and-fishery-evaluation`.

1. Scyphozoan jellyfish
2. Structural epifauna (seapens/whips, sponges, anemones, corals, tunicates)
3. Assorted invertebrates (bivalves, brittle stars, hermit crabs, miscellaneous crabs, sea stars, marine worms, snails, sea urchins, sand dollars, sea cucumbers, and other miscellaneous invertebrates).

Total catch of non-target species is estimated from observer species composition samples taken at sea during fishing operations, scaled up to reflect the total catch by both observed and unobserved hauls and vessels operating in all FMP areas[18]. Catch since 2003 has been estimated using the Alaska Region's Catch Accounting System (Cahalan et al., 2014). This sampling and estimation process does result in uncertainty in catches, which is greater when observer coverage is lower and for species encountered rarely in the catch.

Status and trends: The catch of Scyphozoan jellyfish has fluctuated since 2011 and peaked in 2014 (Figure 80). Highs in jellyfish catch in 2011 and 2014 were followed by sharp drops the following year to catches less than half the size. The catch of jellyfish in 2014 is more than double the catch in 2015 and is more than five times the catch in 2016, which is the lowest over the time period examined. The catch of jellyfish in 2019 is the third lowest since 2011, and is about half the catch in 2018. Jellyfish are primarily caught in the pollock fishery.

The catch of structural epifauna has been relatively steady from 2011 to 2019 (Figure 80). Benthic urochordata, anemones, and sponge comprised the majority of the structural epifauna catch from 2011–2019. Sponge were the dominant component of the structural epifauna catch in 2011 and were primarily caught in non-pelagic trawls. Benthic urochordate caught in non-pelagic trawls were the dominant component of the structural epifauna catch in 2012 and 2015–2019. In 2013 and 2014, anemones caught in the Pacific cod fishery were the dominant part of the structural epifauna catch.

Sea stars comprise more than 85% of the assorted invertebrates catch in all years (2011–2019) and are primarily caught in flatfish fisheries (Figure 80). The catch of assorted invertebrates generally trended upward from 2011—2015, then decreased from 2015 to 2018. The catch in 2019 is up 23% from 2018.

Factors influencing observed trends: The catch of non-target species may change if fisheries or ecosystems change. Because non-target species catch is unregulated and unintended, if there have been no large-scale changes in fishery management in a particular ecosystem, then large-scale signals in the non-target catch may indicate ecosystem changes. Catch trends may be driven by changes in biomass or changes in distribution (overlap with the fishery) or both. Fluctuations in the abundance of jellyfish in the EBS are influenced by a suite of biophysical factors affecting the survival, reproduction, and growth of jellies including temperature, sea ice phenology, wind-mixing, ocean currents, and prey abundance (Brodeur et al., 2008). The lack of a clear trend in the catch of scyphozoan jellies may reflect interannual variation in jellyfish biomass or changes in the overlap with fisheries.

Implications: The catch of structural epifauna species and assorted invertebrates is very low compared with the catch of target species. Structural epifauna species may have become less available to the EBS fisheries (or the fisheries avoided them more effectively) since 2005. Abundant jellyfish may have a negative impact on fishes as they compete with planktivorous fishes for prey resources (Purcell and Arai, 2001), and additionally, jellyfish may prey upon the early life history stages (eggs and larvae) of fishes (Purcell and Arai, 2001; Robinson et al., 2014).

[18]For this contribution the catch of non-target species/groups from the Bering Sea includes the reporting areas 508, 509, 512, 513, 514, 516, 517, 521, 523, 524, and 530. See `https://www.fisheries.noaa.gov/alaska/sustainable-fisheries/alaska-fisheries-figures-maps-boundaries-regulatory-areas-and-zones`.

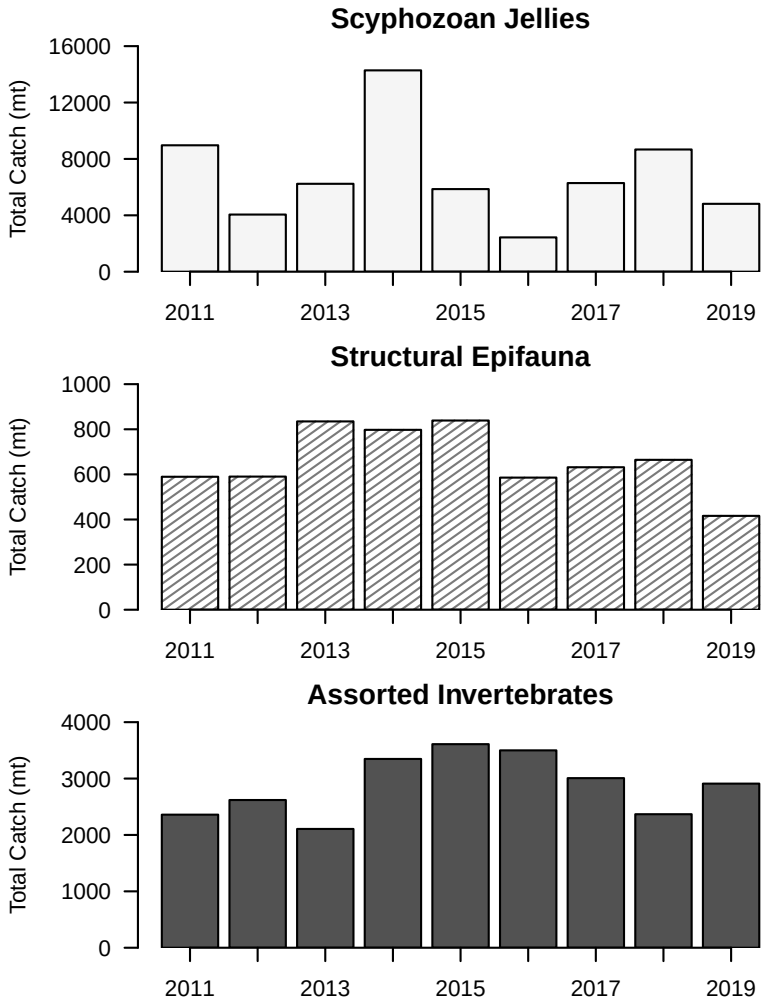

Figure 80: Total catch of non-target species (tons) in EBS groundfish fisheries (2011–2019). **Please note the different y-axis scales** between the species groups.

Seabird Bycatch Estimates for Groundfish Fisheries in the Eastern Bering Sea, 2010–2019

Contributed by Joseph Krieger and Anne Marie Eich
Sustainable Fisheries Division, Alaska Regional Office, National Marine Fisheries Service, NOAA

Contact: Joseph.Krieger@noaa.gov
Last updated: August 2020

Description of indicator: This report provides estimates of the number of seabirds caught as bycatch in commercial groundfish fisheries operating in federal waters of the U.S. Exclusive Economic Zone of the eastern Bering Sea for the years 2010 through 2019. Estimates of seabird bycatch from earlier years using different methods are not included here. Fishing gear types represented are demersal longline, pot, pelagic trawl, and non-pelagic trawl. These numbers do not apply to gillnet, seine, or troll fisheries. Data collection on the Pacific halibut longline fishery began in 2013 with the restructured North Pacific Observer Program.

Estimates are based on two sources of information: (1) data provided by NMFS-certified fishery observers deployed to vessels and floating or shoreside processing plants (AFSC, 2011), and (2) industry reports of catch and production. Observer deployment plans are reviewed and updated annually in the Annual Deployment Plan[19]. The NMFS Alaska Regional Office Catch Accounting System (CAS) produces the estimates (Cahalan et al., 2010, 2014). The main purpose of the CAS is to provide near real-time delivery of accurate groundfish and prohibited species catch and bycatch information for inseason management decisions. CAS also estimates non-target species (such as invertebrates) and seabird bycatch in the groundfish fisheries. The CAS produces estimates based on these two current data sets, which may have changed over time.

Estimates of seabird bycatch from the eastern Bering Sea include the reporting areas 508, 509, 512, 513, 514, 516, 517, 521, and 524[20].

[19]The 2020 plan is available at: https://www.fisheries.noaa.gov/resource/document/2020-annual-deployment-plan-observers-groundfish-and-halibut-fisheries-alaska

[20]https://www.fisheries.noaa.gov/alaska/commercial-fishing/alaska-fisheries-figures-maps-boundaries-/regulatory-areas-and-zones

Table 4: **Estimated** seabird bycatch in eastern Bering Sea groundfish fisheries for all gear types, 2010 through 2019. Note that these numbers represent extrapolations from observed bycatch, not direct observations. See text for estimation methods.

Species Group	2010	2011	2012	2013	2014	2015	2016	2017	2018	2019
Unidentified albatross	0	0	0	0	12	0	0	0	0	0
Short-tailed albatross	10	0	0	0	11	0	0	0	0	0
Laysan albatross	7	28	37	8	13	14	12	28	175	13
Black-footed albatross	9	1	0	0	8	0	0	0	0	0
Northern fulmar	1,745	5,226	2,759	2,733	677	2,334	5,053	3,516	2,808	2,674
Shearwaters	564	156	464	196	116	358	3,161	983	545	3,133
Gull	688	1,558	806	454	576	927	577	372	504	155
Kittiwake	0	7	5	3	4	12	5	22	37	18
Murre	102	14	6	3	47		52	10	0	0
Puffin	9	0	0	0	0	0	10	0	0	0
Auklets	0	0	7	4	67	18	1	25	0	0
Other alcid	0	0	0	0	0	0	0	0	6	6
Cormorant	0	0	0	0	0	3	0	0	0	0
Other birds	0	0	0	0	0	0	0	63	0	0
Unidentified birds	226	348	290	267	73	144	282	253	77	190
Grand Total	3,361	7,337	4,374	3,668	1,604	3,811	9,155	5,271	4,152	6,189

Status and trends: The numbers of seabirds estimated to be caught incidentally in the eastern Bering Sea fisheries in 2019 (6,189 birds) increased from 2018 (4,152 birds) by 49%, and were above the 2010–2018 average of 4,748 birds by 30% (Table 4, Figure 81). Northern fulmars, shearwaters, and gulls were the most common species or species groups caught incidentally in the eastern Bering Sea fisheries in 2019 that could be identified. In 2019, the number of northern fulmars and gulls decreased by 5% and 69%, respectively, compared to 2018, and were below the 2010–2018 average of 2,983 and 718 birds by 10% and 78%, respectively. In 2019, the number of shearwaters was almost six times higher than was estimated in 2018, and was 4.3 times above the 2010–2018 average of 727 birds. As described in the Integrated Seabird Section (see p. 114), this large increase in shearwater bycatch is likely attributed to the shearwater mortality event that was document around Alaska in 2019. No short-tailed albatross or black-footed albatross were reported as taken in the EBS. The number of Laysan albatross decreased by 92% compared to 2018 and was below the 2010–2018 average of 36 birds by 42% (Figure 82).

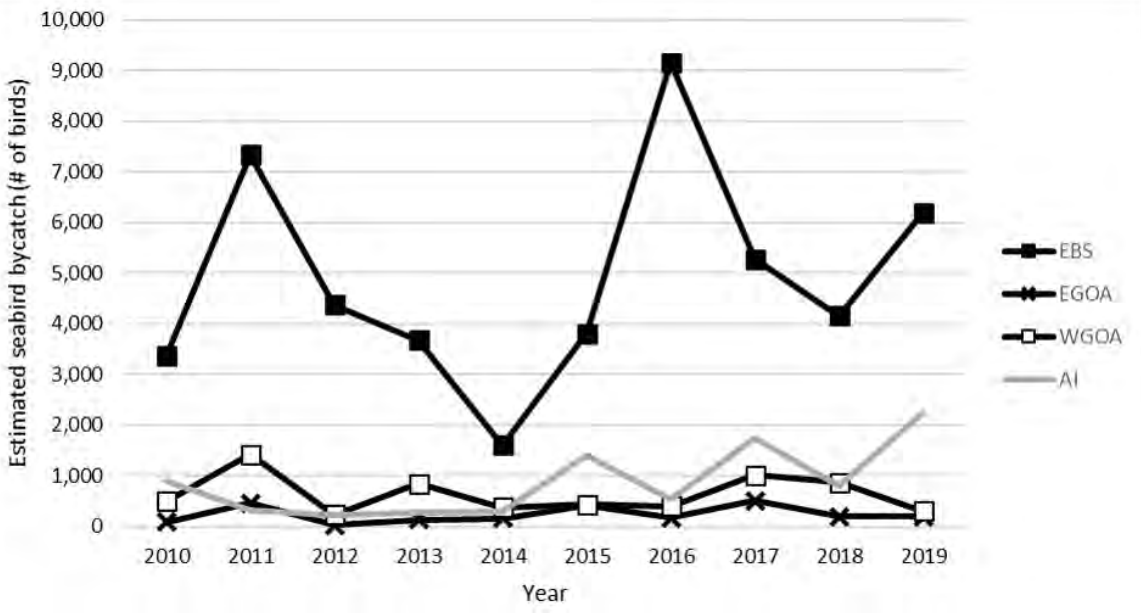

Figure 81: Total estimated seabird bycatch in eastern Bering Sea (EBS), Eastern Gulf of Alaska (EGOA), Western Gulf of Alaska (WGOA), and Aleutian Islands (AI) groundfish fisheries, all gear types combined, 2010–2019.

BSAI Pacific cod fisheries using demersal longline (hook and line) are responsible for the majority of seabird bycatch in the EBS. The average annual seabird bycatch for 2010–2018 was 4,581 birds per year (Table 13 in Krieger and Eich (2020)). In 2019, the estimated seabird bycatch was above the 2010–2018 average by 39% (6,349 birds; Table 13 in Krieger and Eich (2020)). Figure 83 shows the spatial distribution of observed seabird bycatch from 2014–2019 from the Pacific cod hook and line fisheries overlaid onto heat maps depicting fishing effort for the fishery.

Focusing solely on the bycatch of albatross (unidentified, short-tailed, Laysan, and black-footed) in the BSAI Pacific cod fisheries using demersal longline gear, an average of 26 albatross were taken per year, from 2010–2019 (Krieger and Eich, 2020) (Figure 82).

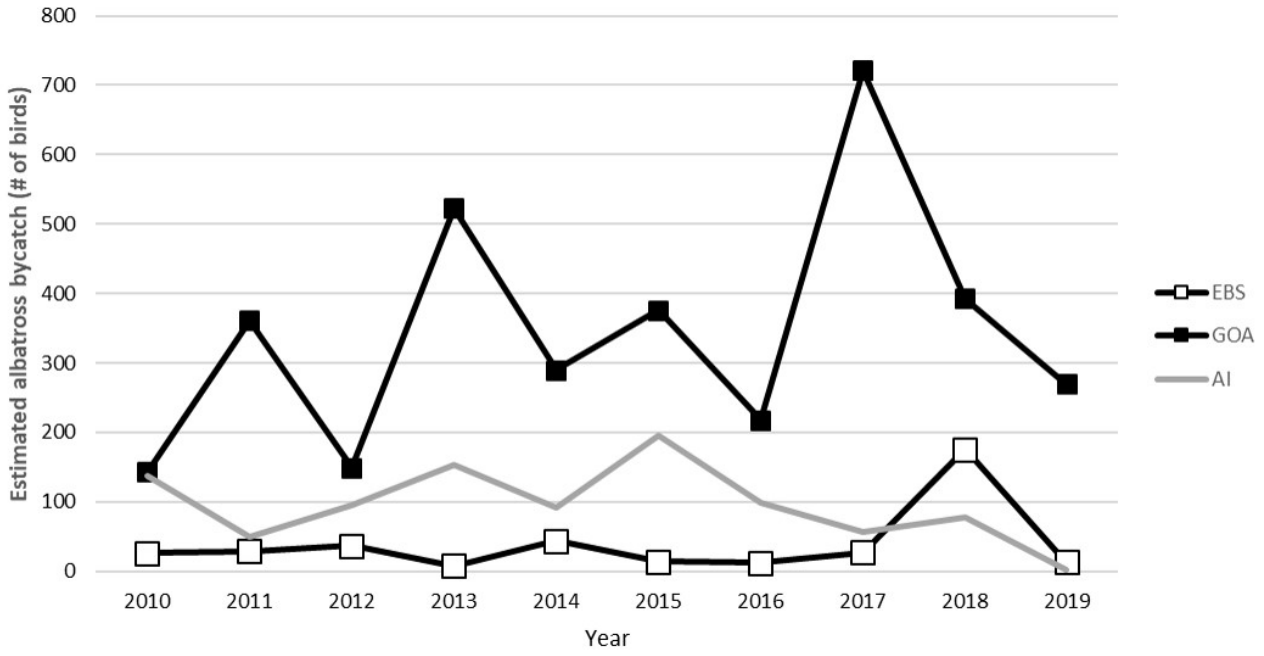

Figure 82: Total estimated albatross bycatch in eastern Bering Sea (EBS), Gulf of Alaska (GOA), and Aleutian Islands (AI) groundfish fisheries, all gear types combined, 2010–2019.

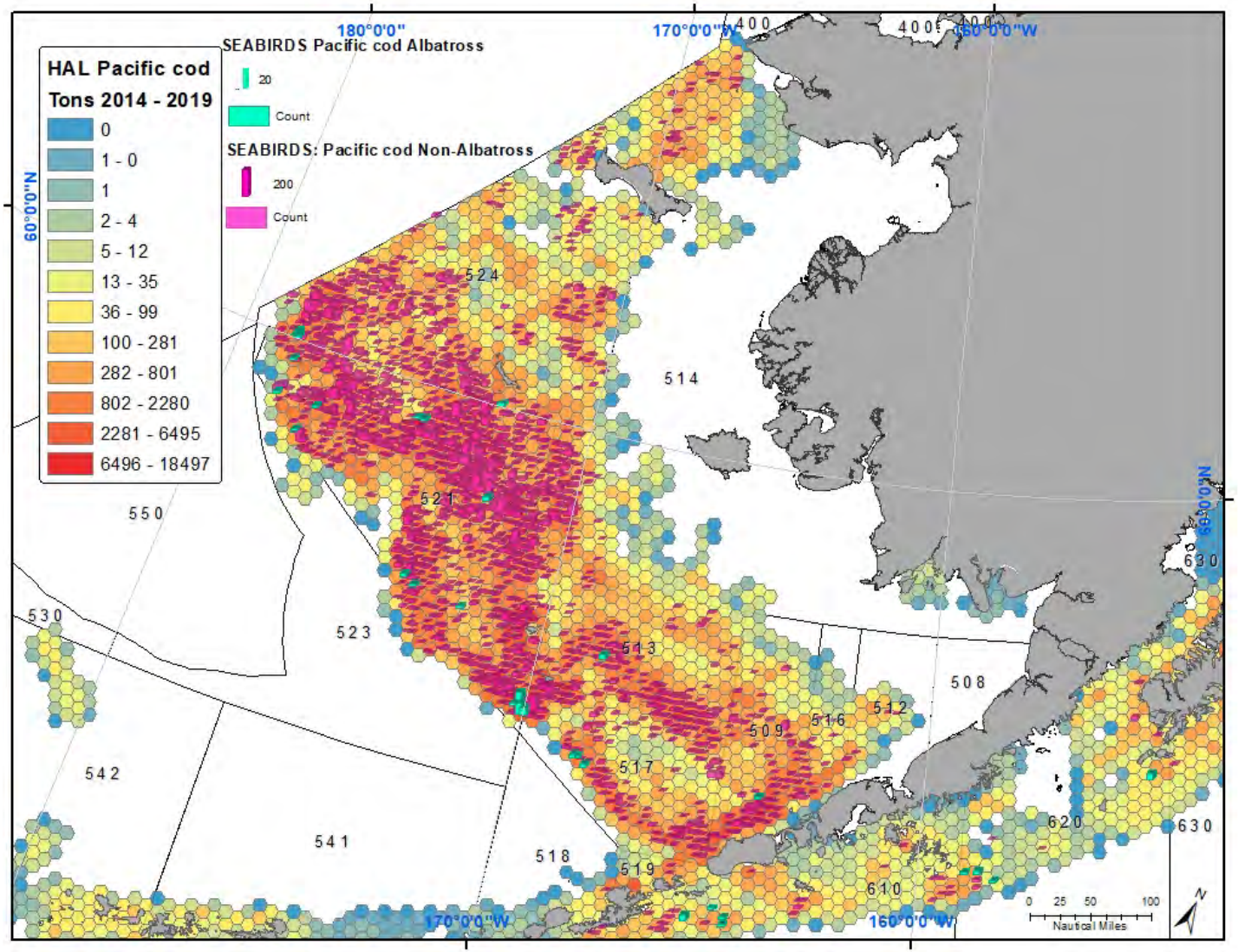

Figure 83: Spatial distribution of observed seabird bycatch from 2014–2019 from the Pacific cod hook and line fisheries. Colored vertical bars indicate the sum of incidental takes at a location grouped within 1/10 of a degree of latitude and longitude. Incidental takes are separated between takes of albatross and takes of non-albatross seabirds. Image includes locations of incidental takes of seabirds overlaid on a heat map depicting fishing effort.

Factors influencing observed trends: There are many factors that may influence annual variation in bycatch rates, including seabird distribution, population trends, prey supply, and fisheries activities.

Vessels fishing with hook and line gear have traditionally been responsible for about 90% of the overall seabird bycatch in Alaska, as determined from the data sources noted above. However, standard observer sampling methods on trawl vessels do not account for additional mortalities from net entanglements, cable strikes, and other sources. Thus, the trawl estimates may be downward biased.

Dietrich and Fitzgerald (2010) found in an analysis of 35,270 longline sets from 2004–2007 that the most predominant species, northern fulmar, only occurred in 2.5% of all sets. Albatross, a focal species for conservation efforts, occurred in less than 0.1% of sets. Thus, while annual seabird bycatch estimates numbers in the 1,000s, given the vast size of the fishery, actual takes of seabirds remains relatively uncommon (Krieger and Eich, 2020).

Implications: Estimated seabird bycatch increased from 2018 to 2019 in the eastern Bering Sea and Aleutian Islands, but this is largely attributed to the shearwater mortality event that occurred throughout Alaska in 2019. Estimated seabird bycatch in the eastern Gulf of Alaska in 2019 remained relatively unchanged from 2018, while seabird bycatch in the western Gulf of Alaska decreased by 66% from 2018 to 2019. This was primarily due to reduced takes of northern fulmars, black-footed albatross, and gulls. These differences indicate localized changes in the Bering Sea, Gulf of Alaska, and Aleutian Islands regarding seabird distribution, fishing effort, and/or seabird prey supply, all of which could impact bycatch.

It is difficult to determine how seabird bycatch estimates and trends are linked to changes in ecosystem components because seabird mitigation gear is used in the longline fleet. There does appear to be a link between poor ocean conditions and the peak bycatch years, on a species-group basis. Fishermen have noted in some years that the birds appear starved and attack baited longline gear more aggressively. This probably indicates changes in food availability rather than distinct changes in how well the fleet employs mitigation gear. A focused investigation of this aspect of seabird bycatch is needed and could inform management of poor ocean conditions if seabird bycatch rates (reported in real time) were substantially higher than normal.

Maintaining and Restoring Fish Habitats

There are no updates to Maintaining and Restoring Fish Habitat indicators in this year's report. See the contribution archive for previous indicators at: `https://access.afsc.noaa.gov/REFM/REEM/ecoweb/`.

Sustainability (for consumptive and non-consumptive uses)

Fish Stock Sustainability Index and Status of Groundfish, Crab, Salmon, and Scallop Stocks

Contributed by George A. Whitehouse
Cooperative Institute for Climate, Ocean, and Ecosystem Studies (CICOES), University of Washington, Seattle WA
Contact: andy.whitehouse@noaa.gov
Last updated: August 2020

Description of indicator: The Fish Stock Sustainability Index (FSSI) is a performance measure for the sustainability of fish stocks selected for their importance to commercial and recreational fisheries[21]. The FSSI will increase as overfishing is ended and stocks rebuild to the level that provides maximum sustainable yield. The FSSI is calculated by awarding points for each fish stock based on the following rules:

1. Stock has known status determinations:
   (a) overfishing level is defined = 0.5
   (b) overfished biomass level is defined = 0.5
2. Fishing mortality rate is below the "overfishing" level defined for the stock = 1.0
3. Biomass is above the "overfished" level defined for the stock = 1.0
4. Biomass is at or above 80% of the biomass that produces maximum sustainable yield (B_{MSY}) = 1.0 (this point is in addition to the point awarded for being above the "overfished" level)

The maximum score for each stock is 4.

In the Alaska Region, there are 35 FSSI stocks and an overall FSSI of 140 would be achieved if every stock scored the maximum value, 4. Over time, the number of stocks included in the FSSI has changed as stocks have been added and removed from Fishery Management Plans (FMPs). To keep FSSI scores for Alaska comparable across years we report the FSSI as a percentage of the maximum possible score (i.e., 100%).

The list of stocks included in the FSSI was revised in 2020 to focus on stocks of heightened commercial and recreational importance. In the Bering Sea and Aleutian Islands (BSAI), the Pribilof Islands blue king crab, Saint Matthew Island blue king crab, Pribilof Islands red king crab, and the black-spotted/rougheye rockfish stocks were removed from the FSSI and added to the group of non-FSSI stocks. The BSAI stock of Kamchatka flounder, the Aleutian Islands Pacific cod stock, and the Bogoslof stock of walleye pollock were added to the BSAI FSSI. These changes resulted in a net reduction from 22 to 21 FSSI stocks in the BSAI (See FSSI Endnotes for stock definitions). With few exceptions, groundfish species (or species complex) in the BSAI are managed as single stocks and not separately for the Bering Sea and Aleutian Islands. As such, the FSSI scores are reported for the BSAI as a whole.

Additionally, there are 28 non-FSSI stocks in Alaska, three ecosystem component species complexes, and Pacific halibut, which are managed under an international agreement. Two of the non-FSSI crab stocks are overfished but are not subject to overfishing. The Pribilof Islands blue king crab stock is in year six of a rebuilding plan, and the North Pacific Fishery Management Council was notified that the Saint Matthew Island blue king crab stock is overfished on October 22, 2018 and have two years from this date to implement a rebuilding plan for this stock. None of the other non-FSSI stocks are known to be subject to overfishing,

[21] `https://www.fisheries.noaa.gov/national/population-assessments/fishery-stock-status-updates`

Table 5: Summary of status for the 21 FSSI stocks in the BSAI, updated through June 2020.

BSAI FSSI (21 stocks)	Yes	No	*Unknown*	*Undefined*	N/A
Overfishing	0	21	0	0	0
Overfished	0	19	2	0	0
Approaching overfished condition	0	19	2	0	0

are overfished, or are approaching an overfished condition. For more information on non-FSSI stocks see the Status of U.S. Fisheries webpage[22].

Status and trends: The overall Alaska FSSI is down from 92% in 2019 to 89% in 2020 (Figure 84). Until 2019, the overall Alaska FSSI had generally trended upwards from 80% in 2006 to a high of 94% in 2018.

As of June 30, 2020, no BSAI groundfish stock or stock complex is subject to overfishing, is known to be overfished, or known to be approaching an overfished condition (Table 5). The BSAI groundfish FSSI score is 59 out of a maximum possible 64.

The BSAI king and Tanner crab FSSI is 19 out of a possible 20. One point was deducted for the Norton Sound red king crab stock's biomass decreasing to below the B/B_{MSY} threshold.

The overall BSAI score is 78 out of a maximum possible score of 84 (Table 6). The overall FSSI has generally trended upward from 74% in 2006 to 93% in 2020 (Figure 85).

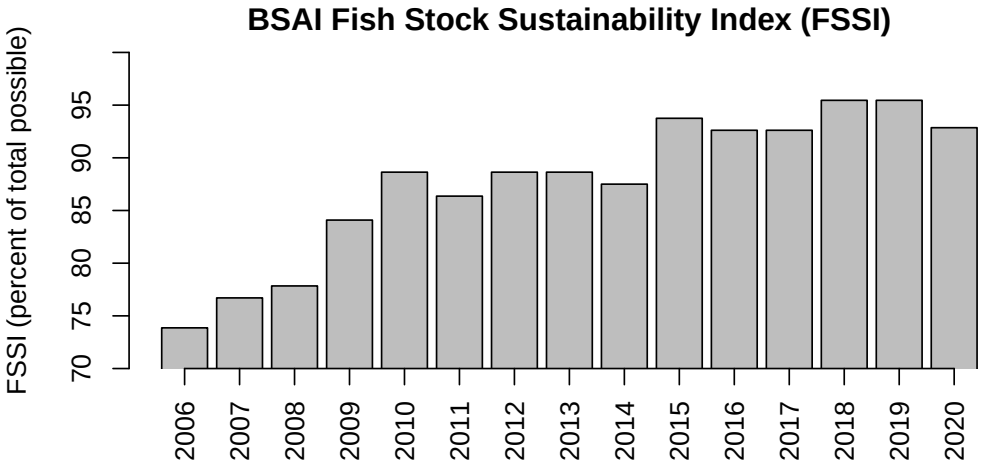

Figure 84: The trend in overall Alaska FSSI, as a percentage of the maximum possible FSSI from 2006 through 2020. The maximum possible FSSI was 140 from 2006 to 2014, 144 from 2015 to 2019, and is 140 in 2020. All scores are reported through the second quarter (June) of each year, and are retrieved from the Status of U.S. Fisheries website.

Factors influencing observed trends: The overall trend in Alaska FSSI has been positive from 2006 through 2019. The decrease in overall score from 2019 to 2020 is the net result of changes in the stocks included in the FSSI plus a loss of one point for the biomass of Norton Sound red king crab decreasing to below 80% of B_{MSY}. Two of the three groundfish stocks added to the BSAI FSSI in 2020 had FSSI scores of 1.5. The Aleutian Islands Pacific cod stock and the Bogoslof stock of walleye pollock lost points for not having known overfished status or known biomass levels relative to their overfished levels or to B_{MSY}. All other BSAI FSSI stocks received the maximum possible score of 4 points.

[22] `https://www.fisheries.noaa.gov/national/population-assessments/status-us-fisheries`

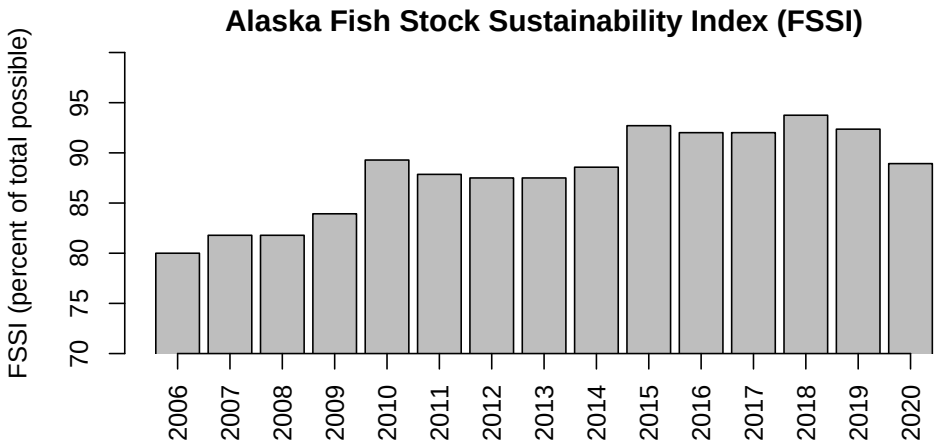

Figure 85: The trend in FSSI for the BSAI region from 2006 through 2020 as a percentage of the maximum possible FSSI. All scores are reported through the second quarter (June) of each year, and are retrieved from the Status of U.S. Fisheries website.

Implications: The majority of Alaska groundfish fisheries appear to be sustainably managed. None of the FSSI stocks in the BSAI are subject to overfishing or known to be overfished.

Table 6: BSAI FSSI stocks under NPFMC jurisdiction updated through June 2020 adapted from the Status of U.S. Fisheries website. See FSSI Endnotes for definition of stocks and stock complexes.

Stock	Overfishing	Overfished	Approaching	Action	Progress	B_{MSY}	FSSI Score
Golden king crab - Aleutian Islands[a]	No	No	No	N/A	N/A	1.554/1.11	4
Red king crab - Bristol Bay	No	No	No	N/A	N/A	0.82	4
Red king crab - Norton Sound	No	No	No	N/A	N/A	0.68	3
Snow crab - Bering Sea	No	No	No	N/A	N/A	0.86	4
Southern Tanner crab - Bering Sea	No	No	No	N/A	N/A	1.09	4
BSAI Alaska plaice	No	No	No	N/A	N/A	1.84	4
BSAI Atka mackerel	No	No	No	N/A	N/A	1.45	4
BSAI arrowtooth flounder	No	No	No	N/A	N/A	2.64	4
BSAI Kamchatka flounder	No	No	No	N/A	N/A	1.4	4
BSAI flathead sole complex[b]	No	No	No	N/A	N/A	1.89	4
BSAI rock sole complex[c]	No	No	No	N/A	N/A	2.1	4
BSAI skate complex[d]	No	No	No	N/A	N/A	1.7	4
BSAI Greenland halibut	No	No	No	N/A	N/A	1.61	4
BSAI northern rockfish	No	No	No	N/A	N/A	1.89	4
BS Pacific cod	No	No	No	N/A	N/A	1.25	4
AI Pacific cod	No	Unknown	Unknown	N/A	N/A	not estimated	1.5
BSAI Pacific Ocean perch	No	No	No	N/A	N/A	1.68	4
Walleye pollock - Aleutian Islands	No	No	No	N/A	N/A	1.09	4
Walleye pollock - Bogoslof	No	Unknown	Unknown	N/A	N/A	not estimated	1.5
Walleye pollock - Eastern Bering Sea	No	No	No	N/A	N/A	1.9	4
BSAI yellowfin sole	No	No	No	N/A	N/A	1.94	4

Box A. Endnotes and stock complex definitions for FSSI stocks listed in Table 6, adapted from the Status of U.S. Fisheries website.

(a) The status of this stock is based on the assessment of two stocks—Eastern and Western Aleutian Islands golden king crab stocks.

(b) The flathead sole complex consists of flathead sole and Bering flounder. Flathead sole accounts for the overwhelming majority of the biomass and is regarded as the indicator species for the complex. The overfished determination is based on the combined abundance estimates for the two species; the overfishing determination is based on the Overfishing Limit (OFL), which is computed from the combined abundance estimates for the two species.

(c) The rock sole complex consists of northern rock sole and southern rock sole (NOTE: These are two distinct species, not two separate stocks of the same species). Northern rock sole accounts for the overwhelming majority of the biomass and is regarded as the indicator species for the complex. The overfished determination is based on the combined abundance estimates for the two species; the overfishing determination is based on the OFL, which is computed from the combined abundance estimates for the two species.

(d) The skate complex consists of Alaska skate, Aleutian skate, Bering skate, big skate, butterfly skate, commander skate, deepsea skate, mud skate, Okhotsk skate, roughshoulder skate, roughtail skate, white-blotched skate, and whitebrow skate. Alaska skate is assessed and is the indicator species for this complex.

Seafood Production

Economic Indicators in the Eastern Bering Sea Ecosystem – Landings

Contributed by Benjamin Fissel[1], Jean Lee[1,2], and Steve Kasperski[1]
[1]Resource Ecology and Fishery Management Division, Alaska Fisheries Science Center, National Marine Fisheries Service, NOAA
[2]Alaska Fisheries Information Network, Pacific States Marine Fisheries Commission
Contact: Ben.Fissel@noaa.gov
Last updated: September 2020

Description of indicator: Landings are a baseline metric for characterizing commercial economic production in the eastern Bering Sea. Landings are the retained catch of fish and are plotted here by functional group (Figure 86). While many species comprise a functional group, it is the handful of species that fishermen target that dominate the economic metrics in each group. The primary target species in the pelagic foragers' functional group are walleye pollock (*Gadus chalcogrammus*), Atka mackerel (*Pleurogrammus monopterygius*), and Pacific ocean perch (*Sebastes alutus*). The primary target species in the apex predators' functional group are Pacific cod (*Gadus macrocephalus*), Pacific halibut (*Hippoglossus stenolepis*), sablefish (*Anoplopoma fimbria*), and arrowtooth flounder (*Atheresthes stomias*). The primary target species in the benthic foragers' functional group are yellowfin sole (*Limanda aspera*), rock sole (*Lepidopsetta bilineata*), and flathead sole (*Hippoglossoides elassodon*). The primary target species in the salmonid functional group are Chinook (*Oncorhynchus tshawytscha*), sockeye (*O. nerka*), and pink (*O. gorbuscha*) salmon. The primary target species in the motile epifauna functional group are king, bairdi, and snow crab. Because of significant differences in the relative scale of landings across functional group landings are plotted in logs.

Status and trends: Aggregate landings in the eastern Bering Sea (EBS) remained stable through 2019. EBS landings are predominantly from the pelagic forager functional group. The primary species landed within this group is pollock whose landings are an order of magnitude larger than that of any other species or functional group. Pelagic forager landings remained stable through 2019 with strong landings of pollock. Trends in the landings of the apex predator functional group are heavily influenced by TAC and catch levels of Pacific cod which dropped in 2019, but were offset by increases in the catch of predator flatfish and rockfish. The net result was a marginal decrease in apex predator landings in 2019. Landings were increasing up to 2008 in the flatfish fisheries which make up the benthic foragers functional group. Total flatfish catches are well below their respective TACs and stocks remain healthy. There was a marginal increase in the landings of benthic foragers through 2019, but landings remained relatively stable. EBS salmon landings have remained largely stable from 2004–2017 with a temporary decline from 2011–2013. Landings in the salmonid functional group also remained stable through 2019. Landings in the crab stocks, which comprise the motile epifauna group, have trended up gradually since 2003 reflecting largely an increased catch of tanner crab. Landings in the motile epifauna group have been on the decline since 2015 with decreases in both the tanner crab and king crab species groups. In 2017 crab catches declined significantly for all species, particularly tanner crab resulting in the significant decline in the index displayed in Figure 86, and have leveled off through 2018 and 2019.

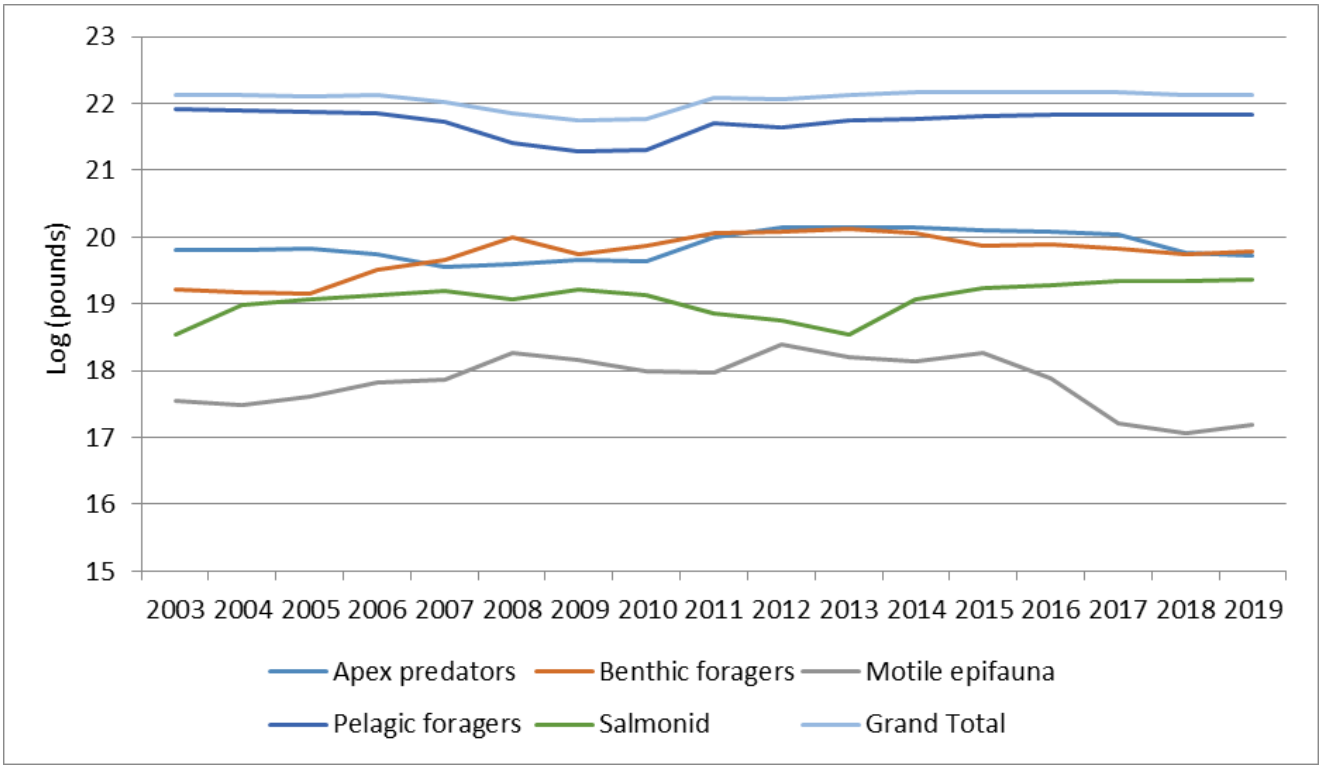

Figure 86: Eastern Bering Sea landings by functional group (log pounds).

Factors influencing observed trends: Between 2008–2010, conservation based reductions in the pollock Total Allowable Catch (TAC) resulted in reduced landings for this functional group. In 2008 Amendment 80 to the BSAI groundfish FMP was implemented rationalizing the major flatfish fisheries which resulted in significant reductions in bycatch. Total catch of the groundfish that comprise the pelagic forager, apex predators, and benthic foragers' functional groups in the EBS is capped at 2 million metric tons. The sum of the Allowable Biological Catches (ABC) for these groups are typically above the cap and TACs are reduced from the ABC through negotiations at the NPFMC to meet the cap requirement. This cap system influences interpretation of trends in landings relative to their underlying stocks as changes in landings may not be the direct result of changes in biomass.

Implications: Landings depict one aspect of the raw stresses from harvesting imposed on the eastern Bering Sea ecosystem's functional group through fishing. This information can be useful in identifying areas where harvesting may be impacting different functional groups in times where the functional groups within the ecosystem might be constrained. What is clear from Figure 86 is that pelagic foragers have been by far largest share of total landings over the 2003–2019 period, while motile epifauna represent the smallest, and declining, share. Monitoring the trends in landings stratified by ecosystem functional group provides insight on the fishing related stresses on ecosystems. The ultimate impact that these stresses have on the ecosystem cannot be discerned from these metrics alone and must be viewed within the context of what the ecosystem can provide.

Profits

Economic Indicators in the Eastern Bering Sea Ecosystem – Value and Unit Value

Contributed by Benjamin Fissel[1], Jean Lee[1,2], and Steve Kasperski[1]
[1]Resource Ecology and Fishery Management Division, Alaska Fisheries Science Center, National Marine Fisheries Service, NOAA
[2]Alaska Fisheries Information Network, Pacific States Marine Fisheries Commission
Contact: Ben.Fissel@noaa.gov
Last updated: September 2020

Description of indicator: Three plots are used to characterize economic value in an ecosystem context for the eastern Bering Sea.

- Ex-vessel value
- First-wholesale value
- Ratio of first-wholesale value to total catch unit value

Ex-vessel value is the un-processed value of the retained catch. Ex-vessel value can informally be thought of as the revenue that fishermen receive from the catch. First-wholesale value is the revenue from the catch after primary processing by a processor. First-wholesale value is a more comprehensive measure of value to the fishing industry as it includes ex-vessel value as well as the value-added revenue from processing which goes to processing sector. The first-wholesale value to total catch unit value is the ratio of value to biomass extracted as a result of commercial fish harvesting. The measure of biomass extracted in this index includes retained catch, discards, and prohibited species catch. This metric answers the question: "how much revenue is the fishing industry receiving per-unit biomass extracted from the ecosystem?" Ex-vessel value and first-wholesale value are plotted by functional group. While many species comprise a functional group, it is the handful of species that fishermen target that dominate the economic metrics in each group.

The primary target species in the pelagic foragers' functional group are walleye pollock (*Gadus chalcogrammus*), Atka mackerel (*Pleurogrammus monopterygius*), and Pacific ocean perch (*Sebastes alutus*). The primary target species in the apex predators' functional group are Pacific cod (*Gadus macrocephalus*), Pacific halibut (*Hippoglossus stenolepis*), sablefish (*Anoplopoma fimbria*), and arrowtooth flounder (*Atheresthes stomias*). The primary target species in the benthic foragers' functional group are yellowfin sole (*Limanda aspera*), rock sole (*Lepidopsetta bilineata*), and flathead sole (*Hippoglossoides elassodon*). The primary target species in the salmonid functional group are Chinook (*Oncorhynchus tshawytscha*), sockeye (*O. nerka*), and pink (*O. gorbuscha*) salmon. The primary target species in the motile epifauna functional group are king, bairdi, and snow crab. Because of significant differences in the relative scale of landings across functional group landings are plotted in logs.

Status and trends: Ex-vessel value is the revenue from landings, consequently trends in ex-vessel value and landings are closely connected. Ex-vessel value is highest in the pelagic forager functional group because of the volume of landings in the pollock fishery. Benthic forager flatfish revenues

decreased from 2012–2015 as a result of decreased prices and, starting in 2015, price increases have increased value while landings remained stable, thus since 2017 revenues have remained relatively flat. Value in the motile epifauna group has been decreasing with decreasing crab landings. The generally increasing trend in salmon value is the result of increased landings. Salmon prices were increasing up to 2018 and decreased in 2019 (Figure 87). Differences in the relative level of the indices between the landings and ex-vessel value reflect differences in the average prices of the species that make up the functional group. Hence, landings of benthic forager flatfish may be larger than salmon, but salmon ex-vessel value is higher because salmon commands a higher price.

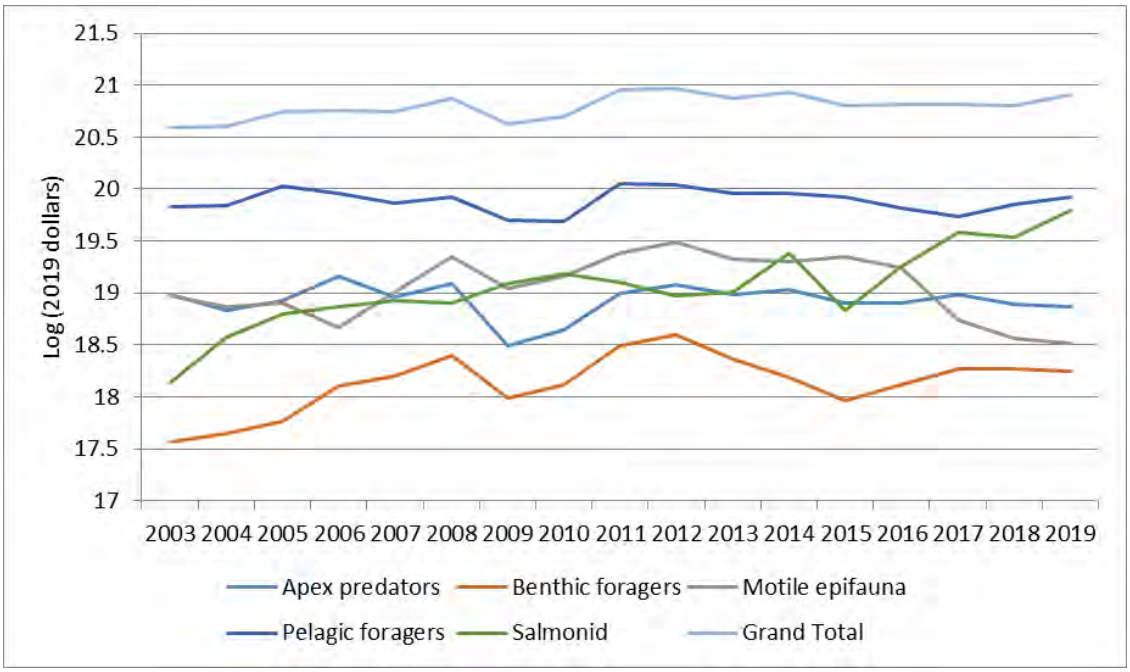

Figure 87: Eastern Bering Sea real ex-vessel value by functional group (log 2019 dollars).

First-wholesale value was generally increasing for each of the functional groups up to about 2008–2010 with stable or increasing landings and gradually increasing prices. After this, variation in landings or in prices have had differential impacts (Figure 88). The value of the pelagic forager group shows a gradual increasing trend as result of relatively stable landings with the exception of 2008–2009 when landings were low. From 2013–2017 prices for pollock decreased as global pollock supply has been high, but increased landings have had the combined effect of marginal increases in value. In 2018 and 2019 prices for pollock increased. First-wholesale value in 2018–2019 fell in the apex predator group as cod landings decreased and the average price of sablefish declined. Benthic forager first-wholesale value decreased from 2012 to 2015 with decreases in flatfish prices as demand for these products plateaued with significant supply. From 2015–2017 supply was stable and prices increased and since 2017 value has remained stable. Increased value in the salmonid functional group since 2015 has been the result of increased landings. Value in the motile epifauna group has been decreasing in recent years with reductions in landings.

The first-wholesale to total catch unit value is analogous to a volumetrically weighted average price across functional groups which is inclusive of discards. However, discards represent a relatively small fraction of total catch. Because of the comparatively larger volume and value from pelagic foragers' the unit value index is more heavily weighted towards this group. The unit value index

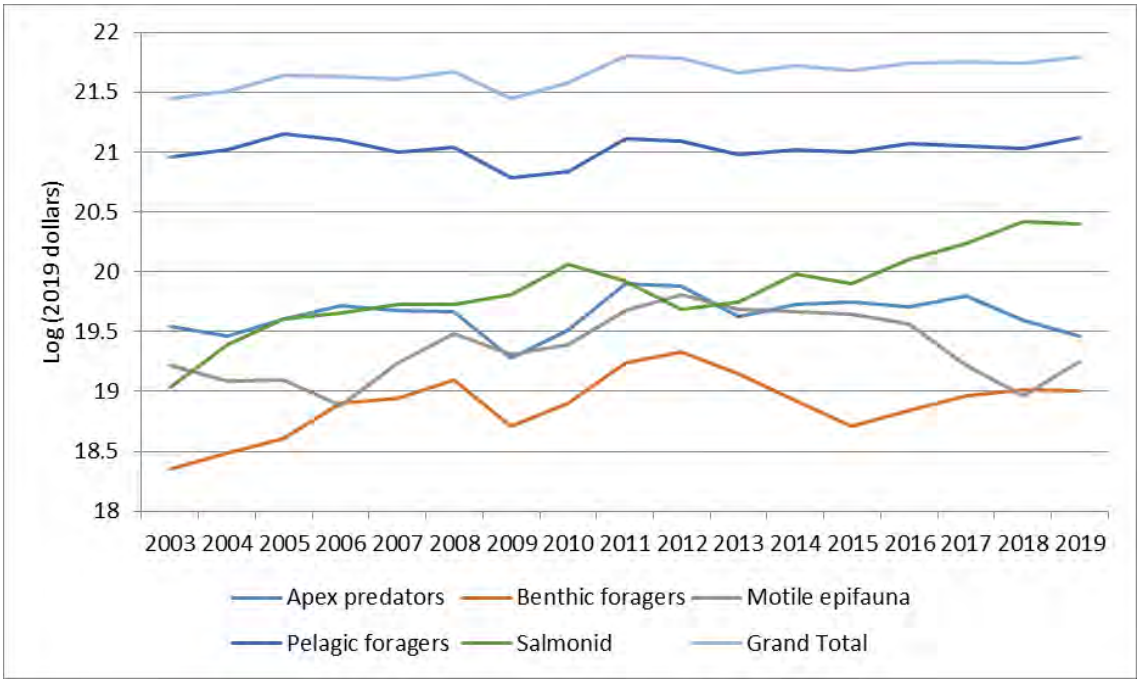

Figure 88: Eastern Bering Sea real first-wholesale value by functional group (log 2019 dollars).

increased from 2003–2008 with generally increasing prices across all functional groups. Salmon and motile epifauna prices also rose in 2010 and have shown significant volatility since. Apex predator prices dipped in 2009 rebounded in 2010–2011, declined in 2013, and have leveled out somewhat since. Benthic forager prices declined through 2009, increased from 2009–2012, and decreased after before leveling out in 2014. The cumulative effect of these price changes is that the first-wholesale unit value index increased to 2008, was relatively volatile at this high level through 2012, then decreased somewhat in 2013, and has vacillated at approximately that level since. The unit value through 2018–2019 increased as many species saw stable or increasing prices, in particular pollock.

Factors influencing observed trends: The reduction in revenue from 2008–2010 was the result of conservation based reductions in the pollock Total Allowable Catch (TAC). Since 2018 strong demand has put upward pressure on whitefish product prices which has filtered through to ex-vessel market. As a result, revenue increased in 2019 in the pelagic forager group despite relatively stable landings. Ex-vessel prices are influenced by a multitude of potential factors including demand for processed products, the volume of supply (both from the fishery and globally), the first-wholesale price, inflation, fishing costs, and bargaining power between processors and fishermen. However, annual variation in the ex-vessel prices tends to be smaller than variations in catch and short to medium term variation in the landings and ex-vessel revenue indices appear similar. The long-term general increasing trend is the influence of a trend of increasing value in the first-wholesale market.

First-wholesale value is the revenue from the sale of processed fish. Some fish, in particular pollock and Pacific cod, are processed in numerous product forms which can influence the generation of revenue by the processing sector. Level shifts in the relative location of the first-wholesale indices compared to the ex-vessel indices are influenced by differences in the amount and types of value-added processing that is done in each functional group.

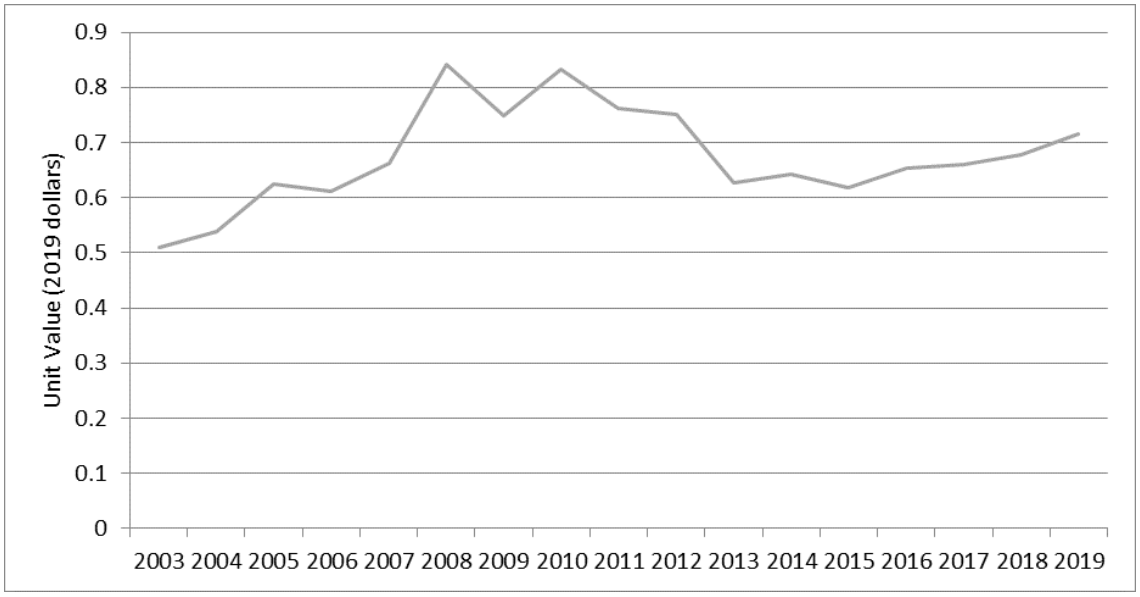

Figure 89: Real first-wholesale to total catch unit value in the eastern Bering Sea (2019 dollars).

Supply reductions in the pollock fishery which began in 2008 resulted in increased first-wholesale prices which account for the significant increase in the 2008 unit value and the relatively high level maintained through 2012. Pollock prices fell somewhat in 2013 with significant global pollock supply.

Implications: The economic metrics displayed here provide perspective on how the human component of the ecosystem utilizes and receives value from the eastern Bering Sea and the species within that ecosystem. Ex-vessel and first-wholesale value metrics area measure of the ultimate value from the raw resources extracted and how humans add value to the harvest for their own uses. In contrast to the landings metrics that are heavily dominated by the pelagic forager functional group, ex-vessel and first wholesale revenues are more evenly distributed across functional groups, which indicates the importance of the groups with lower landings and higher prices to the fishing sector.

Situations in which the value of a functional group are decreasing but catches are increasing indicate that the per-unit value of additional catch to humans is declining. This information can be useful in identifying areas where fishing effort could be reallocated across functional groups in times where the functional groups within the ecosystem might be constrained while maintaining value to the human component of the ecosystem. Monitoring the economic trends stratified by ecosystem functional group provides insight on the fishing related stresses on ecosystems and the economic factors that influence observed fishing patterns. The ultimate impact that these stresses have on the ecosystem cannot be discerned from these metrics alone and must be viewed within the context of what the ecosystem can provide.

Recreation

There are no updates to Recreation indicators in this year's report. See the contribution archive for previous indicators at: `https://access.afsc.noaa.gov/REFM/REEM/ecoweb/`.

Employment

Trends in Unemployment in the Bering Sea

Contributed by Melissa Rhodes-Reese
Pacific States Marine Fisheries Commission
Alaska Fisheries Science Center, National Marine Fisheries Service, NOAA
Contact: melissa.rhodes-reese@noaa.gov
Last updated: September 2020

Description of indicator: Unemployment is a significant factor in the southeastern Bering Sea (SEBS) and northern Bering Sea (NBS) regions, and for groundfish fishery management, as many communities in western Alaska rely upon fisheries to support their economies and to meet subsistence and cultural needs. As with other areas neighboring the Arctic, unemployment is an important indicator of community viability (Rasmussen et al., 2015). Advancements in socio-ecological systems (SES) research has demonstrated the importance of incorporating social variables in ecosystem management and monitoring, and unemployment reflects economic settings of a SES (Turner et al., 2003; Ostrom, 2007). For example, variation in resource access, availability, or employment opportunities may influence human migration patterns, which in turn may decrease human activity in one area of an ecosystem while increasing activity in another.

This section summarizes trends in unemployment over time in the SEBS and NBS. SEBS communities are located within the Lake and Peninsula (facing the Bering Sea), Bristol Bay, Dillingham, and Bethel Borough communities located below 60°N. Communities of the NBS are of the Bethel Borough located above 60°N and those of the Kusilvak and Nome Boroughs. Communities were included if they are geographically located within 50 miles of the coast, based upon their historical involvement in Bering Sea fisheries, and if they were included in one of the North Pacific Fishery Management Council's Bering Sea fishery programs, such as the Community Quota Entity program. Unemployment data were aggregated and weighted to account for varying community populations across Alaska Boroughs. Estimates are presented annually from 2010–2019 (ADLWD, 2019). Population was calculated by aggregating community level data between 1890 and 1990 (DCCED, 2016) and annually from 1990–2018 (ADLWD, 2019).

Status and trends:
Southeastern Bering Sea
The unemployment rate in the SEBS was 2.7% in 2019. This is a slight decrease from 2014 when the unemployment rate was the highest (3.6%) since 2010. Unemployment rates in the SEBS between 2010 and 2019 were lower than State and national rates (Figures 90 and 91).

Northern Bering Sea
The unemployment rate in the NBS was 11.5% in 2019. This is a slight decrease from 2014 when the unemployment rate was the highest (13.7%) since 2010. Unemployment rates in the NBS between 2010 and 2019 were higher than State and national rates (Figures 90 and 91).

Factors influencing observed trends: Alaska State has experienced several boom and bust economic cycles. Peaks in employment occurred during the construction of the Alaska pipeline in the 1970s and oil boom of the 1980s, whereas unemployment peaks occurred following completion of the pipeline, during the oil bust of the late 1980s, and during the great recession of 2007–

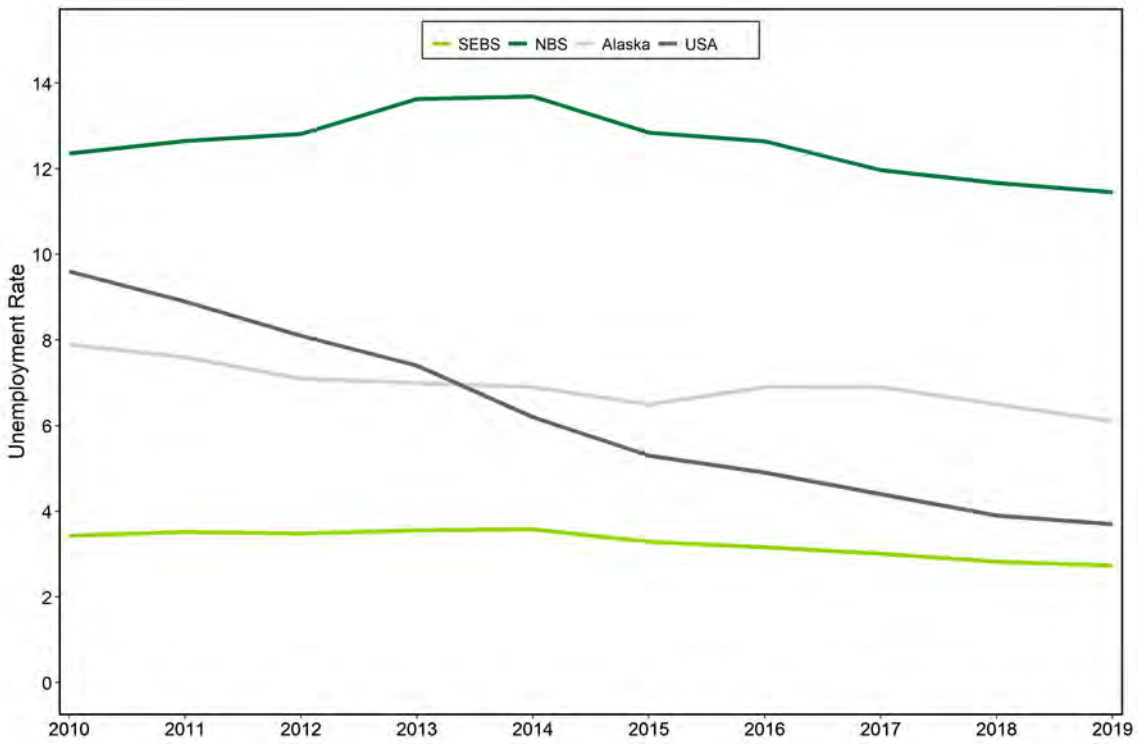

Figure 90: Unemployment rates for the southeastern Bering Sea (SEBS), northern Bering Sea (NBS), Alaska, and USA, 2010–2019.

2009 (ADLWD, 2016)[23]. However, during the great recession, Alaska's employment decreased only 0.4% whereas the national drop was 4.3% partly because of the jobs provided by the oil industry (ADLWD, 2016).

Many communities in the SEBS rely upon seasonal fisheries and construction opportunities for employment, and individuals seek these types of employment in Dillingham (Himes-Cornell et al., 2013). The NBS area had the highest unemployment rates between 2010–2019. Communities in the region rely mainly upon seasonal employment and subsistence activity and year-round employment opportunities are sparse (Himes-Cornell et al., 2013). The SEBS and NBS regions are forecast to experience job loss, similar to State trends since 2015, due to reduced oil revenues (ADLWD, 2018).

Implications: Fisheries contribute to community vitality of the SEBS and NBS, therefore reduced fishing opportunities and employment may lead to out-migration and population decline, particularly in small communities with few job alternatives (Donkersloot and Carothers, 2016). Changes in groundfish policy and management may have implications for small communities and those of the Bering Sea Community Quota Entities. Also, with a large proportion of western Alaska population being Alaska Natives, resource managers may benefit from working with communities holding traditional ecological knowledge (TEK) to incorporate TEK into ecosystem management (Huntington et al., 2004).

[23]For more detailed information see `http://live.laborstats.alaska.gov/pop/estimates/data/ex2.pdf`.

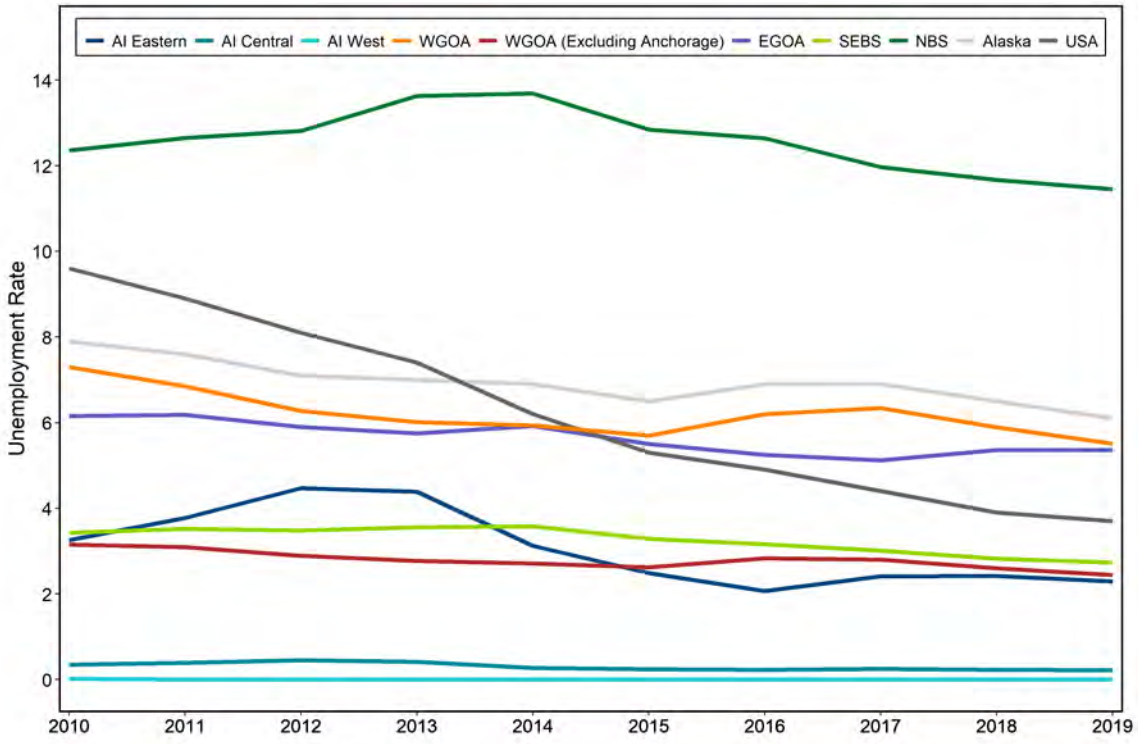

Figure 91: Unemployment rates for all regions, 2010–2019.

Socio-Cultural Dimensions

Defining Fishing Communities

Within the context of marine resource management, what constitutes a fishing community is complex and has been long debated. Fishing communities can be defined geographically, occupationally, or based on shared practice or interests. The Magnuson-Stevens Fisheries Conservation Act (MSA) defines fishing communities as those "substantially dependent on or substantially engaged in the harvest or processing of fishery resources to meet social and economic needs, and includes fishing vessel owners, operators, and crew and United States fish processors that are based in such community" (Magnuson-Stevens Fishery Conservation and Management Act. Public Law, 94, 265). Within the MSA, National Standard 8 requires conservation and management measures to "take into account the importance of fishery resources to fishing communities in order to: (1) provide for the sustained participation of such communities; and (2) to the extent practicable, minimize adverse economic impacts on such communities" (MSA, National Standard 8, last updated 4/26/2018). Identifying and considering appropriate communities is central to effective marine resource management. The National Marine Fisheries Service interprets the MSA definition to emphasize the relevance of geographic place, stating "A fishing community is a social or economic group whose members reside in a specific location..." (50 CFR 600.345–National Standard 8–Communities). Pacific States Marine Fisheries Commission adheres to this definition as well, although it is recognized that taking social networks and shared interests into account "would result in a greater understanding of socioeconomic indicators" (Langdon-Pollock, 2004). While relatively easy to determine, defining fishing community solely on geographical location risks excluding social networks valuable to the flow of people, information, goods, and services. Some managers have turned to "multiple constructions of communities" (Olson, 2005) to better understand fishing communities.

By restricting the definition of fishing community to a geographic place–particularly in the marine environment, Martin and Hall-Arber (2008) argue that geographically restricted notions of community ignore the complexity of social landscapes. The authors expand "community" to include those areas, resources, and social networks on which people depend (Martin and Hall-Arber, 2008). In an effort to acknowledge women's role in fisheries, Calhoun, Conway, and Russel (2016) discuss fishing community in terms of participation in the broader industry (Calhoun et al., 2016). Acknowledging power dynamics and the issue of scale when describing "fishing community', Clay and Olson (2008) complicate the MSA definition, bringing forward the importance of "political, social, and economic relationships".

In the context of the Ecosystem Status Reports, fishing communities were identified by three criteria: 1) geographical location, 2) current fishing engagement (commercial and recreational); and 3) historical linkages to subsistence fishing. Engagement was defined as the value of each indicator as a percentage of the total present in the state. The quantitative indicators used to represent commercial fisheries participation included commercial fisheries landings (e.g., landings, number of processors, number of vessels delivering to a community), those communities registered as homeports of participating vessels, and those that are home to documented participants in the fisheries (e.g., crew license holders, state and federal permit holders, and vessel owners). Recreational fisheries participation included sportfish licenses sold in the community, sportfish licenses held by residents, and the number of charter businesses and guides registered in the community. Given the heavy dependence on subsistence fishing for survival in Alaska, as well as the reliance on river networks for marine resource extraction, a buffer area was created along coastal Alaska to identify

those communities living near coastal resources. Up river communities with historic ties to subsistence fishing were included. Anchorage and Fairbanks were excluded in some analyses in order to avoid skewing results.

The data used were gathered from the Alaska Department of Fish and Game Division of Subsistence database. A broad definition of subsistence "fishing community" was used for this analysis due to the importance of subsistence foods for daily life, particularly in rural Alaska. An estimated 36.9 million pounds of wild foods are harvested annually by rural subsistence users. Residents of more populated urban areas harvest about 13.4 million pounds of wild food under subsistence, personal use, and sport regulations. Given the reliance on subsistence foods, all communities within 50 miles of coastal waters were included in the analysis in order to capture subsistence use of marine resources. In addition, upriver communities identified as highly engaged in subsistence fisheries were included in the analysis. This included communities that historically fit the criteria (given the time period for which data are available (1991 onward). Level of engagement was evaluated by several criteria: 1) the number of Subsistence Halibut Registration Certificates (SHARC) issued to residents; 2) total pounds harvested of all fish and marine invertebrates; 3) the number of salmon harvested; and 4) pounds of marine mammals harvested. In order to document changes in subsistence use, communities once identified as engaged in subsistence fisheries were kept in the analysis regardless of changing engagement.

Contributed by Sarah P. Wise

Trends in Human Population in the Bering Sea

Contributed by Melissa Rhodes-Reese
Pacific States Marine Fisheries Commission
Alaska Fisheries Science Center, National Marine Fisheries Service, NOAA
Contact: melissa.rhodes-reese@noaa.gov
Last updated: September 2020

Description of indicator: Human population is a significant factor in the southeastern Bering Sea (SEBS) and northern Bering Sea (NBS) regions and indicator for groundfish fishery management, as many communities in the region rely upon fisheries to support their local economies and to meet subsistence and cultural needs. Advancements in socio-ecological systems (SES) research has demonstrated the importance of incorporating social variables in ecosystem management and monitoring, and this indicator reflects socio-cultural and economic aspects within SES (Turner et al., 2003; Ostrom, 2007). For example, variation in resource access or availability or employment opportunities may influence human migration patterns, which in turn may decrease human activity in one area of an ecosystem while increasing activity in another.

This section summarizes trends in human population over time in the SEBS and NBS. SEBS communities are located within the Lake and Peninsula (facing the Bering Sea), Bristol Bay, Dillingham, and Bethel Borough communities located below 60°N. Communities of the NBS are of the Bethel Borough located above 60°N and those of the Kusilvak and Nome Boroughs. Communities were included if they are geographically located within 50 miles of the coast, based upon their historical involvement in Bering Sea fisheries, and if they were included in one of the North Pacific Fishery Management Council's Bering Sea fishery programs, such as the Community Quota Entity program. Communities were further divided into two categories as part of this analysis: small (population <1,500) and large (population ≥1,500). Population was calculated by aggregating community level data between 1890 and 1990 (DCCED, 2016) and annually from 1990–2019 (ADLWD, 2018).

Status and trends:
Southeastern Bering Sea
The SEBS is composed of 34 coastal communities with a total population of 10,083 as of 2019. The total population of small communities was 7,756. The community of Dillingham is the only community of this region with a population over 1,500 (2019 population=2,327). The overall population has increased steadily since 1880, with the greatest population increase of 44.2% occurring between 1950 and 1960 (Table 7). This is consistent with Alaska State trends as population change peaked during these periods (over 75% by 1960 and 36.9% by 1990). Population increase leveled off after 1990 with lower rates in the following decades in the SEBS and Alaska overall (ADLWD, 2018).

Between 2010 and 2019, the population of SEBS increased 0.58% which was lower than State trends between 2010–2019 (2.9%). The population of small communities increased 0.78% and Dillingham decreased 0.1% during this time period. The population of the SEBS has remained relatively stable (based on aggregated data), yet 47% of communities in the SEBS experienced population decline between 2010 and 2019 (Figure 92).

Table 7: Southeastern Bering Sea (SEBS) population 1880–2019. Percent change rates are decadal until 2010.

Year	Alaska	% change	SEBS	% change
1880	33,426		1,504	
1890	32,052	-4.1	1,022	-32.05
1900	63,592	98.4	1,203	17.71
1910	64,356	1.2	688	-42.81
1920	55,036	-14.5	1,279	85.9
1930	59,278	7.7	1,369	7.04
1940	72,524	22.3	2,292	67.42
1950	128,643	77.4	3,212	40.14
1960	226,167	75.8	4,633	44.24
1970	302,583	33.8	5,445	17.53
1980	401,851	32.8	7,428	36.42
1990	550,043	36.9	9,339	25.73
2000	626,932	14.0	10,383	11.18
2010	710,231	13.3	10,025	-3.45
2019	731,007	2.9	10,083	0.58

Many SEBS communities are small and/or remote and Alaska Natives comprise up to 82% of the population of small communities in remote areas; the indigenous population in Alaska is greater than any U.S. state (Goldsmith et al., 2004). As of 2016, 15% of Alaska's population was Alaska Native or American Indian (ADLWD, 2017), and as of 2015, 75.7% of the population in the SEBS identified as Native American alone or in combination with another race (DCCED, 2016). In addition, there has been increased migration of Alaska Natives from rural to urban areas (Goldsmith et al., 2004; Williams, 2004), yet the majority of population growth that has occurred in Alaska is of the Caucasian demographic (ADLWD, 2016).

Northern Bering Sea

The NBS is comprised of 61 coastal communities with a total population of 34,057 as of 2019. The population of small communities was 24,108 and large communities was 9,949. The small communities exclude Bethel (population in 2019=6,259) and Nome (population in 2019=3,690) which are the only two communities with populations exceeding 1,500 people. The total NBS population has increased steadily since 1880, with the greatest population increase occurring between 1890 and 1900 (901.1%), and later between 1950 and 1960 (47.6%) (Table 8 and Figure 93). The latter increase is consistent with Alaska State trends as population increased by over 75% between 1950 and 1960. Population increases leveled off after 1990, with lower rates in the following decades in the NBS and Alaska State.

Between 2010 and 2019, the population of the NBS increased 6.06%, which was higher than state trends during this time period (2.9%). Small community populations increased 7.5%, while the population of Bethel increased by 2.94% and Nome by 2.56%. The populations of communities in the NBS have slowly increased with 74.8% of NBS communities experiencing a population increase between 2010 and 2019. Many NBS communities are small and/or remote. As of 2015, 90.2% of the population in NBS identified as Alaska Native alone or in combination with another race (DCCED, 2016).

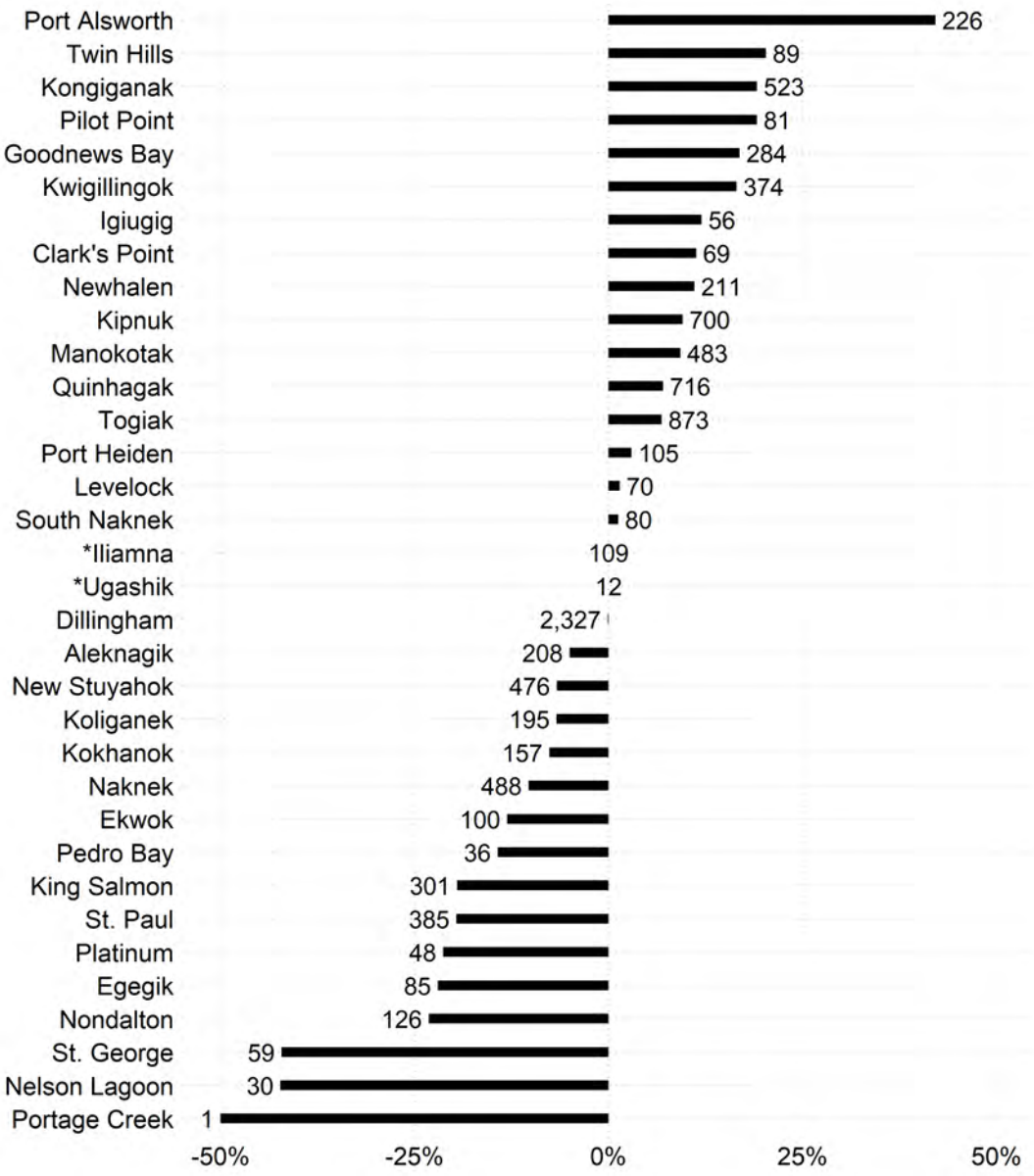

Figure 92: Population and population change of southeastern Bering Sea communities 2010–2019. Bars represent the percentage change and the number represents the 2019 population. Communities with an asterisk experienced no population change.

Factors influencing observed trends: Population trends in Alaska[24] are largely attributed to changes in resource extraction and military activity (Williams, 2004). Historically, the Gold Rush of the late 19th century doubled the State's population by 1900, and later WWII activity and oil development fueled population growth (ADLWD, 2016). However, certain areas have experienced

[24]See the Alaska Department of Labor and Workforce Development "Alaska Economic Trends" magazine that is published monthly for detailed information on factors influencing observed trends in the state at `https://labor.alaska.gov/trends/`

Table 8: Northern Bering Sea (NBS) population 1880–2019. Percent change rates are decadal until 2010.

Year	Alaska	% change	NBS	% change
1880	33,426		3,376	
1890	32,052	-4.1	2,528	-25.12
1900	63,592	98.4	20,453	709.06
1910	64,356	1.2	5,201	-74.57
1920	55,036	-14.5	4,538	-12.75
1930	59,278	7.7	5,527	21.79
1940	72,524	22.3	7,596	37.43
1950	128,643	77.4	9,435	24.21
1960	226,167	75.8	13,940	47.75
1970	302,583	33.8	16,424	17.82
1980	401,851	32.8	20,828	26.81
1990	550,043	36.9	26,157	25.59
2000	626,932	14.0	30,202	15.46
2010	710,231	13.3	32,111	6.32
2019	731,007	2.9	34,057	6.06

population shifts over time, particularly those with military bases—the population of Kodiak declined in the 1990's because of U.S. Coast Guard cut-backs (Williams, 2006). The fishing industry also influences community population. Kodiak and the Aleutian Islands have the most transient populations due to the seafood processing industry (Williams, 2004). Some EBS communities experienced fishery permit loss and population decline (e.g., South Naknek). Factors that influence population shifts include employment, retirement, educational choices, cost of living, climate, and quality of life (Donkersloot and Carothers, 2016).

Overall population growth occurred in the SEBS (1.0%) and NBS (6.1%) between 2010 and 2019. Past increases in the NBS have been attributed to mining and extraction prospects and these activities contributed to high rates of population turnover from migration within the state (ADLWD, 2016). The main factors affecting population growth are natural increase (births minus deaths) and migration, with the latter being the most unpredictable aspect (Williams, 2004; ADLWD, 2016). Between 2012–2016, 59% of Alaska's population was born out of State[25]. In terms of natural growth, from 2013 to 2017 the average annual birth rate in Alaska was 1.5 per 100 people which was higher than the national rate of 1.2 (HAVR, 2018; Martin et al., 2018).

From 2010–2017, the Aleutian chain and Southeast Alaska had the lowest natural increase (0.0–1.0%), whereas the NBS area had the highest (1.5–3.0%). The Kusilvak census area had the highest birth rate (3 births per 100 people; ADLWD (2017)). The estimated natural growth rates of the SEBS had a range of 0.5–3.0% (ADLWD, 2017). The NBS has steadily increased in population with higher than national level birth rates and net migration of less than zero (ADLWD, 2017). The net annual migration of the SEBS was very low (>0) since the region has among the lowest migration rates in the State (Williams, 2004; ADLWD, 2016). The highest net migration occurs in the Gulf of Alaska region; the Matanuska-Susitna Borough has the highest growth rate in the State (ADLWD, 2017).

[25]US Census Bureau. 2018. American Community Survey. `https://www.census.gov/programs-surveys/acs/data.html`

Implications: Population shifts can affect pressures on fisheries resources, however inferences about human impacts on resources should account for economic shifts and global market demand for seafood and other extractive resources of the region. Population change in Alaska is largely fueled by increased net migration rather than natural increase, and there has been increased migration from rural to urban areas. This is evident with population decline of many small communities. Fisheries contribute to community vitality of the SEBS and NBS and reduced fishing opportunities and employment may lead to out-migration and population decline, particularly in small communities with few job alternatives (Donkersloot and Carothers, 2016). Changes in groundfish policy and management, such as increased regulations, may have implications for small communities and those of the Bering Sea Community Quota Entities. Also, with a large proportion of the SEBS and NBS population being Native Alaskans, resource managers may benefit from working with communities holding traditional ecological knowledge (TEK) to incorporate TEK into ecosystem management (Huntington et al., 2004).

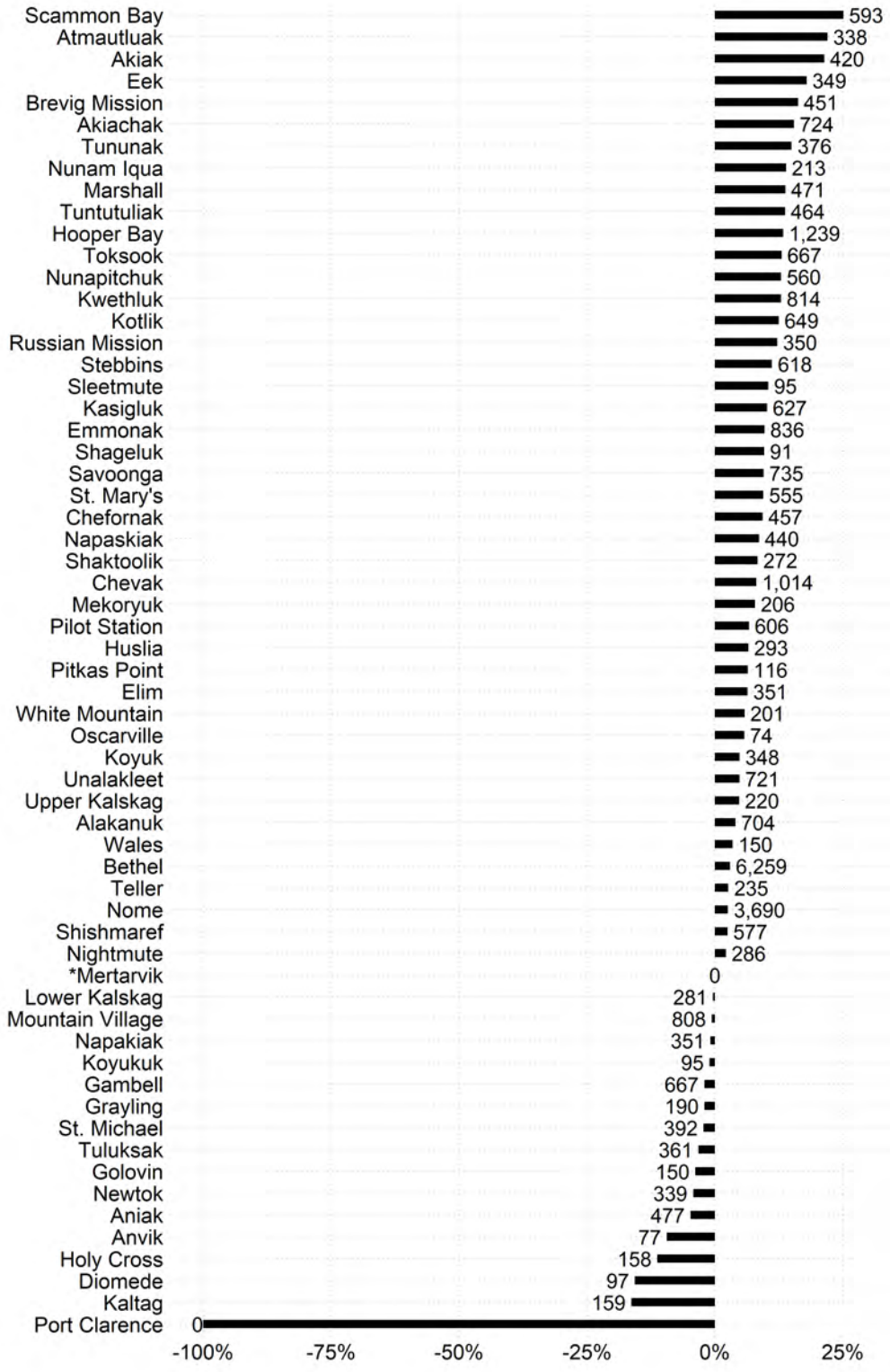

Figure 93: Population and population change of northern Bering Sea communities 2010–2019. Bars represent the percentage change and the number represents the 2019 population. Communities with an asterisk experienced no population change.

K–12 School Enrollment, Graduation Rates, and Dropout Rates in Coastal Communities in the Southeastern and Northern Bering Sea

Contributed by Kim Sparks[1,2] and Sarah Wise[1]
[1]Resource Ecology and Fishery Management Division, Alaska Fisheries Science Center, National Marine Fisheries Service, NOAA
[2]Pacific States Marine Fisheries Commission
Contact: kim.sparks@noaa.gov
Last updated: September 2020

Description of indicator: Ensuring the productivity and sustainability of fishing communities is a core mandate of Federal fisheries management. Community vitality is evaluated here based on K–12 public school enrollment. Enrollment trends are particularly relevant due to the value of schools to community cohesion and identity as well as reflecting conditions for resident families. Declining enrollment trends, particularly school closures, can signal social stressors and is one indicator of community well-being. Communities experiencing enrollment declines or school closures typically experience population out-migration and reduced public services, which threaten the viability of these communities. Public school enrollment rates were analyzed at the community level, and then aggregated to the school district level. In an effort to examine trends over time, data from all years available were included in this analysis. Enrollment statistics for K–12 grades by school and region were compiled for 1995–2019. Previous data naming errors were corrected this year; school data were classified according to the year the data were collected (aka the beginning of the school year). Thus, the most recent data reflects the 2019/2020 school year, but is named as 2019 data. All data originate from the Alaska Department of Education and Early Development[26]. Current school locations and names were verified using the EPA EJ mapping tool[27] and Alaska Department of Education website[28].

The southeastern Bering Sea (SEBS) and northern Bering Sea (NBS) regions each have seven school districts. It should be noted that many school districts overlap with other regions; for the purpose of this analysis, only those schools that fell within the SEBS or NBS regions were included. School graduation rates are based on the four year adjusted cohort graduation rate, which was implemented in Alaska starting with the 2011–2012 school year. Graduation rates are reported for the 2015–2019 cohorts for each school district. Dropout rates are reported by school district from 1990–2019.

Status and trends:
Southeastern Bering Sea
In the SEBS region, there has been a downward trend in school enrollment in most districts with the exception of the Lower Kuskokwim school district, which has increased from 530 students in 1995 to 676 students in 2019 (up 27.5%)(Figure 94). In schools with enrollment under 20 students, the decrease in enrollment is steeper. Several community schools have closed since 2004, including Nelson Lagoon, South Naknek, Portage Creek, Egegik, and most recently St. George in 2017 (Figure 95). After closing in 2012, Clark's Point school re-opened in 2017 with 13 students; it is currently open with 13 students (2019/2020 school year). Despite the fact that enrollment remains tenuously low for these schools, enrollment rates appear to have stabilized since 2017. Graduation rates for

[26]http://www.eed.state.ak.us/stats/
[27]https://ejscreen.epa.gov/mapper/
[28]https://education.alaska.gov/

SEBS school districts vary substantially (Figure 96). Graduation rates for Lower Kuskokwim school district consistently fall in the lower third of school districts analyzed. Alaska's average graduation rates have been 75.6% (2015), 76.1% (2016), and 78.2% (2017). Dropout rates vary for SEBS school districts from 0 to 14%, with increased variability since 2000. The greatest outlier is Dillingham, with a 17.3% dropout rate in 2000.

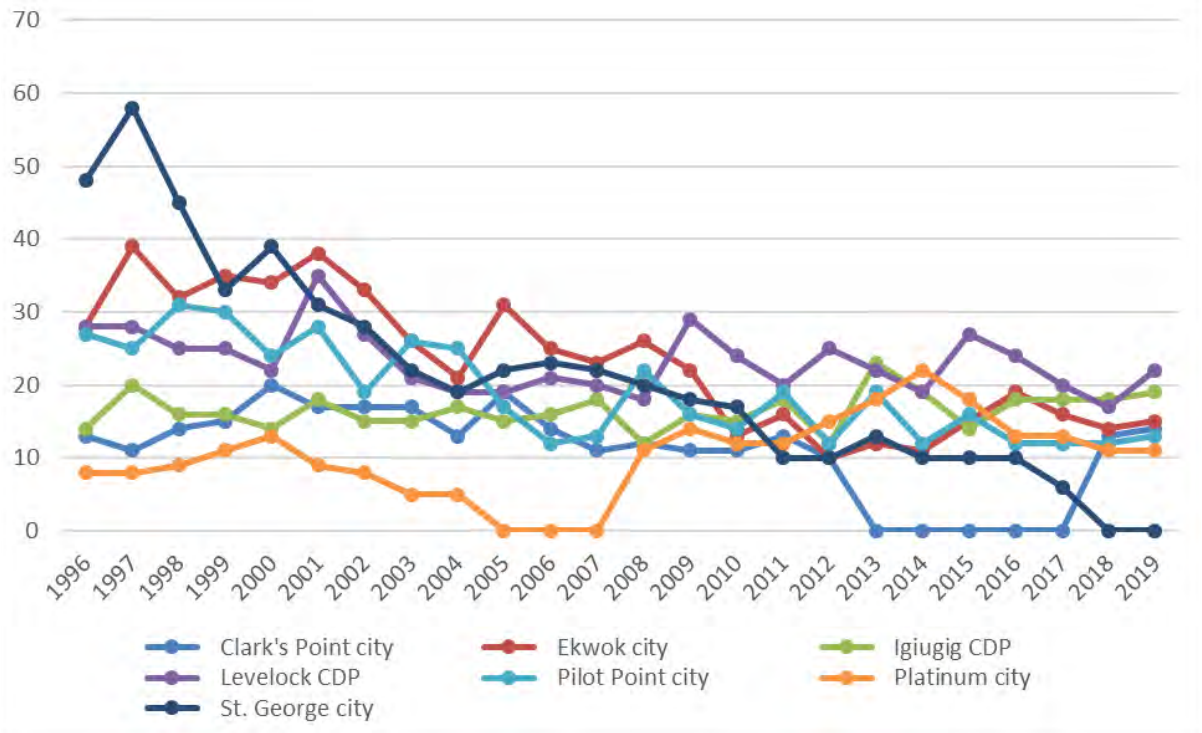

Figure 94: Enrollment for southeastern Bering Sea school districts.

Northern Bering Sea

Unlike many other Alaska regions, NBS school district enrollment levels are generally stable. The Lower Kuskokwim school district increased enrollment from 2,656 students (1995) to 3,442 students (2019), a 27% increase (Figure 97). The Yupiit school district also increased from 379 students (1995) to 463 (2019) (22% increase). There have been two school closures, Pitkas Point (in 2012) and Leonard Seppala High School in Nome (in 2001); however, compared to other regions, the NBS experienced fewer closures overall. NBS has seven schools (11%) with enrollment under 30 students.

The Iditarod and Yukon-Koyukuk school districts are the exception to NBS enrollment stability. Both districts are large, with only a few schools falling into the NBS region (four schools for the Iditarod district and three for Yukon-Koyukuk district). Those schools included in the NBS analysis have declined in enrollment substantially. There remain only two schools with enrollment under 30 students: Blackwell school in Anvik (12 students), and Ella B. Vernetti School in Koyukuk (14 students). The Iditarod school district enrollment has declined 48.8% since 1995, and the Yukon-Koyukuk school district enrollment has declined 40% since 1995.

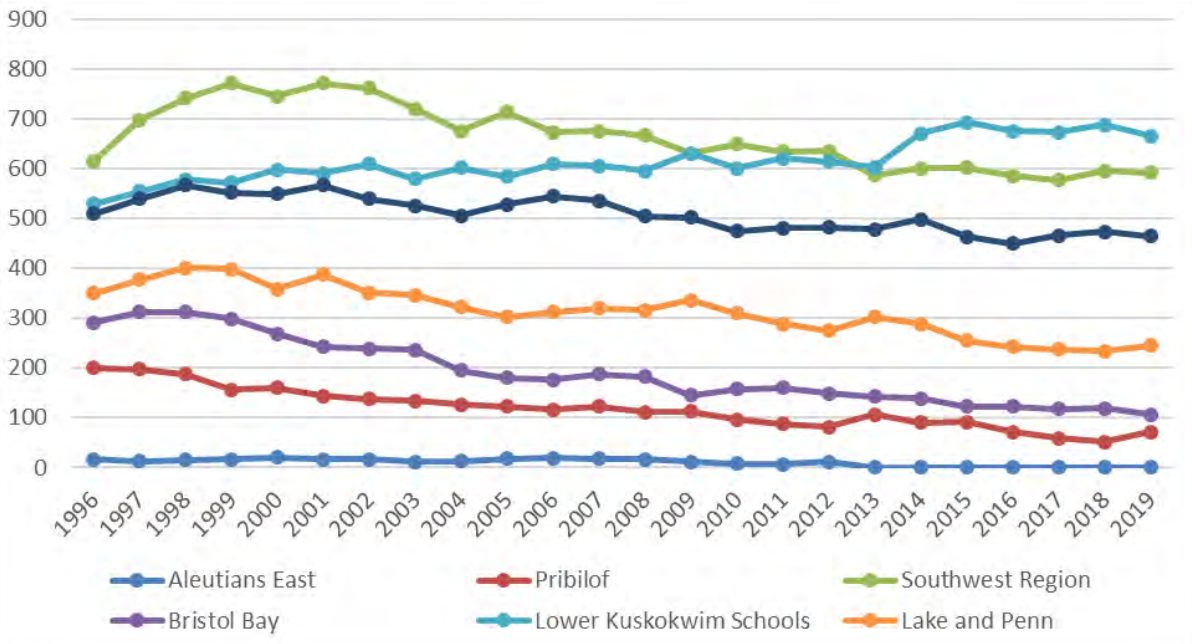

Figure 95: Southeastern Bering Sea school districts with enrollment below 20 students.

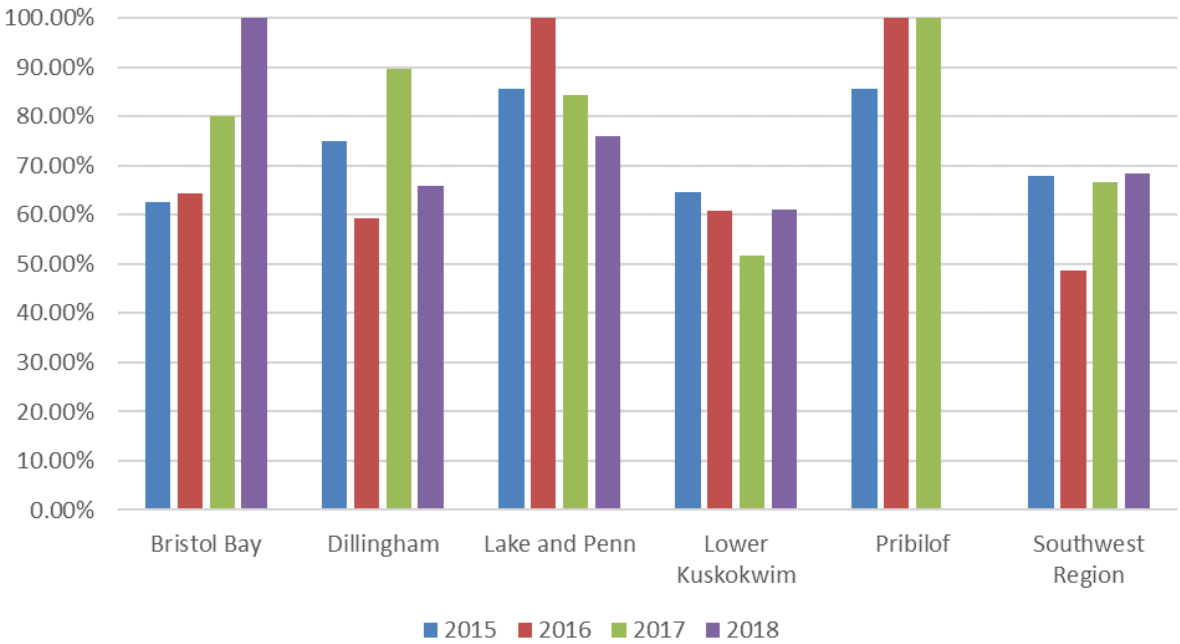

Figure 96: Graduation rates for southeastern Bering Sea school districts, 2015–2019. The State average graduation rate in 2017 was 78.2%.

There is large variation in the graduation rates of NBS school districts, most of which are well below state graduation averages. The graduation rates for Lower Kuskokwim, Nome, and Yupiit school districts consistently fall in the lower third of school districts analyzed for all cohort years (Figure 98). Dropout rates for NBS vary greatly from 0 to 18.6%, with much greater variability since 2000. The greatest outlier is the Yupiit school district, with consistently higher dropout rates. It is also worth noting that the NBS region has the highest dropout rates compared to other regions, with an overall average of 10% for multiple years.

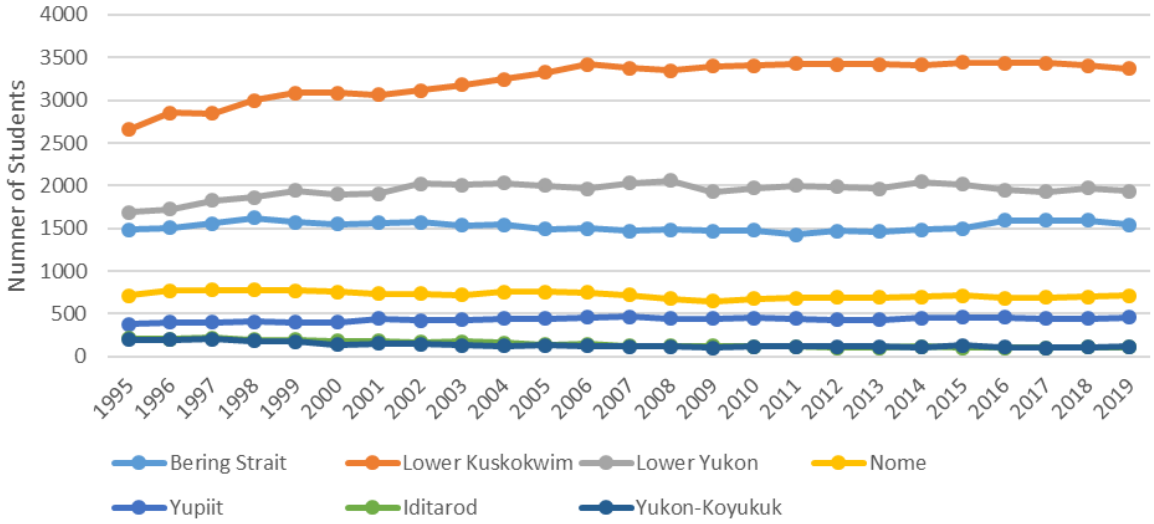

Figure 97: Enrollment for northern Bering Sea school districts.

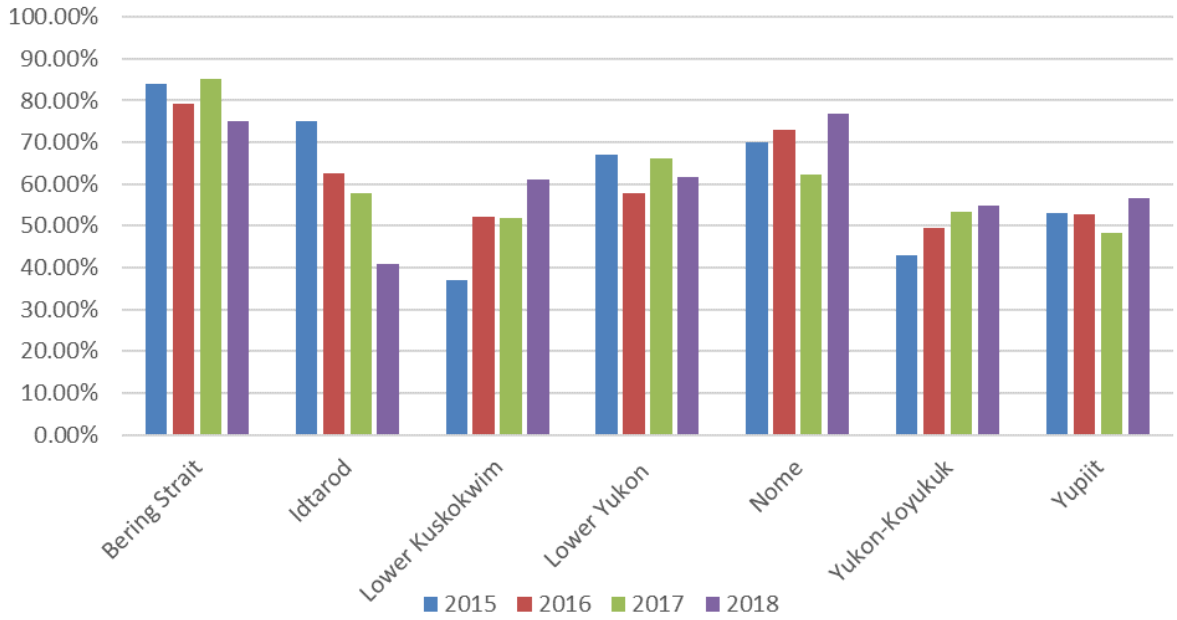

Figure 98: Graduation rates for northern Bering Sea school districts, 2015–2019. The State average graduation rate in 2017 was 78.2%.

Factors influencing observed trends:

Southeastern Bering Sea

The SEBS ecosystem varies substantially in population, community structure, and vitality. The SEBS is a large and diverse area with many small rural communities. High dependence on natural resources and a subsistence way of life shape community structure and social networks, and may drive population shifts according to seasonal availability. A strong reliance on a sharing economy contributes to community well-being and shapes social structures (Goldsmith, 2007). It is possible that school enrollment may shift to the larger communities to benefit from existing social networks. Other factors must be considered including functional ports, airports, or medical facilities to provide support for a viable community structure. Those schools with enrollment under 30 students experience the greatest uncertainty in terms of educational stability.

As of 2019, nine schools had enrollment under 30 students, and four schools reported 15 or fewer students. With greater fluctuation in school enrollment, rural area schools are particularly vulnerable to closure and possible social disruption. The reasons for decreasing enrollment likely involve complex social and economic drivers including migratory patterns, resource availability, and shifting employment opportunities.

Northern Bering Sea

In the NBS ecosystem, limited access to infrastructure may actually stabilize school populations to some degree due to the high reliance on schools for multiple community purposes. Schools in remote villages often serve as meeting places, libraries, places of lodging, and provide access to the internet for the entire community. The closure of a school in these places would have a profound effect. Additional research into the specific reasons for diminishing school enrollment in rural areas, as well as the impacts on these communities, would inform and benefit management decisions.

Implications: Community residents are part of the broader ecosystem, linked through daily informed experience, interaction, and engagement, and a strong sense of place (Masterson et al., 2017). Schools are cultural centers and serve as important indicators of social and economic viability and community well-being (Lyson, 2002, 2005). Within rural communities in particular, schools are valuable symbols for community identity, autonomy, and shared social values (Peshkin, 1978, 1982; Lyson, 2005). Research indicates that school closures negatively affect communities and student achievement (Buzzard, 2016; Tieken and Auldridge-Reveles, 2019). Closed school buildings can be a drain on community and school district resources (Barber, 2018). Patterns of diminishing enrollment and school consolidation suggest a decrease in property values and taxes, economic opportunity, loss in business, as well as fragmented community system and cultural cohesion, and declines in reported quality of life scores (Sell and Leistritz, 1997; Lyson, 2002). Some research finds the rate of participation in community organizations decreases in communities experiencing school closures (Oncescu and Giles, 2014). These findings suggest that reduced enrollment and school closures may flag disruptions in social cohesion, possibly leading to less vibrant and sustainable communities. Because many of these small communities are highly reliant on fisheries and other marine resources, school enrollment can be a strong indication of the linkage between sustainable fisheries and community well-being.

References

Aagaard, K., T. J. Weingartner, S. L. Danielson, R. A. Woodgate, G. C. Johnson, and T. E. Whitledge. 2006. Some controls on flow and salinity in Bering Strait. Geophysical Research Letters **33**.

ADLWD. 2016. Alaska Population Overview: 2015 Estimates. Report, Research and Analysis Section, Alaska Department of Labor and Workforce Development.

ADLWD. 2017. Cities and Census Designated Places (CDPs), 2010 to 2016. Report, Research and Analysis Section, Alaska Department of Labor and Workforce Development.

ADLWD. 2018. Cities and Census Designated Places (CDPs), 2010 to 2017. Report, Research and Analysis Section, Alaska Department of Labor and Workforce Development.

ADLWD. 2019. Cities and Census Designated Places (CDPs), 2010 to 2018. Report, Research and Analysis Section, Alaska Department of Labor and Workforce Development.

AFSC. 2011. Observer Sampling Manual for 2012. Report, Alaska Fisheries Science Center, Fisheries Monitoring and Analysis Division, North Pacific Groundfish Observer Program, 7600 Sand Point Way, NE, Seattle WA, 98115.

Alabia, I. D., J. G. Molinos, S.-I. Saitoh, T. Hirata, T. Hirawake, and F. J. Mueter. 2020. Multiple facets of marine biodiversity in the Pacific Arctic under future climate. Science of The Total Environment **744**:140913.

Alverson, D. L., M. H. Freeberg, S. A. Murawski, and J. Pope. 1994. A global assessment of fisheries bycatch and discards (Vol. 339). Food Agriculture Organization.

Aydin, K., and F. Mueter. 2007. The Bering Sea - a dynamic food web perspective. Deep Sea Research Part II: Topical Studies in Oceanography **54**:2501–2525.

Baduini, C., K. Hyrenbach, K. Coyle, A. Pinchuk, V. Mendenhall, and G. Hunt. 2001. Mass mortality of short-tailed shearwaters in the southeastern Bering Sea during summer 1997. Fisheries Oceanography **10**:117–130.

Baier, C. T., and J. M. Napp. 2003. Climate-induced variability in *Calanus marshallae* populations. Journal of Plankton Research **25**:771–782.

Balch, W., H. R. Gordon, B. Bowler, D. Drapeau, and E. Booth. 2005. Calcium carbonate measurements in the surface global ocean based on Moderate-Resolution Imaging Spectroradiometer data. Journal of Geophysical Research: Oceans **110 (C7)**.

Barber, B. P. 2018. Public School Closures: The Fate of Abandoned School Buildings. Notre Dame Journal of Law, Ethics Public Policy **32**:329 p.

Beamish, R. J., and C. Mahnken. 2001. A critical size and period hypothesis to explain natural regulation of salmon abundance and the linkage to climate and climate change. Progress in Oceanography **49**:423–437.

Berkeley, S. A., M. A. Hixon, R. J. Larson, and M. S. Love. 2004. Fisheries sustainability via protection of age structure and spatial distribution of fish populations. Fisheries **29**:23–32.

Blanchard, F., and J. Boucher. 2001. Temporal variability of total biomass in harvested communities of demersal fishes. Fisheries Research **49**:283–293.

Boldt, J. L., and L. J. Haldorson. 2004. Size and condition of wild and hatchery pink salmon juveniles in Prince William Sound, Alaska. Transactions of the American Fisheries Society **133**:173–184.

Bond, N. A., M. F. Cronin, H. Freeland, and N. Mantua. 2015. Causes and impacts of the 2014 warm anomaly in the NE Pacific. Geophysical Research Letters **42**:3414–3420.

Brenner, R. E., S. J. Larsen, A. R. Munro, and A. M. Carroll. 2020. Run forecasts and harvest projections for 2020 Alaska salmon fisheries and review of the 2019 season. Alaska Department of Fish and Game, Special Publication No. 20-06. Anchorage, AK.

Brodeur, R. D., M. B. Decker, L. Ciannelli, J. E. Purcell, N. A. Bond, P. J. Stabeno, E. Acuna, and G. L. Hunt. 2008. Rise and fall of jellyfish in the eastern Bering Sea in relation to climate regime shifts. Progress in Oceanography **77**:103–111.

Brodeur, R. D., R. L. Emmett, J. P. Fisher, E. Casillas, D. J. Teel, and T. W. Miller. 2004. Juvenile salmonid distribution, growth, condition, origin, and environmental and species associations in the Northern California Current. Fishery Bulletin **102**:25–46.

Broerse, A., T. Tyrrell, J. Young, A. Poulton, A. Merico, W. Balch, and P. Miller. 2003. The cause of bright waters in the Bering Sea in winter. Continental Shelf Research **23**:1579–1596.

Buzzard, R. A. 2016. What Every Policy Maker, School Leader, Parent, and Community Member Needs to Know About the Social, Economic, and Human Capital Costs of Closing a Rural School: A Comprehensive Multi-faceted Investigation. Niagara University.

Cahalan, J., J. Gasper, and J. Mondragon. 2014. Catch sampling and estimation in the Federal groundfish fisheries off Alaska, 2015 edition. Report, U.S. Dep. Commer., NOAA Tech. Memo. NMFS-AFSC-286, 46 p.

Cahalan, J., J. Mondragon, and J. Gasper. 2010. Catch sampling and estimation in the Federal groundfish fisheries off Alaska. Report, U.S. Dep. Commer., NOAA Tech. Memo. NMFS-AFSC-205, 42 p.

Calambokidis, J. 2013. PCFG, PCFA, or Seasonal Resident: An Important But Debated Subgroup by Any Name. Journal of the American Cetacean Society **42(1)**:21–24.

Calhoun, S., F. Conway, and S. Russell. 2016. Acknowledging the voice of women: implications for fisheries management and policy. Marine Policy **74**:292–299.

Catchpole, T., C. Frid, and T. Gray. 2006. Resolving the discard problem - A case study of the English Nephrops fishery. Marine Policy **30**:821–831.

Clucas, I. 1997. A study of the options for utilization of bycatch and discards from marine capture fisheries. FAO fisheries circular **928**:1–59.

Coiley-Kenner, P., T. Krieg, M. Chythlook, and G. Jennings. 2003. Wild resource harvests and uses by residents of Manokotak, Togiak, and Twin Hills, 1999/2000. Alaska Department of Fish and Game Division of Subsistence Technical Paper **No. 275**.

Conner, J., and R. Lauth. 2016. Results of the 2013 eastern Bering Sea continental shelf bottom trawl survey of groundfish and invertebrate resources. Report, U.S. Dep. Commer., NOAA Tech. Memo. NMFS-AFSC-331.

Conners, M. E., K. Y. Aydin, and C. L. Conrath. 2016. Assessment of the octopus stock complex in the Bering Sea and Aleutian Islands. Report, North Pacific Fishery Management Council.

Cooney, R., and K. Coyle. 1982. Trophic implications of cross-shelf copepod distributions in the southeastern Bering Sea. Marine Biology **70**:187–196.

Cooper, D., L. A. Rogers, and T. Wilderbuer. 2020. Environmentally driven forecasts of northern rock sole (Lepidopsetta polyxystra) recruitment in the eastern Bering Sea. Fisheries Oceanography **29**:111–121.

Coyle, K., and G. Gibson. 2017. Calanus on the Bering Sea shelf: probable cause for population declines during warm years. Journal of Plankton Research **39**:257–270.

Coyle, K. O., L. Eisner, F. J. Mueter, A. Pinchuk, M. Janout, K. Cieciel, E. Farley, and A. Andrews. 2011. Climate change in the southeastern Bering Sea: impacts on pollock stocks and implications for the Oscillating Control Hypothesis. Fisheries Oceanography **20**:139–156.

Cross, J. N., J. T. Mathis, N. R. Bates, and R. H. Byrne. 2013. Conservative and non-conservative variations of total alkalinity on the southeastern Bering Sea shelf. Marine Chemistry **154**:100–112.

Danielson, S., O. Ahkinga, C. Ashjian, E. Basyuk, L. Cooper, L. Eisner, E. Farley, K. Iken, J. Grebmeier, and L. Juranek. 2020. Manifestation and consequences of warming and altered heat fluxes over the Bering and Chukchi Sea continental shelves. Deep Sea Research Part II: Topical Studies in Oceanography **177**:104781.

DCCED. 2016. State of Alaska Department of Commerce, Community and Economic Development. Report, Community and Regional Analysis, Community Database Online.

Dietrich, K. S., and S. M. Fitzgerald. 2010. Analysis of 2004-2007 vessel-specific seabird bycatch data in Alaska demersal longline fisheries. Alaska Fisheries Science Center, Resource Ecology and Fisheries Management Division.

Donkersloot, R., and C. Carothers. 2016. The graying of the Alaskan fishing fleet. Environment: Science and Policy for Sustainable Development **58**:30–42.

Duffy-Anderson, J. T., P. Stabeno, A. G. Andrews III, K. Cieciel, A. Deary, E. Farley, C. Fugate, C. Harpold, R. Heintz, and D. Kimmel. 2019. Responses of the northern Bering Sea and southeastern Bering Sea pelagic ecosystems following record-breaking low winter sea-ice. Geophysical Research Letters **46**:9833–9842.

Duffy-Anderson, J. T., P. J. Stabeno, E. C. Siddon, A. G. Andrews, D. W. Cooper, L. B. Eisner, E. V. Farley, C. E. Harpold, R. A. Heintz, and D. G. Kimmel. 2017. Return of warm conditions in the southeastern Bering Sea: Phytoplankton-Fish. PloS one **12**:e0178955.

Dulvy, N., S. Rogers, S. Jennings, V. Stelzenmuller, D. Dye, and H. Skjoldal. 2008. Climate change and deepening of the North Sea fish assemblage: a biotic indicator of warming seas. Journal of Applied Ecology **45**:1029–1039.

Edullantes, B. 2019. ggplottimeseries: Visualisation of Decomposed Time Series with ggplot2. R package version **0.1.0**.

Eisner, L. B., J. M. Napp, K. L. Mier, A. I. Pinchuk, and A. G. Andrews III. 2014. Climate-mediated changes in zooplankton community structure for the eastern Bering Sea. Deep Sea Research Part II: Topical Studies in Oceanography **109**:157–171.

Eisner, L. B., A. I. Pinchuk, D. G. Kimmel, K. L. Mier, C. E. Harpold, and E. C. Siddon. 2018. Seasonal, interannual, and spatial patterns of community composition over the eastern Bering Sea shelf in cold years. Part I: zooplankton. ICES Journal of Marine Science **75**:72–86.

Eisner, L. B., E. C. Siddon, and W. W. Strasburger. 2015. Spatial and temporal changes in assemblage structure of zooplankton and pelagic fish in the eastern Bering Sea across varying climate conditions. Izv TINRO **181**:141–160.

Eisner, L. B., E. M. Yasumiishi, A. G. Andrews III, and C. A. O'Leary. 2020. Large copepods as leading indicators of walleye pollock recruitment in the southeastern Bering Sea: Sample-Based and spatio-temporal model (VAST) results. Fisheries Research **232**:105720.

Elison, T., P. Salomone, T. Sands, G. Buck, K. Sechrist, and D. Koster. 2018. 2017 Bristol Bay area annual management report. Report, Alaska Department of Fish and Game, Fishery Management Report No. 18-11.

Estensen, J., H. Carroll, S. Larson, C. Gleason, B. Borba, D. Jallen, A. Padilla, and K. Hilton. 2018. Annual management report Yukon Area, 2017. Report, Alaska Department of Fish and Game, Fishery Management Report No. 18-28.

Fall, J., C. Brown, N. Braem, L. Hutchinson-Scarbrough, D. Koster, T. Krieg, and A. Brenner. 2012. Subsistence harvests and uses in three Bering Sea communities, 2008: Akutan, Emmonak, and Togiak. ADFG Division of Subsistence, Technical Paper **No. 371**.

FAO. 1995. Code of Conduct for Responsible Fisheries. Food and Agriculture Organization, Rome.

Farley, E., J. Moss, and R. Beamish. 2007. A Review of the critical size, critical period hypothesis for juvenile Pacific salmon. North Pacific Anadromous Fish Commission Bulletin **4**:311–317.

Farley, E. V., A. Starovoytov, S. Naydenko, R. Heintz, M. Trudel, C. Guthrie, L. Eisner, and J. R. Guyon. 2011. Implications of a warming eastern Bering Sea for Bristol Bay sockeye salmon. ICES Journal of Marine Science **68**:1138–1146.

Fetterer, F., K. Knowles, W. N. Meier, M. Savoie, and A. K. Windnagel. 2017. Sea Ice Index, Version 3. Regional Daily Data. Report, Boulder, Colorado USA. NSIDC: National Snow and Ice Data Center.

Funk, F., L. K. Brannian, and K. A. Rowell. 1992. Age Structured Assessment of the Togiak Herring Stock, 1978-1992, and Preliminary Forecast of Abundance for 1993. Report, Alaska Department of Fish and Game, Division of Commercial Fisheries.

Funk, F., and K. A. Rowell. 1995. Population model suggests new threshold for managing Alaska's Togiak Fishery for Pacific herring in Bristol Bay. Alaska Fishery Research Bulletin **2**:125–136.

Goldsmith, O. S. 2007. The remote rural economy of Alaska. Institute of Social and Economic Research, University of Alaska Anchorage.

Goldsmith, S., J. Angvik, L. Howe, A. Hill, and L. Leask. 2004. The Status of Alaska Natives Report. I. Anchorage: Institute of Social and Economic Research, University of Alaska.

Gordon, H. R., G. C. Boynton, W. M. Balch, S. B. Groom, D. S. Harbour, and T. J. Smyth. 2001. Retrieval of coccolithophore calcite concentration from SeaWiFS imagery. Geophysical Research Letters **28**:1587–1590.

Graham, C. J., T. M. Sutton, M. D. Adkison, M. V. McPhee, and P. J. Richards. 2019. Evaluation of growth, survival, and recruitment of Chinook salmon in southeast Alaska rivers. Transactions of the American Fisheries Society **148**:243–259.

Graham, N., R. S. Ferro, W. A. Karp, and P. MacMullen. 2007. Fishing practice, gear design, and the ecosystem approach—three case studies demonstrating the effect of management strategy on gear selectivity and discards. ICES Journal of Marine Science **64**:744–750.

Hare, S. R., N. J. Mantua, and R. C. Francis. 1999. Inverse production regimes: Alaska and west coast Pacific salmon. Fisheries **24**:6–14.

Harley, J. R., K. Lanphier, E. G. Kennedy, T. A. Leighfield, A. Bidlack, M. O. Gribble, and C. Whitehead. 2020. The Southeast Alaska Tribal Ocean Research (SEATOR) Partnership: Addressing Data Gaps in Harmful Algal Bloom Monitoring and Shellfish Safety in Southeast Alaska. Toxins **12**:407.

Harris, R. P., P. H. Wiebe, J. Lenz, H. R. Skjoldal, and M. Huntley. 2000. ICES Zooplankton Methodology Manual. Amsterdam, The Netherlands.

HAVR. 2018. State of Alaska, Department of Health and Social Services. Report, Health Analytics and Vital Records, Vital Statistics 2017 Annual Report.

Haynie, A. C., and L. Pfeiffer. 2013. Climatic and economic drivers of the Bering Sea walleye pollock (*Theragra chalcogramma*) fishery: implications for the future. Canadian Journal of Fisheries and Aquatic Sciences **70**:841–853.

Heintz, R. A., E. C. Siddon, E. V. Farley Jr, and J. M. Napp. 2013. Correlation between recruitment and fall condition of age-0 pollock (*Theragra chalcogramma*) from the eastern Bering Sea under varying climate conditions. Deep Sea Research Part II: Topical Studies in Oceanography **94**:150–156.

Hermann, A., C. Ladd, W. Cheng, E. Curchitser, and K. Hedstrom. 2016. A model-based examination of multivariate physical modes in the Gulf of Alaska. Deep Sea Research Part II: Topical Studies in Oceanography **132**:68–89.

Hilborn, R., T. P. Quinn, D. E. Schindler, and D. E. Rogers. 2003. Biocomplexity and fisheries sustainability. Proceedings of the National Academy of Sciences of the United States of America **100**:6564–6568.

Himes-Cornell, A., K. Hoelting, C. Maguire, L. Munger-Little, J. Lee, J. Fisk, R. Felthoven, C. Geller, and P. Little. 2013. Community profiles for North Pacific fisheries - Alaska. Report, U.S. Dep. Commer., NOAA Tech. Memo, NMFS-AFSC-259, 803 p.

Hirst, A., and R. Lampitt. 1998. Towards a global model of in situ weight-specific growth in marine planktonic copepods. Marine Biology **132**:247–257.

Hobday, A. J., L. V. Alexander, S. E. Perkins, D. A. Smale, S. C. Straub, E. C. Oliver, J. A. Benthuysen, M. T. Burrows, M. G. Donat, and M. Feng. 2016. A hierarchical approach to defining marine heatwaves. Progress in Oceanography **141**:227–238.

Hobday, A. J., E. C. Oliver, A. S. Gupta, J. A. Benthuysen, M. T. Burrows, M. G. Donat, N. J. Holbrook, P. J. Moore, M. S. Thomsen, and T. Wernberg. 2018. Categorizing and naming marine heatwaves. Oceanography **31**:162–173.

Holbrook, N. J., H. A. Scannell, A. S. Gupta, J. A. Benthuysen, M. Feng, E. C. Oliver, L. V. Alexander, M. T. Burrows, M. G. Donat, and A. J. Hobday. 2019. A global assessment of marine heatwaves and their drivers. Nature communications **10**:1–13.

Holsman, K. K., and K. Aydin. 2015. Comparative methods for evaluating climate change impacts on the foraging ecology of Alaskan groundfish. Marine Ecology Progress Series **521**:217–235.

Holsman, K. K., J. Ianelli, K. Aydin, A. E. Punt, and E. A. Moffitt. 2016. A comparison of fisheries biological reference points estimated from temperature-specific multi-species and single-species climate-enhanced stock assessment models. Deep Sea Research Part II: Topical Studies in Oceanography **134**:360–378.

Hsieh, C.-H., C. S. Reiss, J. R. Hunter, J. R. Beddington, R. M. May, and G. Sugihara. 2006. Fishing elevates variability in the abundance of exploited species. Nature **443**:859–862.

Hunsicker, M. E., L. Ciannelli, K. M. Bailey, S. Zador, and L. C. Stige. 2013. Climate and Demography Dictate the Strength of Predator-Prey Overlap in a Subarctic Marine Ecosystem. PLoS ONE **8**:e66025.

Hunt, G. L., P. H. Ressler, G. A. Gibson, A. De Robertis, K. Aydin, M. F. Sigler, I. Ortiz, E. J. Lessard, B. C. Williams, and A. Pinchuk. 2016. Euphausiids in the eastern Bering Sea: A synthesis of recent studies of euphausiid production, consumption and population control. Deep Sea Research Part II: Topical Studies in Oceanography **134**:204–222.

Hunt, G. L., P. Stabeno, G. Walters, E. Sinclair, R. D. Brodeur, J. M. Napp, and N. A. Bond. 2002. Climate change and control of the southeastern Bering Sea pelagic ecosystem. Deep-Sea Research Part II-Topical Studies in Oceanography **49**:5821–5853.

Hunt, G. L., P. J. Stabeno, S. Strom, and J. M. Napp. 2008. Patterns of spatial and temporal variation in the marine ecosystem of the southeastern Bering Sea, with special reference to the Pribilof Domain. Deep-Sea Research Part II-Topical Studies in Oceanography **55**:1919–1944.

Hunt, J., George L., K. O. Coyle, L. B. Eisner, E. V. Farley, R. A. Heintz, F. Mueter, J. M. Napp, J. E. Overland, P. H. Ressler, S. Salo, and P. J. Stabeno. 2011. Climate impacts on eastern Bering Sea foodwebs: a synthesis of new data and an assessment of the Oscillating Control Hypothesis. ICES Journal of Marine Science **68**:1230–1243.

Huntington, H., T. Callaghan, S. Fox, and I. Krupnik. 2004. Matching traditional and scientific observations to detect environmental change: a discussion on Arctic terrestrial ecosystems. Ambio **Special Report Number 13**:18–23.

Ianelli, J., B. Fissel, K. Holsman, T. Honkalehto, S. Kotwicki, C. Monnahan, E. Siddon, S. Stienessen, and J. Thorson. 2019. Assessment of the Walleye Pollock Stock in the Eastern Bering Sea. Report, North Pacific Fisheries Management Council, 605 W 4th Ave, Anchorage, AK 99510.

Ianelli, J., T. Honkalehto, S. Barbeaux, B. Fissel, and S. Kotwicki. 2016. Assessment of Alaska pollock stock in the Eastern Bering Sea. Report, North Pacific Fishery Management Council, 605 W 4th Ave, Anchorage, AK 99510.

Iida, T., K. Mizobata, and S.-I. Saitoh. 2012. Interannual variability of coccolithophore *Emiliania huxleyi* blooms in response to changes in water column stability in the eastern Bering Sea. Continental Shelf Research **34**:7–17.

Jacox, M. G. 2019. Marine heatwaves in a changing climate. Nature **571**:485–487.

Jones, T., L. M. Divine, H. Renner, S. Knowles, K. A. Lefebvre, H. K. Burgess, C. Wright, and J. K. Parrish. 2019. Unusual mortality of Tufted puffins (Fratercula cirrhata) in the eastern Bering Sea. PloS one **14**:e0216532.

JTC. 2020. Joint Technical Committee of the Yukon River U.S./Canada Panel: Yukon River salmon 2019 season summary and 2020 seasonal outlook. Alaska Department of Fish and Game, Division of Commercial Fisheries, Regional Information Report 3A20-01. Anchorage, AK. Report.

Jurado-Molina, J., P. A. Livingston, and J. N. Ianelli. 2005. Incorporating predation interactions in a statistical catch-at-age model for a predator-prey system in the eastern Bering Sea. Canadian Journal of Fisheries and Aquatic Sciences **62**:1865–1873.

Kalnay, E., M. Kananitcu, R. Kistler, W. Collins, and D. Deaven. 1996. The NCEP/NCAR 40-year reanalysis project. Bulletin of the American Meteorological Society **77**:437–471.

Karp, W. A., L. L. Desfosse, and S. G. Brooke. 2011. US National bycatch report. Report, U.S. Dep. Commer., NOAA Tech. Memo., NMFS-F/SPO-117E, 508 p.

Kearney, K., A. Hermann, W. Cheng, I. Ortiz, and K. Aydin. 2020. A coupled pelagic–benthic–sympagic biogeochemical model for the Bering Sea: documentation and validation of the BESTNPZ model (v2019. 08.23) within a high-resolution regional ocean model. Geoscientific Model Development **13 (2)**.

Kelleher, K. 2005. Discards in the world's marine fisheries: an update. Report 9251052891, Food Agriculture Org., Vol. 470.

Kimmel, D. G., L. B. Eisner, M. T. Wilson, and J. T. Duffy-Anderson. 2018. Copepod dynamics across warm and cold periods in the eastern Bering Sea: Implications for walleye pollock (*Gadus chalcogrammus*) and the Oscillating Control Hypothesis. Fisheries Oceanography **27**:143–158.

Krieger, J., and A. Eich. 2020. Seabird bycatch estimates for Alaska groundfish fisheries: 2019. Report, U.S. Dep. Commer., NOAA Tech. Memo. NMFS-F/AKR-24, 40 p.

Ladd, C., L. Eisner, S. Salo, C. Mordy, and M. Iglesias-Rodriguez. 2018. Spatial and Temporal Variability of Coccolithophore Blooms in the Eastern Bering Sea. Journal of Geophysical Research: Oceans **123**:9119–9136.

Ladd, C., and P. J. Stabeno. 2012. Stratification on the Eastern Bering Sea shelf revisited. Deep Sea Research Part II: Topical Studies in Oceanography **65**:72–83.

Langdon-Pollock, J. 2004. West coast marine fishing community descriptions. Report, Pacific State Marine Fisheries Commission, Economic Fisheries Information Network, Portland Oregon.

Lebida, R. C., and D. C. Whitmore. 1985. Bering Sea herring aerial survey manual. Report, Alaska Department of Fish and Game, Division of Commercial Fisheries, Bristol Bay Data Report No. 85-2, Anchorage, AK.

Lefebvre, K. A., L. Quakenbush, E. Frame, K. B. Huntington, G. Sheffield, R. Stimmelmayr, A. Bryan, P. Kendrick, H. Ziel, and T. Goldstein. 2016. Prevalence of algal toxins in Alaskan marine mammals foraging in a changing arctic and subarctic environment. Harmful Algae **55**:13–24.

Litzow, M. A., M. E. Hunsicker, N. A. Bond, B. J. Burke, C. J. Cunningham, J. L. Gosselin, E. L. Norton, E. J. Ward, and S. G. Zador. 2020*a*. The changing physical and ecological meanings of North Pacific Ocean climate indices. Proceedings of the National Academy of Sciences **117**:7665–7671.

Litzow, M. A., M. J. Malick, N. A. Bond, C. J. Cunningham, J. L. Gosselin, and E. J. Ward. 2020*b*. Quantifying a Novel Climate Through Changes in PDO-Climate and PDO-Salmon Relationships. Geophysical Research Letters **47**:e2020GL087972.

Livingston, P. A., K. Aydin, T. W. Buckley, G. M. Lang, M.-S. Yang, and B. S. Miller. 2017. Quantifying food web interactions in the North Pacific–a data-based approach. Environmental Biology of Fishes **100**:443–470.

Long, W. C., K. M. Swiney, C. Harris, H. N. Page, and R. J. Foy. 2013. Effects of ocean acidification on juvenile red king crab (Paralithodes camtschaticus) and Tanner crab (Chionoecetes bairdi) growth, condition, calcification, and survival. PloS one **8**:e60959.

Lovvorn, J. R., C. L. Baduini, and G. L. Hunt. 2001. Modeling underwater visual and filter feeding by planktivorous shearwaters in unusual sea conditions. Ecology **82**:2342–2356.

Lyson, T. 2005. The importance of schools to rural community viability. Report, A Mathematics Educator‘s Introduction to Rural Policy Issues, 59-64.

Lyson, T. A. 2002. What Does a School Mean to a Community? Assessing the Social and Economic Benefits of Schools to Rural Villages in New York. Report, Educational Resources Information Center, 15 p.

Magurran, A. E. 1988. Ecological diversity and its measurement. Princeton University Press, Princeton, N.J.

Mantua, N. J., S. R. Hare, Y. Zhang, J. M. Wallace, and R. C. Francis. 1997. A Pacific Interdecadal Climate Oscillation with Impacts on Salmon Production. Bulletin of the American Meteorological Society **78**:1069–1079.

Martin, J. A., B. Hamilton, M. Osterman, A. Driscoll, and P. Drake. 2018. Births: Final Data for 2017. Report, Report, National Vital Statistics System.

Martin, K. S., and M. Hall-Arber. 2008. The missing layer: Geo-technologies, communities, and implications for marine spatial planning. Marine Policy **32**:779–786.

Martinson, E. C., H. H. Stokes, and D. L. Scarnecchia. 2012. Use of juvenile salmon growth and temperature change indices to predict groundfish post age-0 yr class strengths in the Gulf of Alaska and eastern Bering Sea. Fisheries Oceanography **21**:307–319.

Masterson, V. A., R. C. Stedman, J. Enqvist, M. Tengö, M. Giusti, D. Wahl, and U. Svedin. 2017. The contribution of sense of place to social-ecological systems research: a review and research agenda. Ecology and Society **22 (1)**.

Mathis, J. T., J. N. Cross, and N. R. Bates. 2011. Coupling primary production and terrestrial runoff to ocean acidification and carbonate mineral suppression in the eastern Bering Sea. Journal of Geophysical Research: Oceans **116 (C2)**.

Mathis, J. T., J. N. Cross, N. Monacci, R. A. Feely, and P. Stabeno. 2014. Evidence of prolonged aragonite undersaturations in the bottom waters of the southern Bering Sea shelf from autonomous sensors. Deep Sea Research Part II: Topical Studies in Oceanography **109**:125–133.

Matson, P. G., L. Washburn, E. A. Fields, C. Gotschalk, T. M. Ladd, D. A. Siegel, Z. S. Welch, and M. D. Iglesias-Rodriguez. 2019. Formation, development, and propagation of a rare coastal coccolithophore bloom. Journal of Geophysical Research: Oceans **124**:3298–3316.

McCann, K. S. 2000. The diversity - stability debate. Nature **405**:228–233.

MODIS-Aqua, M. 2018. NASA goddard space flight center, ocean ecology laboratory, ocean biology processing group. Report, DAAC, Greenbelt, MD, USA.

Moore, S. E. 2008. Marine mammals as ecosystem sentinels. Journal of Mammalogy **89**:534–540.

Moore, S. E., K. M. Wynne, J. C. Kinney, and J. M. Grebmeier. 2007. Gray whale occurrence and forage southeast of Kodiak, Island, Alaska. Marine Mammal Science **23**:419–428.

Mueter, F. J., and M. A. Litzow. 2008. Sea ice retreat alters the biogeography of the Bering Sea continental shelf. Ecological Applications **18**:309–320.

Mueter, F. J., and B. L. Norcross. 2002. Spatial and temporal patterns in the demersal fish community on the shelf and upper slope regions of the Gulf of Alaska. Fishery Bulletin **100**:559–581.

Murphy, J. M., K. G. Howard, J. C. Gann, K. C. Cieciel, W. D. Templin, and C. M. Guthrie. 2017. Juvenile Chinook Salmon abundance in the northern Bering Sea: Implications for future returns and fisheries in the Yukon River. Deep-Sea Research Part II-Topical Studies in Oceanography **135**:156–167.

Napp, J. M., and G. L. Hunt. 2001. Anomalous conditions in the south-eastern Bering Sea 1997: linkages among climate, weather, ocean, and Biology. Fisheries Oceanography **10**:61–68.

NPFMC. 2016. Bering Sea/Aleutian Islands Groundfish Fishery Management Plan Amendment Action Summaries. Report, North Pacific Fishery Management Council, 605 W 4th Ave Suite 306, Anchorage, Alaska 99501.

NPFMC. 2017. Fishery Management Plan for Groundfish of the Bering Sea and Aleutian Islands Management Area. Report, North Pacific Fishery Management Council, 605 W 4th Ave Suite 306, Anchorage, Alaska 99501.

Olson, J. 2005. Development in theory: re-placing the space of community: A story of cultural politics, policies, and fisheries management. Anthropological Quarterly **78**:247–268.

Olson, M. B., and S. L. Strom. 2002. Phytoplankton growth, microzooplankton herbivory and community structure in the southeast Bering Sea: insight into the formation and temporal persistence of an *Emiliania huxleyi* bloom. Deep Sea Research Part II: Topical Studies in Oceanography **49**:5969–5990.

Oncescu, J. M., and A. Giles. 2014. Rebuilding a sense of community through reconnection: The impact of a rural school's closure on individuals without school-aged children. Journal of Rural and Community Development **9 (3)**:295–318.

Ortiz, I., F. Weise, and A. Greig. 2012. Marine regions boundary data for the Bering Sea shelf and slope. UCAR/NCAR—Earth Observing Laboratory/Computing, Data, and Software Facility. Dataset. doi **10**:D6DF6P6C.

Ostrom, E. 2007. A diagnostic approach for going beyond panaceas. Proceedings of the National Academy of Sciences **104**:15181–15187.

Parmesan, C., and G. Yohe. 2003. A globally coherent fingerprint of climate change impacts across natural systems. Nature **421**:37–42.

Paul, A., and J. Paul. 1999. Interannual and regional variations in body length, weight and energy content of age-0 Pacific herring from Prince William Sound, Alaska. Journal of fish biology **54**:996–1001.

Pauly, D., V. Christensen, J. Dalsgaard, R. Froese, and F. Torres. 1998. Fishing down marine food webs. Science **279**:860–863.

Peshkin, A. 1978. Growing Up American; Schooling and the Survival of Community. Report, Educational Resources Information Center.

Peshkin, A. 1982. The Imperfect Union. School Consolidation Community Conflict. Report 0226661660, Educational Resources Information Center.

Pierson, J. J., H. Batchelder, W. Saumweber, A. Leising, and J. Runge. 2013. The impact of increasing temperatures on dormancy duration in Calanus finmarchicus. Journal of plankton research **35**:504–512.

Pilcher, D. J., D. M. Naiman, J. N. Cross, A. J. Hermann, S. A. Siedlecki, G. A. Gibson, and J. T. Mathis. 2019. Modeled effect of coastal biogeochemical processes, climate variability, and ocean acidification on aragonite saturation state in the Bering Sea. Frontiers in Marine Science **5**:508.

Platt, T., C. Fuentes-Yaco, and K. T. Frank. 2003. Marine ecology: spring algal bloom and larval fish survival. Nature **423**:398–399.

Purcell, J. E., and M. N. Arai. 2001. Interactions of pelagic cnidarians and ctenophores with fish: a review. Hydrobiologia **451**:27–44.

Queirolo, L. E., L. Fritz, P. Livingston, M. Loefflad, D. Colpo, and Y. DeReynier. 1995. Bycatch, utilization, and discards in the commercial groundfish fisheries of the Gulf of Alaska, eastern Bering Sea, and Aleutian Islands. NOAA Tech. Memo. NMFS-AFSC **58**:148.

Rasmussen, R., G. Hovelsrud, and S. Gearheard. 2015. Community Viability. Copenhagen: Nordisk Ministerråd.

Robinson, K. L., J. J. Ruzicka, M. B. Decker, R. Brodeur, F. Hernandez, J. Quiñones, E. Acha, S. Uye, H. Mianzan, and W. Graham. 2014. Jellyfish, forage fish, and the world's major fisheries. Oceanography **27**:104–115.

Rodionov, S. N., N. A. Bond, and J. E. Overland. 2007. The Aleutian Low, storm tracks, and winter climate variability in the Bering Sea. Deep Sea Research Part II: Topical Studies in Oceanography **54**:2560–2577.

Rogers, L. A., and D. E. Schindler. 2011. Scale and the detection of climatic influences on the productivity of salmon populations. Global Change Biology **17**:2546–2558.

Ruggerone, G. T., B. A. Agler, B. M. Connors, E. V. Farley Jr, J. R. Irvine, L. I. Wilson, and E. M. Yasumiishi. 2016. Pink and sockeye salmon interactions at sea and their influence on forecast error of Bristol Bay sockeye salmon. North Pacific Anadromous Fish Commission Bulletin **6**:349–361.

Ruggerone, G. T., and J. L. Nielsen. 2004. Evidence for competitive dominance of pink salmon (*Oncorhynchus gorbuscha*) over other salmonids in the North Pacific Ocean. Reviews in Fish Biology and Fisheries **14**:371–390.

S, Z., H. G. Jr, T. T, and A. K. 2013. Combined seabird indices show lagged relationships between environmental conditions and breeding activity. Marine Ecology Progress Series **485**:245–258.

Schindler, D. E., R. Hilborn, B. Chasco, C. P. Boatright, T. P. Quinn, L. A. Rogers, and M. S. Webster. 2010. Population diversity and the portfolio effect in an exploited species. Nature **465**:609–613.

Schindler, D. E., P. R. Leavitt, S. P. Johnson, and C. S. Brock. 2006. A 500-year context for the recent surge in sockeye salmon (*Oncorhynchus nerka*) abundance in the Alagnak River, Alaska. Canadian Journal of Fisheries and Aquatic Sciences **63**:1439–1444.

Schlegel, R. W., and A. J. Smit. 2018. heatwaveR: a central algorithm for the detection of heatwaves and cold-spells. Journal of Open Source Software **3**:821.

Sell, R. S., and F. L. Leistritz. 1997. Socioeconomic impacts of school consolidation on host and vacated communities. Community Development **28**:186–205.

Shin, Y.-J., M.-J. Rochet, S. Jennings, J. G. Field, and H. Gislason. 2005. Using size-based indicators to evaluate the ecosystem effects of fishing. ICES Journal of marine Science **62**:384–396.

Shin, Y.-J., L. J. Shannon, A. Bundy, M. Coll, K. Aydin, N. Bez, J. L. Blanchard, M. d. F. Borges, I. Diallo, and E. Diaz. 2010. Using indicators for evaluating, comparing, and communicating the ecological status of exploited marine ecosystems. Part 2. Setting the scene. ICES Journal of Marine Science **67**:692–716.

Sigler, M. F., P. J. Stabeno, L. B. Eisner, J. M. Napp, and F. J. Mueter. 2014. Spring and fall phytoplankton blooms in a productive subarctic ecosystem, the eastern Bering Sea, during 1995–2011. Deep Sea Research Part II: Topical Studies in Oceanography **109**:71–83.

Spencer, P. D. 2008. Density-independent and density-dependent factors affecting temporal changes in spatial distributions of eastern Bering Sea flatfish. Fisheries Oceanography **17**:396–410.

Spencer, P. D., K. K. Holsman, S. Zador, N. A. Bond, F. J. Mueter, A. B. Hollowed, and J. N. Ianelli. 2016. Modelling spatially dependent predation mortality of eastern Bering Sea walleye pollock, and its implications for stock dynamics under future climate scenarios. ICES Journal of Marine Science **73**:1330–1342.

Springer, A. M., C. P. McRoy, and M. V. Flint. 1996. The Bering Sea Green Belt: Shelf-edge processes and ecosystem production. Fisheries Oceanography **5**:205–223.

Springer, A. M., and G. B. van Vliet. 2014. Climate change, pink salmon, and the nexus between bottom-up and top-down forcing in the subarctic Pacific Ocean and Bering Sea. Proceedings of the National Academy of Sciences **111**:E1880–E1888.

Stabeno, P., S. Danielson, D. Kachel, N. Kachel, and C. Mordy. 2016. Currents and transport on the eastern Bering Sea shelf: An integration of over 20 years of data. Deep Sea Research Part II: Topical Studies in Oceanography **134**:13–29.

Stabeno, P. J., and S. W. Bell. 2019. Extreme Conditions in the Bering Sea (2017 - 2018): Record - Breaking Low Sea-Ice Extent. Geophysical Research Letters **46**:8952–8959.

Stevenson, D. E., and R. R. Lauth. 2012. Latitudinal trends and temporal shifts in the catch composition of bottom trawls conducted on the eastern Bering Sea shelf. Deep-Sea Research Part Ii-Topical Studies in Oceanography **65-70**:251–259.

Stockwell, D. A., T. E. Whitledge, S. I. Zeeman, K. O. Coyle, J. M. Napp, R. D. Brodeur, A. I. Pinchuk, and G. L. Hunt. 2001. Anomalous conditions in the south-eastern Bering Sea, 1997: nutrients, phytoplankton and zooplankton. Fisheries Oceanography **10**:99–116.

Swiney, K. M., W. C. Long, and R. J. Foy. 2017. Decreased pH and increased temperatures affect young-of-the-year red king crab (Paralithodes camtschaticus). ICES Journal of Marine Science **74**:1191–1200.

Thorson, J. T., and L. A. Barnett. 2017. Comparing estimates of abundance trends and distribution shifts using single-and multispecies models of fishes and biogenic habitat. ICES Journal of Marine Science **74**:1311–1321.

Thorson, J. T., L. Ciannelli, and M. A. Litzow. 2020. Defining indices of ecosystem variability using biological samples of fish communities: A generalization of empirical orthogonal functions. Progress in Oceanography **181**:102244.

Thorson, J. T., M. L. Pinsky, and E. J. Ward. 2016*a*. Model-based inference for estimating shifts in species distribution, area occupied and centre of gravity. Methods in Ecology and Evolution **7**:990–1002.

Thorson, J. T., A. Rindorf, J. Gao, D. H. Hanselman, and H. Winker. 2016*b*. Density-dependent changes in effective area occupied for sea-bottom-associated marine fishes. Proceedings of the Royal Society B: Biological Sciences **283**:20161853.

Tieken, M. C., and T. R. Auldridge-Reveles. 2019. Rethinking the school closure research: School closure as spatial injustice. Review of Educational Research **89**:917–953.

Tobin, E. D., C. L. Wallace, C. Crumpton, G. Johnson, and G. L. Eckert. 2019. Environmental drivers of paralytic shellfish toxin producing Alexandrium catenella blooms in a fjord system of northern Southeast Alaska. Harmful algae **88**:101659.

Tojo, N., G. H. Kruse, and F. C. Funk. 2007. Migration dynamics of Pacific herring (*Clupea pallasii*) and response to spring environmental variability in the southeastern Bering Sea. Deep Sea Research Part II: Topical Studies in Oceanography **54**:2832–2848.

Trenberth, K., and J. W. Hurrell. 1994. Decadal atmosphere-ocean variations in the Pacific. Climate Dynamics **9**:303–319.

Turner, B. L., R. E. Kasperson, P. A. Matson, J. J. McCarthy, R. W. Corell, L. Christensen, N. Eckley, J. X. Kasperson, A. Luers, and M. L. Martello. 2003. A framework for vulnerability analysis in sustainability science. Proceedings of the National Academy of Sciences **100**:8074–8079.

Vandersea, M. W., S. R. Kibler, P. A. Tester, K. Holderied, D. E. Hondolero, K. Powell, S. Baird, A. Doroff, D. Dugan, and R. W. Litaker. 2018. Environmental factors influencing the distribution and abundance of Alexandrium catenella in Kachemak bay and lower cook inlet, Alaska. Harmful algae **77**:81–92.

Wespestad, V., and D. Gunderson. 1991. Climatic induced variation in Eastern Bering Sea herring recruitment. Report, Proceedings of the International Herring Symposium, Anchorage, AK. Alaska Sea Grant.

Wilderbuer, T., J. T. Duffy-Anderson, P. Stabeno, and A. Hermann. 2016. Differential patterns of divergence in ocean drifters: Implications for larval flatfish advection and recruitment. Journal of Sea Research **111**:11–24.

Wilderbuer, T., W. Stockhausen, and N. Bond. 2013. Updated analysis of flatfish recruitment response to climate variability and ocean conditions in the Eastern Bering Sea. Deep Sea Research Part II: Topical Studies in Oceanography **94**:157–164.

Wilderbuer, T. K., A. B. Hollowed, W. J. Ingraham, P. D. Spencer, M. E. Conners, N. A. Bond, and G. E. Walters. 2002. Flatfish recruitment response to decadal climatic variability and ocean conditions in the eastern Bering Sea. Progress in Oceanography **55**:235–247.

Williams, E. H., and T. J. Quinn. 2000. Pacific herring, (*Clupea pallasii*), recruitment in the Bering Sea and north-east Pacific Ocean, I: relationships among different populations. Fisheries Oceanography **9**:285–299.

Williams, J. 2006. Alaska Population Overview: 2003-2004 Estimates. Report, The State of Alaska Department of Labor and Workforce Development, Research and Analysis Section, Demographics Unit.

Williams, J. G. 2004. Alaska Population Overview: 2003-2004 Estimates. Report, The State of Alaska Department of Labor and Workforce Development, Research and Analysis Section, Demographics Unit.

Winemiller, K. O. 2005. Life history strategies, population regulation, and implications for fisheries management. Canadian Journal of Fisheries and Aquatic Sciences **62**:872–885.

Witherell, D. 2000. Groundfish of the Bering Sea and Aleutian Islands Area: Species Profiles 2001. Report, North Pacific Fishery Management Council, 605 West 4th Avenue, Suite 306, Anchorage, AK 99501. `http://www.fakr.noaa.gov/npfmc/summary_reports/species2001.pdf`

Woillez, M., J. Rivoirard, and P. Petitgas. 2009. Notes on survey-based spatial indicators for monitoring fish populations. Aquatic Living Resources **22**:155–164.

Zador, S. G., and S. Fitzgerald. 2008. Seabird attraction to trawler discards. Report, Alaska Fisheries Science Center, NOAA, NMFS, 7600 Sand Point Way NE, Seattle WA 98115.

Appendix

History of the ESRs

Since 1995, staff at the Alaska Fisheries Science Center have prepared a separate Ecosystem Status (formerly Considerations) Report within the annual Stock Assessment and Fishery Evaluation (SAFE) report. Each new Ecosystem Status Report provides updates and new information to supplement the original report. The original 1995 report presented a compendium of general information on the Gulf of Alaska, Bering Sea, and Aleutian Island ecosystems as well as a general discussion of ecosystem-based management. The 1996 edition provided additional information on biological features of the North Pacific, and highlighted the effects of bycatch and discards on the ecosystem. The 1997 edition provided a review of ecosystem-based management literature and ongoing ecosystem research, and provided supplemental information on seabirds and marine mammals. The 1998 edition provided information on the precautionary approach, essential fish habitat, effects of fishing gear on habitat, El Niño, local knowledge, and other ecosystem information. The 1999 edition again gave updates on new trends in ecosystem-based management, essential fish habitat, research on effects of fishing gear on seafloor habitat, marine protected areas, seabirds and marine mammals, oceanographic changes in 1997/98, and local knowledge.

In 1999, a proposal came forward to enhance the Ecosystem Status Report by including more information on indicators of ecosystem status and trends and more ecosystem-based management performance measures. The purpose of this enhancement was to accomplish several goals:

1. Track ecosystem-based management efforts and their efficacy
2. Track changes in the ecosystem that are not easily incorporated into single-species assessments
3. Bring results from ecosystem research efforts to the attention of stock assessment scientists and fishery managers
4. Provide a stronger link between ecosystem research and fishery management
5. Provide an assessment of the past, present, and future role of climate and humans in influencing ecosystem status and trends

Each year since 1999, the Ecosystem Status Reports have included some new contributions and will continue to evolve as new information becomes available. Evaluation of the meaning of observed changes should be in the context of how each indicator relates to a particular ecosystem component.

For example, particular oceanographic conditions, such as bottom temperature increases, might be favorable to some species but not for others. Evaluations should follow an analysis framework such as that provided in the draft Programmatic Groundfish Fishery Environmental Impact Statement that links indicators to particular effects on ecosystem components.

In 2002, stock assessment scientists began using indicators contained in this report to systematically assess ecosystem factors such as climate, predators, prey, and habitat that might affect a particular stock. Information regarding a particular fishery's catch, bycatch, and temporal/spatial distribution can be used to assess possible impacts of that fishery on the ecosystem. Indicators of concern can be highlighted within each assessment and can be used by the Groundfish Plan Teams and the Council to justify modification of allowable biological catch (ABC) recommendations or time/space allocations of catch.

We initiated a regional approach to the ESR in 2010 and presented a new ecosystem assessment for the eastern Bering Sea. In 2011, we followed the same approach and presented a new assessment for the Aleutian Islands based on a similar format to that of the eastern Bering Sea. In 2012, we provided a preliminary ecosystem assessment on the Arctic. Our intent was to provide an overview of general Arctic ecosystem information that may form the basis for more comprehensive future Arctic ecosystem assessments. In 2015, we presented a new Gulf of Alaska report card and assessment, which was further divided into Western and Eastern Gulf of Alaska report cards beginning in 2016. This was also the year that the previous Alaska-wide ESR was split into four separate report, one for the Gulf of Alaska, Aleutian Islands, eastern Bering Sea, and the Arctic[29].

The eastern Bering Sea and Aleutian Islands ecosystem assessments were based on additional refinements contributed by Ecosystem Synthesis Teams. For these assessments, the teams focused on a subset of broad, community-level indicators to determine the current state and likely future trends of ecosystem productivity in the EBS and ecosystem variability in the Aleutian Islands. The teams also selected indicators that reflect trends in non-fishery apex predators and maintaining a sustainable species mix in the harvest as well as changes to catch diversity and variability. Indicators for the Gulf of Alaska report card and assessment were also selected by a team of experts, via an online survey first, then refined in an in-person workshop.

Originally, contributors to the Ecosystem Status Reports were asked to provide a description of their contributed indicator, summarize the historical trends and current status of the indicator, and identify potential factors causing those trends. Beginning in 2009, contributors were also asked to describe why the indicator is important to groundfish fishery management and implications of indicator trends. In particular, contributors were asked to briefly address implications or impacts of the observed trends on the ecosystem or ecosystem components, what the trends mean and why are they important, and how the information can be used to inform groundfish management decisions. Answers to these types of questions will help provide a "heads-up" for developing management responses and research priorities. In 2018, a risk table framework was developed for individual stock assessments as a means of documenting concerns external to the stock assessment model, but relevant to setting the Acceptable Biological Catch (ABC) value. These concerns could be categorized as those reflecting the assessment model, the population dynamics of the stock, and environmental and ecosystem concerns—including those based on information from Ecosystem Status Reports. In the past, concerns used to justify an ABC below the maximum calculated by the assessment model were documented in an ad hoc manner in the stock assessment report

[29]The Arctic report is under development

or in the minutes of the groundfish Plan Teams or Scientific and Statistical Committee reviews. With the risk table, formal consideration of concerns—including ecosystem—are documented and ranked, and the stock assessment author presents a recommendation for the maximum ABC or a value lower. Five risk tables were completed in 2018 as a test case. After review, the Council requested risk tables to be included in all stock assessments in 2019.

In Briefs were started in 2018 for the Eastern Bering Sea, 2019 for the Gulf of Alaska, and 2020 for the Aleutian Islands. These more public-friendly succinct versions of the full ESRs are now planned to be produced in tandem with the ESRs.

In 2019, risk tables were completed for all full assessments. Ecosystem scientists collaborated with stock assessment scientists to use the Ecosystem Status Reports to help inform the ecosystem concerns in the risk tables.

Ecosystem and Socioeconomic Profiles (ESPs) were initiated in 2017 (Sablefish) and ESR editors began working closely with ESP teams in 2019 (starting with GOA walleye pollock). These complimentary annual status reports inform groundfish management and alignment in research that feeds these reports increases efficiency and collaboration between ecosystem and stock assessment scientists.

This report represents much of the first three steps in Alaska's IEA: defining ecosystem goals, developing indicators, and assessing the ecosystems (Figure 99). The primary stakeholders in this case are the North Pacific Fishery Management Council. Research and development of risk analyses and management strategies is ongoing and will be referenced or included as possible.

Figure 99: The IEA (integrated ecosystem assessment) process.

It was requested that contributors to the Ecosystem Status Reports provide actual time series data or make them available electronically. The Ecosystem Status Reports and data for many of the time series presented within are available online at: `http://access.afsc.noaa.gov/reem/ecoweb/`. These reports and data are also available through the NOAA-wide IEA website at: `https://www.integratedecosystemassessment.noaa.gov/regions/alaska`.

Past reports and all groundfish stock assessments are available at: `https://www.fisheries.noaa.gov/alaska/population-assessments/north-pacific-groundfish-stock-assessment-and-fishery-evaluation.`

If you wish to obtain a copy of an Ecosystem Considerations Report version prior to 2000, please contact the Council office (907) 271-2809.

Responses to SSC comments from December 2019

This year, as in the past, the ESRs were insightful, well-written, and well-edited. Both chapters were helpful in providing a context within which to assess the stocks of commercially harvested fish in the Federal waters off Alaska. The editors and authors have been very responsive to the comments and suggestions provided by the SSC in 2018, with many improvements evident. The SSC appreciates the positive impacts of the additional resources devoted to the ESRs. These additional resources allowed for a more in-depth analysis of recent environmental changes, such as the examination of the reappearance of the heatwave in 2019 in the Gulf of Alaska, and the extraordinary conditions in the northern Bering Sea in both 2018 and 2019.

Thank you. This year we provide updates to the Eastern Bering Sea (Siddon), Gulf of Alaska (Ferriss & Zador, with Rob Suryan providing coordination with Gulf Watch Alaska), and Aleutian Islands (Ortiz & Zador) Ecosystem Status Reports (ESRs). We anticipate updating the Eastern Bering Sea and Gulf of Alaska ESRs in 2021 as NOAA continues to support and provide resources to these Reports.

Given the rapidly changing conditions in the EBS, there is increased need for information about the effects of climate on the carrying capacity of the EBS and GOA marine ecosystems. This need is great in both the southeastern Bering Sea and the northern Bering Sea. Likewise, there is cause for concern because the western Gulf of Alaska has remained in heatwave conditions for most of 2019, and summer sea surface temperatures were similar to the warmest temperatures during the 2014 - 2016 marine heatwave. ***The SSC strongly recommends the conduct of annual surveys of not only groundfish, but also zooplankton across the entire eastern Bering Sea and the GOA.*** *This additional coverage should not be at the expense of biennial surveys of the Aleutians and Bering Sea slope.*

The AFSC has engaged in extensive survey planning and prioritization in 2020, in collaboration with the North Pacific Fisheries Management Council, in the context of responding to COVID-19 and balancing research and monitoring needs.

There were several lines of evidence indicating concern about the lack of large zooplankton on the EBS shelf. *The Rapid Zooplankton Assessment indicated low abundances of large copepods and euphausiids. The effects of these low abundances are especially apparent in the reproductive success of seabirds that are obligate planktivores, like the* Aethia *auklets. Although fish-eating seabirds had relatively good reproductive success, auklets had poor reproductive success and*

abandoned colonies in the Pribilof Islands, as well as at St. Lawrence and Hall Islands (next to St. Matthew Island). These reproductive failures, coupled with the die-off of short-tailed shearwaters due to starvation in July/August, are compelling evidence for a poor plankton prey base.

These implications of changes in foodweb structure and carrying capacity are of particular concern in the NBS. The SSC recognizes the challenge to find indicators of benthic communities, and recommends continued efforts to integrate data on benthic infauna and epifauna into the ESR, perhaps exploring data from the NBS separately from those available in the southeastern Bering Sea (e.g., diet of flatfish, crab, gray whales, ice seals; changes in benthic community structure in the NBS). For updated information, it may be useful to contact some of the academic investigators working in the NBS, such as Jackie Grebmeier.
The high mortality rates of gray whales and ice seals in the EBS and of seals in the Chukchi Sea may be a matter of concern. They reflect the general decline in several benthic species (e.g., northern rock sole, yellowfin sole, Tanner crab, red king crab). Together, these declines may be signaling a decrease in benthic productivity. Direct measurements of motile epifauna biomass are available from the bottom trawl surveys and the timeseries from the standard (southern) grid is presented in the EBS Report Card. Indirect measurements of benthic infauna and epifauna are inferred from trends in biomass of the benthic forager guild (e.g., Yellowfin sole, Northern rock sole). The addition of benthic sampling methods (e.g., beam trawl) is under consideration for ecosystem surveys conducted over the shelf.

There was a high reported number (179) of Laysan albatrosses bycaught in the EBS. If all were indeed Laysan, the population implications do not seem overly bad, as there is a large population of Laysan albatrosses in the North Pacific. However, if these numbers include mis-identified endangered short-tailed albatrosses, these losses could have serious conservation impacts. The SSC is concerned that observers are well trained in differentiating Laysan and short-tailed albatrosses.
Response from the Alaska Regional Office: "We have great confidence in the observer's ability to correctly identify a short-tailed albatross. That species is strongly emphasized during their annual training and observers are instructed to err on the side of caution if they even think they have one.

Please note: the numbers presented in the ESR are estimated takes of laysan albatross. Since we do not have full observer coverage on all boats, we have to extrapolate actual reported takes on observed vessels out to unobserved vessels. This can sometimes result in an actual take of 4 or 5 albatross being extrapolated out to 25 or 30."

Comments applicable to both the EBS and the GOA ESRs
These are very long reports and it is likely that few readers will read them in their entirety. Their greatest value is in the syntheses and in the sections that focus attention on emerging ecosystem-wide problems and key messages. Presently, there are a number of areas in the ESRs where there are several overlapping contributions on the same subject. It would shorten the ESRs and make the information more comprehensible if the authors could collaborate to produce a single contribution on a given subject that summarizes the current situation. As an example, ***the SSC recommends that there be a single, short, but comprehensive (integrated) contribution on sea temperatures in each region*** *(presently, 17 Figures in the GOA ESR). The integrated section on seabirds might provide a good example. Synthesis products, presentations, discussions with assessment authors, and collaboration among contributors are among the high value outcomes of the ESR reports.*
The EBS ESR continued with the Integrated Seabird Information (p. 114) section in the 2020 ESR based on this feedback from the SSC. In addition, a new Physical Environment Synthesis (p. 50) is

presented in the 2020 ESR as an overview of the physical oceanographic conditions impacting the eastern Bering Sea. The synthesis section merges across information sources, from broad-scale to local-scale, in the following section: Climate Overview, Regional Highlights, Sea Ice, Winds, Sea Surface Temperature, and Bottom Temperature.

The GOA ESR is taking an iterative approach to creating a single, comprehensive contribution on sea temperatures. In the 2020 ESR, we have combined all the sea temperature data into one section (Physical Environment) and we have combined three sub-regional temperature datasets into a single figure, to reduce the total number of figures. We also provide a short summary of temperature data at the beginning of the Physical Environment section. The 2020 ESR has 8 sea temperature figures. The 2021 ESR will include a further revised synthesis of temperature data when we receive the biennial survey updates and have a full suite of data to work with.

In both the EBS and GOA, there are several Ecosystem or Community Indicators that could be much more informative if split up into different species groups. Mean Community Life Span, Mean Community Length, Mean Community Weight, Mean Community Trophic level (not in this year's reports) are often indices that are driven by the abundance of one or two species. In the EBS, pollock dominate the statistics, and in the GOA, forage fish may drive the averages. ***The SSC suggests calculating these indices with and without the dominant species****, or in several species groups that make some ecological sense.*
The lead contributor has provided a response to this comment: "We agree that these indices can be driven by an abundant species, such as walleye pollock. For the eastern Bering Sea, and in the absence of 2020 trawl survey data, we have recalculated the 2019 submissions for Mean Lifespan of the Fish Community, Mean Length of the Fish Community, and the Stability of Groundfish Biomass, with and without walleye pollock to illustrate the effect they have on these groundfish indicators.

In the GOA there are many species of pelagic forage fishes (e.g., herring, capelin, etc.) that collectively could drive the value of fish community indicators. The indicators Mean Lifespan of the Fish Community, Mean Length of the Fish Community, and Stability of Groundfish Biomass are specific to the portion of the groundfish community that are efficiently sampled with bottom-trawling gear used by the AFSC during their biennial summer survey of the GOA. While many species of pelagic forage fish are occasionally encountered during the survey, most are not consistently sampled well enough to be included in the biomass index, including sandlance, capelin, and other pelagic smelts. Herring and eulachon are included in the survey index, so we have recalculated the 2019 GOA contributions with and without herring and eulachon to examine their influence on these community indicators."

The SSC strongly supports the production of the 'In Brief' versions of the ESRs *aimed at conveying a summary of ecosystem information to the public. The 'In Brief' report on the EBS from 2018 was well-received by communities, and the 2019 versions for both the EBS and GOA look excellent. The SSC continues to encourage these efforts, as well as further attempts to provide information back to the communities that have provided information for the ESR.*
Thank you – we agree! We will be producing 2020 'In Brief' versions of the EBS, GOA, and AI ESRs this year. In addition, in collaboration with AFSC communications team, we are producing story maps and short educational outreach videos to further describe the 2020 ESRs to a broader audience.

In the human dimensions section of the ESRs, the utility of a number of the indicators would

be improved with the addition of a spatial dimension. Seafood production, value, and unit value indicators are presented at the EBS-level only, and unemployment is presented at the EBS and NBS levels only, which does not allow for discernment of changing patterns over time at a sub-regional or community scale. Trends in population are presented at a community level but, like observed trends of unemployment, there is no apparent nexus of changes in ecosystem- or fishery-specific variables to changes in human dimension indicators (e.g., no community level time series data on federally managed fisheries engagement are presented that would provide a perspective on potential relationships between these data and observed population trends).

Overall, the human dimensions section would benefit from a series of maps that show the relationships between the various geographic units discussed and the location of communities within those geographies (and the larger ecosystem geographies). It would also be beneficial to clarify the relationship between the type of human dimensions data that are contained in ESRs, ESPs, SAFEs, the Economic SAFE, and the apparently new and to-be-defined documents that will contain the fishing community information that was removed from the current version of the Economic SAFE. This would provide clarity and consistency in meeting the data needs to address social and community focused management obligations under National Standard 2 and National Standard 8 while avoiding redundancy of effort.
Eco-regional maps with identified communities are in development and will be included in next year's ESRs. The level of analysis (e.g., EBS-level) is consistent with the ESR scope. For sub regional and community scale, this data is available in the ESP (stock specific), ACEPO (Groundfish and crab FMPs), and Econ SAFE (economic information) documents. The Economic and Social Science Research group at AFSC continues to refine and communicate this suite of documents. Examples of these efforts include presentations by Stephen Kasperski at the September 2020 Groundfish Plan Team, the November 2020 Groundfish Plan Team, and the SSC in their February meeting.

Comments Specific to the Eastern Bering Sea Ecosystem Status Report:
The SSC was pleased to note that most report card indicators have current data.

The SSC appreciated the section detailing which patterns were reflective of 2018 vs 2019 vs cumulative impacts. This format made it easier to see the influence of two years of low sea ice and the differences and potential connectivity between the southeastern Bering Sea and NBS. It was also helpful to understand which observations were the result of lagged-effects or cumulative effects of changes to the ecosystem.

The EBS ESR includes several leading indicators of pollock recruitment that yield, in some cases, contradictory results. It would be useful to assess alternative hypotheses as to why these differences were found. For instance, what role could the differences between the winters of 2017/18 and 2018/19 have played?
We agree that further investigation into the mechanistic relationships and drivers of pollock recruitment is warranted. We look forward to the opportunity to explore these relationships through the development of the ESP for EBS pollock in 2021.

Current Conditions 2019 section:
Page 21: Note that both species of kittiwakes are primarily fish eaters, with some plankton taken by both species.
Thank you - we appreciate the clarification and have better described trends for fish-eating and planktivorous seabirds in the 2020 Integrated Seabird Information section (p. 114).

Page 21: The comments about the movements of cod (and other fish from the Inner Shelf Domain) seem a bit too speculative.
Thank you - we presented this as a possible explanation of increased abundance of Pacific cod in the 2019 standard bottom trawl survey as an alternative hypothesis.

Noteworthy Items section:
SSC greatly appreciates the excellent contributions on marine mammal ecology *provided by the Marine Mammal Laboratory (MML) and others. The SSC hopes that the MML will continue to provide reports in the future, as they add greatly to our understanding of probable stressors in the Eastern Bering Sea ecosystem.*

The SSC appreciates the inclusion of data on northern fur seals from bioenergetic models and ongoing foraging studies. In the southeastern Bering Sea, the new information tying female fur seal foraging to a lack of prey, especially of age-0 and age-1 pollock, suggests that these forage fish (and possibly others) are less abundant around St. Paul Island than was previously the case. For some forage, such as capelin, there may have been a movement to cooler waters in the 1980s. For others, there may be increased consumption by predators such as arrowtooth flounder, adult pollock and Pacific cod. Alternatively, the EBS coccolithophore blooms (Figure 45) may have some impact on the ability of fur seals to locate and capture prey. These blooms cannot account for the declines in the 1970s, 1980s and 1990s, before there were major blooms in the SEBS. Collectively, the results of the foraging effort and bioenergetics studies suggest that lactating females on St. Paul Island are having difficulty finding food in close proximity to the rookery, which could adversely affect pup growth rates and contribute to the ongoing population decline on St. Paul Island. It is not clear how adjustments to fishing pressures might influence the availability of age-0 and age1 pollock near St. Paul Island and still protect Pribilof Island Blue King Crab.
This SSC comment was relayed to the contributors of the 2019 Noteworthy section entitled 'Contrasting Trends in Northern Fur Seal Foraging Effort Between St. Paul and Bogoslof Islands: 2019 Preliminary Results' on 30 March 2020. During 2020, MML was unable to conduct the vast majority of field research in the Bering Sea due to COVID-19 travel restrictions. We look forward to receiving contributions from MML in 2021.

At the October preview, the SSC requested information on Harmful Algal Blooms (HABs). Some interesting examples were provided in the Ecosystem Recap section. Particularly noteworthy were the reports that saxitoxin was detectable in the stomach contents of all pollock sampled. In the future, it would be useful to have more information on the occurrence of HABs in the components of the EBS marine ecosystem, as well as some context on typical 'background levels'.
In the 2020 ESRs, a new contribution from the Alaska HAB Network is included. Results from shellfish and phytoplankton monitoring showed a consistent presence of harmful algal blooms (HABs) throughout the Gulf of Alaska and Aleutian Islands in 2020; results from samples collected in the northern Bering Sea are still pending (p. 136).

Ecosystem Status Indicators section:
The SSC welcomes the addition of the new, excellent section on sea ice *in the Bering Sea. The SSC hopes that it will still be relevant in coming years! If this contribution on sea ice continues in subsequent years, it may not be necessary for the EBS FOCI contribution to cover these topics. It would be useful for all indices to use a standardized year; the ice-year is presently 1 August to 31 July, but later in the document the SST-year is 1 September to 31 August.*
The new Physical Environment Synthesis (p. 50) provides a succinct section on sea ice dynamics (p. 54). Within the Physical Environment Synthesis, the 'year' is defined seasonally as follows:

Autumn (Sept-Nov), Winter (Dec-Feb), Spring (Mar-May), and Summer (Jun-Aug) in all cases except the indicator of annual ice extent that remains 1 August to 31 July to account for the seasonal ice cycle in an annualized index.

It would be interesting to see the salinity data and to see how it might reveal transport mechanisms. This is an area for additional investigation.
After close examination, it was unclear what contribution this comment refers to.

Figure 39: 2019 has a VERY sharp peak in chlorophyll compared to 2018. How might that affect the availability of phytoplankton for zooplankton? It would be useful to see a figure from a year with ice (e.g., 2017).
In the 2020 ESR, the contributors of chlorophyll information provided a more comprehensive analysis in terms of temporal (2003–2020) and spatial (8 regions) coverage (p. 74).

Figure 42: Very nice to see the hotspots around the Pribilofs and in the Chirikov Basin near where the Anadyr water (nutrient rich) meets the fresh coastal water (nutrient depleted). The maps of stability and Chl-a are potentially quite useful.
This SSC comment has been replayed to the contributors of the 2019 contribution entitled 'Phytoplankton Biomass and Size Structure During Late Summer to Early Fall in the Eastern Bering Sea'. During 2020, the BASIS survey was canceled due to COVID-19 travel restrictions. We look forward to receiving updates to this contribution in 2022.

The SSC supports continued exploration of the use of VAST models *as an update of the large copepod (*Calanus marshallae/glacialis, Metridia pacifica*) index. However, we caution that the 2008 estimate should be carefully examined. This estimate is suspect given that the estimate increased, as did the variance. Neither of these outcomes would be expected.*
The lead contributor has provided a response to this comment: "The relationship between large copepods and age-3 pollock abundances was improved using the copepod indices from the VAST spatio-temporal model particularly for years when sampling was limited. For example, the VAST model-based indices compared to sample-based indices predicted a higher abundance of large copepods in 2008, a year when the sample coverage did not extend into the outer shelf. The outer shelf is where M. pacifica and Neocalanus spp. are found in the highest concentrations and where Calanus spp. are often observed in high numbers.

The reduced number of observations in the outer shelf in 2008 combined with the biological variation in the observations of large copepods in that region could lead to the increased variance. Regarding the higher model-based estimate compared to the sample-based estimate, while we wouldn't expect them to be dramatically different, it is possible for a model-based estimate to be different than the sample-based estimate for a few reasons: (1) model-based estimate accounts for spatial correlation and (2) inclusion of unsampled areas in the extrapolation grid for density estimates."

*In discussions about zooplankton, it is important to differentiate small species of copepods from early life stages of large species that will grow and accumulate lipid stores in summer. It is these large species that support the overwintering of age-0 pollock. In the same vein, it could be useful to distinguish among copepod species that store lipids (*Calanus *spp. and* Neocalanus *spp.) and those that do not (*Metridea *spp. and* Eucalanus bungii*), and therefore have low nutritional value to fish.*
This comment has been addressed by the contributors in the 2020 ESR contribution entitled 'Current and Historical Trends for Zooplankton in the Bering Sea' in the first paragraph of the Factors Influencing Observed Trends section (p. 82).

The new condition factor analysis for age-0 Pacific cod and walleye pollock provides a useful update to previous work. ***The SSC requests that criteria for assigning the categories "warm", "cold" and "average" to year-classes be clearly defined.*** *The figures show data from 2003–2018, but it is not clear whether the categorization was based on this time series or some other period.*
The authors of this contribution agree that a more clear definition when assigning thermal categories to years is warranted and will address this when the contribution can be updated next in 2023 (no BASIS survey sample collections in 2019–2021 and then a 1-year lag in processing the energetics samples collected in 2022).

The SSC found the Bering Strait project on HABs of great interest. However, no details, contact information, etc. was available. A full contribution would be nice.
In the 2020 ESRs, a new contribution from the Alaska HAB Network is included. Results from shellfish and phytoplankton monitoring showed a consistent presence of harmful algal blooms (HABs) throughout the Gulf of Alaska and Aleutian Islands in 2020; results from samples collected in the northern Bering Sea are still pending (p. 136).

Figure 55: The energy content of most of these salmon seems low. How does that relate to ocean survival and salmon returns?
This SSC comment has been relayed to the contributors of the 2019 contribution entitled 'Total Energy Trends Among Juvenile Fishes in the Northern Bering Sea'. During 2020, the northern Bering Sea surface trawl survey was canceled due to COVID-19 travel restrictions. We look forward to receiving updates to this contribution in 2022.

Page 120: "In contrast, surface silicate (silicic acid) is found in higher concentrations than nitrogen and inter-annual variations are reliably detectable making silicate a possible indicator of nutrient availability in surface waters." But why is surface silicate important if it is N that is limiting?
This SSC comment has been relayed to the contributors of the 2019 contribution entitled 'Implications for Age-0 Walleye Pollock (*Gadus chalcogrammus*) Condition Based on Late Summer Surface Silicic Acid Concentrations'. During 2020, the BASIS survey was canceled due to COVID-19 travel restrictions. We look forward to receiving updates to this contribution in 2023 (no BASIS survey sample collections in 2019–2021 and then a 1-year lag in processing the samples collected in 2022).

Page 125/126: The average energy content of age-0 pollock in warm years between 2003 and 2017 accounts for 72% of the variation in age-1 recruits per spawning biomass, but only 9% in cold years (Figure 84) due to two years with very high recruitments in 2008 and 2012. In the exceptionally cold year of 2012, much ice and a large cold pool may have pushed adult cod and pollock off much of the shelf. It has been hypothesized that in cold years with a large cold pool, the amount of predation on age-0 pollock is reduced.
Agreed. In fact, this is pointed to in the 2019 contribution entitled 'Condition of Age-0 Walleye Pollock and Pacific Cod' under Implications: "For age-0 pollock, the relationship between average energy content and recruitment to age-1 under warm years suggests that bottom-up processes (i.e., higher metabolic demands, poor prey quality and quantity) have a strong impact on survival and subsequent recruitment success. The model fit under cold years suggests survival and recruitment success are more variable and likely the result of a suite of processes, including bottom-up and top-down pathways."

Figure 80: Relationships between estimated mean abundance of large copepods (sum of Calanus marshallae/glacialis, Metridia pacifica, *and* Neocalanus *spp.) during the age-0 life stage of pollock,*

and the estimated abundance of age-3 pollock. It might be interesting to repeat this analysis without Metridia.
This SSC comment has been relayed to the contributors of the 2019 contribution entitled 'Large Copepod Abundance (Sample-Based and Modeled) as an Indicator of Pollock Recruitment to Age-3 in the Southeastern Bering Sea'.

Integrated Seabird Section: ***The SSC commends the authors and editors in assembling this section.*** *It provides an excellent overview and avoids repetition. It also spurred valuable collaborations among the contributors. It would be nice to have a two- or three-sentence summary statement at the end.*
The 2020 ESR continued with the Integrated Seabird Information (p. 114) section and, based on this feedback from the SSC, it now contains a Summary section.

Figure 97: The SSC recommends providing the raw numbers of bycaught west coast Chinook salmon, at least in the text. An increase in the proportion of west coast salmon could just indicate a decreasing capture of salmon from other stocks.
The contribution entitled 'Stock Compositions of Chinook and Chum Salmon Bycatch in Bering Sea Trawl Fisheries' will no longer be presented in the ESRs because the information is presented in bycatch reports through the Council process and is, for the purposes of the ESRs, out-dated.

Figure 101: Could the bycatch of assorted benthic invertebrates be affecting crab stocks?
Sea stars comprise more than 85% of the assorted invertebrates catch in all years (2011–2019), so it is unlikely that bycatch of assorted benthic invertebrates would have a large impact on crab stocks.

Human Dimensions section:
This section would benefit from a thorough edit, as there are apparent errors in the population tables (e.g., Scammon Bay population) and they lack clarity in labeling. The migration pattern figures and school enrollment data conflate boroughs and census areas (the differences between which equate to different relationships between communities therein).
These SSC comments were relayed to the contributors; the population and unemployment data were carefully reviewed and clarified in the 2020 ESR. The migration pattern figures were not included in the 2020 ESR.

Page 198 "The closure of a school in either of these places would have a profound effect." What are these places?
This SSC comment was relayed to the contributors and has been revised for clarity in the 2020 ESR.

Methods Description for the Report Card Indicators

For each plot, the mean (green dashed line) and ±1 standard deviation (SD; green solid lines) are shown as calculated for the entire time series. Time periods for which the time series was outside of this ±1 SD range are shown in yellow (for high values) and blue (for low values).

The shaded green window shows the most recent 5 years prior to the date of the current report. The symbols on the right side of the graph are all calculated from data inside this 5-year moving window (maximum of 5 data points). The first symbol represents the "2016–2020 Mean" as follows: '+ or -' if the recent mean is outside of the ±1 SD long-term range, '.' if the recent mean is within

this long-term range, or 'x' if there are fewer than 2 data points in the moving window. The symbol choice does not take into account statistical significance of the difference between the recent mean and long-term range. The second symbol represents the "2016–2020 Trend" as follows: if the magnitude of the linear slope of the recent trend is greater than 1 SD/time window (a linear trend of >1 SD in 5 years), then a directional arrow is shown in the direction of the trend (up or down), if the change is <1 SD in 5 years, then a double horizontal arrow is shown, or 'x' if there are fewer than 3 data points in the moving window. Again, the statistical significance of the recent trend is not taken into account in the plotting.

The intention of the figure is to flag ecosystem features and the magnitude of fluctuations within a generalized "fisheries management" time frame (i.e., trends that, if continued linearly, would go from the mean to ±1 SD from the mean within 5 years or less) for further consideration, rather than serving as a full statistical analysis of recent patterns.